Stress resistance of *Enterobacteriaceae* in food and water

by

Zhiying Wang

A thesis submitted in partial fulfillment of the requirements for the degree of

Doctor of Philosophy

in

Food Science and Technology

Department of Agricultural, Food and Nutritional Science

University of Alberta

ABSTRACT

Bacterial species in the order *Enterobacterales* populate diverse ecological niches including soil, water, nematodes, insects, plants, and vertebrates. Many *Enterobacteriaceae* temporarily inhabit the intestine of vertebrate hosts but also survive and thrive in extra-intestinal habitats to transit between host individuals. These species acquire stress resistance genes to overcome dispersal limitations and environmental stresses; this stress resistance also challenges pathogen control in the food industry and hospitals. The research described in this thesis aimed to investigate the role of stress resistance genes in host adaptation and their impact on food safety and public health. Samples from Daqu fermentation, wastewater, and fresh water contained *Enterobacteriaceae* that harbored a genomic island termed the transmissible locus of stress tolerance (tLST), which confers extreme heat resistance. Functional genomics demonstrated that the tLST also confers resistance to chlorine and other oxidizing chemicals, and identified 7 proteins encoded by the tLST are necessary for heat or chlorine resistance. Comparative genomics demonstrated that the tLST is particularly present in those *Enterobacteriaceae* that occur in plant-associated habitats as well in the intestine of vertebrates. The frequency of the tLST in clinical isolates of *Klebsiella* and *Cronobacter* species suggests that tLST-mediated resistance may contribute to their persistence in hospitals. The function of the genomic island was also characterized by competition experiments of isogenic tLST-positive and tLST-negative strains. These demonstrated that the fitness gain during lethal challenge with chlorine is associated with a substantial fitness cost in the absence of chemical or physical stressors.

The presence of tLST excluded virulence factors of several pathogens including *Shigella*, Shiga-toxin producing *E. coli*, uropathogenic *E. coli*, and *Salmonella*. To determine whether the accessory genome of *Salmonella* also includes genes that contribute to stress resistance,

comparative and functional genomic analyses were used to identify genes related to the resistance of *Salmonella* to desiccation and dry heat. Of the 289 genes that were differentially distributed in resistant and sensitive strains of *Salmonella*, 7 genes were confirmed to contribute to dry-heat resistance or high-pressure resistance by expression in sensitive strains. Taken together, this study improves the understanding of the contribution of genetic determinants to stress resistance and host adaptation in *Enterobacteriaceae*, which allow improved control of pathogenic *Enterobacteriaceae*.

PREFACE

This thesis is an original work by Zhiying Wang, which is written according to the guidelines provided by FGSR.

Chapter 2 is in preparation for submission as Zhiying Wang, David J. Simpson, Na Li, Jinshui Zheng, Malinda S. Thilakarathna, and Michael G. Gänzle, "Ecology, diversity and evolution of *Enterobacterales*" to the ISME journal. Chapter 3 has been published as Zhiying Wang, Pan Li, Lixin Luo, David J. Simpson, and Michael G. Gänzle. (2018), "DaQu fermentation selects for heat resistant *Enterobacteriaceae* and bacilli", Applied and Environmental Microbiology, 84(21);e01483-18. Chapter 4 has been published as Zhiying Wang, Yuan Fang, Shuai Zhi, David J. Simpson, Alexander Gill, Lynn M. McMullen, Norman F. Neumann, Michael G. Gänzlea. (2020), "The locus of heat resistance confers resistance to chlorine and other oxidizing chemicals in *Escherichia coli*", Applied and Environmental Microbiology, 86(4);e02123-19. Chapter 5 has been published as Zhiying Wang, Huifeng Hu, Tongbo Zhu, Jinshui Zheng, Michael G. Gänzle, and David J. Simpson. (2021), "Ecology and function of the transmissible locus of stress tolerance in *Escherichia coli* and plant-associated *Enterobacteriaceae*". mSystems, 6(4):e00378-21. Chapter 6 has been published as Zhiying Wang, Tongbo Zhu, Zhao Chen, Jianghong Meng, David J. Simpson, and Michael G. Gänzle. (2021)."Genetic determinants of stress resistance in desiccated *Salmonella enterica*" by Applied and Environmental Microbiology, 87(23):e01683-21.

Dr. Michael G. Gänzle and Dr. David J. Simpson contributed to the experimental design and manuscript edits (Chapters 2 to 6). Dr. Jinshui Zheng and Na Li collected and analyzed the genomic data (Chapter 2). Dr. Malinda S. Thilakarathna provided suggestions on plant-associated lifestyle (Chapter 2). Dr. Pan Li and Dr. Lixin Luo provided Daqu samples (Chapter 3). Dr. Yuan

Fang contributed to the methodology establishment (Chapter 4). Dr. Alexander Gill provided the data of Shiga toxin-producing *Escherichia coli* (Chapter 4). Dr. Norman F. Neumann brought the concept of the relationship between the tLST and virulence factors (Chapter 4). Dr. Lynn M. McMullen provided suggestions and edited the manuscript (Chapter 4). Dr. Jinshui Zheng and Huifeng Hu contributed to the bioinformatic analysis and data visualization (Chapter 5). Tongbo Zhu contributed to the experiments (Chapters 5 and 6). Dr. Zhao Chen and Dr. Jianghong Meng contributed to the whole genome sequencing and manuscript editing (Chapter 6). I was responsible for searching references, designing the studies, conducting experiments and writing the manuscripts of entire thesis.

ACKNOWLEDGMENTS

First and foremost, I would like to express my deep and sincere gratitude to my supervisor Dr. Michael G. Gänzle for providing me the opportunity to pursue my Ph.D. and for his countless mentorship, support, encouragement, and guidance throughout the program. I would like to extend my deepest gratitude to Dr. Lynn M. McMullen and Dr. Norman F. Neumann for being my supervisory committee members and for their support, guidance, and constructive criticism of my research. My profound appreciation goes to my external examiner Dr. Linda J. Harris and my defense examiner Dr. Casey Fowler for sparing their valuable time to read and evaluate my thesis.

I want to express my appreciation to China Scholarship Council, Alberta Innovates Technology Futures, and Dr. Michael E. Stiles Graduate Scholarship in Applied Microbiology for financial support.

I am grateful to Dr. David J. Simpson for support, training, and mentorship. My honest thanks go to Dr. Jinshui Zheng, Tongbo Zhu, Dr. Yuan Fang, and Huifeng Hu for working with me to complete my research. My sincere thanks go to my labmates in lab 2-50: Dr. Yalu Yan, Dr. Yuanyao Chen, Dr. Ziyi Hu, Dr. Weilan Wang, Dr. Qing Li, Dr. Nuanyi Liang, Dr. Justina Zhang, Dr. Ying Hu, Kaixing Tang, Gautam Gaur, Luis E. Rojas, Zhaohui Xu, Zhen Li, Jin Xie, Zheng Zhao, Nanzhen Qiao, Vi Pham, Oanh Nguyen, Chandre Van De Merwe, Felicitas Pswarayi, Rami Althnaibat, Lilian Morceli, and many others for being good friends, critical colleagues, and patient audiences. I also would like to thank my friends, Dr. Hongmin Dong, Amritha J. Prasad, Brasathe Jeganathan, and Yujie Lu. My five years would not be memorable and enjoyable without your company. Finally, my deepest gratitude goes to my parents, my husband Hongbing Fan, and my daughter Mishu Fan for their endless love, trust, and encouragement throughout my life. Words cannot express my thanks for your tremendous support and encouragement.

TABLE OF CONTENTS

LIST OF TABLES

LIST OF FIGURES

LIST OF ABBREVIATIONS

4-HPA: 4-hydroxyphenylacetic acid

AITC: allyl isothiocyanate

ANOVA: one-way analysis of variance

ARG: antibiotics resistance gene

aTC: anhydrotetracycline

cAAI: core-genome average amino acid identity

CFU: colony forming units

Cm: chloramphenicol

ddPCR: droplet digital polymerase chain reaction

FAM: 6-carboxyfluorescein

gapA: glyceraldehyde-3-phosphate dehydrogenase A

GFP: green fluorescent protein

HEX: 6-carboxy-2,4,4,5,7,7-hexachlorofluorescein

IAA: indole-3-acetic acid

IPTG: isopropyl β-D-1-thiogalactopyranoside

LB: Luria-Bertani

LHR: locus of heat resistance

LSD: least significant difference

MDR: multidrug-resistant

MMC: mitomycin C

NCBI: National Center for Biotechnology Information

PAA: peroxyacetic acid

qPCR: quantitative polymerase chain reaction

RAPD: random amplified polymorphism DNA

RFP: red fluorescent protein

roGFP2: reduction-oxidation-sensitive green fluorescent protein 2

RT-qPCR: reverse transcription-quantitative polymerase chain reaction

sgRNA: single guide RNA

SGSC: Salmonella Genetic Stock Centre

SOB: super optimal broth

Spec: spectinomycin

STEC: Shiga toxin-producing *E. coli*

T2SS: Type II Secretion System

T3SS: Type III Secretion Systems

T6SS: Type VI Secretion Systems

T_A: annealing temperature

tLST: transmissible locus of stress tolerance

T_m: melting temperature

TSA: trypticase soy agar

UPEC: uropathogenic *E. coli*

VRBG: violet red bile glucose

WT: wild type

X-gal: 5-bromo-4-chloro-3-indolyl-β-D-galactopyranoside

CHAPTER 1: General Introduction and Thesis Objectives

1.1. Introduction

Enterobacterales are among most common human pathogens, including pathogenic *Escherichia coli*, *Klebsiella*, and *Salmonella*. Members of this order are also a prominent cause of nosocomial infections with multidrug-resistant (MDR) organisms (Blake et al., 2003). Research on *Enterobacterales* has focused on their role as human, animal, or plant pathogens, or as indicators of fecal contamination. *Enterobacterales* are present on a variety of foods including fruits, vegetables, ready-to-eat meat, poultry, eggs, nuts and dairy products, as well as fish and other seafoods (Baylis et al., 2011). In addition, carbapenem-resistant *Enterobacteriaceae*, the largest family in the *Enterobacterales*, as well as fluoroquinolone-resistant *Salmonella* and *Shigella*, are of major concern (Tacconelli et al., 2018), and a substantial body of research has focused on the understanding of MDR systems, their prevalence, and their transmission. However, the commensal population and strains inhabiting non-human-related niches are understudied. The extra-intestinal lifestyles of both commensal and pathogenic *Enterobacterales* may inform on the evolutionary mechanisms that are related to the emergence of MDR and other resistance phenotypes.

Enterobacterales populate diverse ecological niches including soil, water, nematodes, insects, plants and vertebrates (Scheutz and Strockbine, 2005). Evolution of *Enterobacterales* to adapt to different environments involves acquisition of stress resistance genes through horizontal gene transfer. For example, the transmissible locus of stress tolerance (tLST) is a 15 kb genomic island and is a reliable indicator of heat resistance in *Enterobacterales*, potentially posing a threat to food safety and public health (Mercer et al., 2015). Control measures to mitigate the risk of heat resistant pathogens require information on the reservoir and selective pressure for tLST-positive

Enterobacterales, and the presence of the genomic island in pathogenic *Enterobacterales*. A high frequency of tLST-positive *E. coli* was identified in cheese and wastewater (Marti et al., 2016; Zhi et al., 2016). Strains of tLST-positive *E. coli* were enriched in cheese after thermization and in wastewater after chlorine treatment, showing high resistance to heat (Marti et al., 2016; Zhi et al., 2016) . The knowledge of the human-made and natural reservoirs for tLST and the information on whether the genomic island mediates cross-resistance to heat stress, chlorine stress and other stressors remain unknown.

The tLST can be widely transferred among *Enterobacterales* including one strain of *Salmonella* and some opportunistic human pathogens such as *Cronobacter* and *Klebsiella* (Boll et al., 2017; Mercer et al., 2017b). The frequency of tLST-positive in pathogenic strains is important for understanding its functional overlap with virulence factors. Virulence factors in *Shigella*, Shiga toxin-producing *E. coli* (STEC) and uropathogenic *E. coli* (UPEC) are of particular concern. *Shigella* species, which is one of the leading causes of diarrheal disease among children, possesses a large virulence plasmid that is unique to virulent strains of *Shigella* and enteroinvasive *E. coli* (Pilla et al., 2017). Stx-encoding prophages and the locus of enterocyte effacement of UPEC are important determinants of pathogenicity, causing urinary tract infections and diarrhea in humans (Minardi et al., 2011). Of note, the tLST is rarely identified in *Salmonella* (Mercer et al., 2017b), but it is frequently associated with strains or species in the environment or in association with plants (Botzler, 1987; Dong et al., 2003; Schmid et al., 2009), which implies the tLST may contribute to the adaptation to plant-associated habitats. It remains unclear whether the tLST is associated with lifestyles and virulence factors or not.

The low frequency of the tLST in *Salmonella* and the significant dry resistance of *Salmonella* indicates that *Salmonella* use other genetic determinants for stress resistance.

Desiccation resistance is an essential capability for *Salmonella* to survive or persist in non-host environments during host transition, which contributes to outbreaks of foodborne disease with low a_W foods ($a_W < 0.85$). Mechanisms of desiccation resistance overlap with those of heat resistance, oxidative resistance, starvation resistance and acid resistance; however, mechanisms of heat resistance of desiccated *Salmonella* remain largely unexplored.

Taken together, multiple stresses that *Enterobacterales* face in environment shape their evolution and affect their lifestyles. This thesis generally aimed to improve our understanding of the contribution of genetic determinants including the tLST to stress resistance and host adaptation in *Enterobacterales*, which allow improved control of pathogenic *Enterobacterales*.

1.2. Hypothesis

The extra-intestinal lifestyle of *Enterobacterales* selects for genes of accessory genome that mediate stress resistance and impede control of pathogenic *Enterobacterales* in the food supply and in health care facilities.

1.3. Objectives

1) New perspectives of the evolution and lifestyles of *Enterobacterales* (Chapter 2).

2) Characterization of tLST-positive isolates from Daqu fermentation and wastewater (Chapters 3 and 4).

3) Investigation of the resistance to oxidizing chemicals conferred by the tLST and the relationship between the tLST and virulence factors (Chapter 4).

4) Investigation of the functions of tLST-encoding proteins to heat and chlorine resistance and their ecological roles (Chapter 5).

5) Identification of genetic factors that determine the dry-heat resistance on desiccated *Salmonella* cells (Chapter 6).

CHAPTER 2. Ecology, Diversity and Evolution of *Enterobacterales*

2.1. Introduction

The order *Enterobacterales* populate diverse ecological niches including soil, water, nematodes, insects, plants, and vertebrates (Scheutz and Strockbine, 2005). Members of the *Enterobacterales* substantially contribute to foodborne disease, nosocomial infections, and community-onset infections in humans (Blake et al., 2003; Lasko and Nicolau, 2020). Carbapenem-resistant *Enterobacteriaceae* as well as fluoroquinolone-resistant *Salmonella* and *Shigella* are listed by the WHO as priority pathogens, control of which requires novel antibiotics (Tacconelli et al., 2018; Voor in 't holt et al., 2020).

Owing to the relevance of specific *Enterobacterales* to food production and human health, research on *Enterobacterales* focused on plant pathogens and human pathogens. Most *Enterobacterales* species, however, are harmless to humans and may even promote plant growth. The alternative lifestyles of (opportunistic) pathogens and plant commensal bacteria are obscured by the wealth of literature on the pathogenic lifestyle of related taxa. For example, the terms "*Cronobacter"* and *"*plants" retrieve 135 publications (Aug 4, 2021) on Pubmed but only two of those refer to the plant-associated lifestyle of the genus while the remainder focuses on pathogenicity or occurrence and persistence in food or processing plants. Species inhabiting non-human-related niches are understudied and under-represented in genome sequence databases.

The taxonomic reorganization of the *Enterobacterales* (Adeolu et al., 2016) provides a framework to assess their roles as commensals of insects, plants, nematodes, or as environmental microorganisms. This communication aims to assess whether phylogeny and lifestyles of *Enterobacterales* inform on evolutionary mechanisms that facilitate the emergence of antibiotic resistant pathogens as well as improved tools for their control.

2.2. Taxonomy of *Enterobacterales*

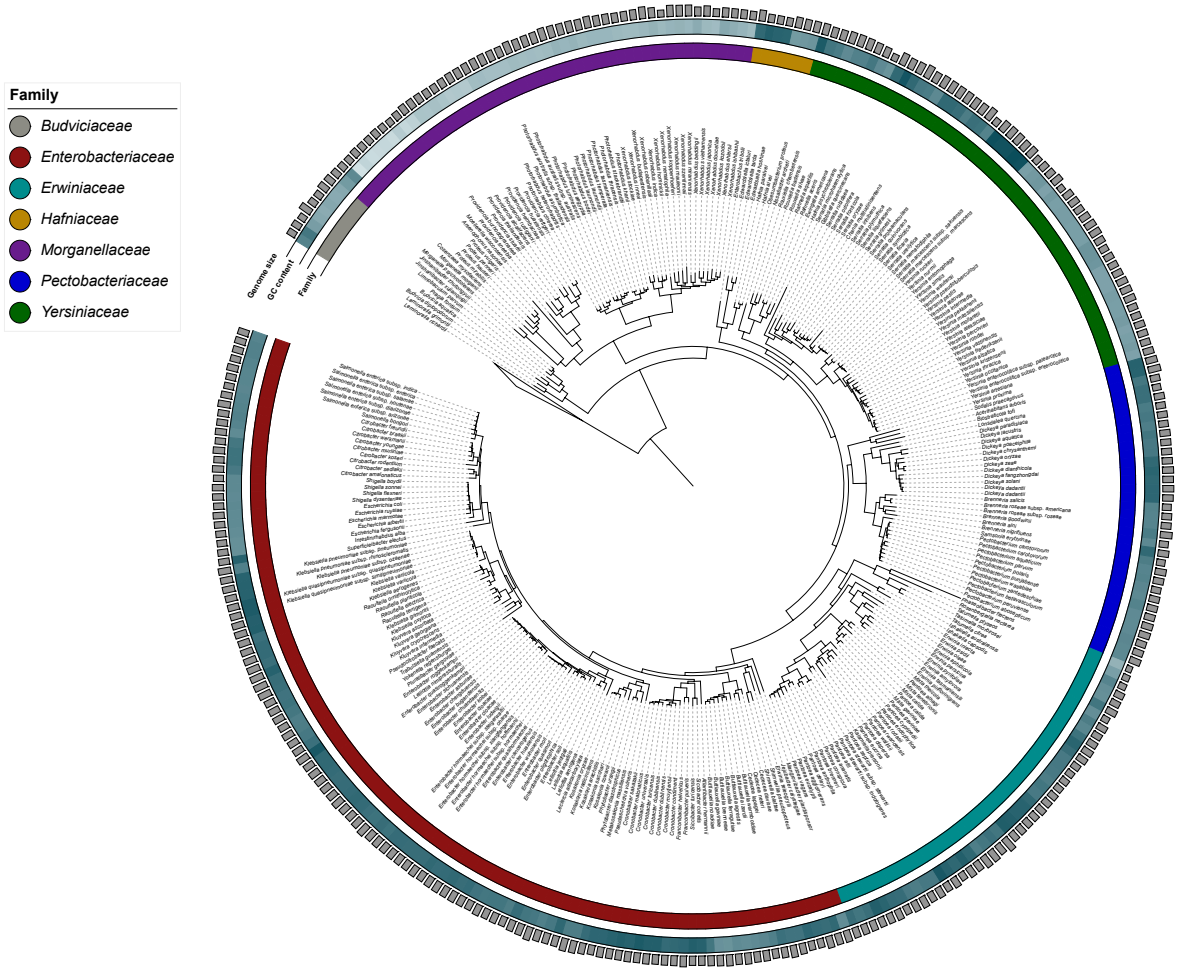

Figure 2.1. Core genome phylogenetic tree of *Enterobacterales*. All the type strains belonging to 310 type species of with genome data available until June 10th, 2021 were used for analysis (Table S2.1.), with 28 genomes from the family *Pasteurellales* as outgroup. Each genome sequence was annotated by Prokka. The pan and core protein clusters of all these genomes were constructed using FastOrtho. Each of the 1306 core genes shared by at least 90% of the 338 genomes was aligned by Muscle and cleaned by TrimAl. The phylogenomic analysis is based on the concatenated alignment of these alignments. The maximum likelihood tree was inferred by RAxML-NG with the best model (LG+I+G) estimated by ModelFinder. The inner ring indicates the family that the species belongs to. The Middle ring color gradient indicates the GC content of the used genomes, with the lighter for lower and darker for Higher. The out bar chart showed the genome size for each strain.

All *Enterobacterales* belonged to the family *Enterobacteriaceae* (Adeolu et al., 2016) until genome-scale taxonomy established the order *Enterobacterales* containing 7 families (Adeolu et

al., 2016) (Figure 2.1.). Core genome phylogeny corrected the taxonomic position of several genera (Alnajar and Gupta, 2017; Soutar and Stavrinides, 2020) and added 8 new genera (Baek et al., 2019; Ge et al., 2021; Jiang et al., 2020; Soutar and Stavrinides, 2020; Xu et al., 2020). Currently, the order includes 364 species or subspecies within 69 genera and 7 families (Table S2.1.).

To validate if phylogenetic groups in the *Enterobacterales* encompass phylogenetic diversity that corresponds to bacterial orders, pairwise core-genome average amino acid identity (cAAI) values were calculated (Figure 2.2.; Table S2.2.). cAAI values (Figure 2.2.) support conclusions from the phylogenetic tree (Figure 2.1.) as intra-family cAAI values are generally higher than inter-family cAAI values. The *Morganellaceae* comprise two clades, one containing the genera *Photorhabdus* and *Xenorhabdus*, the other all other genera. cAAI values inform that these clades are as distantly related to each other as to other *Enterobacterales*. The lowest pairwise cAAI value within the *Enterobacterales* is 66%, indicating they are more closely related than other bacterial orders. For example, the lowest intra-family cAAI value among *Lactobacillaceae* is 51% with several intra-genus cAAI values lower than 66% (Zheng et al., 2020). The relatively high cAAI values within the *Enterobacterales* imply that diversification of species in *Enterobacterales* is mediated by horizontal gene transfer rather than mutations in the core genome.

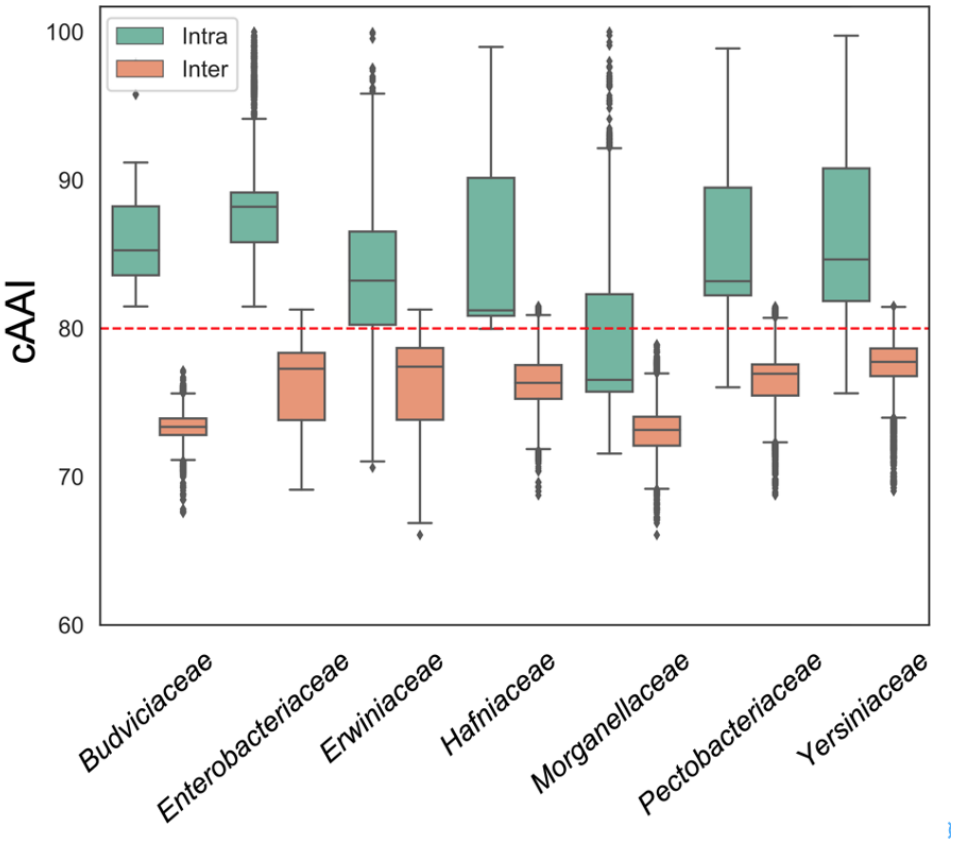

Figure 2.2. Boxplot of cAAI. Pairwise cAAI values were computed by CompareM based on the 1306 core protein sequences of each genome (Table S2.2.).

2.3. Lifestyles of *Enterobacterales*

To elucidate the order's evolution, we assigned lifestyles related to insect-, nematode- or vertebrate-associated, environmental, and plant associated habitats to each species (Figure 2.3.).

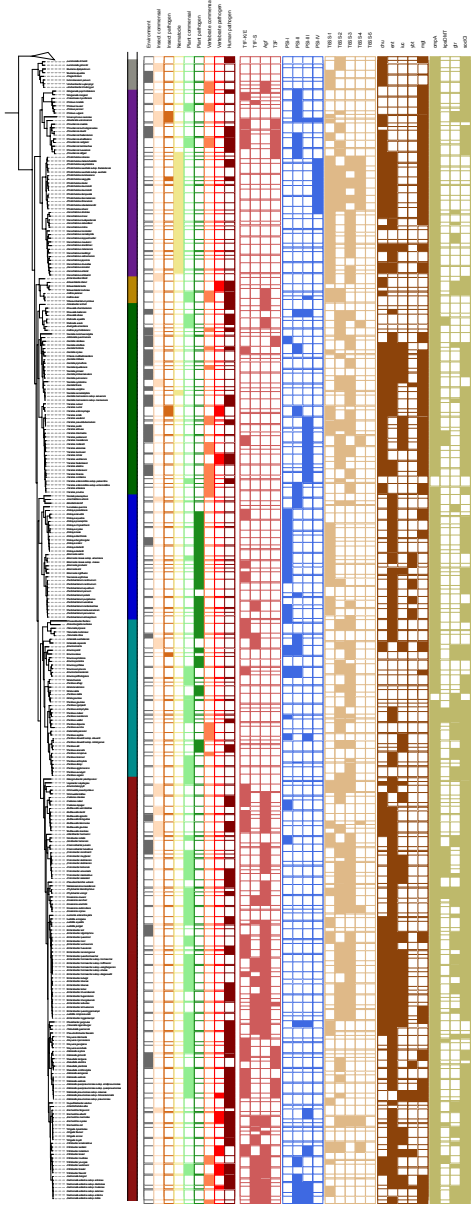

Figure 2.3. Connections among niches of the type strains, secretion systems and virulence factors. The assignment of species to lifestyle was based on different references (Table S2.3.), which included natural habitats of the species as environmental, insect commensal, insect insect pathogen, nematode, plant commensal, plant pathogen, vertebrate commensal, vertebrate pathogen, or human pathogen. PSI-I to PSI-II and T6SS-1 to T6SS-5 respectively represent the 4 and 5 subtypes of type III and type VI secretion system. The virulence factors included those involved in adherence, such as T1F-K/E (Type 1 fimbriae of both *K. pneumoniae* and *E. coli*), T1F-S (Type 1 fimbriae of *Salmonella*), Agf (Thin aggregative fimbriae of *Salmonella*) and T3F (Type 3 fimbriae); iron uptake, such as *chu* (Hemin uptake), *ent* (Enterobactin, Siderophore), *iuc* (Aerobactin, Siderophore), *ybt* (Yersiniabactin, Siderophore), *mgt* (Magnesium uptake), and invasion, such as *ompA* (Outer membrane protein A), *kbsDMT* (K1 capsule), *grt* (Endotoxin), *sodCI* (Stress protein).

Environment and plants. *Enterobacterales* occur in low-temperature marine and aquatic environments, soils, rhizosphere, and plants. Environmental genera including *Pectobacteriaceae* and many *Erwiniaceae* occur in soil (Figures 2.3. and 2.4.). *Enterobacterales*, particularly *Erwiniaceae* and *Enterobacteriaceae*, occur as growth-promoting commensal members of plant microbiota (Figures 2.3. and 2.4.). Plant-associated species occupy the rhizosphere, phyllosphere or as endophytes (Figure 2.4.). **Nematodes.** The genera *Xenorhabdus* and *Photorhabdus* are symbionts of nematodes (Forst et al., 1997). Symbionts of insect-pathogenic nematodes colonize the gut of juvenile nematodes, are transferred into the insect hemolymph upon infection and kill the larvae, providing nutrients for the nematode (Goodrich-Blair et al., 2007). **Insect hosts.** Many insects harbor commensal *Enterobacterales* (Figure 2.3.). Almost all aphids contain a symbiont of the genus *Buchnera* (Munson et al., 1991). Insect-associated species are distributed across all 7 families of the *Enterobacterales* but *Enterobacteriaceae* do not include insect pathogens (Figure 2.3.). **Vertebrate hosts.** *Enterobacterales* include vertebrate commensals and pathogens (Figure 2.3.). *Shigella* became restricted to humans as hosts through acquired virulence plasmids and genome decay (Berg et al., 2005). Some of the 2500 *Salmonella enterica* serovars cause infections only in specific host species, e.g. human-specific typhoidal serovars Typhi, Paratyphi A, and Paratyphi C, whereas non-typhoidal serovars cause gastroenteritis of varying severity in diverse hosts (Achtman et al., 2012). Many genera have only been reported as clinical isolates or pathogens but the limited literature available on these genera implies that their habitat is not primarily related to humans (Blekher et al., 2000; Kämpfer et al., 2014; Mlaga et al., 2017; Potter et al., 2018; Rekha et al., 2020; Teng et al., 2020).

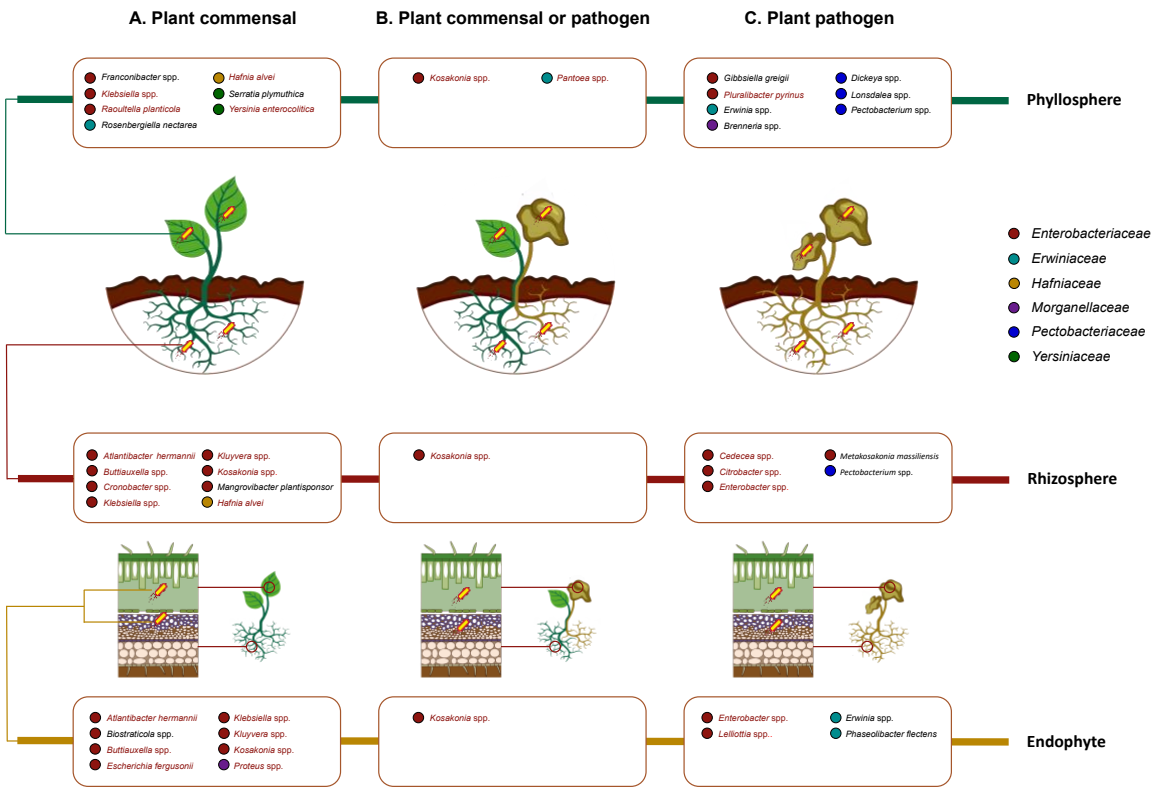

Figure 2.4. Plant-associated *Enterobacterales* in phyllosphere, rhizosphere and endophytes of plants. Human pathogens are highlighted in red. The assignment of genera/species to phyllosphere, rhizosphere and endophytes was based on different references (Table S2.4.).

2.4. Blended lifestyles and dispersal.

Blended lifestyles that include (temporary) persistence in multiple habitats are common for many *Enterobacterales*. Vertebrate animals, insects, and nematodes mediate the dispersal of *Enterbacterales* (Figure 2.5.). **Nematodes and insects.** *Photorhabdus luminescens* and *Xenorhabdus bovienii* utilize nematodes as vectors for transportation to insects, only killing when directly injected into the hemolymph (Rahoo et al., 2011). **Plants and insects.** Several phytopathogens use insects as vectors for transmission (Rossmann et al., 2018). The phytopathogen *Erwinia tracheiphila* persistently colonizes beetle vectors to overcome dispersal

limitations (Shapiro et al., 2014). **Plants and vertebrates.** Intestinal *Enterobacterales* including *Citrobacter* and *Escherichia* are commonly present in water, soil, and on plants (Figure 2.3.), which suggests an environmental or plant-associated lifestyle of these species. *Escherichia fergusonii* is a seed endophyte in coffee (Silva et al., 2012) and many strains of *Escherichia coli* can adhere to both roots and leaves using a plasmid-borne Type II Secretion System (T2SS) (Holmes et al., 2020). The mucosal pathogen of mice, *Citrobacter rodentium,* shares virulence factors with pathogenic *E. coli*. *Citrobacter* species were recovered from vegetables and fruits samples (Adegun et al., 2019). *Citrobacter freundii* causes canker in white mulberry (Allahverdi et al., 2016) but it is also a universal fish pathogen causing injury and high mortality (Jeremić et al., 2003). **Environment and vertebrates.** *Serratia* and *Yersinia* thrive in a diverse number of environments including water, soil, and parasitic to symbiotic colonization of the digestive tracts of various animals (NAGANO et al., 1997; Petersen and Tisa, 2013). *Yersinia pestis* acquired a single operon that enables persistence and biofilm-formation in flea guts. Persistence in fleas enabled a new dispersal vehicle and flea bites provided a new point of entry into susceptible hosts, including rodents and humans (Hinnebusch and Erickson, 2008). *Y. pestis* evolved from the free-living *Yersinia pseudotuberculosis* which also causes infectious disease in humans (Gu et al., 2007). Interrogating 14082 metagenome datasets with *Yersinia* species revealed that 42.4% and 32.9% of *Yersinia* species were present in environmental and vertebrate-associated sources respectively (Figure S2.1.), indicating a blended lifestyle of the majority of the genus. **Wide dispersal.** Plant-pathogenic *Pectobacterium* overcome dispersal limitation using nematodes, insects, or birds (Nykyri et al., 2014). For example, *Pectobacterium stewartii* gain entry into plants via the wounds created by the feeding flea beetles (Walterson and Stavrinides, 2015). *E. fergusonii* and *Klebsiella oxytoca* were isolated from wild birds in different regions, suggesting that birds are

vectors for their transmission (Yahia et al., 2020). *Enterobacter*, *Cronobacter, Kosakonia*, and *Klebsiella* widely occur on plants (Figure 2.4.), including those consumed by humans. The consumption of these plants facilitates the transfer of bacteria from plants to humans. In agricultural production, feces of wild animals, the application of animal manure, or the use of contaminated irrigation water on crops contaminate plants (Alegbeleye et al., 2018), resulting in human colonization or infection (Ercumen et al., 2017; Fink-Gremmels and van der Merwe, 2019; Solomon et al., 2002).

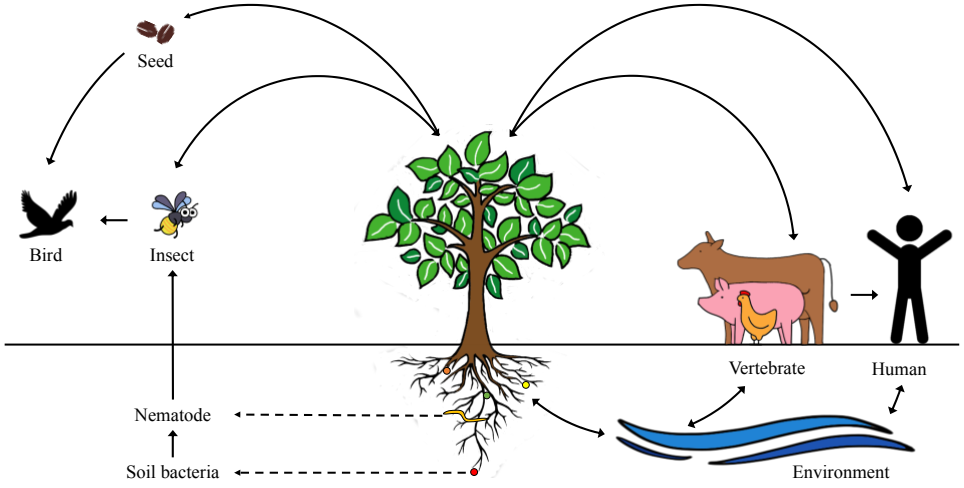

Figure 2.5. Lifestyle and transmission paths of *Enterobacterales*. *Enterobacterales* can be dispersed via vertebrates, insects, nematodes, water and plants.

2.5. Relationship of lifestyles and phylogeny

Where sufficient information is available, lifestyle assignments associate with phylogenetic grouping. *Enterobacteriaceae*, comprise species adapted to vertebrate hosts, plants or the environment. *Yersiniaceae* include predominantly species with environmental lifestyles but also occur invertebrates. The *Erwiniaceae* include mostly plant-associated bacteria including plant

pathogens, and virtually all *Pectobacteriaceae* are plant pathogens. *Xenorhabdus* and *Photorhabdus* form a nematode associated clade within the *Morganellaceae,* demonstrating the two phylogenetic clades also match the lifestyles. These phylogeny-lifestyle associations allow for the identification of lifestyle transitions and adaptations. A gradual transition of lifestyles can be observed in the family *Enterobacteriaceae* (Figure 2.3.). The environmental/plant-associated *Shimwellia* and *Mangrovibacter* are most closely related to the ancestral *Jejubacter* (Figures 2.1. and 2.2.), while *Cronobacter*, *Kosakonia*, *Enterobacter*, and *Klebsiella*, which are more distant to the ancestral node, represent a blended lifestyle that includes plant-associated niches, and vertebrate intestines; these organisms are also relevant as opportunistic human pathogen. Vertebrate adapted species including *Shigella* and *Salmonella* Typhi are the most distant group to *Buttiauxella* (Figures 2.1. and 2.2.). This observation implies that the last common ancestor of *Enterobacteriaceae* was originally plant adapted. A possible scenario for evolution and lifestyle switches relates to the use of animals as a tool to overcome dispersal association, eventually adapting to persistence in the intestine of animals.

Adaptation to narrow ecological niches reduces bacterial genome size and G+C content, particularly in vertically transmitted symbionts (Fisher et al., 2017; Moran et al., 2008). For example, the G+C content of the obligate symbionts *Buchnera aphidicola* (aphids) and *Wigglesworthia glossinidia* (tsetse fly) is 26.3% and 23.7%. Their genome sizes are 616 to 792 kb, which is just above the threshold of minimal size (580 kb) for bacterial genomes (McCutcheon, 2010; Shigenobu et al., 2000). Related free-living *Enterobacterales* have larger genomes (2–8 Mb) (Figure 2.1.). Human-restricted human pathogens including *Shigella, Y. pestis*, and *S.* Typhi have more recently diverged from their environmental ancestors but also experienced substantial gene loss and a slightly reduced G+C content (Holt et al., 2008; Parkhill et al., 2001). Many of the

monophyletic serotypes of *Salmonella* evolved as pathogens to specific hosts (McQuiston et al., 2008; Zou et al., 2016), driven by horizontal gene transfer (Brown et al., 2003). For example, distinct lineages of *S.* Typhimurium correlated well with the CRISPR sequences and prophage profiles (Fu et al., 2017), indicating that different lineages are no longer infected by the same phages, which reduces horizontal gene transfer (Fu et al., 2017).

Co-evolution of hosts and their symbionts results in co-speciation, shown by "co-phylogenetic" patterns (Fisher et al., 2017). Symbionts adapted to promote host-level fitness and vice-versa (Groussin et al., 2020). The symbiotic association between the obligate symbiont *B. aphidicola* and its aphid hosts (Douglas, 1998) was dated back to about 250 million years (Hoy, 2019). The strict vertical transmission of only a few symbiont bacterial cells from one host generation to the next results in low symbiont recombination rates, leading to gene loss and genome reduction (Campbell et al., 2015; Moran and Mira, 2001). In contrast, facultative symbionts are not required for host reproduction but increase their proportion of hosts by conferring fitness benefits (Moran et al., 2005). Facultative symbionts undergo horizontal transfer within and between species and are often shared between divergent host groups (Sandström et al., 2001). *Sodalis glossinidius* is a facultative symbiont of tsetse flies (Nováková and Hypša, 2007), but also an obligate symbiont of weevils and chewing lice (Fukatsu et al., 2007), indicating that a facultative symbiont lost the ability of horizontal transmission and is evolving into an obligate symbiont (Moran et al., 2008).

2.6. Genetic adaptation

The core genome carries essential genes and does not reflect evolution by horizontal gene transfer to occupy novel niches. Therefore, differentially distributed genes in accessory genomes are shown in Figure 2.6. Each family is characterized by a unique set of accessory genes (Figure

2.6.). When bacteria switch to a new lifestyle, flagellar motility and attachment are considered prerequisites for successful colonization (Harshey, 2003). *Enterobacterales* possess five distinct flagellar systems (flag-1 to flag-5). Flag-4 is predominant for insect endosymbionts including *Sodalis* and *W. glossinidia* (De Maayer et al., 2020). The adhesion fimbriae of human pathogenic *Klebsiella* and *Salmonella* are also present in other *Enterobacterales* including human pathogens (Figure 2.3.). This suggests that flagella systems and fimbriae are acquired with lifestyle changes.

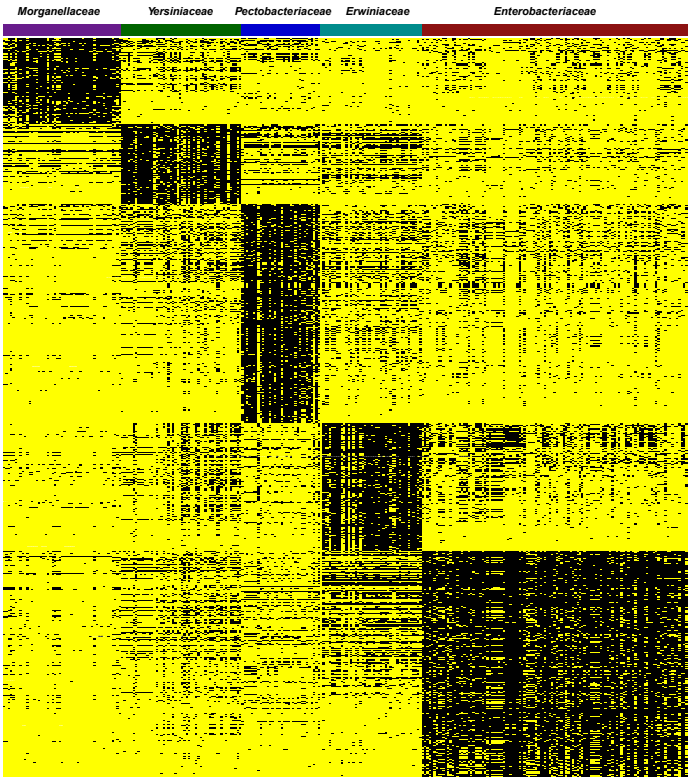

Figure 2.6. Heatmap of family specific gene clusters. The family enriched gene families were estimated by Scoary on the gene cluster table obtained from FastOrtho. Only both sensitivity and specificity above 70% were used for display, with black for presence and yellow for absence.

Type III Secretion Systems (T3SS) evolved from flagella (Diepold and Armitage, 2015) and are often laterally transferred, resulting in a lifestyle change. Currently, seven families of T3SS are described, four target animals and three target plants (Büttner, 2012; Troisfontaines and

Cornelis, 2005). The Hrp1 family, the only plant-specific T3SS found in *Enterobacterales,* is primarily found in *Erwiniaceae* and *Pectobacteriaceae* but also some members of *Yersiniaceae* and *Enterobacteriaceae* (Figure 2.3.). Only the family *Erwiniaceae* and the genus *Cedecea* include members with both plant and animal specific T3SSs (Figure 2.3.). Interestingly, after the split from *Erwiniaceae, Cedecea* is among the ancestral genera of *Enterobacteriaceae*, suggesting the progenitor of *Enterobacteriaceae* had both plant- and animal-focused lifestyles and that the loss of the plant T3SS played a role in lifestyle adaptation. In our analysis, *Budviciaceae*, *Morganellaceae*, and *Hafniaceae* lack the plant specific Hrp1 T3SS while it is identified in *Yersiniaceae*, *Erwiniaceae*, *Pectobacteriaceae* and *Enterobacteriaceae* (Figure 2.3.). This suggests that *Enterobacterales* emerged initially as an (invertebrate) animal adapted group before *Pectobacteriaceae* and *Erwiniaceae* split off and became plant adapted with *Enterobacteriaceae* further evolving into vertebrate-adapted organisms.

The Type VI Secretion Systems (T6SS) also injects proteins into neighboring cells (Filloux, 2009)., The T6SS, initially associated with bacterial virulence, was recently hypothesized to primarily prepare the ground for virulence by clearing the niche of bacterial competitors (Navarro-Garcia et al., 2019). T6SS gene clusters categorize into five groups based on gene organizations and homologies: T6SS-1-5, which are involved in different pathogenic pathways (Barret et al., 2011; Boyer et al., 2009). The distribution of T6SS groups appears correlated with ecological niches (Figure 2.3.). Nematode-associated *Enterobacterales* often possess a combination of T6SS-1 and T6SS-3. Interestingly, *Photorhabdus* requires multiple loci of T6SS (from 3 to 4). T6SS-4 is associated with plant habitats or vertebrate intestines (Boyer et al., 2009). T6SS-1 is absent in *Erwiniaceae* which contains numerous plant pathogens/commensal. The T6SS-2 is distributed among obligate/opportunistic human pathogens, indicating its impact on systemic infection in

humans. The function of T6SS-5 remains unknown and it is only present in *Morganella psychrotolerans* and *Moellerella wisconsensis* (Figure 2.3.).

Enterobacterales produce enterobactin, aerobactin, and yersiniabactin (Lawlor et al., 1987; Raymond et al., 2003), which are siderophores critical for host-pathogen interactions (Schaible and Kaufmann, 2004). Enterobactin binds iron (Fe^{3+}) with higher affinity than yersiniabactin, followed by aerobactin (Brock et al., 1991; Perry et al., 1999; Raymond et al., 2003). Enterobactin plays a more important role at low iron concentration, while the inverse is true of yersiniabactin (Lawlor et al., 2007). *Enterobacterales* frequently harbor multiple systems in one genome (Figure 2.3.). The adaption of *Enterobacterales* to different lifestyles also depends on the methods available for acquiring iron in a given environment (Lau et al., 2016). *Enterobacterales* that use the low-affinity aerobactin often also use one or more of the high-affinity systems (Figure 2.3.), possibly to save energy by first using low-affinity siderophores unless a higher affinity siderophore is needed. The presence of multiple iron transport systems reflects the importance of iron and the optimization of its acquisition in the lifestyles. Bacterial siderophores acquire the soluble iron (Fe^{2+}) from the soil, promoting the growth and yield of plants, but also contribute greatly to the pathogenicity of plant pathogens including *Erwiana amylovora*. They may also aid in survival in the gut and allow competition with siderophore-producing intestinal bacteria (Valdebenito et al., 2006). For example, *Shigella flexneri* grows in different environments using its two ferrous and six ferric iron transport systems (Wyckoff et al., 2009). Taken together, the type of siderophores that are utilized by bacteria are co-opted by plant/animal hosts.

Other genes and operons inform on *Enterobacterales* lifestyles (Figures 2.3. and 2.7.). The *gtr* operons are dominant in *Enterobacteriaceae* and occasionally present in *Erwiniaceae* (Figure 2.3.), indicating these operons correspond with plant- and vertebrate-associated lifestyles. The L-

fucose utilizing *fuc* operon is related to vertebrate-associated lifestyle, while the aguAB and *pqq* operons, promoting plant growth, are associated with plant-adapted lifestyle (Figure 2.7.).

2.7. Role of antibiotic resistance

The spread of antibiotic resistance has been attributed to the use of antibiotics in the prevention or treatment of disease in humans and farm animals, posing a substantial threat to both (Koutsoumanis et al., 2021; WHO, 2015). Therapeutic antibiotic use started more than 80 years ago (D'Costa et al., 2011) and antibiotic growth promoters have been used in agricultural animal production about 50 years ago (Dibner and Richards, 2005). However, bacterial antibiotic resistance predates humanity (D'Costa et al., 2011) and is found in ecosystems unassociated with human activity (Clemente et al., 2015). Antibiotics are involved in microbial warfare (Cornforth and Foster, 2015), in cell-to-cell signaling networks, enriching bacterial lineages and clones, and contributing to local colonization processes (Baquero et al., 2013). The dataset of type strain genomes allowed testing of the hypothesis whether the evolution of antibiotic resistance in the *Enterobacterales* predates the human use of antibiotics. Firstly, the dataset was rarefied to include only type strains and thus avoided the sampling bias; secondly, many type strains were isolated before antibiotics were used in human or veterinary medicine. Only few nematode-associated *Morganellaceae* are chloramphenicol resistant and some of *Yersiniaceae* are mainly beta-lactam- and quinolone-resistant (Figure 2.8.). *Pectobacterium zantedeschiae* is the only type strain that carries antibiotic resistance genes in *Pectobacteriaceae* (Figure 2.8.). Few *Erwiniaceae* members are resistant to quinolones (Figure 2.8.). Surprisingly, *Enterobacteriaceae* but only few pathogens in the family harbored numerous antibiotic resistance genes (Figure 2.8.), which may reflect that

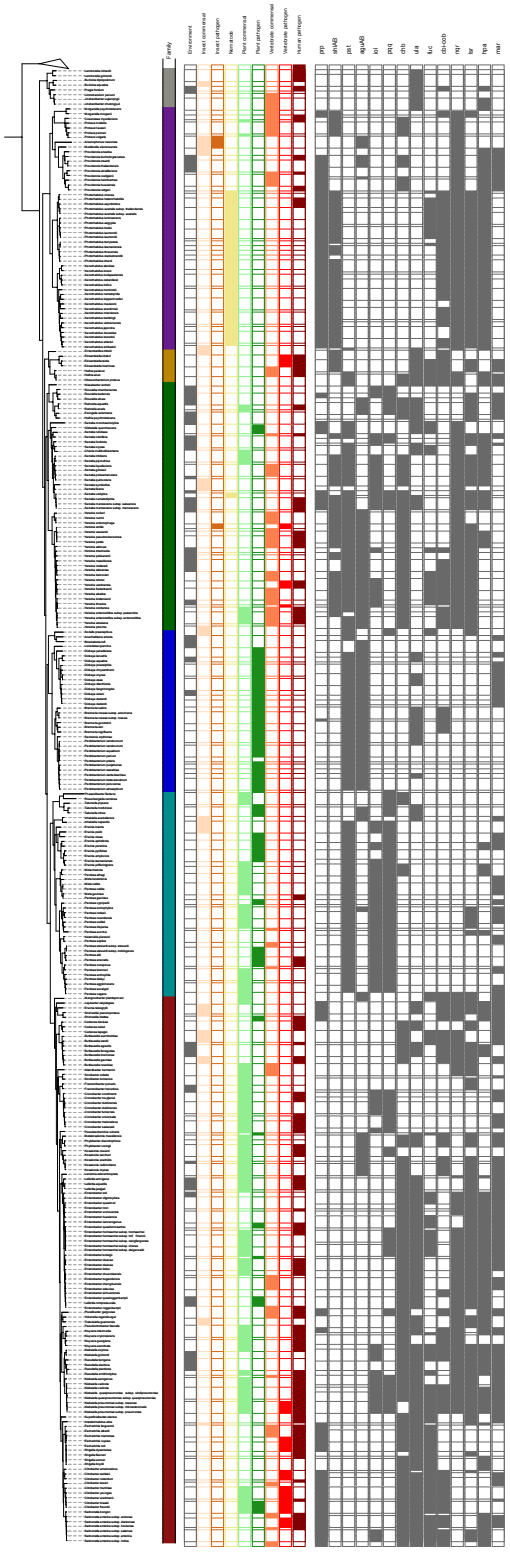

Figure 2.7. The presence and absence of some family or niches specific genes involved in different metabolic pathways. Genes are abbreviated as follows: prp, prpBCDE, propionate catabolism; shlAB, hemolysin; pst, pstSACB, phosphate import; aguAB, agmatine utilization; pqq, pqqBCDEF,

Figure 2.7. legend (con't):
(con;pyrroloquinoline quinone biogenesis; chb, chitobiose operon, utilization of the beta-glucosides chitobiose and cellobiose; ula, ulaABCDEFG, L-ascorbate utilization; fuc, L-fucose operon, L-fucose fermentation; cbi-cob, cbi operon and cob operon, cobalamin (vitamin B12) biosynthesis; nqr, nqr operon, Na+-translocating NADH-quinone reductase; lsr, lsr operon, transport and processing of Autoinducer 2; hpa, 4-hydroxyphenylacetic acid (4-HPA) degradation; mar, marAB, multiple antibiotic resistance.

type strains of pathogens were mostly isolated prior to 1943 (Supplementary Table S2.5.). Overall, antibiotic resistance genes appear to be present irrespective of antibiotic use and is apparently selected for by blended lifestyles which includes many of the *Enterobacteriaceae*.

2.8. Conclusions

The ESKAPE pathogens *Enterococcus faecium*, *Staphylococcus aureus*, *Klebsiella pneumoniae*, *Acinetobacter baumannii*, *Pseudomonas aeruginosa*, and *Enterobacter* spp. are currently the greatest challenge in preventing nosocomial infections as many are multi-drug resistant (Pendleton et al., 2013). *Enterococcus faecium* (Gouliouris et al., 2019; Jha et al., 2005), *Klebsiella* and *Enterobacter* in *Enterobacteriaceae* are associated with both plants and vertebrates. *Pseudomonas aeruginosa* is an environmental species that is ubiquitous in soil and water ecosystems (Streeter and Katouli, 2016). Antibiotic resistance in these ESKAPE pathogens thus relates to blended lifestyles. Blended lifestyles necessitate large genomes, supporting persistence in multiple ecosystems, and horizontal gene transfer, providing the opportunity for nosocomial infections. Genes supporting hospital persistence or human infections are often acquired and maintained in response to selective pressure in aquatic or plant-associated habitats, e.g. siderophores, biofilm formation in *Pseudomonas* (Ueda and Saneoka, 2015), and tLST-encoded chlorine and heat resistance in *Cronobacter*, *E. coli*, and *Klebsiella* (Wang et al., 2020). They also support human to human transmission of pathogens such as *Salmonella* through survival in plants (Fatica and Schneider, 2011). Blended lifestyles of *Enterobacterales,* including

Enterobacteriaceae, also question the usefulness of coliforms or even fecal coliforms as reliable indicators of fecal contamination in food and water analysis.

The discovery of antibiotics to control pathogenic *Enterobacterales* in human and animal health and agriculture initiated 70 years ago, and the wide use of antibiotics facilitates the emergency of resistant bacteria (D'Costa et al., 2011). Research that only focuses on human pathogens is not enough to know the real life of pathogenic *Enterobacterales*. An evolutionary overview of this order is needed. The large-scale comparative genomic analysis allows the elucidation of *Enterobacterales'* adaptation to diverse habitats and lifestyles. Available genomic information and blended lifestyles suggest that foodborne and nosocomial pathogens in the *Enterobacterales* have an evolutionary origin with nematodes and plants and that control depends on understanding alternative lifestyles and extraintestinal evolutionary origin. Blended lifestyles facilitate gene acquisition, large genomes, and provides a selective pressure for antibiotic resistance independent of human activity. Understanding the origin of pathogenic bacteria and their role in nature will provide insight into the control of pathogenic *Enterobacterales*.

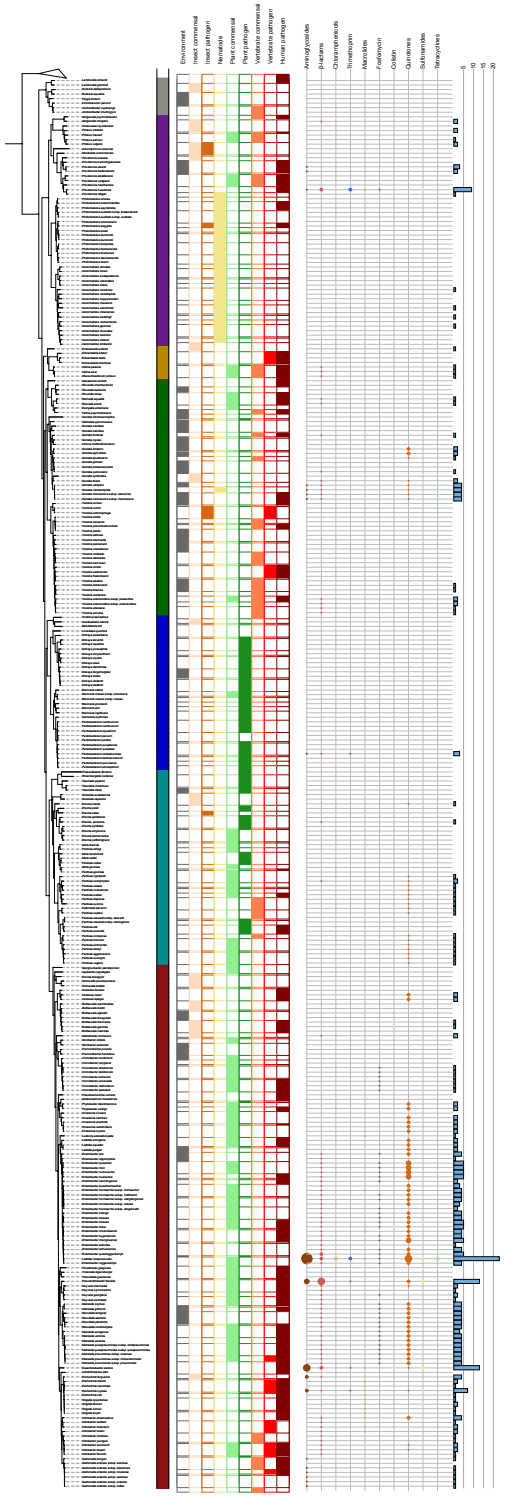

Figure 2.8. Antibiotics resistance genes (ARGs) distributions. All the ARGs were predicted from the annotated proteins of each genome by ABRicate based on the Resfinder database. The circle size on the middle lines represents the number of ARGs identified from each genome conferring to the same class of drugs. The height of the bar chart on the right refer to the total ARG number of predicted from each genome.

CHAPTER 3. Daqu Fermentation Selects for Heat Resistant *Enterobacteriaceae* and Bacilli

3.1 Introduction

Thermal processing is widely used to kill unwanted vegetative cells and endospores in foods (Doyle, 2012). The heat resistance of vegetative cells or endospores of the same species varies substantially (Esty and Meyer, 1922; Liu et al., 2015). Due to the difference of heat resistance in target organisms, heat-resistant strains may tolerate thermal food preservation processes that are lethal to a majority of strains of the same species (Dlusskaya et al., 2011; Margosch et al., 2006). Comparative genomic analyses have identified transferrable genomic islands that confer heat resistance to bacterial endospores (Berendsen et al., 2016a) and *Enterobacteriaceae* (Mercer et al., 2015). Knowledge regarding the genetic determinants of bacterial heat resistance not only allows for the rapid identification of heat-resistant strains but also facilitates the identification of environmental conditions that select for heat resistance.

Heat resistance of endospores is enhanced by the *spoVA*^{2mob} operon (Berendsen et al., 2016a). The *spoVA*^{2mob} operon has previously been identified in *Bacillus subtilis*, *Bacillus licheniformis*, *Bacillus amyloliquefacien*s, *Bacillus cereus* and *Bacillus thermoamylovorans*; cloning of the *spoVA*^{2mob} operon increased spore heat resistance, with the effect increasing with the copy number of the operon (Berendsen et al., 2016b; Krawczyk et al., 2016). *spoVA*^{2mob}-mediated heat resistance of bacterial endospores relates to the uptake of dipicolinic acid during sporulation (Kort et al., 2005; Tovar-Rojo et al., 2002). Heat resistance of *Enterobacteriaceae* including *Escherichia coli*, *Salmonella, Cronobacter* and *Enterobacter cloacae*, is mediated by a genomic island termed the transmissible locus of stress tolerance (tLST) (Kamal et al., 2021; Mercer et al., 2017b, 2015). The tLST increases the D_{60} value (decimal reduction time [i.e., the time required to kill 90% of the microorganisms] at 60 °C) relative to that of tLST-negative strains

of the same species 10- to 100-fold (Li and Gänzle, 2016). The tLST-encoded proteins include heat shock proteins that prevent or repair protein misfolding and aggregation (Lee et al., 2018; Mercer et al., 2017a). Both the tLST and the *spoVA*^{2mob} operon are mobile genetic elements and may transfer to pathogenic bacteria or spoilage organisms; therefore, heat resistance provided by the tLST and the *spoVA*^{2mob} operon challenges the control of pathogens in food system by thermal processing (Li and Gänzle, 2016; Sadiq et al., 2016).

The reservoir and selective pressure for tLST-positive or *spoVA*^{2mob}-positive microorganisms remain unknown; to date, conclusions on environmental conditions selecting for tLST-positive *E. coli* were based solely on the frequency of tLST-positive isolates in specific ecosystems (Ma and Chui, 2017; Mercer et al., 2017b; Zhi et al., 2016). Ecosystems that maintain a temperature of 60 °C for an extended period may select for heat-resistant bacteria. One example is Daqu, a traditional starter culture used for production of spirits and vinegar from cereals. Daqu is produced from cereals by a spontaneous solid-state fermentation which includes three phases: shaping (fermentation stage), ripening (maturation stage) and drying (Xiu et al., 2012). Daqu fermentation supports growth of amylolytic fungi and bacilli; amylolytic enzymes produced in Daqu support starch saccharification and ethanol production in subsequent fermentation stages (Li et al., 2016). The temperature is a key process parameter to control the evolution of microbiota (Xiao et al., 2017). Depending on the type of fermentation, the temperature increases during the fermentation stages to reach a maximum ranging from 45 to 65 °C and declines to ambient temperature during maturation and drying stages (Wang et al., 2011). In traditional Daqu fermentations, temperature control is achieved by forced ventilation and by manually turning over the Daqu blocks (Xiu et al., 2012). Mesophilic organisms including fungi, bacilli, *Enterobacteriaceae*, *E. cloacae*, and lactic acid bacteria are dominant representatives of the Daqu

fermentation microbiota (Wang et al., 2011; Xiao et al., 2017). Daqu comprising *Enterobacteriaceae* and bacilli provides a good model for studying the effect of temperature on the selection for heat resistant strains containing the tLST or the *spoVA*^{2mob} operon.

Previous studies mainly demonstrated the mechanisms of functional genes mediating heat resistance (Berendsen et al., 2016a; Krawczyk et al., 2017; Mercer et al., 2017a, 2015), but the environmental selective pressure for heat resistance genes in natural and human-made ecosystems remains unclear. Therefore, this study aimed to investigate the environmental selective pressure for heat-resistant organisms in food fermentation. The tLST-positive and *spoVA*^{2mob}-positive bacteria were screened in the Daqu matrix, followed by verification of the heat resistance of each isolate. The cell counts of *Enterobacteriaceae* and sporeformers were also assessed during Daqu production, as well as the copy numbers of the tLST and the *spoVA*^{2mob} operon. Moreover, the influence of temperature on the selection for heat-resistant bacteria was determined by evaluating the copy numbers of the tLST and the *spoVA*^{2mob} operon during Daqu processing.

3.2. Materials and methods

3.2.1. Sample collection

Daqu samples were obtained by Li *et al.* (Li et al., 2016, 2015b) from two independent industry-scale fermentations. The stacked layers of Daqu blocks were manually turned every 2 days during the fermentation stage to allow adequate aeration and to control the pile temperature. During the 17-day fermentation, the temperatures of the blocks was strictly controlled (Li et al., 2016) according to traditional solid-state fermentation techniques such as stacking and opening windows and doors, with a small variation in the Daqu core temperature (pile temperature) between the four fermentation rooms; afterwards, for the 13-day maturation, samples were dried and cooled to room temperature. The core temperatures of Daqu blocks were recorded every day.

In enumeration and isolation, samples were collected on day 17 (the end of fermentation stage) and day 30 (the end of maturation stage) and were analyzed. For quantitative PCR (qPCR) analysis, samples were collected separately at day 0 (40 °C~45 °C) and days 4 (42 °C~47 °C), 6 (46 °C~51 °C), 11 (53 °C~58 °C), 15 (45 °C~50 °C) and 30 (<25 °C) based on the temperature control during the fermentation process (Figure 3.1.). Samples were collected from two replicate fermentation rooms at each time point, and two samples per fermentation room were obtained. Two technical replicates were analyzed by qPCR. Daqu samples were ground to powder in a sterile grinder and then transferred into a sterile stomacher bag (Stomacher Lab System, London, UK) to obtain about 500 g of sample. All samples were dried and frozen at -20 °C immediately for further analysis.

3.2.2. Enumeration and isolation

Dry samples (10 g) were mixed with 90 ml of buffered peptone water (Oxiod), soaked at 4 °C for 30 min, and homogenized (Stomacher Lab Blender 400; Seward Medical, London, UK) for 2 min. Duplicate counting plates were prepared using appropriate dilutions. For plating, 50 μL of the dilution was spread on the surface of a dried plate with a spiral plater (Don Whitley Scientific, Shipley, UK). The total bacteria count was determined on Luria-Bertani (LB) (Difco) plates after incubation at 37 °C for 24 h. For the estimation of bacterial spores, a 10% (wt/vol) sample suspension was heated at 80 °C for 30 min and enumerated as described above. Serial dilutions of homogenate were surface plated on Violet red bile glucose (VRBG) agar (Oxiod) and incubated at 44 ˚C for 18 h, separately. After incubation, the colonies appearing on the selected plates were counted and calculated as colony forming units (CFU) per gram of dry Daqu sample. Three representative colonies of each morphology were isolated and stored in glycerol at -80 °C.

3.2.3. Identification of isolates

For sequencing analysis, genomic DNA of bacteria was extracted from pure cultures of isolates using a DNeasy blood and tissue kit (Qiagen, Hilden, Germany) according to the manufacturer's instructions. The genomic DNA was then used as a template for PCR to amplify the bacterial 16S rRNA using the primers 27F/1492R (Eden et al., 1991) and Phusion High-fidelity DNA Polymerase (Fisher Scientific). Amplified 16S rRNA fragments were analyzed on 1% (wt/vol) agarose gels stained with SYBRsafe (Invitrogen, Burlington, Ontario, Canada). After purification with a GeneJET Gel Extraction and DNA Cleanup Micro Kit (Thermo Fisher Scientific, Waltham, MA), the 16S rRNA were sequenced with Sanger sequencing by the Molecular Biology Service Unit of the University of Alberta (Canada). The 16S rRNA sequences were compared with sequences of type strains using the sequence match tool of the Ribosomal Database Project (https://rdp.cme.msu.edu/seqmatch/seqmatch_intro.jsp).

3.2.4. PCR screening of DaQu isolates for the *spoVA*^{2mob} operon and tLST

All isolates were screened for heat resistance with primers targeting the last gene of the *spoVA*^{2mob} operon and three fragments of the tLST in *Escherichia coli* AW1.7. Primers used in this study are shown in the Table 3.1. To detect the presence of the *spoVA*^{2mob} operon, primers were designed to selectively amplify the last gene of the *spoVA*^{2mob} operon of *B. amyloliquefaciens* DSM7 (GenBank accession no. FN597644.1).

3.2.5. Preparation of vegetative cells and spores of bacilli

Vegetative cells of *Bacillus* and *Brevibacillus* were prepared for heat testing at 60 °C. All strains were grown in LB broth at 37 °C with agitation at 200 rpm for 12 h. After being subcultured at 1% dilution three times, cultures were examined by microscopic observation under bight field

to verify that more than 99.9% of the cells had not sporulated. Spore suspensions of 10 isolates from Daqu in water were prepared as described previously (Margosch et al., 2006).

3.2.6. Determination of heat resistance of bacilli and *K. cowanii*

Vegetative cells of bacilli were treated at 60 °C for 1, 3, 5, or 7 min as previously described (Dlusskaya et al., 2011). After heating, appropriate dilutions were plated on LB agar and incubated at 37 °C for 24 h. After incubation, CFUs were calculated.

Spore suspensions were transferred to 25 μL of Dade Accupette pipettes (P4518-25). The glass capillaries were heat sealed, placed in an oil bath at 110 °C for 0, 5, 10, 20, 30, 60, 180, or 300 s, and rapidly cooled in water. The cell counts of heat-treated spore suspensions were determined as described above.

To confirm the contribution of the tLST in the heat resistance of *K. cowanii*, pLHR was transformed into tLST-negative FUA10121 by electroporation. Transformants were plated on LB agar containing 15 mg/L tetracycline-hydrochloride. The construction of pLHR was described previously (Mercer et al., 2015). Four strains of *K. cowanii* (FUA1601, FUA1341, FUA1348 and FUA1349) were treated at 60 °C for 1, 3, 5, or 7 min. The cell counts of heat-treated culture were determined as described above.

3.2.7. Nonlinear model of spores for thermal inactivation

A modified model originating from the Weibull frequency distribution was proposed to describe nonlinear survival curves of spores (Mafart et al., 2001).

$$\log\frac{N}{N_0} = k \times t^p$$

where N presents the number of surviving cells after a duration of heat treatment time t, while N_0 is the initial population. For a given temperature (110 °C), parameter distributions are k and p, and

these two values were determined by nonlinear curve fit procedure in Sigma Plot 12.5. If the survival does not change with time, parameters of k and p are 1 and -0.01, respectively.

3.2.8. Quantification of copy number of the tLST and the *spoVA*^{2mob} operons

qPCR was used for determining the copy number of *spoVA*^{2mob} operons, tLST and 16S rRNA in Daqu community DNA. Community DNA was isolated from 1 g of Daqu powder using the E.Z.N.A. soil DNA kit (Omega Bio-Tek, Doraville, GA). The 7500 fast real-time PCR instrument and 7500 software v 2.0.5 (Applied Biosystems) were used for qPCR amplification and detection. qPCR reactions were prepared in duplicates of 25 μL reaction mixture in MicroAmp optical 96-well reaction plates and sealed with optical adhesive film (Applied Biosystems). Each reaction well contained 50 ng of template DNA, 12.5 μL of 2 × SYBR green PCR master mix (Qiagen, Hilden, Germany), and 0.5 mmol each of forward and reverse primers. Nuclease-free water was used as the negative control. The thermal cycling protocol was as follows: initial denaturation for 10 min at 95 °C, followed by 40 cycles of 30 s at 95 °C, 30 s at melting temperature (T_m), and specific extension time at 72 °C. The fluorescence signal was measured at the end of each extension step at 72 °C. After the amplification, a melting curve analysis with a temperature gradient of 0.1 °C/s from 70 to 95 °C was performed to confirm that only the specific products were amplified. Finally, the samples were cooled down to 4 °C. Table 3.1. shows the sizes of the amplified products and their melting temperatures, for determining of specific PCR product amplification. The standard curves for the *spoVA*^{2mob} operon, tLST and 16S rRNA ranged from 1×10^3 to 1×10^9 copies/μL. All curves were linear in the range tested ($r^2 > 0.999$) by the duplicate reactions. A high amplification efficiency (0.98) was determined for all three target genes.

3.2.9. Determination of copy number of the *spoVA*^{2mob} operon per genome

DNA was isolated from each strain using a Qiagen DNeasy blood and tissue kit (Qiagen). The qPCR assay for determination of *spoVA*^{2mob} operons is described above. The genome copies can be calculated as follows:

$$\text{Genome copies} = \frac{m}{n \times 1.096 \times 10^{-12}}$$

Where n is genome size (in base pairs) and m is the amount of genomic DNA in one PCR (in nanograms). The average genome sizes of *B. amyloliquefaciens*, *B. velezensis*, and *B. subtilis* were determined with completed genomes of these species that were available in the National Center for Biotechnology Information (NCBI) database in November 2017. The average genome sizes (numbers of genomes) were as follows: *B. amyloliquefaciens*, 3.97 ± 0.10 Mb (53); *B. subtilis*, 4.11 ± 0.28 Mb (166); *B. velezensis,* 4.00 ± 0.11 Mb (97).

3.2.10. Frequency of the *spoVA*^{2mob} operon in genome-sequenced bacilli

The sequence of the *spoVA*^{2mob} operon (Berendsen et al., 2016a) was BLAST searched against all completed genomes of species matching *spoVA*^{2mob}-positive isolates obtained in the present study. The BLAST search was performed on 4 May 2018 using the NCBI nucleotide BLAST against 74 genomes of *B. licheniforms*, 1 genome of *Br. parabrevis*, 185 genomes of *B. subtilis*, 54 genomes of *B. amyloliquefacien*, and 118 genomes of *B. velezensis* (total of 432 genomes).

3.2.11. Statistical analysis.

Data were subjected to analysis of variance (ANOVA) using SPSS 21.0 (SPSS Inc., Chicago, IL, USA) software. The least significant difference (LSD) was used to test the difference among means. Differences between means were evaluated as significant at a *P* value of <0.05.

3.3. Results

3.3.1. Temperature profile of Daqu piles

To determine the temperature profile of the Daqu fermentation from which isolates were obtained, the temperature profile in replicate batches of Daqu was monitored during fermentation and maturation (Figure 3.1.). Microbial activity increased the Daqu temperature to more than 45 °C after 4 days of fermentation. The fermentation stage consists of the thermophilic and cooling stages. At the thermophilic stage, the temperature increased to about 60 °C, followed by a decrease to 45 °C at the cooling stage and a 13-day maturation stage at room temperature. A temperature of more than 55 °C, which is typically sufficient to kill *Enterobacteriaceae* within minutes or hours (Li and Gänzle, 2016; Nazarowec-White and Farber, 1997), was maintained for more than 4 days.

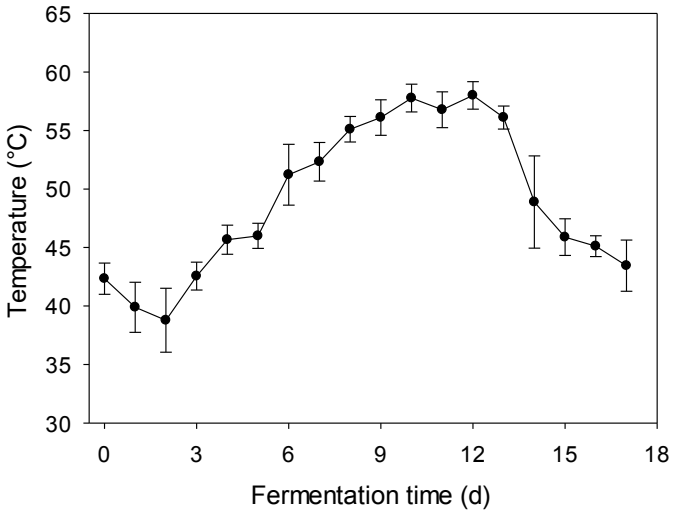

Figure 3.1. Temperature profile of Daqu piles during the fermentation stage (day 1 to day 17). The temperature remained at ambient temperature throughout the maturation and drying stages (data not shown). Data represent means ± standard deviations from four fermentation rooms in triplicate.

3.3.2. Identification of bacilli and *Enterobacteriaceae* from Daqu

To characterize isolates with respect to their heat resistance, two Daqu samples were obtained from the fermentation and maturation stages. Plate counts were determined on Luria-Bertani (LB) and violet red bile glucose (VRBG) agars (Table 3.2.), and representative isolates were identified at the species level (Tables 3.3. and 3.4.). Samples were analyzed after several months of storage at -20 °C and using protocols for selective enumeration; therefore, cell counts may not fully reflect the counts at the time of fermentation. Endospore-forming organisms increased after 13 days of maturation. Isolates of endospore-forming organisms belonged to *B. licheniformis*, *Brevibacillus parabrevis*, *B. subtilis*, *B. amyloliquefaciens* and *B. velezensis* (Table 3.3.). Cell counts of *Enterobacteriaceae* increased from 5.48 log CFU/g to 6.64 log CFU/g by the end of maturation. Eleven isolates of *Enterobacteriaceae* were identified as *Kosakonia cowanii, Cronobacter sakazakii, Enterobacter hormaechei*, *and Pantoea calida* (Table 3.4.).

3.3.3. The tLST and the *spoVA*^{2mob} operon screening of isolates

PCR was performed to identify the presence of the tLST and the *spoVA*^{2mob} operon in all isolates of *Enterobacteriaceae* and spore-forming bacteria, respectively. Two and three isolates from the fermentation stage and the maturation stage, respectively, were *spoVA*^{2mob}-positive (Table 3.3.). *K. cowanii* FUA1601 from the fresh DaQu samples was tLST-positive (Table 3.4.).

3.3.4. The tLST confers heat resistance on *K. cowanii*

To determine whether the tLST confers heat resistance on *K. cowanii*, the survival of tLST-positive *K. cowanii* FUA1601 at 60 °C was compared to survival of tLST-negative *K. cowanii* FUA1341, FUA1348, FUA1349 (Figure 3.2.). The survival rate of three tLST-negative *K. cowanii* isolates was significantly lower than that of tLST-positive *K. cowanii* FUA1601 ($P < 0.05$). To

further confirm the role of tLST in heat resistance, the entire tLST sequence was cloned to pRK767 to form pLHR (Mercer et al., 2015), and pLHR was transferred into tLST-negative *K. cowanii* FUA10121. The heat resistance of the transformant *K. cowanii* FUA10121 (pLHR) was equivalent to the that of the tLST-positive wild-type strain (Figure 3.2.).

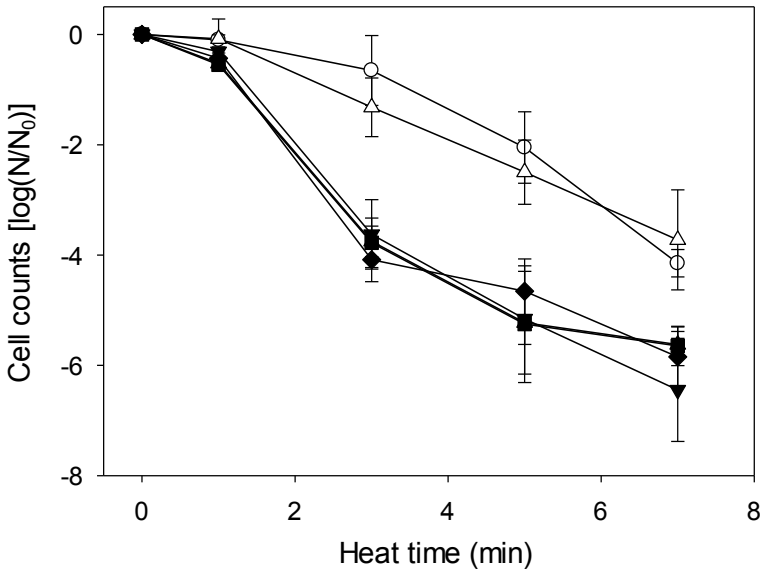

Figure 3.2. Cell counts after treatment at 60 °C for six strains of *Kosakonia cowanii*. White circles, tLST-positive *K. cowanii* FUA1601 isolated from Daqu; white triangles, tLST-negative *K. cowanii* FUA10121 (pLHR) isolated from Daqu; black triangles, tLST-negative *K. cowanii* FUA10121 isolated from Daqu; black inverted triangles, tLST-negative *K. cowanii* FUA1341 isolated from malted oats; black squares, tLST-negative *K. cowanii* FUA1348 isolated from malted oats; black diamonds, tLST-negative *K. cowanii* FUA1349 isolated from malted oats. Data are shown as means ± standard deviations from three independent experiments.

3.3.5. Heat resistance of endospores is dependent on the copy number of the *spoVA*^{2mob} operon

To determine heat resistance of vegetative cells and endospores of bacilli possessing the *spoVA*^{2mob} operon, survival was assessed at 60 °C for vegetative cells (Figure 3.3.) and at 110 °C for spores (Figure 3.4.). Vegetative cells of bacilli were heat sensitive irrespective of the presence

of the *spoVA*^{2mob} operon (Figure 3.3.). In contrast, the presence of the *spoVA*^{2mob} operon increased the heat resistance in spores (Figure 3.4.). Cell counts of *spoVA*^{2mob}-negative strains were reduced by approximately 7 log CFU/mL after 30 s at 110 °C, while cell counts of *spoVA*^{2mob}-positive strains were reduced by less than 1 log CFU/mL (Figure 3.4.).

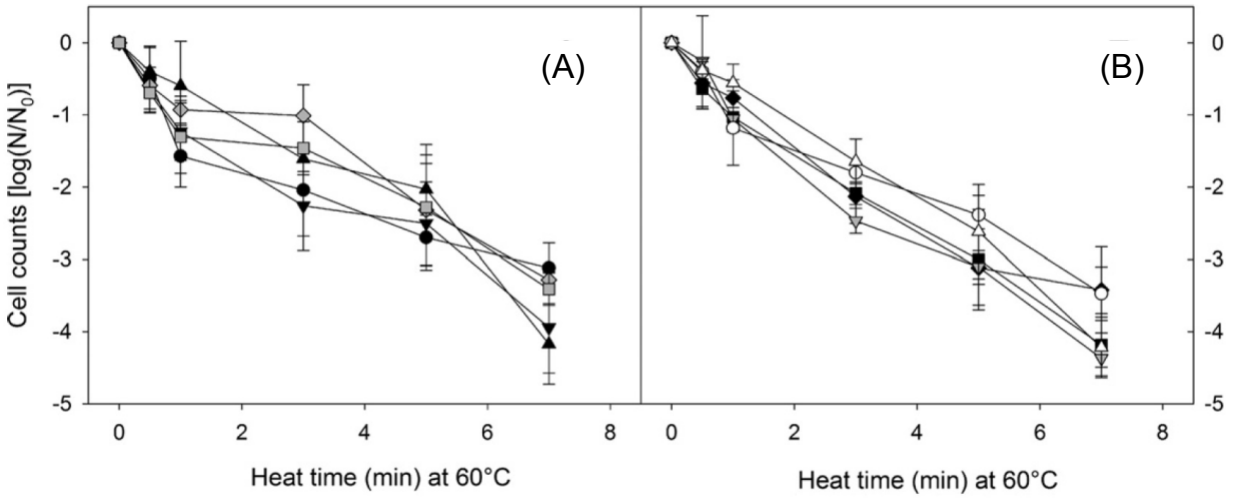

Figure 3.3. Cell counts of *Bacillus* and *Brevibacillus* isolates after treatment of vegetative cells at 60 °C. **Panel A.** Heat treatment of vegetative cells of 5 isolates from the fermentation stage. Black circles, *B. licheniformis* FUA2146; black triangles, *Br. parabrevis* FUA2147; black inverted triangles, *B. subtilis* FUA2148; gray diamonds, *B. amyloliquefaciens* FUA2149; grey squares, *B. subtilis* FUA2150. **Panel B.** Heat treatment of vegetative cells of 5 isolates from the maturation stage. Black diamonds, *B. licheniformis* FUA2151; black squares, *Br. parabrevis* FUA2152; grey inverted triangles, *B. amyloliquefaciens* FUA2153; white circles, *B. amyloliquefaciens* FUA2154; white triangles, *B. velezensis* FUA2155. Black, gray, and white symbols represent strains with 0, 1, and 2 copies of the *spoVA*^{2mob} operon per genome (Table 3.3.). Data are shown as means ± standard deviations from three independent experiments.

Because heat resistance of spores was reported to depend on the copy number of the *spoVA*^{2mob} operon (Berendsen et al., 2016a), we also determined the copy number of the *spoVA*^{2mob} operon in Daqu isolates (Table 3.3). The lowest copy number of the *spoVA*^{2mob} operon in *B. subtilis* FUA2150 was calculated as 0.69; however, because the number of copies per genome must be an integer, the deviation from 1 was assumed to represent experimental error. The copy numbers of the *spoVA*^{2mob} operon in *B. amyloliquefaciens* FUA2149 and FUA2153 were comparable to *B.*

subtilis FUA2150 and were similarly assumed to be 1. The copy numbers of the *spoVA*^{2mob} operon of *B. amyloliquefaciens* FUA2154 and *B. velezensis* FUA2155 were determined experimentally as 1.42 and 1.27, respectively. These numbers are twice as high as the copy number in *B. subtilis* FUA2150 and likely represents two *spoVA*^{2mob} operons per genome.

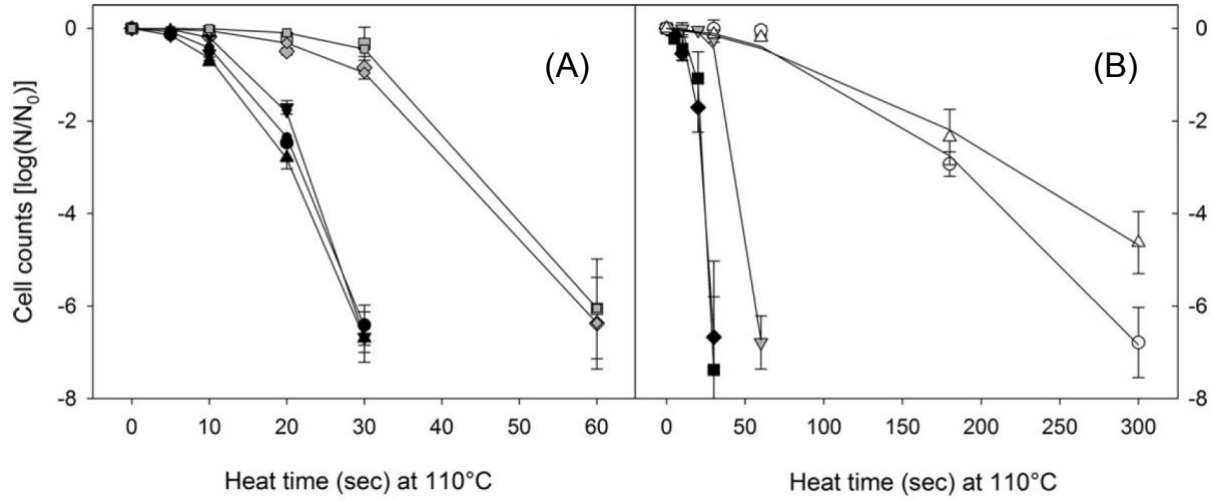

Figure 3.4. Cell counts of *Bacillus* and *Brevibacillus* isolates after treatment of spore preparations at 110 °C. **Panel A**. Heat treatment of spores of 5 isolates from the fermentation stage. Black circles, *B. licheniformis* FUA2146; black triangle, *Br. parabrevis* FUA2147; black inverted triangles, *B. subtilis* FUA2148; grey diamonds, *B. amyloliquefaciens* FUA2149; grey squares, *B. subtilis* FUA2150. **Panel B.** Heat treatment of spores of 5 isolates from the maturation stage. Black diamonds *B. licheniformis* FUA2151; black squares, *Br. parabrevis* FUA2152; grey inverted triangles, *B. amyloliquefaciens* FUA2153; white circles, *B. amyloliquefaciens* FUA2154; white triangles, *B. velezensis* FUA2155. Black, gray, and white symbols represent strains with 0, 1, and 2 copies of the *spoVA*^{2mob} operon per genome (Table 3.3.). Data are shown as means ± standard deviations from three independent experiments.

The survival of bacterial endospores at 110 °C clearly related to the copy number of the *spoVA*^{2mob} operon (Figure 3.4.). To determine whether a quantitative relationship exists between the number of *spoVA*^{2mob} copies per genome and the heat resistance, survivor curves at 110 °C were fitted to the Weibull model (Figure 3.4.). The use of the nonlinear Weibull model was chosen because all thermal death time curves exhibited pronounced shouldered. The relationship between the inactivation rate *k*, the shape parameter *p*, and the *spoVA*^{2mob} copy number is shown in Figure

3.5. The inactivation rate of spores of the five strains lacking the *spoVA*^{2mob} operon was approximately 0.32 min at 110 °C. The average inactivation rate of strains carrying one or two *spoVA*^{2mob} operons was 0.86 and 4.5 min 110 °C, respectively; plotting the gene copy number versus the inactivation rate revealed a log-linear relationship with a correlation coefficient (r^2) of 0.96 (Figure 3.5.). Remarkably, the shape factor, which indicates tailing or shoulders, was also dependent on the copy number of the *spoVA*^{2mob} operon. The shoulder effect decreased with increasing copy numbers of the *spoVA*^{2mob} operon (Figure 3.4.); the shape factor *p* was correlated to the operon copy number, with an r^2 of 0.96 (Figure 3.5.).

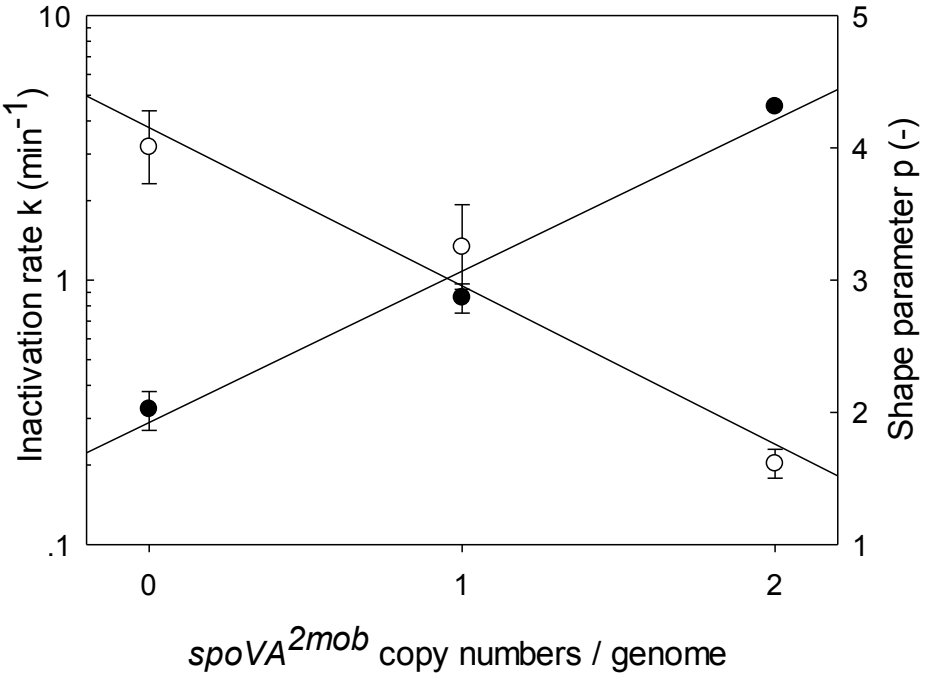

Figure 3.5. Weibull parameters *k* and *p* of 10 *Bacillus* and *Brevibacillus* isolates from Daqu. The values obtained for the inactivation rate *k* (●) and the shape parameter *p* (○) at 110 °C were averaged for all isolates with 0 (5 strains), 1 (three strains), or 2 (two strains) copies of the *spoVA*^{2mob} operon per genome. Lines represent log-linear regression (*k*) and linear regression (*p*) of copy numbers and the parameters of the Weibull model.

3.3.6. Increase of copy numbers of the tLST and the *spoVA*^{2mob} operon during Daqu fermentation process

A high frequency of the tLST and the *spoVA*^{2mob} operon in isolates indicates selection for heat-resistant strains during fermentation. To provide further evidence that Daqu fermentation selects for tLST- and *spoVA*^{2mob}-positive *Enterobacteriaceae* and bacilli, respectively, we quantified the copy numbers of these two genes relative to total bacterial 16S rRNA throughout the fermentation process. The copy numbers of the tLST, the *spoVA*^{2mob} operon and 16S rRNA genes were measured at 6 time points of Daqu fermentation (Figure 3.6.). The abundance relative to 16S rRNA genes of both the tLST and the *spoVA*^{2mob} operon increased during Daqu fermentation.

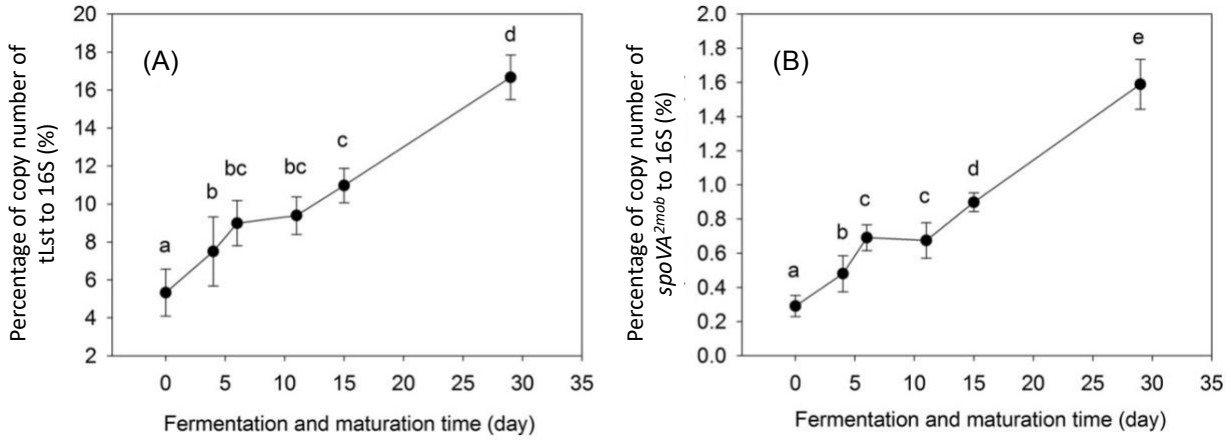

Figure 3.6. Relative abundance of gene copies of the tLST and *spoVA*^{2mob} operon in Daqu community DNA during fermentation and maturation. **Panel A.** Copy numbers of the tLST relative to the copy number of bacterial 16S rRNA genes. **Panel B.** Copy number of the *spoVA*^{2mob} operon relative to the copy number of bacterial 16S rRNA genes. Data represent means ± standard deviations from four replicates. Values in the same panel that do not share a lowercase letter are significantly different ($P < 0.05$).

The increase of the tLST and the *spoVA*^{2mob} operons were significant after only 4 and 6 days of fermentation (Figure 3.6.), corresponding to increases of fermentation temperature to 45 °C and 52 °C (Figure 3.1.), respectively. In the entire process, the relative abundance of the tLST increased

more than 3-fold; the relative abundance of the *spoVA*^{2mob} operon increased more than 5-fold (Figure 3.6.).

3.3.7. Frequency of *spoVA*^{2mob}-positive bacilli in genomes deposited in the NCBI database

To determine whether the frequency of the s*poVA*^{2mob} operon in bacilli isolated from Daqu is higher than the frequency of other strains of the same species, we identified the frequency of s*poVA*^{2mob}-positive BLAST results with the s*poVA*^{2mob} operon as a query sequence. For the *Bacillus* spp. of interest, 432 genome sequences are available; of these, 6 of 74 genome sequences of *B. licheniformis*, 0 of 1 genome sequence of *Br. parabrevis*, 4 of 185 genome sequences of *B. subtilis*, 4 of 53 genome sequences of *B. amyloliquefaciens*, and 2 of 118 genome sequences of *B. velezensis* were s*poVA*^{2mob}-positive. In 23 out of the 24 finished genomes of *Bacillus* spp. that contained s*poVA*^{2mob}, the operon was carried on a chromosome.

3.4. Discussion

The tLST and the *spoVA*^{2mob} operons confer heat resistance on *Enterobacteriaceae* and bacilli, respectively (Berendsen et al., 2016a; Mercer et al., 2015). This study quantified the tLST and the *spoVA*^{2mob} operon in a Daqu fermentation, demonstrating that the temperature profile of Daqu fermentation can provide selective pressure for these genomic islands and related heat-resistant strains.

Samples used in this study were dried and stored frozen to isolate community DNA for culture-independent analysis of the presence of genes coding for heat resistance. In addition, a total of 29 microbial strains were isolated to verify that tLST- or *spoVA*^{2mob}-positive *Enterobacteriaceae* and bacilli, respectively, have a higher resistance to heat than negative isolates of the same species and origin. Plant-associated *Enterobacteriaceae* including *C. sakazakii*, *K. cowanii* and *E. hormaechei*, were frequently isolated. *K. cowanii* was classified as *Enterobacter* until 2013 (Tall

et al., 2015; Yan and Fanning, 2015). The diversity of isolates thus conforms to prior reports that plant-associated *Enterobacteriaceae* are abundant representatives of Daqu microbiota, comparable to other Daqu fermentation from different locations under same temeperature profile (Li et al., 2016, 2015a, 2015b). Of note, plant-associated *Enterobacteriaceae* and particularly *C. sakazakii* are also opportunistic pathogens. *C. sakazakii* and *K. cowanii* persist for extended periods in low-moisture foods, including infant formula, and can cause nosocomial infections in preterm neonates (Jaradat et al., 2014; Mardaneh and Soltan-Dallal, 2014).

This study additionally demonstrated that DaQu fermentation selects for heat-resistant and tLST-positive *K. cowanii*. The heat resistance of tLST-positive *Kosakonia* from Daqu is comparable to previously published heat resistance of tLST-positive *Enterobacter* spp. (Mercer et al., 2017b) and confirms that the tLST is a reliable marker for heat resistance (Mercer et al., 2017b, 2015). The relative abundance of *Enterobacteriaceae* in Daqu, about 25% of total isolates (Li et al., 2015a), matches the relative abundance of the tLST copies (this study), indicating that a substantial proportion of *Enterobacteriaceae* carry the tLST. Even when considering that multiple copies of the tLST may be present in one strain, this study demonstrates that an increase of the fermentation temperature exerts a strong selective pressure for tLST-positive *Enterobacteriaceae*. A high frequency of tLST-positive *Escherichia coli* organisms has been previously found from meat(Guragain et al., 2021; Mercer et al., 2015), cheese (Marti et al., 2016), and wastewater (Zhi et al., 2016); however, the tLST has not been identified in spontaneous solid-state fermentation or in *K. cowanii*. The temperature of Daqu ranged from 55 to 60 °C for 6 days; at this temperature range, even tLST-positive *Kosakonia* and *Enterobacter* spp. are usually killed within minutes of exposure (Figure 3.3., Mercer et al., 2017b). A reduction of the water activity induces accumulation of compatible solutes and enhances the heat resistance of tLST-positive

Enterobacteriaceae (Breeuwer, 2014; Feeney et al., 2014; Pleitner et al., 2012). The low moisture content of Daqu may thus enhance the selective advantage of tLST-mediated heat resistance of *Kosakonia* during fermentation.

Bacillus spp. constitute a significant portion of the microbial population in Daqu (Wang et al., 2011; Xiao et al., 2017; Xiu et al., 2012); their endospores survive under low-moisture conditions and at high temperatures (Bond and Favero, 1977). This study demonstrated that the count of spores increased during fermentation; the taxonomic identification of spore-forming bacteria matched prior reports on Daqu microbiota (Tables 3.1. and 3.2.) (Shanqimuge et al., 2015; Wang et al., 2011). More surprisingly, 50% of the isolates of sporeformers were *spoVA*^{2mob}-positive. The frequency of *spoVA*^{2mob}-positive bacilli isolated from Daqu is more than 10-fold higher than the proportion of *spoVA*^{2mob}-positive isolates for which genome sequence data has been accessible in the Genebank genome database. Moreover, most *spoVA*^{2mob}-positive bacilli and all isolates with two *spoVA*^{2mob} copies per genome were obtained from the maturation stage. Heat-resistant and *spoVA*^{2mob}-positive bacilli were identified as *B. subtilis*, *B. amyloliquefaciens* and *B. velezensis*.

The high proportion of *spoVA*^{2mob}-positive isolates (Tables 3.1. and 3.2.) together with the strong increase of the relative abundance of the *spoVA*^{2mob} operon in community DNA (Figure 3.6) indicates a strong selective pressure for the operon during fermentation. This selective pressure is likely exerted on spore survival. The *spoVA*^{2mob} operon is controlled by a sporulation-specific promoter, and the genes in this operon are specifically expressed during sporulation (den Besten et al., 2017); accordingly, the operon impacts heat resistance of spores but not of vegetative cells (Figures 3.3. and 3.4.). The Daqu fermentation temperature is substantially below the temperature range that allows rapid inactivation of *spoVA*^{2mob}-negative endospores (Figure 3.3.) (Berendsen et

al., 2016a, 2015; Esteban et al., 2015). The 4- to 5-fold increase of the proportion of *spoVA*^{2mob}-positive bacterial endospores during Daqu fermentation suggests that the operon also improves long-term survival of *Bacillus* endospores at the temperature range of 50 to 60 °C, which is not well documented in the experimental literature.

The heat resistance of *Bacillus* endospores depended not only on the presence but also on the copy number of the *spoVA*^{2mob} operon, consistent with a prior report (Berendsen et al., 2016b). Kinetic modeling of spore inactivation in combination with quantification of the *spoVA*^{2mob} copy numbers allowed establishment of quantitative relationships. The inactivation rate was strongly influenced by the *spoVA*^{2mob} copy numbers, as indicated by the log-linear relationship (Figure 3.5.). Remarkably, the shape parameter *p* was also dependent on the presence and copy number of the *spoVA*^{2mob} operon. For log-linear thermal death time curves, the shape parameter is 1; tailing is represented by a shape parameter below 1, and values for *p* that are higher than 1 indicate a shoulder (Peleg and Cole, 2000; Weibull, 1951). Physiological mechanisms that relate to shouldering and tailing phenomena are poorly investigated (Mathys et al., 2007). The *spoVA*^{2mob} operon strongly impacted the shoulder effect in thermal death time curves (Figures 3.4. and 3.5.); this phenomenon warrants further investigations.

3.5. Conclusions

In conclusion, the Daqu fermentation analyzed in this study appears to have selected for mobile genetic elements conferring heat resistance in *Enterobacteriaceae* and bacilli. Both the tLST and the *spoVA*^{2mob} operon were enriched by the end of Daqu processing, and the relative abundance of the two increased approximately 3 and 5 times, respectively. *Bacillus* endospores exhibit a much higher resistance to heat than *Enterobacteriaceae*; it is therefore remarkable that the tLST and the *spoVA*^{2mob} operon, which confer resistance on *Enterobacteriaceae* and *Bacillus*

spores, respectively, are enriched in the same food fermentation. Current knowledge allows identification of ecosystems which select for tLST-positive *E. coli*; however, the selective pressure for other *Enterobacteriaceae* is unknown. All current isolates of *spoVA*^{2mob}-positive bacilli were obtained from commercial food products (Berendsen et al., 2015); data on natural habitats that provide selective pressure for this operon are unavailable. This study extends prior knowledge by indicating that heat resistance may contribute to ecological fitness for *K. cowanii* and *Bacillus* spp. in food fermentations and may account for their abundance in fermentation microbiota. Daqu is the one of only a few food fermentations for which fermentation temperatures reach or exceed 60 °C; moreover, it is also one of only a few fermentations dominated by bacilli and *Enterobacteriaceae* (Gänzle, 2015). The selective pressure for heat-resistant *Enterobacteriaceae* and bacilli in food fermentations is therefore unprecedented. The identification of the tLST and the *spoVA*^{2mob} operon as likely indicators of fitness of *Enterobacteriaceae* and bacilli in Daqu fermentation may provide insight into environmental sources of heat-resistant spoilage organisms. The presence of heat-resistant *Kosakonia* spp. and *Bacillus* spp. in Daqu is not a food safety concern; however, both genomic islands are mobile and transferable to pathogenic bacteria or toxin-producing bacteria by horizontal gene transfer. Our study may contribute to the identification of the source of heat resistant spoilage organisms and pathogens that may contaminate the food supply.

Table 3.1. Sequences of primers for PCR

Primer	Sequence (5'→3')	T_m (°C)	Product size (kb)	References
27F	AGAGTTTGATCCTGGCTCAG	58	1.5	Eden et al.,
1492R	GGCTACCTTGTTACGACTT			1991
Det-hyp-2mob-F	GTGCCTGAATGGTTAGATATAGC	68	0.86	This study
Det-hyp-2mob-R	TTATCCTTTTAAAATAGGGGTCACTTTATC			
Lhr2-F	TACAAGATTGCCCTGGAAGT	60	0.20	Mercer et al.,
Lhr2-R	CTTGATCGAATCCTGGTTGG			2015
HR-F1	TTAGGTACCGCTGTCCATTGCCTGA	62	1.8	Mercer et al.,
HS-R1	AGACCAATCAGGAAATGCTCTGGACC			2015
HR-F2.2	GAGGTACCTGTCTTGCCTGACAACGTTG	64	2.8	Mercer et al.,
HR-R2	TATCTAGAATGTCATTTCTATGGAGGCATG AATCG			2015
HS-F1	GCAATCCTTTGCCGCAGCTATT	64	2.8	Mercer et al.,
HR-R3	GTCAAGCTTCTAGGGCTCGTAGTTCG			2015

Table 3.2. Culture-dependent analysis of Daqu microbiota at fermentation stage (day 17) and maturation stage (day 30)

Bacteria/Medium	Fermentation stage		Maturation stage	
	Cell count (CFU/g)[a]	No. of Isolates	Cell count (CFU/g)[a]	No. of Isolates
Total plate count	5.48×10^7	2	4.06×10^7	6
Endospores[b]	2.24×10^3	5	2.02×10^5	5
VRBG[c] Agar	3.02×10^5	5	4.38×10^6	6

[a]Data are means of two technical replicates.

[b]Endospores were enumerated after heating to 80 °C for 30 min.

[c]VRBG, violet red bile glucose.

Table 3.3. Identification and copy number of the *spoVA*^{2mob} operon in 10 isolates from Daqu

Stage	Closest type strain	Strain	Type strain	Identity (%) to type strain	*spoVA*^{2mob} copy no./ genome[a,b]	*spoVA*^{2mob} copy# / genome[c]
Fermentation	*Bacillus licheniformis*	FUA2146	ATCC 14580	99.7	- [d]	0
	Brevibacillus parabrevis	FUA2147	IFO 12334T	98.7	-	0
	Bacillus subtilis	FUA2148	DSM 10	99.4	-	0
	Bacillus amyloliquefaciens	FUA2149	DSM 7	100.0	0.71 ± 0.04	1
	Bacillus subtilis	FUA2150	DSM 22148	99.2	0.69 ± 0.08	1
Maturation	*Bacillus licheniformis*	FUA2151	ATCC 14580	99.7	-	0
	Brevibacillus parabrevis	FUA2152	IFO 12334T	100.0	-	0
	Bacillus amyloliquefaciens	FUA2153	DSM 7	98.6	0.89 ± 0.12	1
	Bacillus amyloliquefaciens	FUA2154	NBRC 15535	100.0	1.42 ± 0.17	2
	Bacillus velezensis	FUA2155	CBMB 205	99.6	1.27 ± 0.31	2

[a]Mean ± standard deviations in triplicate.

[b]Measured copy numbers.

[c]Adjusted copy number;

[d]-, not detected

Table 3.4. Identification and presence of tLST of 11 isolates from Daqu

Stage	Closest type strain	Strain	Type strain	Identity (%) to type strain	Presence of tLST[a]
Fermentation	*Kosakonia cowanii*	FUA10116	CIP 107300	100.0	–
	Cronobacter sakazakii	FUA10117	ATCC 29544	99.1	–
	Cronobacter sakazakii	FUA10118	ATCC 29544	100.0	–
	Enterobacter hormaechei	FUA10119	CIP 103441	99.3	–
	Pantoea calida	FUA10120	1400/07	99.1	–
Maturation	*Kosakonia cowanii*	FUA1601	CIP 107300	100.0	+
	Kosakonia cowanii	FUA10121	CIP 107300	99.9	–
	Cronobacter sakazakii	FUA10122	ATCC 29544	98.9	–
	Cronobacter sakazakii	FUA10123	ATCC 29544	98.8	–
	Enterobacter hormaechei	FUA10124	CIP 103441	95.3	–
	Pantoea calida	FUA10125	1400/07	99.6	–

[a]-, negative; +, positive

CHAPTER 4. The Transmissible Locus of Stress Tolerance Confers Resistance to Chlorine and Other Oxidizing Chemicals in *Escherichia coli*

4.1 Introduction

Escherichia coli is a common member of the microbiota of the gastrointestinal tract of vertebrate animals. Most strains of *E. coli* are nonpathogenic, but pathogenic strains cause enteric and extraintestinal diseases (Croxen et al., 2013; Sarowska et al., 2019). An important source of exposure to pathogenic *E. coli* is contaminated water used for irrigation, drinking and the processing of fruits and vegetables (Beuchat, 2002; Odonkor and Ampofo, 2013). Water sanitation can be achieved by ozonation, UV light, and, most commonly, chlorination (Macauley et al., 2006; Ridgway and Olson, 1982). Hypochlorous acid (HOCl), the active compound of water chlorination, reacts with multiple cellular macromolecules, such proteins, nucleic acids and lipids (Harrison and Schultz, 1976). However, bacteria develop resistance to chlorination, and recovery of viability by bacterial cells following chlorination has been observed (Bommer et al., 2018). In particular, strains of *E. coli* isolated from wastewater showed high resistance to chlorine (Zhi et al., 2016).

Chlorine-specific resistance in *E. coli* involves three chlorine-sensitive transcription factors, *hypT*, *rclR* and *nemR*, which are activated by specifically by chlorine ion oxidation (Drazic et al., 2013; Gray et al., 2013; Parker et al., 2013). The chlorine resistance of *E. coli* is also mediated through the RpoS-regulated general stress response (Du et al., 2015), the oxidative stress regulons *oxyR* and *soxR* (Cabiscol Català et al., 2000; Hillion and Antelmann, 2015), and heat shock proteins (Winter et al., 2005). An overview of the mechanisms affecting chlorine resistance in *E. coli* is shown in Figure 4.1.

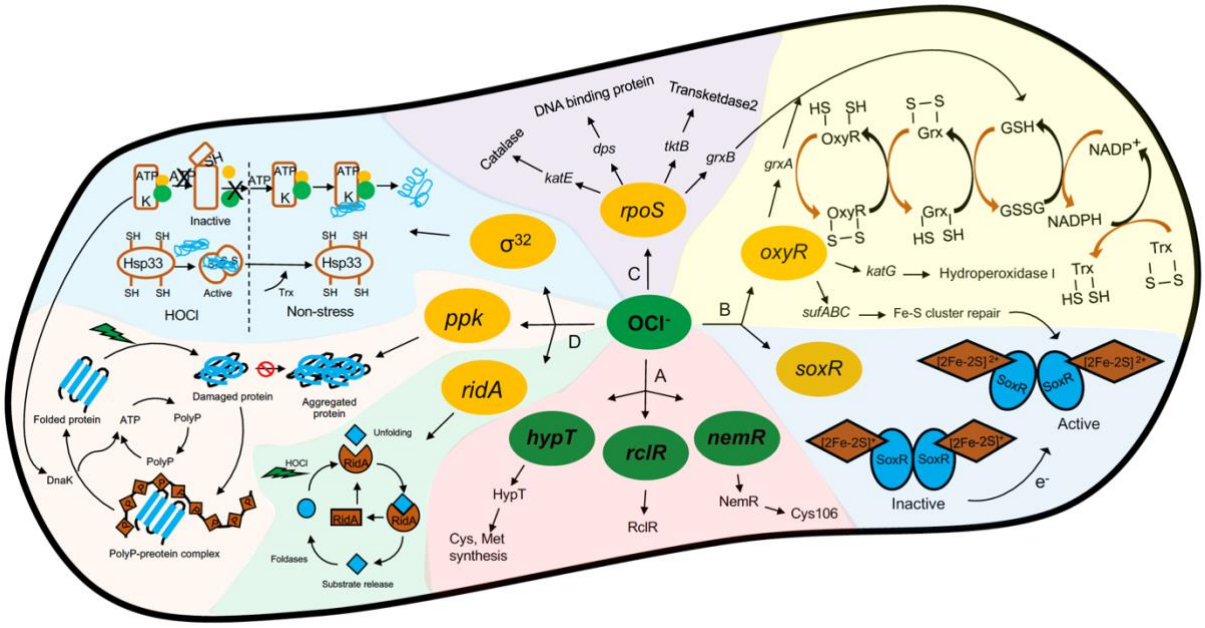

Figure 4.1. Cytoplasmic determinants of chlorine resistance in *E. coli*. (A) Chlorine-specific transcription factors. HypT is specially activated by chlorine through methionine oxidation, and Cys4 becomes oxidized and inhibits DNA binding to avoid unnecessary regulation of target genes (Drazic et al., 2013). Proteins encoded by *rclR* form a membrane-associated complex responsible for reducing cellular components specifically oxidized by chlorine (Parker et al., 2013). The NemR-mediated chlorine response relies on the reversible oxidative modification of the conserved Cys106 (Gray et al., 2013). (B) Oxidative stress response. The insufficiency of NADPH leads to SoxR reduction, and the oxidized Fe−S clusters trigger a conformational change of SoxR (Siedler et al., 2013). Chlorine activates OxyR by the formation of a disulfide bond (Cabiscol Català et al., 2000), and then OxyR is regenerated by the glutaredoxin-glutathione-glutathione reductase (Grx/GSH/Gor) system upon return to nonstress conditions (Hillion and Antelmann, 2015). Oxidized OxyR activates the *grxA* and *katG*, encoding enzymes involved in chlorine resistance, and *sufABC* for the repair of damaged Fe–S clusters (Cornelis et al., 2011). (C) General stress response. RpoS regulates the transcription of *katE* (encoding catalase), *dps* (encoding a DNA-binding protein), *tktB* (encoding transketdase2), and *grxB* (encoding glutaredoxin2), which act against chlorine resistance (Du et al., 2015). (D) Prevention of protein aggregation. The reduced Hsp33 in chlorine leads to the simultaneous formation of two intramolecular disulfide bonds and binds to unfolding substrate proteins, whereas Dnak is inactivated because of the low ATP level. When cellular ATP levels are restored, Hsp33 becomes reduced, and bound substrates are transferred to the DnaK system for refolding (Winter et al., 2005). Inorganic polyphosphate (PloyP) forms stable complexes with unfolding proteins. After the relief of stress, polyphosphate can be reconverted to ATP, which can be used by DnaK to refold polyphosphate-protected proteins (Gray and Jakob, 2015). RidA is N-chlorinated by chlorine and then binds to a wide range of unfolded client proteins, preventing their aggregation. Under nonstress condition, the chlorine is removed, leading to the release of the client protein and protein refolding (Müller et al., 2014).

A high proportion of chlorine-resistant isolates of *E. coli* recovered from wastewater also harbor the transmissible locus of stress tolerance (tLST) (Zhi et al., 2016), a genomic island that mediates extreme heat resistance in *E. coli* (Mercer et al., 2015). The genes on the tLST are predicted to encode proteins associated with response to heat shock, cell envelope stress, and oxidative stress (Mercer et al., 2017a). The putative mechanisms of tLST-mediated heat resistance (Mercer et al., 2017a) overlap the chlorine resistance mechanisms (Figure 4.1.). The tLST-encoded heat shock proteins sHSP20, $ClpK_{GI}$ and $sHSP_{GI}$ may prevent chlorine-mediated protein aggregation. The tLST additionally encodes a homologue of the oxidoreductase thioredoxin. The activities of the enzymes encoded in the tLST indicate a potential role in resistance to chlorine and oxidative stresses during water treatment, although this role has not been confirmed experimentally. Moreover, it remains unknown to what extent heat resistance and chlorine resistance overlap with the presence of *E. coli* virulence factors. Current knowledge is thus insufficient to assess the frequency of pathogenic strains of *E. coli* that use tLST-mediated resistance to oxidative water treatment. Of particular concern are Shiga toxin-producing *E. coli* (STEC) strains that cause foodborne and waterborne illness outbreaks (Beer et al., 2015; Heiman et al., 2015; Kintz et al., 2017). The definitive virulence factor of STEC is Shiga toxin (also termed verotoxin), and STEC strains may have high infectivity, with a 1 to 10% risk of infection upon exposure to a single cell (Croxen et al., 2013; Teunis et al., 2008). In addition, a growing body of evidence suggests that uropathogenic *E. coli* (UPEC) appears to differentially survive wastewater treatments and may also be transmitted by contaminated water (Adefisoye and Okoh, 2016; Anastasi et al., 2010; Boczek et al., 2007; Foxman, 2010). UPEC strains do not share a defined set of virulence factors but are described on the basis of their ability to cause infections in the urinary tract and bladder.

This study therefore aimed to investigate whether the tLST confers resistance to chlorine in *E. coli* and to determine the frequency of the tLST in strains of STEC and UPEC.

4.2. Materials and methods

4.2.1. Collection and screening of *E. coli* from wastewater and groundwater

Ten tLST-positive strains and 10 tLST-negative strains of *E. coli* were selected from a total of 70 strains that had been isolated from wastewater previously (Zhi et al., 2016). In addition, 70 *E. coli* isolates collected from wastewater effluents during routine monitoring programs were provided by a municipal water treatment plant in Alberta, Canada. These samples were collected from undigested sludge, digested sludge, and biosolids from a lagoon prior to agricultural land application. Strains of *E. coli* were subcultured from most-probably-number tubes in EC-broth (Oxoid) after 24 h of incubation. The methods used to confirm the identification of *E. coli* and to detect specific virulence or resistance markers are outlined below. Sixty-five groundwater isolates positive for *stx1*, *stx2*, or both were collected from routine screening of well water samples submitted to the Alberta Provincial Laboratory for Public Health. Isolates were screened for the presence of the tLST with primers targeting three fragments of the tLST in *E. coli* AW1.7. Primers used in this study are listed in Table 4.1.; a list of isolates used in the study is provided in Table S4.1. in the supplemental material.

4.2.2. Determination of chlorine resistance

Chlorine resistance was determined by mixing 200 µL of overnight cultures with 6.5 µL of a 3% (wt/wt) sodium hypochlorite solution (Sigma-Aldrich, St. Louis, MO) to a concentration of 15 mM NaClO, followed by incubation for 25 min at 20 °C. The reaction was terminated by the addition of 6.5 µL of 10% $Na_2S_2O_3$ (Sigma-Aldrich, St. Louis, MO). Treatment conditions were

selected to achieve a reduction of cell counts ranging from about 1 to 7 log CFU/mL. To benchmark the effect of the tLST on chlorine resistance against the previously described contribution of the tLST to heat resistance, the heat resistance of overnight cultures of *E. coli* was determined as described previously (Mercer et al., 2015). Cell counts of cultures before and after treatment were determined by surface plating on LB agar and incubation at 37 °C for 24 h. Results are expressed as log-transformed ratios of cell counts before treatment to cell counts after treatment [$\log(N_0/N)$].

4.2.3. Effect of the tLST on resistance to oxidizing chemicals

To assess the contributions of different regions of the tLST to survival under oxidative stress, *E. coli* MG1655 was transformed with plasmids pRK767, pLHR, pRF1, pRF2, pRF3, and pRF1-2 (Mercer et al., 2015) (Tables 4.2. and 4.3.). The pRK767 plasmid was used as a vector control for MG1655. Oxidative stress was induced by treatment of the transformants for 5 min with 32 mM NaClO, 120 mM H_2O_2 (30% [wt/wt] in H_2O; Sigma-Aldrich, St. Louis, MO), 105 mg/L peroxyacetic acid (PAA, 32 % [wt/wt] in acetic acid, pH=1.5; Sigma-Aldrich, St. Louis, MO), 5.80 mM KIO_4 (Thermo Fisher Scientific, Waltham, MA, USA), 10 mM acrolein (Thermo Fisher Scientific, Waltham, MA, USA), or 75 mg/L allyl isothiocyanate (AITC; Alfa Aesar Co., Inc.). Reactions were terminated by adding 10% $Na_2S_2O_3$ to achieve a final concentration of 16 to 63 mM. The cell counts were determined as described above.

4.2.4. Measurement of cytoplasmic oxidation by a roGFP2-based probe

The fusion protein roGFP2-Orp1 was designed to measure H_2O_2 in biological systems (Degrossoli et al., 2018). Plasmid encoding roGFP2-Orp1 was transformed into *E. coli* MG1655, along with plasmids carrying the whole or part of tLST (pRK767, pLHR, pRF1, pRF2, pRF3, pRF1-2). (Table 4.2. and 4.3.). Ampicillin (100 mg/L) and tetracycline (15 mg/L) were added into

the cultivation media to maintain both plasmids. Exponential-phase cultures of transformants were incubated with 100 μM IPTG (Isopropyl β-D-1-thiogalactopyranoside; Thermo-Fisher Scientific, USA) at 37 ˚C overnight to induce the expression of the reduction-oxidation-sensitive green fluorescent protein 2 (roGFP2). Cells were washed twice in phosphate-buffered saline (PBS) buffer (pH 7.4) and were treated with NaClO (32 mM), H_2O_2 (120 mM), or PAA (105 mg/L) for 5 min. Nontreated cells served as controls. Reactions were terminated by adding 10% $Na_2S_2O_3$. Cultures (100 μL) were placed in the wells of a black, clear-bottom 96-well plate (Corning, New York, USA) and fluorescence was measured at excitation wavelengths of 405 and 488 nm and at the emission wavelength of 530 nm. The ratio of the fluorescence intensity obtained at the excitation wavelength of 405 nm to that obtained at 488 nm was used to evaluate the oxidation level of roGFP (Degrossoli et al., 2018).

4.2.5. Determination of membrane lipid oxidation by C_{11}-BODIPY$^{581/591}$

E. coli MG1655 transformed with different plasmids (pRK767, pLHR, pRF1, pRF2, pRF3, pRF1-2) (Table 4.2. and 4.3.) were treated with NaClO (32 mM), H_2O_2 (120 mM), or PAA (105 mg/L) for 5 min. Oxidized *E. coli* served as nonstained control. Nonoxidized *E. coli* prepared with C11-BODIPY$^{581/591}$ (Thermo Fisher Scientific, Waltham, MA, USA) served as a nontreatment control. In brief, 1.5 ml of each culture was washed with 2 ml ice-cold 50 mM Tris-HCl (pH 8.0) containing 20% (wt/vol) sucrose and resuspended in 2 ml Tris-HCl buffer. The outer membrane was disrupted by addition of 0.2 mL lysozyme solution (5 mg/mL lysozyme in 0.25 M Tris-HCl [pH 8.0]) and 0.4 mL EDTA (0.25 M; pH 8.0) (Gänzle et al., 1999). After incubation at 37 °C for 30 min, cell pellets were suspended with 10 mM citrate buffer (pH 7.0) with addition of 10 μM of C_{11}-BODIPY$^{581/591}$, followed by incubation in the dark for 30 min at 37 °C and 200 rpm. Flow cytometry was performed using a BD LSRFotessa X-20 system (BD Biosciences, San Jose, CA,

USA) equipped with 488-nm excitation from a blue air laser at 50 mW and 561-nm excitation from a yellow air laser at 50 mW to excite green (530±30 nm) and red (586±15 nm) fluorescence. Single cells were quantified by forward scatter and side scatter gating on the flow cytometer. In brief, samples were centrifuged, resuspended, and diluted with 1 mL of PBS (pH 7.4) to keep the detected cell number per second (e/s) in the range of 300 to 3,000 events/s. Sample injection and acquisition were started simultaneously and continued until 10,000 events were recorded. Data were recorded by BD FACSDiva software and analyzed by FlowJo (both from BD Biosciences, San Jose, CA, USA). The single-cell population was defined by selecting the cell population located along the diagonal of the "FSC-A; FSC-H" dot plot. The population was divided into four subpopulations by red and green fluorescence reference lines. The reference lines were determined from untreated samples, where at least 96% of the population was negative for red and green fluorescence.

4.2.6. Flow cytometric determination of GFP fluorescence

E. coli O104:H4 Δ*stx*$_2$:*gfp*:*amp* is derived from a STEC strain, with in-frame replacement of the prophage-harbored *stx*$_2$ with a *gfp::amp* cassette (Fang et al., 2017). The fusion of GFP in the Stx2 prophage provides a reporter for protein expression under the control of the Shiga toxin promoter. *E. coli* O104:H4 is tetracycline resistant, a characteristic that interferes with the antibiotic resistance of the other plasmids used in this study. Therefore, the tetracycline resistance gene on plasmids pRK767, pLHR, pRF1, pRF2, pRF3, and pRF1-2 was replaced with chloramphenicol resistance gene from pKD3 (Datsenko and Wanner, 2000). PCRs were carried out using Phusion High-Fidelity DNA polymerase (Thermo Scientific) according to the manufacturer's guidelines. The gene encoding chloramphenicol resistance was amplified by the Priming site 1 and Priming site 2 primers (Table 4.1.). Plasmids pRK767, pLHR, pRF1, pRF2,

pRF3, and pRF1-2 were digested with HindIII to remove the tetracycline resistance gene, and the chloramphenicol resistance gene was then ligated into the plasmid as a HindIII/HindIII insert. The direction of the insert was confirmed by the amplification with the primers targeting Priming site 1 and M13-F/pUC-F (Table 4.1.). The recombinant plasmids were electroporated into *E. coli* O104:H4 Δ*stx*$_2$:*gfp*:*amp* (Table 4.2. and 4.3.). Exponential-phase cultures of these transformants were treated with mitomycin C (MMC; 0.5 mg/L) for 3 h or with NaClO (10 mM), H_2O_2 (2.5 mM), or PAA (50 mg/L) for 1 h. Control samples were incubated in the same manner without stressors. The method used for the detection of the population of fluorescent cells was similar to that described in reference Hu et al. (2016). Samples were divided into two subpopulations, and the percentage values of GFP-positive cells were calculated.

4.2.7. Quantification of *stx*$_2$ prophage expression in tLST-positive and tLST-negative strains in response to oxidative stress

Exponential-phase cultures of *E. coli* O104:H4 Δ*stx*$_2$:*gfp*:*amp*(pRK767) and *E. coli* O104:H4 Δ*stx*$_2$:*gfp*:*amp*(pLHR) were centrifuged and were resuspended in LB broth containing mitomycin C (0.5 mg/L) or H_2O_2 (2.5 mM), followed by incubation at 37 °C for 1 h. Corresponding treatment of cultures without any addition served as control. After treatment, cells were harvested from samples; RNA was isolated using the RNAprotect Bacteria reagent and the RNAeasy minikit (Qiagen) and was reverse transcribed to cDNA with a QuantiTect reverse transcription kit (Qiagen) according to the manufacturer's protocols. The expression of *gfp* and *recA* was quantified by using SYBR green reagent (Qiagen) and a 7500 Fast PCR system (Applied Biosystems, Foster City, CA, USA). Negative controls included DNase-treated RNA and nontemplate controls. The gene coding for glyceraldehyde-3-phosphate dehydrogenase A (*gapA*) served as the reference gene. The ratios of expression of the *gfp* and *recA* in *E. coli* O104:H4 Δ*stx*$_2$:*gfp*:*amp*(pRK767) to their

expression in *E. coli* O104:H4 Δ*stx*$_2$:*gfp*:*amp*(pLHR) under induced and control conditions were calculated according to the method of Pfaffl (2001). The primers used for the quantification of gene expression are listed in Table 4.1.

4.2.8. Determination of the effects of the tLST on prophage induction in different STECs

The construction of the *p*R'*::rfp*::*chl* reporter system has been described previously (Zhang et al., 2018). To measure the effect of the tLST on the induction of Shiga toxin prophages with different promoters, the tetracycline resistance gene in plasmids pLHR and pRK767 was replaced with the kanamycin resistance gene derived from pKD4 (Datsenko and Wanner, 2000) as described above, and the resulting plasmids were electroporated into *E. coli* FUA1303, *E. coli* FUA1311, and *E. coli* FUA1399. Strains were additionally transformed with *p*R'*::rfp*::*chl* plasmids to obtain transformants where red fluorescent protein (RFP) expression is controlled by the native phage promoter that also controls the expression of the chromosomally encoded prophage, or to obtain RFP expression by alternate phage promoters that are not encoded on the chromosome of the host (Table 4.2. and 4.3.). The expression of *rfp* was measured by flow cytometry as described elsewhere (Zhang et al., 2018).

4.2.9. Detection of the *uspC-IS30-flhDC* marker and virulence genes in *E. coli* wastewater isolates and detection of the tLST in STEC

PCR screening of 102 STEC strains for the three tLST fragments was performed using multiplex PCR with the same primers and protocol that were used for the wastewater and groundwater strains (Table 4.1.).

Seventy *E. coli* wastewater isolates were screened for the presence of the *uspc-IS30-flhDC* marker (Zhi et al., 2019, 2016), as an indicator for a naturalized global lineage of wastewater isolates, and for five virulence genes associated with UPEC (*papC*, *iroN*, *fuyA*, *ibeA* and *saf/foc*).

The genomic DNA of *E. coli* strains was extracted from bacterial cultures by using a DNeasy blood and tissue kit (Qiagen, Hilden, Germany) according to the manufacturer's instructions. Lists of genes and primers are provided in Table 4.1. High-resolution melting (HRM) analysis-qPCR was conducted on a Rotor-Gene Q (Qiagen) system using a Type-it HRM PCR Kit (Qiagen) (Lin and Gänzle, 2014) to detect the target genes listed in Table 4.1. with group-specific primers according to the manufacturer's protocols. Based on the primer annealing temperature (T_A), three pairs of primers with the same T_A but different melting temperatures (*Tm*) of the amplicons were combined in the multiplex PCRs. The melting temperatures of PCR products are presented in Table 4.1. The PCR was optimized with the following conditions: initial denaturation at 95 °C for 5 min, followed by 45 cycles of denaturation at 95 °C for 10s, annealing at the T_A for 30 s, and extension at 72 °C for 30 s. During the HRM analysis stage, the temperature was increased from 65 °C to 95 °C at the speed of 0.1 °C per step and was held for 2 s at each step. Results are presented as means ± standard deviations for three biological replicates.

4.2.10. Statistical analysis

Data were obtained in 10 biological replicates (for the oxidation of membrane lipids) or 3 biological replicates (for all other assays) and are expressed as means ± standard deviations. Data were analyzed by one-way analysis of variance (ANOVA) using SPSS software, version 21.0 (SPSS Inc., Chicago, IL, USA). The least significant difference (LSD) was used to test the difference among means using a *P* value of <0.05.

4.3. Results

4.3.1. The tLST confers resistance to oxidizing chemicals on *E. coli*

A previous study found that 59% of 70 *E. coli* isolates from chlorinated sewage carried the tLST (Zhi et al., 2016). In contrast, none of the STEC groundwater isolates tested in this study

carried the tLST. To test the hypothesis that the tLST contributes to chlorine resistance, the heat and chlorine resistance of 10 tLST-positive and 10 tLST-negative *E. coli* strains isolated from wastewater was determined (Figure 4.2.). Ten tLST-positive wastewater isolates were randomly selected and matched with 10 randomly selected tLST-negative isolates. Two tLST-positive strains, *E. coli* AW1.3 and *E. coli* AW1.7, and the tLST-negative strain *E. coli* AW1.7ΔpHR1 served as

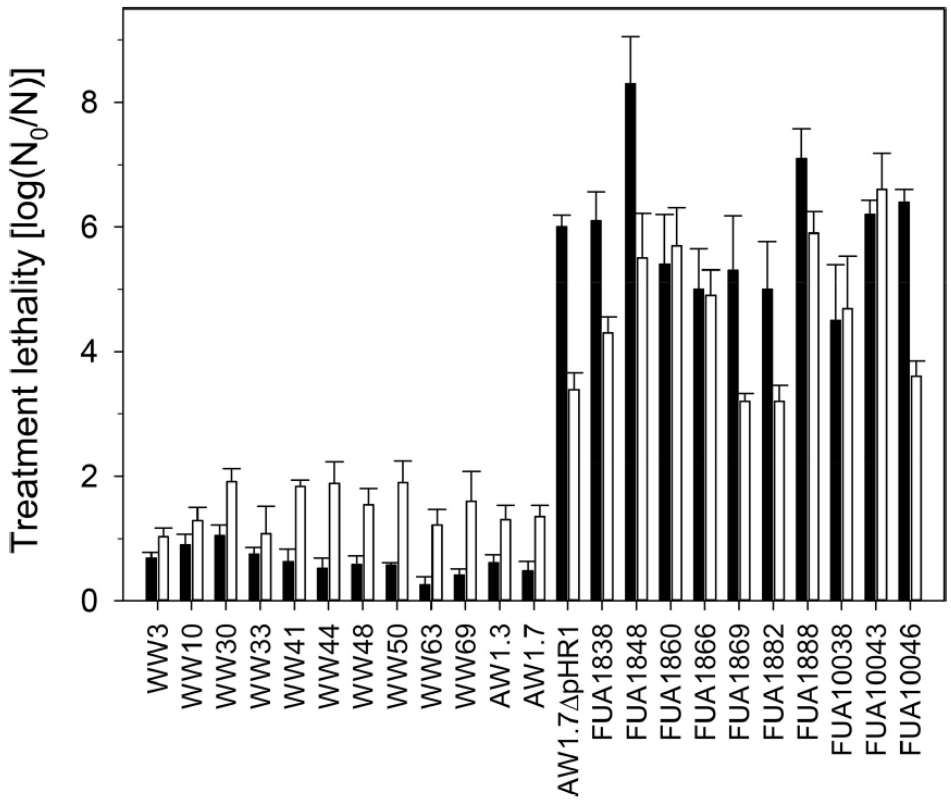

Figure 4.2. Lethality of treatments with heat or chlorine to 23 strains of *E. coli*. The treatment lethality is expressed as the log-transformed ratio of cell counts before treatment (N_0) to cell counts after treatment (N). Filled bars represent cells treated after 60 °C for 5 min; open bar represent cells treated with 15 mM NaClO for 25 min. *E. coli* AW1.7ΔpHR1 and FUA strains are tLST negative; the other 12 strains are tLST positive. Data are shown as means ± standard deviation from three independent experiments.

controls. The reductions in the cell counts of *E. coli* AW1.7 after heat and chlorine treatments were about 6 and 2 log CFU/mL lower, respectively, than the reduction in the cell counts of *E. coli* AW1.7ΔpHR1, a heat-sensitive derivative of AW1.7. Similarly, the lethality of chlorine treatment

against tLST-positive wastewater isolates ranged from 1 to 2 log(N_0/N) [while log(N_0/N) is the log-transformed ratio of cell counts before treatment to cell counts after treatment], while chlorine lethality against tLST-negative wastewater isolates ranged from 3.5 to 6 log(N_0/N) (Figure 4.2.).

The contributions of genes encoded by the tLST to resistance to chlorine and other oxidants were confirmed by cloning fragments of the tLST into *E. coli* MG1655, followed by determination of the lethality of NaClO, H_2O_2, peroxyacetic acid (PAA), and KIO_4. Acrolein and allyl isothiocyanate (AITC) were additionally used as oxidizing chemicals that *E. coli* may encounter in natural habitats. The tLST or tLST fragments were introduced into *E. coli* MG1655 after cloning into the low-copy-number vector pRK767. *E. coli* MG1655 transformed with pRK767 served as vector control (Figure 4.3.). Cloning of the tLST protected against challenge with NaClO, H_2O_2, and PAA but provided no protection against KIO_4, acrolein, or AITC. Protection against NaClO, H_2O_2, and PAA was provided by all plasmids encoding the full-length tLST or fragment 1 or 2; plasmid pRF3 was less effective (against NaClO and H_2O_2) or ineffective (against PAA). Remarkably, cloning of the tLST or any of its parts into of tLST-negative *E. coli* increased the sensitivity to AITC (Figure 4.3.).

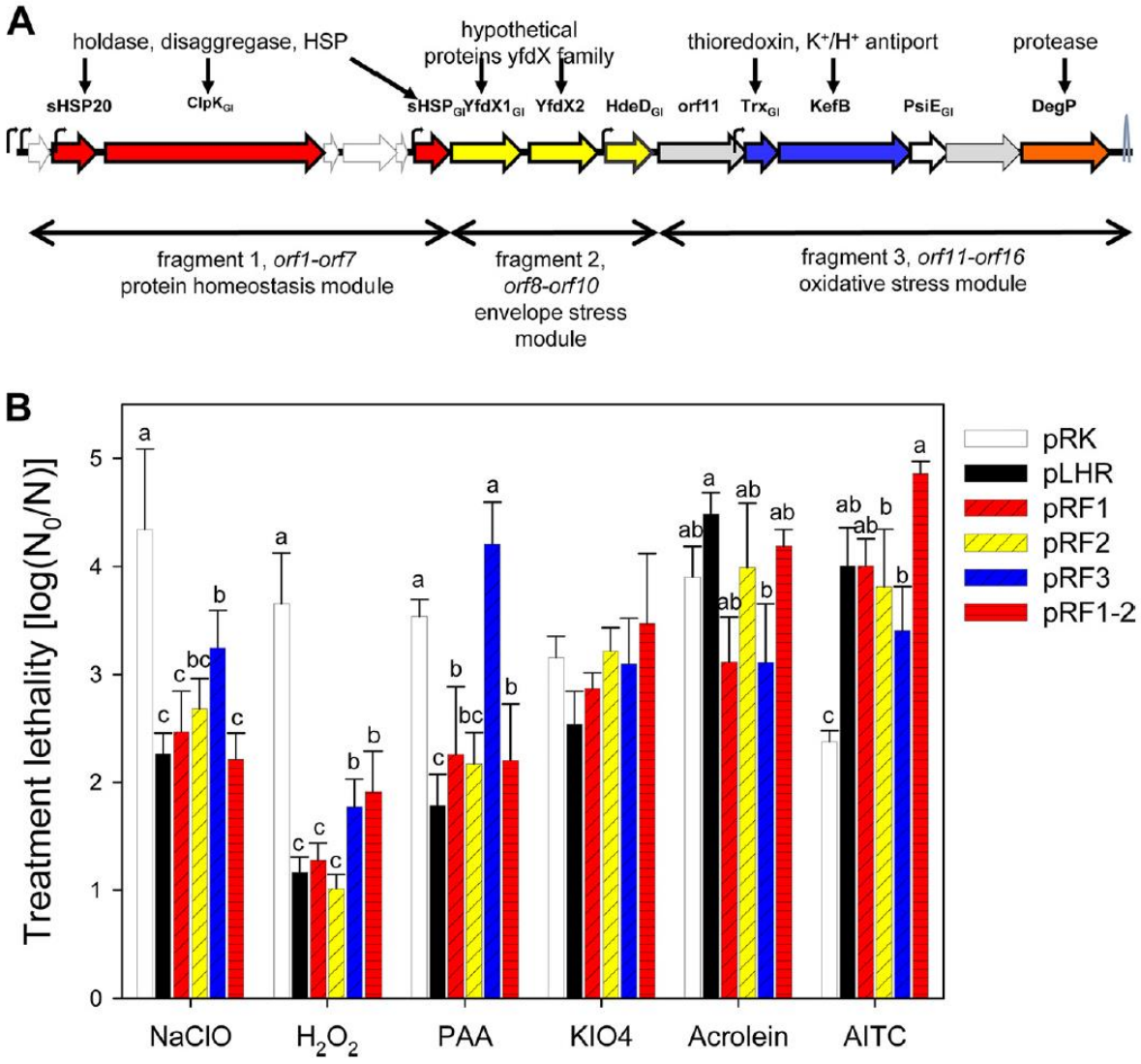

Figure 4.3. Panel A. Schematic representation of the transmissible locus of stress tolerance (tLST1) and putative functions located on the genomic island. Genes that are expressed in *E. coli* MG1655(pLHR) are framed and printed in boldface. Proteins are color coded based on their predicted function: red, heat shock proteins; yellow, hypothetical proteins with a possible relationship to envelope stress; blue, genes related to oxidative stress; orange, DegP with possible relationship to signaling in the Cpx, EvgA and σ^E pathways. Genes carry the subscript "GI" for genomic island if an orthologue of the same gene is present in *E. coli* genomes. Open reading frames are numbered if there is no known function associated with the genes. Predicted promoters are indicated by arrows; the gray caret on the right indicates a predicted terminator. The three fragments of the tLST that were used to assemble pRF1, pRF2, pRF3, and pRF1-2 are indicated below the diagram. Modified according to Mercer et al., (2017a).

Panel B. Lethality of treatment with different oxidants to cultures of *E. coli* MG1655 expressing the tLST or specific fragments of the tLST that are carried on pRF1, pRF2, pRF3, or pRF1-2. Treatment lethality is expressed as the log-transformed ratio of cell counts before treatment (N_0) to cell counts after treatment (N). Cells were treated with 32 mM NaClO, 120 mM H_2O_2,105 mg/L peroxyacetic acid (PAA), 5.80 mM KIO_4, 10 mM acrolein, or 75 µg/mL allyl-isothiocyanate (AITC) for 5 min. Reactions were

Figure 4.3. legend (con't):
terminated by adding an equivalent volume of 10% $Na_2S_2O_3$ as a reducing agent. Values for different plasmids within a treatment that do not have a common lowercase letter are significantly different (P<0.05). Data are shown as means ± standard deviations from three independent experiments.

4.3.2. The tLST prevents the oxidation of multiple cellular targets

The oxidation of cytoplasmic proteins and membrane lipids was assessed in *E. coli* MG1655 transformed with the complete tLST or tLST fragments. Oxidation of cytoplasmic proteins was assessed with the probe roGFP2_Orp1 and ratiometric fluorescence spectroscopy (Degrossoli et al., 2018). Oxidation of the probe enhances green fluorescence when excited at 488 nm but not at 405 nm. For the non-oxidized probe, the ratio of fluorescence intensity at an excitation wavelength of 405 nm to that at an excitation wavelength of 488 nm was equal to 1. Oxidation of the probe increases the green fluorescence and decreases the 405/488-nm fluorescence intensity ratio. In comparison to that for untreated *E. coli* MG1655, a decreased fluorescence ratio of roGFP2_Orp1 upon treatment of *E. coli* MG1655 with NaClO, H_2O_2, or PAA indicated that the probe was oxidized (Figure 4.4.). Insertion of the full tLST sequence reduced the oxidation of the probe, as indicated by a higher 405/488-nm fluorescence ratio (Figure 4.4.). pRF1 prevented probe oxidation as effectively as the full-length tLST, while pRF2 or pRF3 had a fluorescence ratio similar to that of the empty vector of pRK767, indicating that pRF2 and pRF3 had little or no effect on probe oxidation. The protective effects of the tLST against the oxidation of cytoplasmic proteins can thus be attributed to the heat shock proteins encoded by fragment 1 on pRF1.

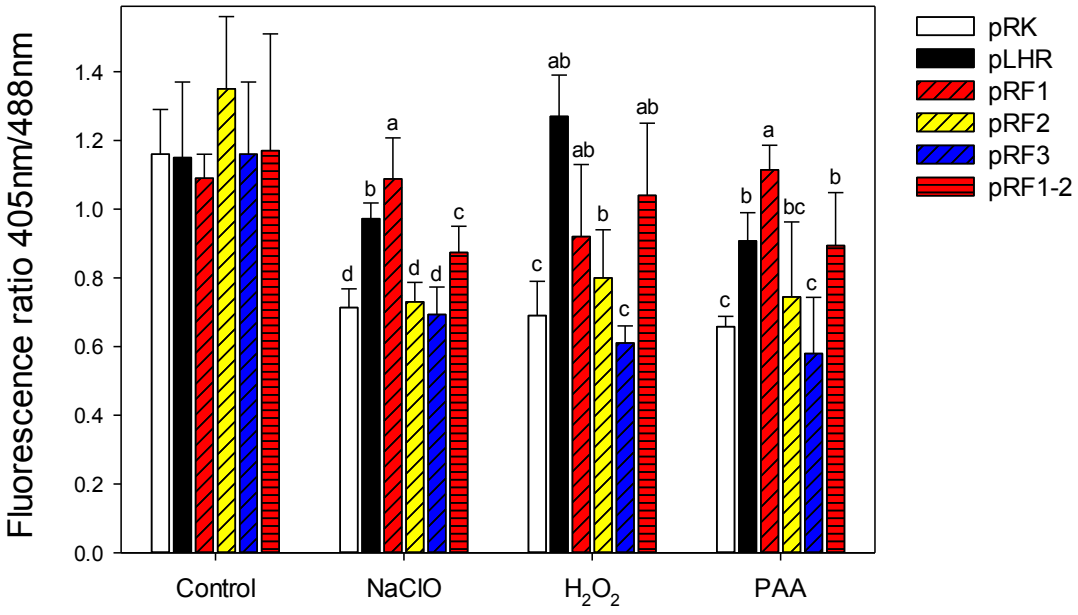

Figure 4.4. Oxidation of roGFP2-based probes expressed in *E. coli* MG1655 with different plasmids (pRK767, pLHR, pRF1, pRF2, pRF3, pRF1-2) after exposure to different oxidants. The ratio of the fluorescence intensity at an excitation wavelengths of 405 to the fluorescence intensity at an excitation wavelength of 488 nm was calculated to indicate the oxidation level in the cytoplasm. Cells either left untreated (control) or were treated for 5 min with 32 mM NaClO, 120 mM H_2O_2, or 105 mg/L peroxyacetic acid (PAA). Values for different plasmids within a treatment that do not have a common lowercase letter are significantly different (P<0.05). Data are means ± standard deviations from three independent experiments.

The oxidation of membrane lipids was determined with the fluorescent probe C11-BODIPY$^{581/591}$, which is sensitive to lipid peroxides in membranes (Fang et al., 2020). The presence of the tLST consistently decreased the population of oxidized cells after treatment of *E. coli* MG1655 or AW1.7 with oxidizing chemicals; a corresponding increase in the population of unoxidized cells was observed after H_2O_2 or PAA treatment (Figure 4.5.; see also Table S4.2. in the supplemental material). A consistent effect of fragments of the tLST was observed only after treatment with H_2O_2; the presence of tLST fragment pRF3 or pRF1-2 resulted in a high number of

unoxidized cells and a correspondingly reduced number of oxidized cells following treatment with H_2O_2.

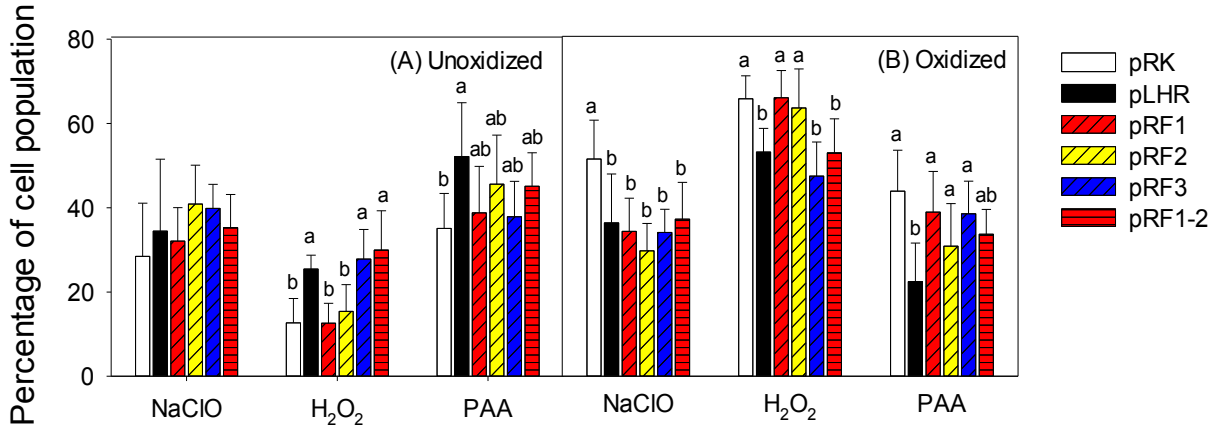

Figure 4.5. Flow cytometric quantification of the oxidation of membrane lipids in *E. coli* MG1655 with different plasmids (pRK767, pLHR, pRF1, pRF2, pRF3, pRF1-2) by use of C11-BODIPY$^{581/591}$ after different treatments. Shown are the levels of stained, unoxidized cells (A) or strained, oxidized cells (B) as percentage of the total cell population Cells were treated for 5 min with 32 mM NaClO, 120 mM H_2O_2, 105 mg/L peroxyacetic acid (PAA). Values for different plasmids within a treatment that do not have a common lowercase letter are significantly different (P<0.05). Data are means ± standard deviations from 10 independent experiments.

4.3.3. The tLST reduces the peroxide-induced induction of the Stx prophage in *E. coli* O104:H4

The expression of the late genes in the Shiga toxin prophage in *E. coli* O104:H4 is induced by oxidative stress (Fang et al., 2017). Quantification of green fluorescent protein (GFP) fluorescence in the reporter strain *E. coli* O104:H4 Δ*stx*$_2$*::gfp*::*amp* is thus an indirect indication of cytoplasmic oxidative stress (Fang et al., 2017). The tLST or tLST fragments were cloned into *E. coli* O104:H4 Δ*stx*$_2$*::gfp*::*amp* to determine the effect of the tLST on the expression of the Shiga toxin prophage. H_2O_2, NaClO and PAA induced GFP expression in *E. coli* O104:H4 Δ*stx*$_2$*::gfp*::*amp* (Figure 4.6.). Cloning of pLHR, pRF1, or pRF1-2 reduced the expression of the

prophage after treatment with any of the three oxidizing chemicals but not after treatment with the positive control mitomycin C (MMC). Cloning of pRF3 reduced prophage induction after treatment with MMC but not after treatment with NaClO or PAA; a modest reduction in the percentage of GFP-expressing cells was observed after treatment with H_2O_2 (Figure 4.6.). The tLST thus reduces the level of oxidative-stress-induced prophage expression, and this effect is predominantly attributable to fragment 1 on pRF1.

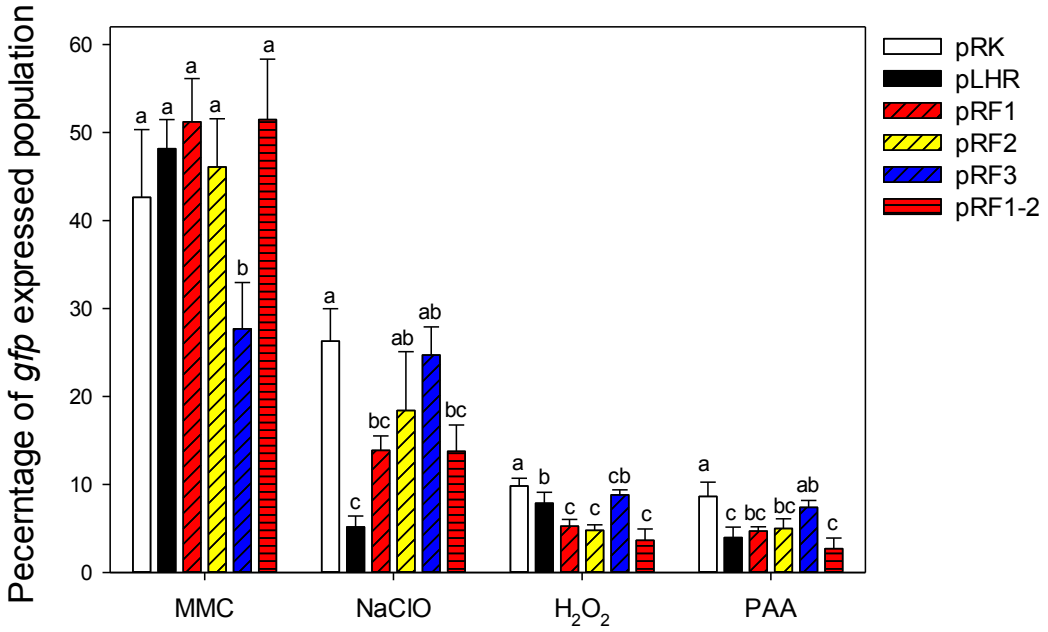

Figure 4.6. Quantification of *stx* expression in the reporter strain *E. coli* O104:H4 Δ*stx*2:*gfp*:*amp* (FUA1302) with different plasmids (pRK767, pLHR, pRF1, pRF2, pRF3, pRF1-2) after exposure to different inducers. Exponential-phase *E. coli* O104:H4 Δ*stx*2:*gfp*:*amp* were incubated at 37 °C with the addition of mitomycin C (MMC; 0.5 mg/L) for 3 h, NaClO (10 mM) for 1 h, H_2O_2 (2.5 mM) for 1 h, or peroxyacetic acid (PAA; 50 mg/L) for 1 h. GFP florescence was quantified by flow cytometry. Values for different plasmids within each treatment that do not have a common lowercase letter are significantly different (P<0.05). Data are means ± standard deviations from at least three independent experiments.

The inhibition of prophage induction by the tLST was confirmed by quantification of *gfp* expression by reverse transcription-quantitative PCR (RT-qPCR). The expression of *gfp* after induction by MMC or H_2O_2 relative to that for uninduced controls was quantified in *E. coli*

O104:H4 Δ*stx*$_2$*::gfp*::*amp*(pLHR) and O104:H4 Δ*stx*$_2$*::gfp*::*amp*(pRK). The tLST reduced the expression of *gfp* after H_2O_2 treatment but not after MMC treatment (Figure 4.7.A.), a finding consistent with the data obtained by flow cytometry (Figure 4.6.). To determine whether the effect of the tLST on prophage induction relates to the RecA-dependent SOS response (Fang et al., 2017), the expression of *recA* was also quantified. The tLST did not affect the expression of *recA* after induction with MMC or H_2O_2 (Figure 4.7.B.).

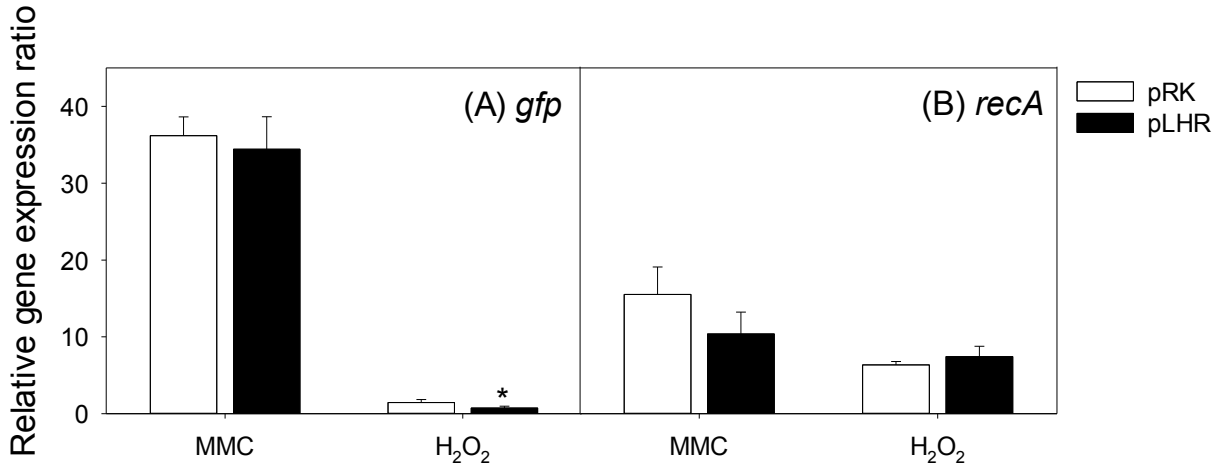

Figure 4.7. Expression of *gfp* (A) and *recA* (B) in *E. coli* O104:H4 Δ*stx2*:*gfp*:*amp* after mitomycin C or H_2O_2 treatment. Relative gene expression was quantified by RT-qPCR with *gapA* as the housekeeping gene and untreated exponential-phase cultures as reference conditions. Exponential-phase cultures were treated with LB broth containing mitomycin C (MMC; 0.5 mg/L) or with H_2O_2 (2.5 mM) for 40 min. Values for different plasmids within a treatment that do not have a common lowercase letter are significantly different (P<0.05). Data are means ± standard deviations from three independent experiments.

4.3.4. The tLST does not interfere with the induction of some but not all of the Stx prophages in *E. coli*

The influence of the tLST on the expression of the Shiga toxin prophage in *E. coli* O104:H4 implies that the genetic island may interfere with the conversion of the prophage to the lytic cycle. The low prevalence of the tLST observed in STEC may indicate that the presence of the tLST

selects against Shiga toxin prophages, or vice versa. About 2% of strains of *E. coli* strains harbor the tLST (Mercer et al., 2015); however, only 0.5% of 615 clinical isolates of STEC and/or *E. coli* O157 have been reported to harbor the tLST (Ma and Chui, 2017). Screening of 100 STEC strains revealed that none of them carried the tLST or parts of the tLST and that none of them exhibited a level of heat resistance equivalent to that of tLST-positive strains (Table S4.3., Gill et al., 2019). The sequence diversity of the late promoter *p*R' region of Stx prophages affects the efficiency of Stx expression in different strains of STEC (Zhang et al., 2018). Therefore, the effects of the tLST on gene expression from different *p*R' regions in native STEC and in heterologous hosts were compared. To investigate if the tLST inhibits the expression of the same *p*R' region in different strains, pLHR and pRK767 were introduced into *E. coli* O157:H7 CO6CE900 (FUA1399), *E. coli* O157:H7 1935 (FUA1303), and *E. coli* O45:H2 05-6545 (FUA1311). These strains were additionally transformed with P*p*1302::*rfp*::*chl*, which carries the *rfp* gene, coding for red fluorescent protein (RFP), under the control of the late promoter of the *E. coli* O104:H4 11-3088 prophage (Tables 4.2. and 4.3.) (Zhang et al., 2018). Prophage expression was induced with H_2O_2, and RFP expression was quantified by flow cytometry. The presence of the tLST resulted in a reduced proportion of cells expressing RFP in all three strains, but the extent of inhibition differed among strains (Figure 4.8.). The effect of the tLST on the expression of the *p*R' region was further evaluated with RFP under the control of promoter *p*R' regions derived from *E. coli* FUA1399, FUA 1303 and FUA1311. Reporter plasmids were cloned in homologous and heterologous hosts. The presence of the tLST decreased the proportion of *E. coli* FUA1399 cells that expressed RFP from promoters *p*1399-28 and *p*1399-79, but the proportion of cells that expressed RFP remained unchanged with *p*1303-s1 and increased with *p*1303-2a in *E. coli* FUA1303 and with *p*1311 in *E. coli* FUA1311. These results demonstrate that the induction of the Shiga toxin promoter in the

presence of the tLST was diverse, due to the sequence diversity of the *p*R' region and prophage-encoded regulatory proteins in different strains.

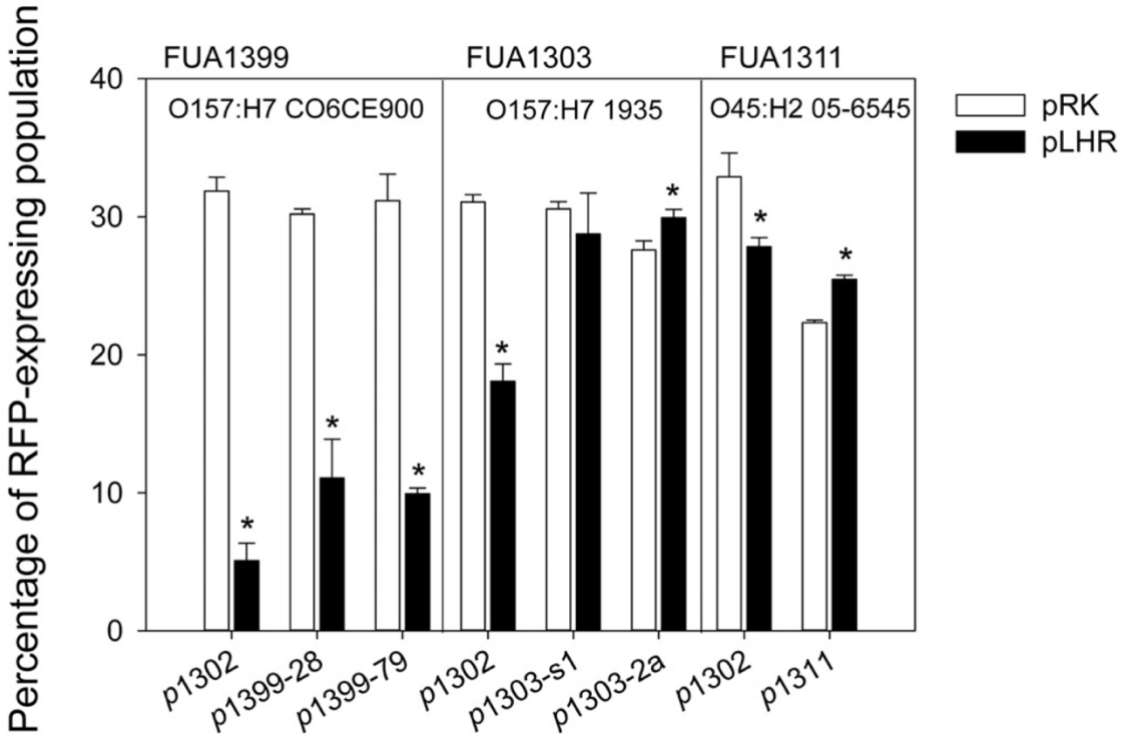

Figure 4.8. The effect of the tLST on the expression of RFP under the control of *p*R' promotors derived from Shiga toxin-producing *E. coli*. Data are the percentage of cells expressing RFP after induction with H_2O_2. RFP florescence was quantified by flow cytometry. The graph compares STEC strains carrying pLHR with STEC strains carrying pKR767 as a control. Promotor activity was assessed with *p*R'::*rfp*::*chl* cloned into three strains of STEC. Plasmid *p*R'::*rfp*::*chl* containing the *p*R' promotor derived from *E. coli* O104:H7 (FUA1302), was cloned into all strains. In addition, each strain was transformed with a plasmid harboring a fusion of *p*R'::*rfp*::*chl* with the *p*R' promotor(s) present in that strain; i.e., *p*1399-28 and *p*1399-79 in *E. coli* O157:H7 CO6CE900 (FUA1399), *p*1303-s1 and *p*1303-2a in *E. coli* O157:H7 1935 (FUA1303), and *p*1311 in *E. coli* O45:H2 05-6545 (FUA1311). Significant differences ($P<0.05$) in promotor activity between strains with pLHR and strains with pRK767 are indicated by an asterisk. Data are means ± standard deviations from three independent experiments.

4.3.5. The tLST is correlated with the absence of most UPEC virulence factors

Seventy *E. coli* wastewater isolates were screened for the tLST, a wastewater marker (IS*30*), and five virulence factors of UPEC to identify tLST-positive strains of UPEC (Table 4.4.). Among

the 70 isolates, 22.9% (16/70) were tLST-positive and 40% (28/70) carried virulence factors that are typical for UPEC. Two of 16 tLST-positive strains carried *fyuA*, which encodes the yersiniabactin receptor (Spurbeck et al., 2012). The other 14 tLST-positive strains excluded UPEC virulence factors. Conversely, 26 of the 28 strains with UPEC virulence factors, and in particular all strains with multiple virulence factors, were tLST-negative (Table 4.4.) Both IS*30*-positive strains carried the tLST, matching prior results (Zhi et al., 2016).

4.4. Discussion

The tLST positive strains of *E. coli* have been observed at increased frequency in wastewater after chlorination, pointing to a contribution of the tLST to chlorine resistance (Zhi et al., 2016). This study documented, with multiple and complementary experimental methods (Degrossoli et al., 2018; Fang et al., 2020; Naguib, 1998), that the tLST protects against oxidative stress. The use of multiple methods to quantify the survival and oxidation of cellular components not only confirmed the protective effect of the tLST but also provided information on the mechanisms of protection.

4.4.1. The tLST and stress resistance in *E. coli*

The tLST protected against NaClO, H_2O_2, and peroxyacetic acid but not against KIO_4, acrolein, or AITC. Acrolein is generated *in vivo* by the chemical conversion of β-hydroxy propionaldehyde, a metabolite of intestinal bacteria including *Salmonella enterica* and *Lactobacillus reuteri* (Engels et al., 2016; Stevens and Maier, 2008). AITC is formed from glucosinolates in plants of the *Brassicaceae* family upon cellular injury and reacts with sulfhydryl groups and disulfide bonds (Kojima, 1971). KIO_4 has been suggested to contribute to electrochemical inactivation of *E. coli*, but the mechanisms of activity remain unclear (Okochi et al., 2005). The selective protective effect of the tLST against oxidizing organic and inorganic

chemicals may relate to differences in the chemical reactivity and permeance of the compounds for the cytoplasmic targets. The presence of the tLST consistently increased resistance to chlorine and peroxides, which are a mainstay in the sanitation of water and in food-processing plants; therefore, further experiments focused on these chemicals.

The tLST encodes proteins that are involved in protein folding or disaggregation and may protect against oxidative stress (Figure 4.1.) (Mercer et al., 2015). The heat shock proteins encoded by the protein homeostasis module (fragment 1), sHSP20, $ClpK_{GI}$, and $sHSP_{GI}$, prevent protein aggregation or disaggregate proteins (Lee et al., 2018; Mercer et al., 2017a). In agreement with the function of these proteins, transformation of *E. coli* with this portion of the tLST provided the greatest protection of cytoplasmic proteins from oxidation but was less protective of membrane lipids. The tLST fragment 3 did not protect against chlorine or the oxidation of cytoplasmic components but decreased the oxidation of membrane lipids (Figures 4.3. to 4.5.). The role of the oxidation of membrane lipids in chlorine resistance is poorly documented (Figure 4.1.). The oxidative stress module (Fragment 3) encodes for thioredoxin, KefB and DegP. Thioredoxin protects against oxidative stress through thiol-disulfide exchange reactions (Holmgren, 1979). KefB may have a function related to oxidative stress; it is a K^+/H^+ antiporter that protects against two electrophiles, methylglyoxal and N-ethylmaleimide (Ferguson et al., 1993a). The serine protease DegP is a periplasmic chaperone that prevents or reduces the iron-induced oxidation of membrane proteins (Skórko-Glonek et al., 1999). Fragment 2 encodes $YfdX1_{GI}$ and YfdX2, two hypothetical proteins of unknown function, and $HdeD_{GI}$, a stress protein whose relation to oxidative stress is unknown (Mates et al., 2007). These genes protected against chlorine and provided limited protection against the oxidation of membrane lipids but did not prevent the oxidation of cytoplasmic proteins. These findings not only confirm the previous designation of

fragment 2 as an "envelope stress module" (Mercer et al., 2017a) but also suggest additional, undescribed mechanisms of protection. Taking these findings together, the contribution of the tLST to chlorine resistance is based on the protection of multiple cellular targets by different parts of the tLST. The multifaceted mechanisms of protection provided by the tLST also explain its contribution to resistance to multiple stressors, including heat, chlorine, and peroxides (Lee et al., 2018, 2015; Mercer et al., 2017a, 2015).

Two distinct tLST variants in *E. coli* confer equivalent heat resistance (Boll et al., 2017). tLST 2 is a 19-kb genomic island that contains 5 open reading frames (ORFs) that are not carried by the tLST but lacks two proteins encoded by the tLST (Boll et al., 2017; Mercer et al., 2015). Proteins that are present in both versions of the genomic island include sHSP20, $ClpK_{GI}$, $sHSP_{GI}$, $YfdX1_{GI}$, YfdX2, KefB, *orf15*, and DegP; these proteins appear to be essential for the role of the genomic island in bacterial stress resistance.

4.4.2. The tLST and virulence of *E. coli*

The tLST is a mobile genetic element that occurs in diverse members of the *Gammaproteobacteria* and *Betaproteobacteria*. The tLST has been identified in one *Salmonella* strain and in several isolates of *Cronobacter* spp. and *Klebsiella* spp. (Boll et al., 2017; Mercer et al., 2017b). The frequency of the tLST in STEC is very low compared to that in the general population of *E. coli* (Ma and Chui, 2017; this study). Genes coding for Shiga toxin production are invariably found in the late region of prophages. Shiga toxin production by *E. coli* has been proposed to protect against predatory protozoa, which are significant *E. coli* predators in the rumen but are less prevalent in other ecosystems that are relevant for the evolution of *E. coli* (Łoś et al., 2013). Expression of the Shiga toxin is upregulated in the lytic cycle of the phage, which is lethal to the host cell, but it has been hypothesized that Shiga toxin production by engulfed cells will kill

the predator, reducing predation on the remainder of the population. Accordingly, STEC are highly associated with diverse ruminant hosts (Imamovic et al., 2009). One explanation of the low overlap of the tLST and Shiga toxin production in *E. coli* is ecological incompatibility; i.e., ecosystems that select for maintenance of the Shiga toxin select against the tLST, and vice versa. Molecular incompatibility is an alternative explanation; i.e., the tLST interferes with the expression of Shiga toxin prophages and hence reduces or abolishes the ecological advantage conferred by lysogeny.

The lytic cycle of the Shiga toxin prophage is regulated by the DNA repair protein RecA and is induced in response to DNA damage and/or oxidative stress. If the tLST protects against oxidative stress it also reduces Shiga toxin production in response to predation by protozoa and may reduce the selective pressure to maintain the Shiga toxin prophages in STEC. Reduced expression of GFP as an indicator for Stx expression was observed in *E. coli* O104:H4 but not for all Shiga toxin prophages in other STEC strains. Different Shiga toxin prophages respond differently to inducing agents (Łoś et al., 2009; Zhang et al., 2018). In this study it was observed that all the prophage promoters investigated responded to H_2O_2, but not all responded to mitomycin C, which is routinely used to induce lambdoid prophages, including Shiga toxin prophages. In summary, the tLST interfered with the induction of some, but not all, Shiga toxin prophages. Thus, it does not appear that the tLST is generally incompatible with the contribution of Shiga toxin to the ecological fitness of *E. coli* in response to protozoan predation. The assumption that the tLST increases fitness in ecological niches in which Shiga toxin prophages do not provide a selective advantage, is a more likely explanation for the low cooccurrence of these two mobile genetic elements in *E. coli.*

Naturalized strains of *E. coli* found in wastewater possess the tLST, are resistant to chlorine, and carry as many as 44 different virulence genes associated with UPEC (Zhi et al., 2019, 2016).

UPEC strains appear to differentially survive wastewater treatment processes, including chlorination and UV-C irradiation (Adefisoye and Okoh, 2016; Anastasi et al., 2013, 2010). Interestingly, the proportion of antibiotic-resistant UPEC cells has been reported to be higher in water after treatment with chlorine (Rijavec et al., 2006; Xi et al., 2009). Collectively, these studies led us to hypothesize that antibiotic resistance correlates with the increased likelihood of UPEC surviving wastewater treatment (chlorination and oxidation). The tLST-positive *E. coli* and UPEC strains were found to exist in wastewater, and the prevalence of the tLST in waste water isolates of *E. coli*, 23%, is about 10-fold higher than that in the general population of *E. coli,* 2%. Surprisingly, this study found low co-occurrence of the tLST and UPEC virulence factors in 70 wastewater isolates. This finding should be confirmed by screening a larger number of strains or genomes, but it suggests that the tLST may not account for the resiliency of UPEC in surviving wastewater treatment processes and attests to the diverse mechanisms by which microbes evolve resistance to wastewater treatment processes.

4.5. Conclusions

In conclusion, the tLST confers resistance to heat and oxidative stress on *E. coli*. The protein homeostasis module provided protection to the contents of the cytoplasm while the oxidative stress module provided protection to membrane lipids. In addition, the reduction effect of the tLST on Shiga toxin expression was specific to the late promoter regions and regulatory proteins. The low prevalence of the tLST in STEC and UPEC strains indicates that the selective pressure for maintenance of the tLST in *E. coli* is different from the selective pressure that maintains Shiga toxin prophages and UPEC virulence factors. This study also shows that water chlorination selects for tLST-positive *E. coli* strains that are heat- and chlorine resistant.

Table 4.1. PCR primers used in this study

Gene target	Primer name	Primer sequence (5'-3')	T_A[a] (°C)	Tm[b] (°C)	Reference
LHR-F1	LHRmF1-F	GCCCGGTGTCGAGGAGAAGG	62.5		This study
	LHRmF1-R	AAGAATGGCCGAGTTCATTGGAGG	59.4		This study
LHR-F2	LHRmF2-F	GCGCGATGCCAAGCAGAACG	62.4		This study
	LHRmF2-R	TGAACGCGCCATTGACCAAGG	60.8		This study
LHR-F3	LHRmF3-F	GGAGACGCTGAGCTTTCTGTCCG	61.7		This study
	LHRmF3-R	CGCAGCAGCCAGTAGGTCG	61.1		This study
LHR-F1	LHRF1-F	TCGTCTACAAGCGTGATCC	58	88.03±0.27	This study
	LHRF1-R	GTCACGCAAACGGATGG			
LHR-F2	LHRF2-F	TCCGAGCTAAGGTGGAATG	58	82.84±0.22	This study
	LHRF2-R	CTGCTTGCCACTTCGTTATC			
LHR-F3	LHRF3-F	ACCGAGCTGATTGAAGGA	58	86.13±0.32	This study
	LHRF3-R	AGCGACACCACGATGAT			
chl^r/*kan*^{r}	Priming site 1	ATCGAAAGCTTGTGTAGGCTGGAGCTG	60		(Datsenko and Wanner, 2000)
	Priming site 2	TAAGGAGGATATTCATATG			
	M13/pUC-F	CCCAGTCACGACGTTGTAAAACG	60		Invitrogen
gfp	gfp-F	TTCTTCAAGTCCGCCATG	55		(Fang et al., 2017)
	gfp-R	TGAAACGGCCTTGTGTAGTATC			
recA	recA-F	ATTGGTGTGATGTTCGGTAA	55		(Fang et al., 2017)
	recA-R	GCCGTAGAGGATCTGAAATT			
gapA	gapA-F	GTTGACCTGACCGTTCGTCT	55		(Fang et al., 2017)
	gapA-R	ACGTCATCTTCGGTGTAGCC			
uspC-IS30-*flhDC*	flh-IS-F	CGGGGAACAAATGAGAACAC	60	80.33±0.37	Zhi et al., (2016)
	flh-IS-F	TGGAGAAACGACGCAATC			
ibeA	ibeA-F	AGGCAGGTGTGCGCCGCGTAC	62	81.90±0.54	White et al., (2011)
	ibeA-R	TGGTGCTCCGGCAAACCATGC			
papC	papC-F	GTGGCAGTATGAGTAATGACCGTTA	60	84.69±0.17	White et al., (2011)
	papC-R	ATATCCTTTCTGCAGGGATGCAATA			
saf/foc	sfa/foc-F	CTCCGGAGAACTGGGTGCATCTTAC	60	83.25±0.22	White et al., (2011)
	sfa/foc-R	CGGAGGAGTAATTACAAACCTGGCA			
fyuA	fuyA-F	TGATTAACCCCGCGACGGGAA	62	87.74±0.23	White et al., (2011)
	fuyA-R	CGCAGTAGGCACGATGTTGTA			
iroN	iroN-F	AAGTCAAAGCAGGGGTTGCCCG	62	84.78±0.31	White et al., (2011)
	iroN-R	GACGCCGACATTAAGACGCAG			

[a] Primer annealing temperature

[b] Melting temperature. Results are shown as means ± SD (n=8).

Table 4.2. Plasmids used in this study and antibiotics used for plasmid maintenance

tLST plasmids ((Mercer et al., 2015)	Modified LHR plasmids (this study)	Probe plasmids ((Degrossoli et al., 2018)	Promoter plasmids (Zhang et al., 2018)
Tetracycline (15 mg/L)	Chloramphenicol (34 mg/L) or kanamycin (30 mg/L)	Ampicillin (100 mg/L)	Chloramphenicol (34 mg/L)
pRK767::*tet*^{r}	pRK767::*chl*^{r}	pCC_roGFP2_Orp1	P*p*1302:: *rfp*::*chl*^{r}
pLHR::*tet*^{r}	pLHR::*chl*^{r}		P*p*1303-1::*rfp*::*chl*^{r}
pRF1::*tet*^{r}	pRF1::*chl*^{r}		P*p*1303-2a::*rfp*::*chl*^{r}
pRF2::*tet*^{r}	pRF2::*chl*^{r}		P*p*1311::*rfp*::*chl*^{r}
pRF3::*tet*^{r}	pRF3::*chl*^{r}		P*p*1399-28::*rfp*::*chl*^{r}
pRF1-2::*tet*^{r}	pRF1-2::*chl*^{r}		P*p*1399-79::*rfp*::*chl*^{r}
	pRK767::*kan*^{r}		
	pLHR::*kan*^{r}		

Table 4.3. Strains used in this study

Strain and FUA number[a]	Description	Promoter/Probe plasmids use in the strain	Reference
E. coli MG1655		Host for tLST plasmids and probe plasmid	
E. coli O104:H4 11-3088 Δ*stx*::*gfp*::*amp*^{r}	*stx* gene replaced with *gfp*	Host for modified tLST plasmids	(Fang et al., 2017)
E. coli O104:H4 11-3088 FUA1302	*stx2a*		(Mercer et al., 2015)
E. coli O157:H7 1935 FUA1303	*stx1*, *stx2a*	Host for pRK767::*kan*^{r}, pLHR::*kan*^{r} and P*p*1302:: *rfp*::*chl*^{r}, P*p*1303-1:: *rfp*::*chl*^{r}, or P*p*1303-2a:: *rfp*::*chl*^{r}	
E. coli O45:H2 05-6545 FUA1311	*stx1*	Host for pRK767::*kan*^{r}, pLHR::*kan*^{r} and P*p*1302:: *rfp*::*chl*^{r} or P*p*1311::*rfp*::*chl*^{r}	
E. coli O157:H7 CO6CE900 FUA1399	*stx2a*	Host for pRK767::*kan*^{r}, pLHR::*kan*^{r} and P*p*1302:: *rfp*::*chl*^{r}, P*p*1399-28::*rfp*::*chl*^{r} or P*p*1399-79::*rfp*::*chl*^{r}	

[a] the FUA number was used for plasmid nomenclature, i.e. the origin of the promoter is identified by the FUA number.

Table 4.4. Screening of the transmissible locus of stress tolerance (tLST), IS30 and virulence genes in 70 wastewater *E. coli* strains (+: positive and -: negative). Screening results for each strains are shown in Table S4.1. of the supplementary material.

Number of strains	Targets						
	tLST	IS30	*ibeA*	*papC*	*saf/foc*	*fyuA*	*iroN*
2	+	+	-	-	-	-	-
2	+	-	-	-	-	+	-
12	+	-	-	-	-	-	-
4	-	-	+	+	+	+	+
1	-	-	-	+	+	+	+
1	-	-	+	-	+	+	+
4	-	-	+	-	-	+	+
1	-	-	-	-	-	+	+
3	-	-	-	+	-	+	-
1	-	-	+	-	-	+	-
1	-	-	-	-	+	+	-
2	-	-	+	-	-	-	-
7	-	-	-	-	-	+	-
1	-	-	-	-	-	-	+
28	-	-	-	-	-	-	-

CHAPTER 5. Ecology and Function of the Transmissible Locus of Stress Tolerance in *Escherichia coli* and Plant-associated *Enterobacteriaceae*

5.1 Introduction

Enterobacteriaceae occupy diverse ecological niches, including environmental, plant-associated, and vertebrate-associated habitats (Adeolu et al., 2016). Plant-associated organisms include *Klebsiella*, *Enterobacter*, and *Cronobacter*, which occur as seed endophytes and promote plant growth (Hinton and Bacon, 1995; Loaces et al., 2011; Pavlova et al., 2017). Some of these plant-associated bacteria also colonize the intestine of vertebrates, including humans, and cause opportunistic infections in humans (Healy et al., 2010; Kakatkar et al., 2017). In the genus *Escherichia, E. fergusonii* is found as a seed endophyte (Silva et al., 2012); *Escherichia coli* is more commonly found as commensal or pathogen of vertebrates but also occurs in environmental niches and retains genes for plant colonization (Byappanahalli et al., 2006; Holmes et al., 2020). Strains of *Escherichia coli* rarely form stable associations with specific host individuals, and the population genetics of *E. coli* reveals only very recent phylogenetic signatures of host adaptation (Pupo et al., 2000; Tenaillon et al., 2010). Niche specialization is largely mediated by lateral gene transfer (Croxen et al., 2013; Holt et al., 2020; Mercer et al., 2015). The roles of mobile genetic elements, including the virulence plasmid pINV of *Shigella*, Stx-encoding prophages, and the locus of enterocyte effacement of enteropathogenic *E. coli*, in genome plasticity and virulence of *E. coli* are well understood (Croxen et al., 2013; Herold et al., 2004; Schmidt and Hensel, 2004). In contrast, the contribution of mobile genetic elements to the ecological fitness of *E. coli* and other *Enterobacteriaceae* in extraintestinal habitats is poorly documented (Holmes et al., 2020; Jang et al., 2017; Luo et al., 2011).

The transmissible locus of stress tolerance (tLST), previously termed locus of heat resistance (LHR), is a genomic island in *E. coli* and related *Enterobacteriaceae* which confers

resistance to heat and chlorine (Gajdosova et al., 2011; Kamal et al., 2021; Mercer et al., 2017b, 2015; Wang et al., 2020, 2018). Genomic islands with similar sequence and function were designated $tLST2_{C604\text{-}10}$ and $tLST2_{FAM21805}$ (Boll et al., 2017). Different tLST variants confer equivalent heat resistance, which indicates that only those genes that are present in all variants of tLST are essential, including the small heat shock protein sHsp20, the heat shock disaggregase ClpK, the small heat shock protein $sHsp_{GI}$, the periplasmatic chaperones PscA, and PscB, the potassium efflux system KefB, *orf14* with unknown function, and the periplasmic protease DegP (Boll et al., 2017; Mercer et al., 2015). Genomic, proteomic and physiological analyses also indicated that those tLST genes are essential to confer the full heat resistance phenotype (H. Li et al., 2020; Mercer et al., 2017a, 2015; Wang et al., 2020). The contribution of individual genes to the resistance phenotype and their ecological role, however, remain to be established. The sHsps and ClpG ($ClpK_{GI}$) increase heat resistance through protein homeostasis (Lee et al., 2018; Mogk and Bukau, 2017). Cloning of sHsps and $ClpK_{GI}$, however, did not confer full resistance to heat or chlorine (Mercer et al., 2017b, 2015; Wang et al., 2020), and the function of other core proteins remains unknown.

The frequency of the tLST in *E. coli* is about 2% (Mercer et al., 2015), but the tLST rarely co-occurs with virulence genes in *E. coli* (Wang et al., 2020), and the tLST has only rarely been identified in *Salmonella* (Boll et al., 2017; Mercer et al., 2017b; Nguyen et al., 2017). The tLST is highly conserved in different species of *Enterobacteriaceae* and is consistently flanked by mobile genetic elements, implying recent lateral gene transfer (Mercer et al., 2015). Species that include strains harboring the tLST (also) occur in the environment or in association with plants in addition to a lifestyle as opportunistic pathogens (Botzler, 1987; Dong et al., 2003; Johnston-Monje and Raizada, 2011; Schmid et al., 2009), however, it remains unclear whether the tLST is related to

the plant associated lifestyle of these organisms. This study, therefore, aimed to determine the distribution of the tLST in the *Enterobacteriaceae* as well as the fitness cost that is associated with its maintenance to assess whether the genomic island links to adaptation to plant-associated habitats. Experiments that determined the ecological fitness of *E. coli* mutants with deletions in single open reading frames of the tLST were informed by determination of the function of core genes of the tLST.

5.2. Materials and methods

5.2.1. Phylogenetic analysis of the tLST in *Enterobacterales*

A total of 30,033 draft genomes of *Enterobacteriaceae* were retrieved from GenBank (Table S5.2.) and annotated with Prodigal (Hyatt et al., 2010). The four sequence variants of the tLST (Figure 5.1.A.) were screened against the 30,033 genomes using BLASTp (http://blast.ncbi.nlm.nih.gov/Blast.cgi) with cutoff values of 80% coverage and an E value $\leq 10^{-5}$. Nine sequences of $tLST2_{FAM21805}$, 16 sequences of $tLST2_{c604\text{-}10}$, 34 sequences of tLSTa, and 175 sequences of tLST1 were used for the construction of a phylogenetic tree of the tLST. Roary was used to find the ortholog protein families of the 4 versions of the tLST, and 10 proteins were classified as the core genome of the tLST with an identity threshold of 80%. These 10 open reading frames (ORFs) were aligned by Muscle (v3.8.31) and joined by an in-house Python script for use as input file to IQ-tree (v1-6.12). The best model, "HIVb+F+R3", was selected by ModelFinder. The maximum likelihood tree was visualized using Interactive Tree of Life (Letunic and Bork, 2019).

Metadata that is available with the genome sequences were used to select clinical and environmental *C. sakazakii* strains, 102 and 267 genomes, respectively, as well as clinical and environmental *K. pneumoniae* strains, 250 and 360, respectively, which were screened using

BLASTn for the presence of tLST1 (NZ_LDYJ01000141) with an 80% query cover cutoff of the nucleotide sequence. All available *C. sakazakii* and environmental *K. pneumoniae* isolates were used; for genomes from clinical isolates of *K. pneumoniae*, only one strain was selected from each depositing source.

5.2.2. Screening of the tLST and plant growth-promoting genes in *K. pneumoniae*

Briefly, genomes of *K. pneumoniae* isolates from different sources were obtained from Refseq database, 84 strains were from animals; 170 strains were from the environment, 121 strains were from humans, and 57 strains were from plants. Prokka 1.14.6 was used for genome annotation. The presence of tLST1, *nthA* (56938764), *phnA* (948621), *phnH* (948619), *phnI* (948605), *phnJ* (948606), *phnK* (948611), *phnL* (948612), *phnM* (948613), and *nifH* (56937870) were screened by BLASTp with cutoff values of 80% coverage of the amino acid sequence and an E value $\leq 1\times10^{-5}$. BLAST results were filtered with an in-house Python script.

5.2.3. Determination of heat and chlorine resistance in environmental and clinical isolates

The strains from FUA10289 to FUA10298 were isolated from water collected at different geographic locations (Table S5.3.). Water (1 mL) was spread with an L-shape cell spreader on Luria-Bertani (LB) agar plates, and the plates were incubated at room temperature for 48 h. After incubation, 10 colonies from each morphology per place were re-streaked on LB plates. Clonal isolates were eliminated by random amplified polymorphism DNA (RAPD)-PCR. The RAPD-PCR protocol consisted of in initial denaturing step of 1 min at 96 °C, followed by 3 cycles at 96 °C for 3 min, 35 °C for 5 min, and 75 °C for 5 min and 32 cycles of denaturing at 96 °C for 1 min, 55 °C for 2 min, and 75 °C for 3 min. Isolates from the same sample that displayed identical RAPD patterns were considered clonal isolates; one representative per isolate was identified at the species level by Sanger sequencing of the 16S rRNA genes. The presence of different versions of

the tLST in water isolates and clinical isolates of *Klebsiella* (Table S5.3.) was determined with primers shown in (Table S5.4.). To determine the heat resistance, overnight cultures of strains were treated at 60 ℃ for 0, 5, 10, 15, and 20 min. To determine the chlorine resistance, overnight cultures of strains were treated with 32 mM NaClO for 0, 3, 5, and 12 min. The reaction was terminated by the addition of 50 μL of 10% $Na_2S_2O_3$. Appropriate dilutions before and after treatment were plated on LB agar and incubated at 30 °C for 24 h. Results are expressed as the log-transformed ratio of cell counts before and after treatments [$\log(N/N_0)$].

5.2.4. Construction of *E. coli* MG1655 *lacZ*::LHR

The tLST was inserted into *lacZ* operon in *E. coli* MG1655 (WT) by the no-SCAR (Scarless Cas9 Assisted Recombineering) system (Reisch and Prather, 2015). To construct the single guide RNA (sgRNA) plasmid, a set of primers (sgRNA-*lacZ*-F/R) was used to PCR amplify the pKDsg-cr4 backbone. The 20 bp spacer sequence specific for *lacZ* was synthesized in primers to construct pKDsg-*lacZ*. The plasmid pLHR (Mercer et al., 2015) was purified using a Qiagen plasmid midiprep kit (Qiagen). The plasmid was digested with the DraI enzyme (Thermofisher) to linearize the plasmid. *E. coli* MG1655 that possessed both the pCas9cr4 and pKDsg-*lacZ* were grown to an optical density at 600 nm (OD_{600}) of approximately 0.5 in super optimal broth (SOB) medium with chloramphenicol (34 mg/L) and spectinomycin (50 mg/L) at 30 °C. λ red was induced with the addition of 50mM L-arabinose, incubated for 20 minutes, and the cells were then made electrocompetent by washing with 10% ice-cold glycerol. The linearized pLHR (500 ng) was electroporated into the induced cells, and 950 μL of super optimal broth with catabolite repression (SOC) medium was added; after 2 h, the culture was transferred to LB broth containing chloramphenicol (Cm; 34 mg/L), spectinomycin (spec; 50 mg/L), and anhydrotetracycline (aTC; 100 μg/L) and incubated at a 30°C shaker overnight. To select the mutant, 200 μL of the overnight

culture was heated at 60 °C for 5 min and plated on LB with IPTG (Isopropyl β-D-1-thiogalactopyranoside; 0.2 mM) and 5-bromo-4-chloro-3-indolyl-β-D-galactopyranoside (X-gal; 40 mg/L). After incubation at 37 °C overnight, white colonies grown on the plate were confirmed with primers tLST-16-F/*lacZ*-upstream, tLST-2-R/*lacZ*-downstream, and *pscA*-check-F/R. Afterwards, the colonies were patched on plates with or without Cm (34 mg/L) to test the loss of pKDsg-*lacZ*. The pKDsg-p15 plasmid was electroporated into *E. coli* MG1655 *lacZ*::LHR (pCas9cr4) to cure the plasmid pCas9cr4. The transformants were recovered in SOC for 1 h at 30 °C and then aTC (100 μg/L) was added and incubated for additional 2 h before plating on LB plated with spec (50 mg/L) and aTC (100 μg/L). After overnight growth at 37 °C, the resultant colonies were patched onto LB plates with and without Cm (34 mg/L) to test the loss of the pCas9cr4. Finally, *E. coli* MG1655 *lacZ*::LHR (pKDsg-p15) cells were grown at 42 °C to lose the plasmid, and colonies were tested on the spec plates (50 mg/L).

5.2.5. Deletion of 13 genes encoded by the tLST (Δ*orf* mutants)

E. coli MG1655 *lacZ*::LHR carrying plasmid pKD46 (Datsenko and Wanner, 2000) was cultured in LB broth containing 100 mg/L ampicillin and 10 mM L-arabinose at 30°C until turbidity at 600 nm reached 0.4~0.6. The cells were harvested and washed three times with ice-cold 10% glycerol to prepare electrocompetent cells. A PCR amplicon containing the chloramphenicol resistance gene (amplified from pKD3) flanked upstream and downstream by sequences of the target genes was obtained using primers in Table S5.4. PCRs were carried out using Phusion high-fidelity DNA polymerase (Thermo Scientific) according to the manufacturer's guidelines. Afterwards, the PCR products containing the 40- to 220-bp homologous sequence arms at each end of the chloramphenicol resistance cassette were electroporated into electrocompetent cells. Transformants were screened on LB agar containing 25 mg/L chloramphenicol. Knockouts

were confirmed with three pairs of primers (Up/Down, check-F/R and cm-insert/Down) shown in Table S5.4. Next, the chloramphenicol cassette was removed by pCP20 transformation (Cherepanov and Wackernagel, 1995), and the mutants were tested for loss of antibiotic resistance. The *E. coli* mutants used in this study are listed in Table S5.5.

5.2.6. Genetic complementation of the genes comprising tLST

For plasmid complementation, *sHsp20*, *clpK*$_{GI}$, *sHsp*$_{GI}$, *pscA*, *pscB*, *hdeD*$_{GI}$ and *kefB* were amplified using primers in Table S5.4. The PCR products were cloned into pCA24N as NotI/HindIII inserts and were transformed into *E. coli* DH5α. The plasmids pCA-*sHsp20*, pCA-*clpK*$_{GI}$, pCA-*sHsp*$_{GI}$, pCA-*pscA*, pCA-*pscB*, pCA-*hdeD*$_{GI}$, and pCA-*kefB* were electroporated into their corresponding mutants. The pCA24N was used as vector control and was electroporated into *E. coli* MG1655 *lacZ*::LHR. All transformants carrying either pCA24N or pCA24N-based recombinant vectors were plated on LB medium containing 34 mg/L chloramphenicol. The expression of insertions was induced by 1mM IPTG.

5.2.7. Determination of heat and chlorine resistance of *E. coli*

To assess the contribution of different open reading frames of the tLST to survival under heat and oxidative stresses, heat resistance and chlorine resistance were determined with the WT and *E. coli* MG1655 *lacZ::*LHR and its Δ*orf* mutants. Strains were grown overnight in LB broth at 37°C with 200 rpm agitation. To determine the heat resistance, 50 μL of overnight culture in a 200-μL PCR tube was treated at 63 °C for 5 min and cooled to 4 °C. Chlorine resistance under a neutral condition (pH7) was determined by mixing 200 μL of overnight cultures with 2.8 μL of 23% (vol/vol) sodium hypochlorite solution (Sigma-Aldrich, St. Louis, MO), followed by incubation for 5 min at room temperature. The reaction was terminated by the addition of 50 μL of 10% $Na_2S_2O_3$. To determine the chlorine resistance under an alkaline condition, 200 μL of

overnight cultures was centrifuged at 5,300 × g for 5 min, and then the pellet was resuspended in 200 µL of LB broth containing 8 mM NaClO at pH 11.0±0.4. After a 5-min incubation at room temperature, the reaction was terminated by washing cells with LB broth. Cell counts of cultures before and after treatment were determined by surface plating on LB agar and incubating at 37 °C for 18 h. Results are expressed as the log-transformed ratio of cell counts before and after treatments [$\log(N_0/N)$].

5.2.8. Measurement of cytoplasmic oxidation by roGFP2-based probe

The fusion protein roGFP2-Orp1 was used to measure oxidative levels in biological systems (Degrossoli et al., 2018). Plasmid encoding roGFP2-Orp1 was transformed into the WT and *E. coli* MG1655 *lacZ*::LHR and its Δ*orf* mutants. The plasmids were maintained by adding ampicillin (100 mg/L) to the cultivation media. After treatment with chlorine, the ratio of the fluorescence intensities obtained at the excitation wavelength of 488 and 405 nm was used to evaluate the oxidation of roGFP2 as described (Wang et al., 2020).

5.2.9. Determination of membrane lipid oxidation by C_{11}-BODIPY$^{581/591}$

E. coli MG1655 *lacZ*::LHR and its Δ*orf11*, Δtrx_{GI}, Δ*kefB*, Δ*orf14*, Δ*orf15*, and Δ$degP_{GI}$ mutants were treated with 50 mM NaClO at pH 7 for 5 min, and 50 µL of 10% $Na_2S_2O_3$ was added to stop the reaction. Oxidized *E. coli* without staining treatment served as a control. Membrane lipid oxidation was measured with flow cytometry as in reference (Wang et al., 2020).

5.2.10. Ecological fitness of WT and *E. coli* MG1655 *lacZ*::LHR and its Δ*orf* mutants

To access the impact of the tLST on the ecological fitness of *E. coli*, pairwise growth competition in LB broth was carried out. Briefly, *E. coli* MG1655 *lacZ*::LHR and the WT were inoculated into 5 mL of LB broth at an initial concentration of 10^3 CFU/mL for each strain and

incubated at 37 °C and 200 rpm for 24 h. The culture was then diluted 1:10^3 into fresh LB broth and incubated under the same conditions. The culture was maintained for 12 inoculation cycles. Chlorine treatment was performed every 2, 4, or 8 inoculation cycles, and the non-treated group served as a control. After a full inoculation cycle, cultures were treated with 32 mM NaClO for 5 min at room temperature and were washed by LB two times to remove the residual NaClO, followed by subculturing. To investigate the role of *sHsp20*, $hdeD_{GI}$, and *kefB* in the maintenance of tLST under selective conditions, Δ*sHsp20*, Δ$hdeD_{GI}$, and Δ*kefB* mutants were inoculated along with WT in 5 mL of LB broth as described above. Chlorine treatment was applied as described above every two inoculation cycles. In addition, cultures were treated at 60 °C for 5 min every two inoculation cycles. After each inoculation cycle but before lethal treatments, where applicable, cells were stored at -20 °C for enumeration by droplet digital PCR.

QX200 droplet digital PCR (ddPCR) system (Bio-Rad) with TaqMan probes was used to determine the ratio of cells of *E. coli* MG1655 *lacZ*::LHR and the WT. The primers and probes are shown in Table S5.4. Each ddPCR mixture consisted of 11 μL of 2× ddPCR SuperMix for probes (no dUTP) (Bio-Rad), 1.1 μL of culture from the competition experiment, 0.5 mM each forward and reverse primers of tLST and *lacZ*, and 0.5 mM both probes. The nuclease-free water was added to obtain the final volume of 22 μL. The reaction mixture (20 μL) was loaded into a DG8 cartridge (Bio-Rad) together with 20 μL of droplet generation oil (Bio-Rad) and placed in the QX200 droplet generator (Bio-Rad) to generate approximately 20,000 droplets in a 96-well PCR plate. The plate was subjected to amplification in a C1000 Touch thermal cycler (Bio-Rad) under the following condition: 1 cycle at 95 °C for 5 min, 40 cycles at 94 °C for 30 s and 60 °C for 60 s, 1 cycle at 98 °C for 10 min, and ending at 4 °C. After amplification, tLST and *lacZ* were detected in the 6-carboxyfluorescein (FAM) channel and the 6-carboxy-2,4,4,5,7,7-

hexachlorofluorescein (HEX) channel by the QX200 droplet reader (Bio-Rad), respectively, and fluorescence was analyzed with QuantaSoft software (Bio-Rad). Results are expressed as the log-transformed ratio of the gene copy number of *E. coli* MG1655 *lacZ*::LHR to that of the WT. Competition experiments using WT and Δ*orf* mutants were analyzed with the same methodology with primers and probes shown in Table S5.4.

5.2.11. Statistical analysis

Data of treatment lethality and oxidation level in cytoplasm or membrane lipids were analyzed with one-way analysis of variance (ANOVA). The effects of treatments, strains, and time on the log-transformed ratio of strains in competition assays were tested with a two-way ANOVAs, with both treatments/strains and time treated as fixed factors. Statistical analyses were performed with SPSS 21.0 (SPSS Inc., Chicago, IL, USA). The least significant difference (LSD) was used to test the difference among means using a P value of <0.05. Data are presented as means ± standard deviations from at least three biological replicates.

5.3. Results

5.3.1. Distribution of tLST in *Enterobacterales*

Four main sequence variants of the tLST have been identified (Figure 5.1.A.) (Schmid et al., 2009). The sequences of different tLSTs were used as query sequences to assess the occurrence and frequency of the tLST in *Enterobacteriaceae*. In total, 953 of the 30,033 *Enterobacteriaceae* genomes harbor the tLST (Figure S5.1. and Table S5.2.); of these 953 sequences, 234 were nonredundant. Fewer than 10 genomes are available for most species of the *Enterobacteriaceae* while pathogenic microorganisms are overrepresented; this sampling bias prevents quantitative interpretation of the data. Nevertheless, a high proportion of genomes of the genera *Cronobacter*, *Enterobacter*, and *Klebsiella* included the tLST (Figure S5.1. and Table S5.1.). The proportion of

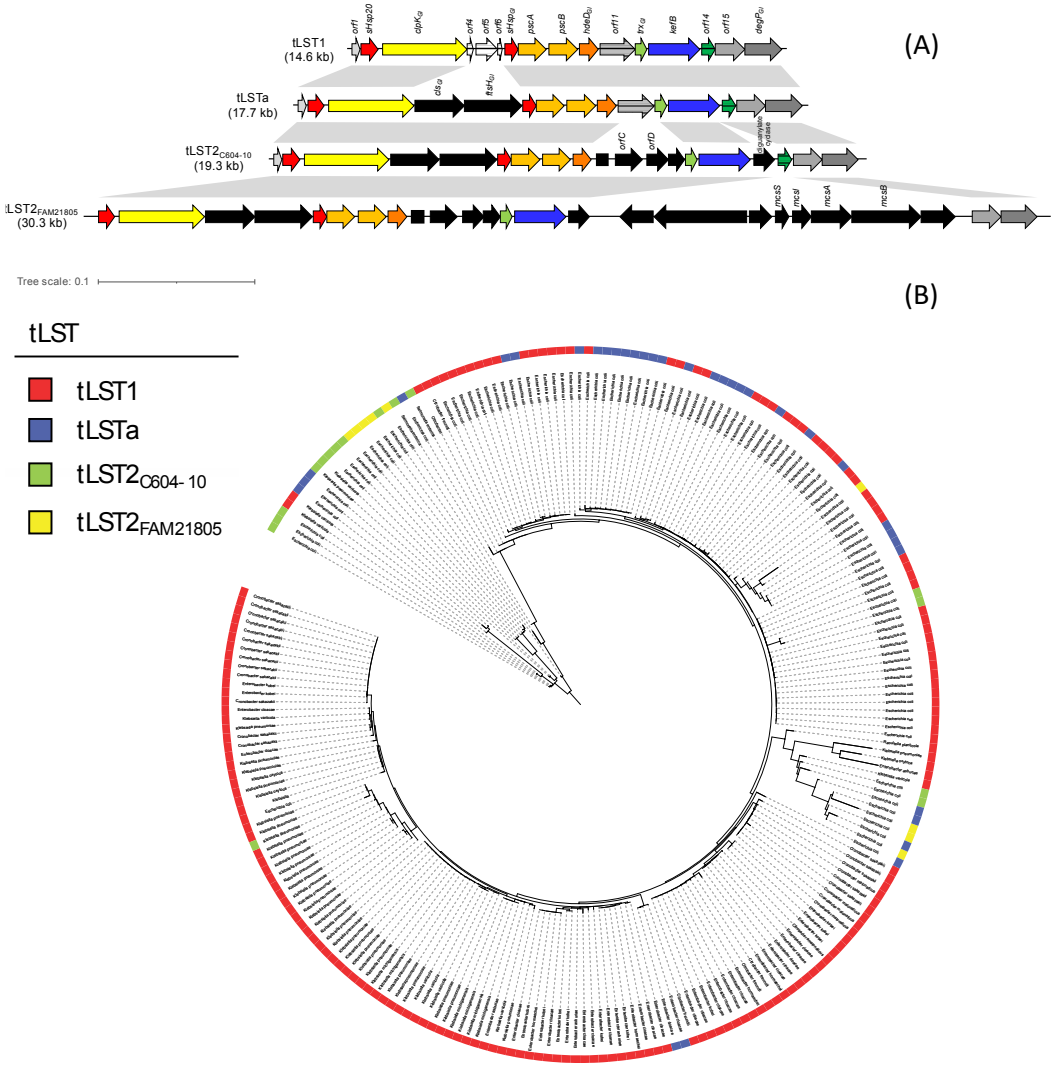

Figure 5.1. Major sequence variants of the locus of heat resistance **(Panel A)** and their distribution in *Enterobacterales* **(Panel B)**.

Panel A. Schematic representation of sequence variants of the tLST. ORFs absent on tLST1 are marked in black; partially disrupted ORFs are marked with stripes. The sequences was obtained from GenBank under the accession numbers LDYJ01000141 (tLST1), CP010237 (tLSTa), CP016838 ($tLST2_{C604\text{-}10}$), and KY416992 ($tLST2_{FAM21805}$). Gray shading indicates sequences with more than 80% nucleotide identity.

Panel B. Phylogenetic tree of the tLST from *Enterobacteriaceae*. A phylogenetic tree was constructed based on tLST sequences extracted from 234 tLST-positive *Enterobacteriaceae*. The presence of tLST1, tLSTa, $tLST2_{C604\text{-}10}$, and $tLST2_{FAM21805}$ is annotated using a color-coded arrangement. Different bacterial species are also color-coded.

E. coli and *Salmonella* genomes that include the tLST was about 2% and less than 0.1%, respectively (Table S5.1.). A sufficient number of genomes is available for *Klebsiella pneumoniae* and *Cronobacter sakazakii* to allow differentiation of the frequency of the tLST by source of isolation. In this analysis, genomes of *K. pneumoniae* were rarefied to include only one strain from each depositing source. Of the 355 genomes of *C. sakazakii*, 8% of genomes of environmental origin and 8% of clinical isolates included the tLST. In *K. pneumoniae*, 2% and 4% of genomes of environmental and clinical isolates, respectively, harbor the tLST (Table S5.1.).

5.3.2. Core and accessory genes harbored by different variants of the tLST in the *Enterobacteriaceae*

The 234 nonredundant tLST-sequences representing different sequence variants are depicted in a phylogenetic tree of aligned tLST sequences (Figure 5.1.B.). The different tLST variants do not form monophyletic clusters, but tLSTa and tLST2 sequences are interspersed among the larger number of tLST1 sequences (Figure 5.1.B.). This indicates a mosaic structure of the genomic island which is shaped by recombination events and horizontal gene transfer. The tLST sequences from *E. coli* were predominantly located between 10:00 and 4:00 (Figure 5.1.B.), while tLST sequences from *Klebsiella*, *Cronobacter*, and *Enterobacter* were located predominantly between 4:00 and 10:00. The uniform clustering of tLST sequences from *E. coli*, however, may also relate to sampling bias, as this species was represented by a much larger number of genomes than other species. In addition, tLST sequences from other species were interspersed with the *E. coli* cluster, and individual sequences of *E. coli* were identified among tLST sequences of other strains, again indicating recent lateral gene transfer. Among the different tLST variants that are present in the *Enterobacteriaceae*, tLST1 is most frequently present (Figure 5.1.B.). tLST1 is the shortest tLST variant that confers full heat resistance (Mercer et al., 2017b, 2015). Accessory

genes that are present in other tLST variants do appear not to contribute to heat resistance; therefore, further studies focused on the core genes of tLST1.

5.3.3. Co-occurrence of tLST and plant growth-promoting genes

Enterobacteriaceae that live in association with plants include *Klebsiella* and *Cronobacter*. Core genes harbored by the tLST were screened in *K. pneumonia* genomes, the species for which most genomes were available (Figure 5.2.). The percentages of tLST-positive genomes in strains isolated from the environment, humans, or plants were substantially higher than the percentage of tLST-positive genomes of isolates from animals. Genomes of strains of *K. pneumoniae* also harbor genes that support mutualistic relationships with plants. Genes that are functionally necessary in indole-3-acetic acid (IAA) production (*nthA*), phosphate solubilization and uptake (*phnA*, *phnH*, *phnI*, *phnJ*, *phnK*, *phnL*, *phnM*), and nitrogen fixation (*nifH*) were also identified in *K. pneumonia* genomes (Figure 5.2.). Co-occurrence of the tLST and genes related to promotion of plant growth may indicate that the tLST contributes to the plant-associated lifestyle of *K. pneumoniae* rather than its lifestyle as a nosocomial pathogen. The tLST was absent in genomes of *K. pneumonia* possessing *nthA* and rarely co-occurred with *nifH*. All genomes were predicted to have a set of genes for phosphate transport and degradation, irrespective of the presence of the tLST.

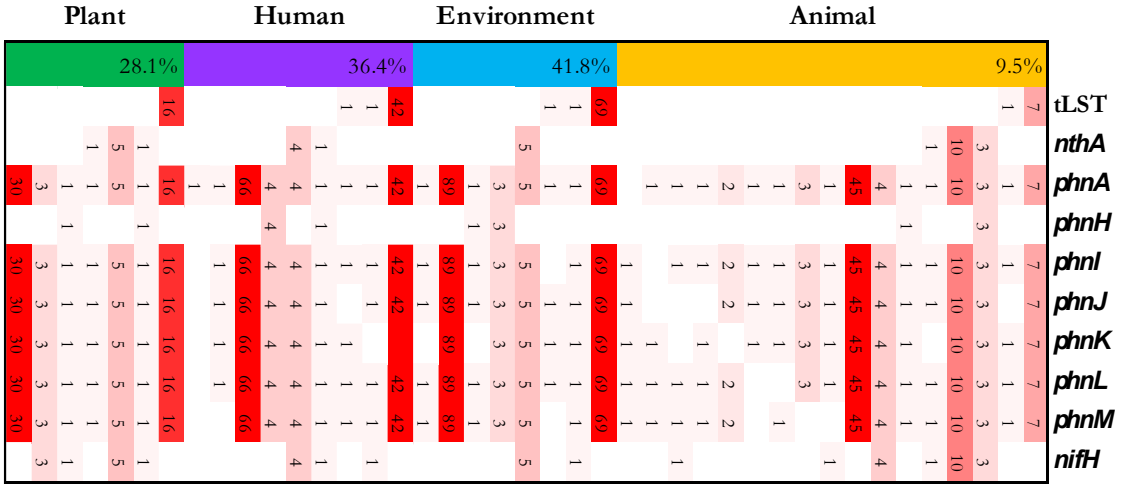

Figure 5.2. Distribution of tLST and plant growth-promoting genes in *K. pneumoniae*. Genomes of *K. pneumoniae* were selected by their different lifestyles. The numbers inside the yellow, blue, purple, and green boxes represent the percentages of tLST in *K. pneumoniae* inhabiting animal (8/84), environment (71/170), human (44/121) and plant (16/57), respectively. Besides the tLST, each column represents a gene that is involved in the biosynthetic pathway of common plant growth-promoting features in *K. pneumoniae*, such as *nthA* (indole-3-acetic acid production), *phnX* family (phosphate solubilization and uptake) and *nifH* (nitrogen fixation). The heatmap shows individual genome count. Each row represents the genomes with a panel of genes, and the numbers inside red boxes indicate the numbers of these genomes. Absence of genes is represented by white boxes.

5.3.4. Contribution of tLST to heat and chlorine resistance in *Klebsiella* spp. and *E. coli*

To compare the function of tLST between *Klebsiella* spp. and *E. coli*, the two species for which a sufficient number of tLST-positive strains are available, for heat and chlorine resistance, 10 tLST-positive and tLST-negative strains of *Klebsiella* spp. and 7 strains of *E. coli* were compared (Figure 5.3.). Resistance to heat and chlorine was determined by the presence of the tLST, not by the taxonomic position (*Klebsiella* or *Escherichia*) or the source of isolation (clinical or environmental). Because the contribution of tLST1 to heat resistance in *K. pneumoniae* was comparable to its contribution to heat resistance in *E. coli*, subsequent experiments were carried out with *E. coli* MG1655.

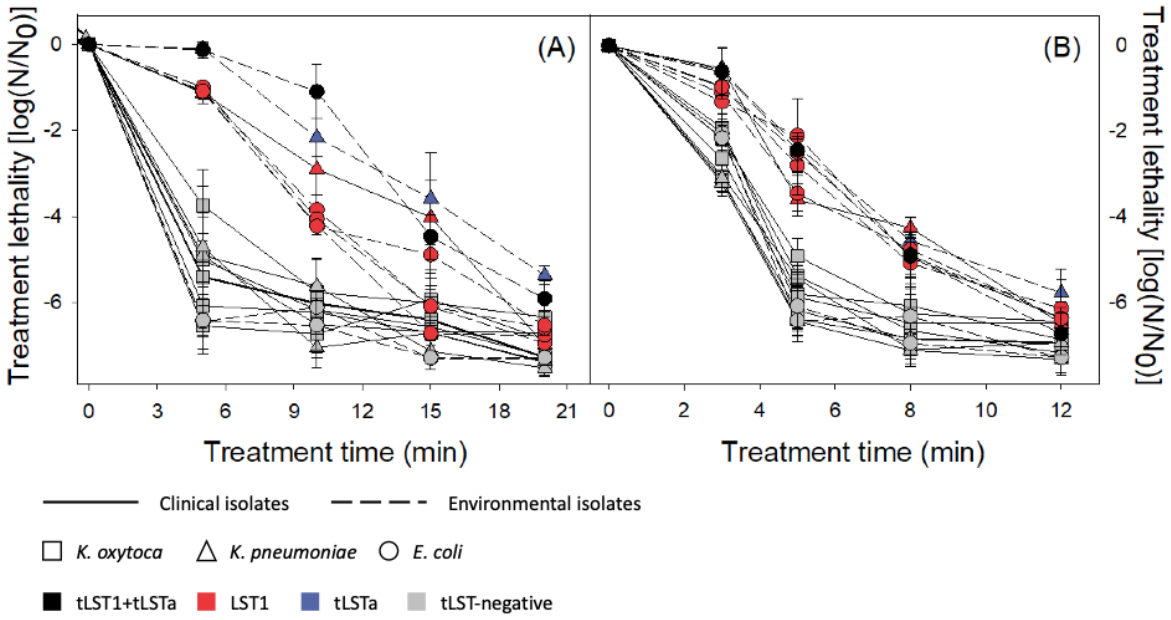

Figure 5.3. Lethality of heat and chlorine in environmental and clinical isolates of *K. oxytoca*, *K. pneumoniae*, and *E. coli*. **Panel A.** Strains were treated at 60 °C for 0, 5, 10, 15, and 20 min. **Panel B.** Strains were treated at 32 mM NaClO for 0, 3, 5, 8, and 12 min. Grey squares represent tLST-negative strains *K. oxytoca* FUA10326, FUA10327, FUA10328, FUA1261, FUA1266, and FUA1271; blue triangles represent *K. pneumoniae* FUA1427 carrying tLST1; green triangles represent *K. pneumoniae* FUA10298 carrying tLSTa; grey triangles represent tLST-negative *K. pneumoniae* FUA10329 and FUA10340; Black circles represent *E.coli* FUA10297 carrying both versions of tLST1 and tLSTa; blue circles represent *E. coli* FUA10289, FUA10291, FUA10292, and FUA10296 carrying tLST1; and grey circles represent tLST-negative strains *E.coli* FUA10290 and FUA10293. Solid lines indicate clinical isolates, and dotted lines indicate environmental isolates. Data are shown as means ± standard deviations from three independent experiments.

5.3.5. Contribution of genes harbored by the tLST to heat and chlorine resistance

To determine the function of individual genes of the tLST, the heat and chlorine resistance were assessed in *E. coli* MG1655 (wild type [WT]), *E. coli* MG1655 *lacZ*::LHR, and derivatives of *E. coli* MG1655 *lacZ*::LHR lacking one each of the genes harbored by the tLST1(Δ*orf* mutants) (Figure 5.4.). Deletions were introduced in all 13 functional genes of the tLST, excluding the truncated and dysfunctional *orf4, orf5,* and *orf6* (Figure 5.1.). The deletion of *shsp20*, *clpK*$_{GI}$, *shsp*$_{GI}$, *pscA*, *pscB* and *hdeD*$_{GI}$ reduced both heat and chlorine resistance. The deletion of *kefB*

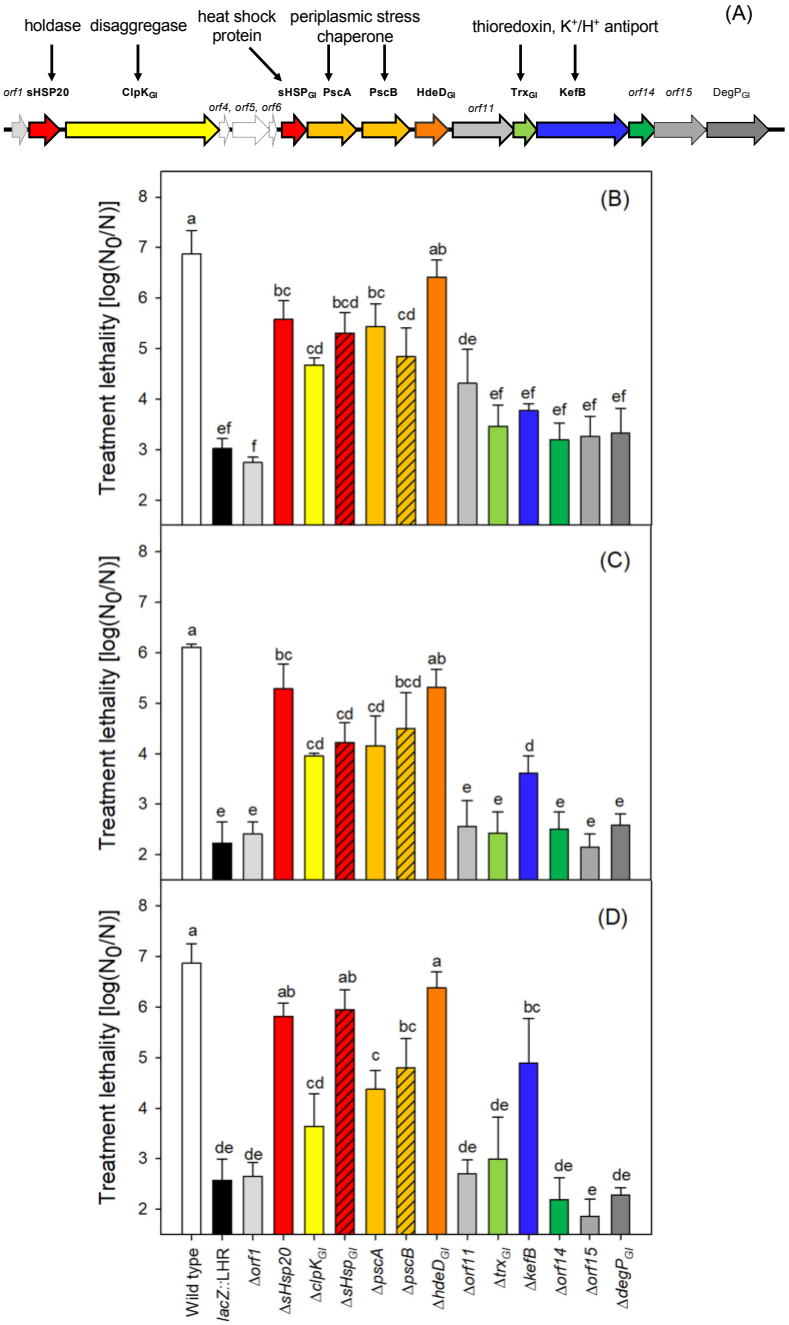

Figure 5.4. Impact of genes harbored by the tLST on heat and chlorine resistance. **Panel A.** Schematic representation of the transmissible locus of stress tolerance (tLST1) and putative functions encoded by genes located on the genomic island. Genes that are known to be expressed in *E. coli* MG1655 (pLHR) are framed and printed in bold font (Li et al., 2020). Proteins are color coded based on their predicted function: red, heat shock proteins; orange, hypothetical proteins with a possible relationship to envelope stress; and green and blue, genes related to oxidative stress. Genes carry the footnote "GI" for genomic island if an orthologue of the same gene is present in genomes of *E. coli*. Open reading frames are numbered if there is no known function associated with the genes; predicted functions of proteins are

Figure 5.4. legend (con't):
written above. Modified according to (Mercer et al., 2017a). **Panel B.** Lethality of treatments at 63 °C for 5 min to cultures of WT and derivative strains carrying tLST or tLST with single deletion. **Panel C.** Lethality of treatments with 50 mM NaClO for 5 min at pH 7. **Panel D.** Lethality of treatment with 8 mM NaClO for 5 min at pH 12. The treatment lethality was expressed as the log-transformed ratio of cell counts before treatment (N_0) over the cell counts after treatment (N). Values for different strains after the same treatment that do not have a common lowercase letter are significantly different (P<0. 05). Data are shown as means ± standard deviations from three independent experiments.

reduced chlorine resistance, particularly under alkaline conditions. Complementation of *shsp20*, *clpK*$_{GI}$, *shsp*$_{GI}$, *pscA*, *pscB*, *hdeD*$_{GI}$, and *kefB* restored heat and chlorine resistance to the level observed in *E. coli* MG1655 *lacZ*::LHR (pCA24N) (Figure S5.2.). In summary, 7 of the 13 core genes of the tLST (Figure 5.1.) are required to confer resistance to heat or chlorine.

5.3.6. Contribution of tLST-harbored genes to protect multiple cellular components against chlorine

To determine the role of tLST-harbored genes in protecting specific components of the cytoplasm and membrane, the oxidation of cytoplasmic proteins and membrane lipids was assessed in the WT and *E. coli* MG1655 *lacZ*::LHR and its Δ*orf* mutants by using the probes roGFP2-Orp1 (Degrossoli et al., 2018) and C11-BODIPY$^{581/591}$ (Fang et al., 2017), respectively. After treatment with chlorine, oxidation of roGFP2-Orp1 decreases the fluorescence of green fluorescence protein 2 (GFP2) and the ratio of the fluorescence intensity at excitation wavelength of 488/405 nm. In comparison to that of *E. coli* MG1655 *lacZ*::LHR, a decreased fluorescence ratio of roGFP2-Orp1 in Δ*sHsp20*, Δ*clpK*$_{GI}$, and Δ*sHsp*$_{GI}$ mutants indicated that these three genes prevented protein oxidation (Figure 5.5.A.). The deletion of *kefB* reduced the proportion of cells with unoxidized membrane lipids and increased the number of cells with oxidized membrane lipids (Figure 5.5.B.). On the contrary, the deletion of *orf11*, *trx*$_{GI}$, *orf14*, *orf15*, and *degP*$_{GI}$ did not change (P<0.05) the ratio of unoxidized and oxidized cells. Moreover, the deletion of *kefB* caused the same change in

membrane potential as in the WT after chlorine treatment (Figure S5.3.). In summary, *sHsp20*, *clpK*$_{GI}$ and *sHsp*$_{GI}$ decreased the oxidation of cytoplasmic proteins, while *kefB* decreased the oxidation of membrane lipids and contributed to maintenance of a polarized membrane.

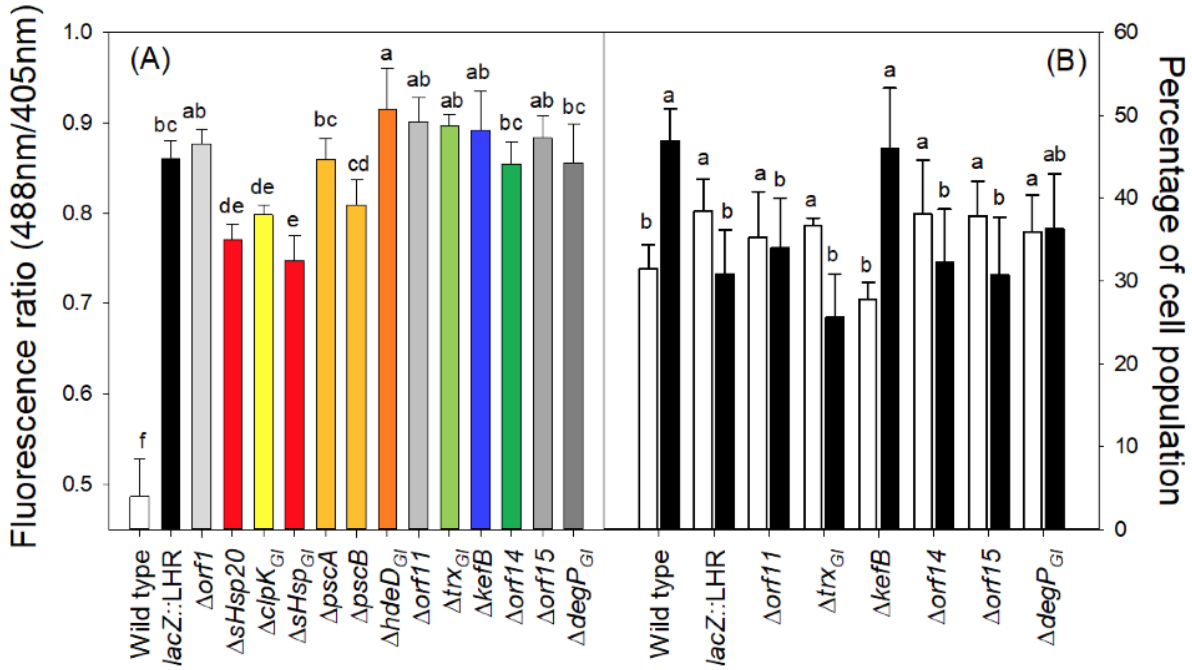

Figure 5.5. Effect of the tLST or the tLST with deletions in single open reading frames on the oxidation of cytoplasmic proteins (**Panel A)** or the cytoplasmic membrane (**Panel B).** Values for different strains that do not have a common lowercase letter are significantly different (P<0.05). Data are shown as means ± standard deviations from three independent experiments.

Panel A. Oxidation of roGFP2-based probes expressed in *E. coli* MG1655 *lacZ*::LHR and its Δ*orf* mutants after chlorine treatment. The ratio of the fluorescence intensity at excitation wavelengths of 488 and 405 nm was calculated to indicate the oxidation of cytoplasmic proteins. Cells were treated with 50 mM NaClO for 5 min at pH 7, and the reaction was terminated by adding an equivalent volume of 10% $Na_2S_2O_3$ as a reducing agent.

Panel B. Flow cytometric quantification of the oxidation of membrane lipids in *E. coli* MG1655 *lacZ*::LHR and its Δ*orf* mutants after chlorine treatment. White bars indicate the percentages of the population of stained and unoxidized cells; black bars indicate stained and oxidized cells. Cells were treated with 50 mM NaClO for 5 min at pH 7, and the reaction was terminated by adding an equivalent volume of 10% $Na_2S_2O_3$ as reducing agent.

5.3.7. The tLST impacts the ecological fitness of *E. coli*

To determine the effect of the tLST on the ecological fitness of *E. coli*, the ratio of *E. coli* MG1655 *lacZ::*LHR to the WT was determined in competition assays that included periodic lethal chlorine challenges, or not. A decreasing ratio of *E. coli* MG1655 *lacZ*::LHR to WT demonstrates a growth advantage of the WT compared to the growth of *E. coli* MG1655 *lacZ*::LHR (Figure 5.6.A.). The tLST-positive strain was also outcompeted when chlorine challenges were applied every 4 or 8 inoculation cycles (Figure 5.6.A.). Applying a lethal chlorine challenge every 2 inoculation cycles maintained the tLST-positive and tLST-negative strains at equal cell counts (Figure 5.6.A.).

To determine whether single gene deletions in the tLST reduce its fitness cost, the ratio of Δ*shsp20*, Δ$hdeD_{GI}$, or Δ*kefB* mutants to the WT in competition assays was assessed with lethal heat or chlorine stress applied every 2 inoculation cycles, i.e., under conditions that maintained the tLST-positive and tLST-negative strains at equal cell counts (Figure 5.6.A.). The ratio of strains with single deletions to the WT decreased more slowly than that of strains with full-length tLST to the WT, indicating that deletion of these genes reduced the fitness cost of the tLST but also reduced the fitness gain of the tLST after challenge with heat and chlorine. The Δ*kefB* mutant maintained equal cell counts with the WT in competition experiments with heat stress but not in competition experiments with chlorine stress (Figure 5.6.B.), in keeping with the observation that the *kefB* deletion did not reduce tLST-mediated heat resistance. Overall, these competition experiments with strains carrying single deletions in the tLST suggest that all core genes need to be present in the tLST to maintain the ecological advantage relative to the fitness cost.

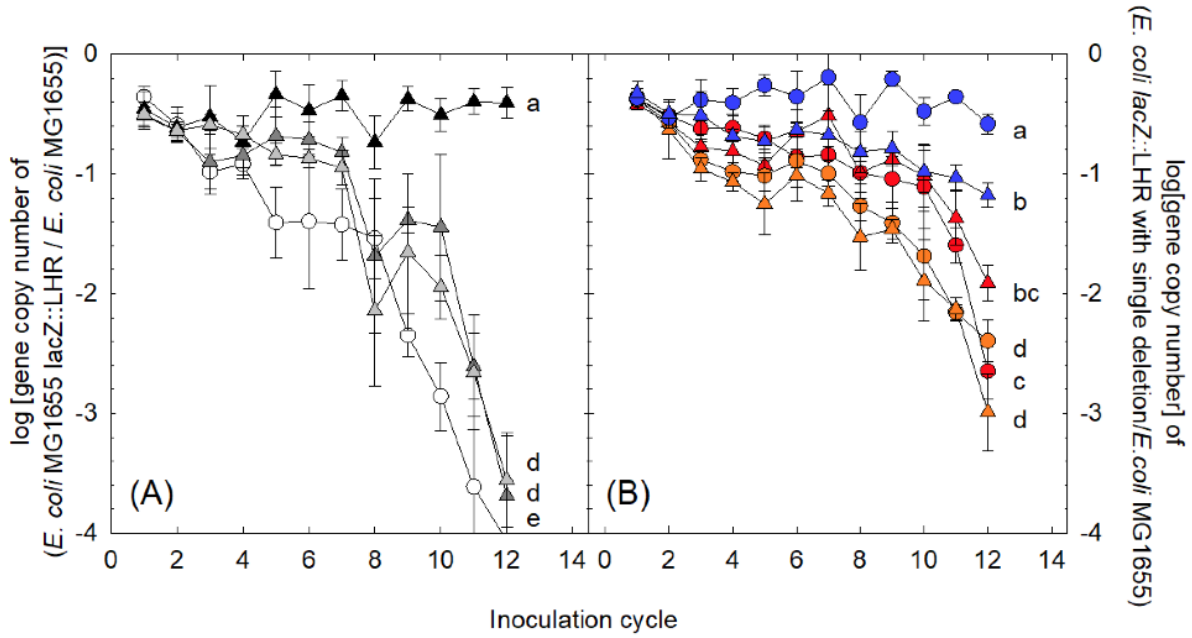

Figure 5.6. Effect of the tLST on the ecological fitness of WT as determined in competition experiments with *E. coli* MG1655 *lacZ*::LHR or Δ*orf* mutants and WT. Different curves that do not have a common lowercase letter indicate that the effect of treatment or strains on the ecological fitness is significantly different (P<0.05).

Panel A. Competition experiments with *E. coli* MG1655 *lacZ*::LHR and WT with or without chlorine treatment. The abundance of tLST was expressed as the log-transformed ratio of gene copy numbers of *E. coli* MG1655 *lacZ*::LHR to that of WT. White circles represent cultures in LB without intermittent lethal challenge; black triangles represent cultures treated with 32 mM NaClO for 5 min at pH 7 every two inoculation cycles; dark grey triangles represent cultures treated with 32 mM NaClO for 5 min at pH 7 every four inoculation cycles; and light grey triangles represent cultures treated with 32 mM NaClO for 5 min at pH 7 every eight inoculation cycles. Data are shown as means ± standard deviations from three independent experiments. The detection limit of the assay was a ratio of 4 or -4 log(gene copy number [*E. coli* MG1655 *lacZ*::LHR/WT]).

Panel B. Competitions between Δ*sHsp20* mutant and WT (red), Δ$hdeD_{GI}$ mutant and WT (orange), Δ*kefB* mutant and WT (blue) in binary competitions with regular lethal heat or chlorine treatments. The abundance of Δ*orf* mutants was expressed as the log-transformed ratio of gene copy numbers of Δ*sHsp20*/Δ$hdeD_{GI}$/Δ*kefB* mutants to that of WT. Circle symbols represent cells treated at 60 °C for 5 min every two inoculation cycles, and triangle symbols represent cells treated with 32 mM NaClO for 5 min at pH 7 every two inoculation cycles. Data are shown as means ± standard deviations from three independent experiments. The detection limit of the assay was a ratio of 4 or -4 log(gene copy number [Δ*orf* mutant/WT]).

5.4. Discussion

The tLST is present in all the phyla of *Proteobacteria* with the exception of *Epsilonproteobacteria* (Kamal et al., 2021; Mercer et al., 2015). Almost all the tLST-positive genomes within *Enterobacterales* are found in the family *Enterobacteriaceae*, while only 5 tLST-positive genomes were identified in other families of the *Enterobacterales* (Kamal et al., 2021). Members of the *Enterobacterales* have diverse lifestyles and are associated with soil and aquatic habitats or with host organisms, including plants, nematodes, insects, animals, and humans (Scheutz and Strockbine, 2005). The order also includes human and animal pathogens, e.g. *E. coli*, *Salmonella enterica*, and *Yersinia pestis*, and phytopathogens, e.g. *Pectobacterium carotovorum*, *Dickeya solani*, and *Pantoea ananatis*. Interestingly, the proportion with the tLST is low in enteric pathogens (Wang et al., 2020; this study) and in plant pathogens (Kamal et al., 2021), suggesting that the tLST and an obligate pathogenic lifestyle are ecologically incompatible. Moreover, the tLST was not associated with plant growth-promoting features such as IAA production, phosphate transport, and nitrogen fixation. This study found a high prevalence of tLST in *Enterobacter*, *Cronobacter*, *Citrobacter*, and *Klebsiella*, which suggests that the tLST provides a selective advantage for those bacteria with a "blended lifestyle" that includes colonization of plants as well as temporary persistence in vertebrates but not for vertebrate-associated organisms, including enteric pathogens, or organisms that occur predominantly or exclusively in plants and/or insects. This pattern was discernible with genome sequence data available in 2014 (Mercer et al., 2015), 2019 (this study), and 2021 (Kamal et al., 2021), suggesting that it will remain with increasing amount of available genome sequence data. The elucidation of mechanisms of resistance to environmental stressors that is provided the tLST may improve our understanding of why the tLST increases the ecological fitness of specific species of *Enterobacteriaceae*.

5.4.1. tLST-comprising genes and stress resistance of *E. coli*

tLST protects against heat and oxidative stress in *E. coli* (Boll et al., 2017; Mercer et al., 2015; Wang et al., 2020), and different fragments of the tLST protect different cellular components (H. Li et al., 2020; Wang et al., 2020). Four distinct tLST variants were found in *Enterobacteriaceae*. Core genes of the tLST1 are retained in all sequence variants of the genomic islands, but larger tLST versions include accessory genes (Boll et al., 2017; Nguyen et al., 2017). Different sequence variants of the tLST do not form monophyletic clades but likely result from recent insertions and deletions to an ancestral tLST which also occurs in *Betaproteobacteria* (Boll et al., 2017; Nguyen et al., 2017). This study focused on the contribution of core genes of the tLST to heat and chlorine resistance.

The genes *shsp20*, *clpK*$_{GI}$, *shsp*$_{GI}$, *pscA*, *pscB*, and *hdeD*$_{GI}$ protected against both heat and chlorine, but *kefB* protected only against chlorine. The mechanism by which these genes effect chlorine resistance is summarized in Figure 5.7. sHsp20, ClpK$_{GI}$, and sHsp$_{GI}$ are involved in protein folding and disaggregation (Lee et al., 2018; H. Li et al., 2020; Mercer et al., 2015) (Figure 5.7.). The periplasmic proteins PscA and PscB, previously designated YfdX1 and YfdX2, are heat stable and retain the native α-helical secondary structure up to 50 °C (Saha et al., 2016). YfdX decreased the aggregation of the insulin B-chain *in vitro*, showing ATP-independent chaperon-like activity (Saha et al., 2016). YfdX is water-soluble, indicating that it is not an integral membrane protein; the presence of a predicted signal peptide in the N terminus indicates localization in the periplasm. Owing to their chaperon activity (Saha et al., 2016) and their role in protection against multiple stressors (this study), these two YfdX family proteins were renamed as periplasmic stress chaperons (Psc). HdeD is also a periplasmic protein contributing to acid resistance (Hommais et al., 2004). KefB is a potassium/proton antiporter that protects against electrophiles (Masuda et al.,

1993) and is the only protein of the tLST that specifically contributes to chlorine resistance. KefB exchanges intracellular potassium and extracellular protons, leading to acidification of the cytoplasm (Ferguson et al., 1993b). This rapid decrease in the intracellular pH protected the *E. coli* cell against chlorine stress under alkaline condition by maintaining the membrane potential (Figure S5.3.).

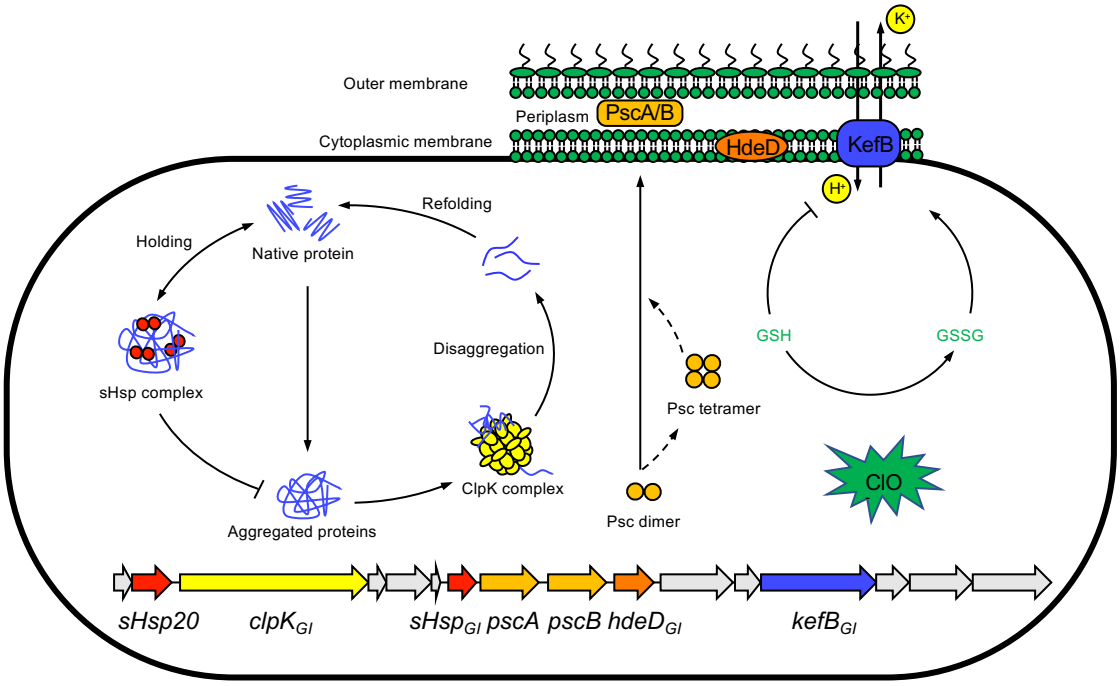

Figure 5.7. Schematic overview of the relevant tLST-comprising genes in response to chlorine stress in *E. coli*. $sHsp_{GI}$ and $ClpK_{GI}$ refold or solubilize the denatured proteins as disaggregase (Lee et al., 2018; Mogk and Bukau, 2017). sHsp20 cooperates with $ClpK_{GI}$ as a holding chaperone (Lee et al., 2015). Products of *pscA*, *pscB*, and HdeD have a chaperone-like activity (Lee et al., 2019) and may interact with chlorine in the periplasm. The *nemR-gloA* operon is derepressed via the oxidation of cysteine residues. The production of S-D-lactoylglutathione by GloA actives KefB potassium efflux system which protects the membrane lipids against chlorine (Lee and Park, 2017).

5.4.2. Fitness gain and fitness cost of the tLST.

The tLST is particularly frequent in species that are found in the intestine of vertebrates but also occur as plant endophytes. The frequency of the tLST in other genera of

Enterobacteriaceae that predominantly or exclusively occur in insects, vertebrate hosts, or in plants was substantially lower. To date, the ecology of the tLST has been studied mainly in anthropogenic habitats. The frequency in the general population of *E. coli* is approximately 2% (Mercer et al., 2015). DaQu fermentation, which starts at ambient temperature and increases to 50 to 60 °C, selects for tLST-positive *Enterobacteriaceae* (Wang et al., 2018). tLST-positive strains of *E. coli* are also enriched in chlorine-treated wastewater (Zhi et al., 2016) and in raw-milk cheese (Marti et al., 2016), reflecting the selective pressure of chlorination and thermization at 60 °C, respectively. The selective pressure for maintaining the tLST in natural ecological niches remains unknown. Competition experiments demonstrated that the tLST is associated with substantial fitness cost, in keeping with the observation that tLST-encoded proteins are among the most abundant proteins in *E. coli* (H. Li et al., 2020). The fitness cost of the tLST were compensated for only by frequent lethal challenges with heat or chlorine. The competition experiments also demonstrated that deletion of single tLST-harbored genes reduced the fitness gain but did not significantly decrease the fitness cost, indicating selective pressure for maintenance of all core genes of the tLST. The selective pressure that maintains the tLST in specific members of the *Enterobacteriaceae* remains unknown (Kamal et al., 2021) but likely serves to overcome dispersal limitation by improving survival outside of plant or vertebrate hosts.

5.4.3. Contribution of tLST on dispersal and persistence of nosocomial pathogens

Several of the *Enterobacteriaceae* that frequently harbor the tLST are nosocomial pathogens (Davin-Regli et al., 2019; Holý and Forsythe, 2014; Koutsoumanis et al., 2020; Sanders and Sanders, 1997). *Enterobacter*, *Klebsiella*, and *Cronobacter* also upregulate or acquire antimicrobial resistance genes, which leads to concerns related to the spread of antibiotic resistance in healthcare settings (Da Silva et al., 2012; Mezzatesta et al., 2012). The high proportion of tLST-

positive clinical isolates of *K. pneumoniae* compared to that of *K. pneumoniae* isolates from other sources suggests that the tLST-mediated resistance to disinfection agents may facilitate persistence in hospitals. A tLST-positive *K. pneumoniae* isolate from a hospital chlorination tank influent was also resistant to 10 antibiotics (Popa et al., 2020). A pattern of higher frequency of the tLST in clinical isolates of *C. sakazakii* was not observed; however, 73.5% of genomes of clinical isolates of *C. sakazakii* clinical strains possessed the *shsp20* and *clpK* genes of the tLST, while only 24.3% of the environmental strain had these genes. Variants of the tLST also occurs in *Betaproteobacteria* (Kamal et al., 2021). Remarkably, the nosocomial pathogen *Pseudomonas aeruginosa* clone C strains is tLST positive and resistant to heat and oxidative stress (Kamal et al., 2019; Lee et al., 2015). The relatively high prevalence of the tLST in clinical isolates of *Klebsiella* and *P. aeruginosa* may indicate that the tLST contributes to the persistence of nosocomial pathogens in the hospital environment. Although the co-occurrence of the tLST and antibiotic resistance in *Enterobacteriaceae* remains to be explored, the occurrence of antibiotic-resistant pathogens that are also resistant to chlorine may further impede their control in hospitals.

5.5. Conclusions

In conclusion, the tLST is rarely present in intestinal pathogens and in strictly plant-associated *Enterobacterales* but is frequently present in those *Enterobacteriaceae* that have a "blended lifestyle", which includes plant habitats and vertebrate intestines, but are also of importance as multidrug-resistant opportunistic or nosocomial pathogens. An estimation of the fitness cost versus fitness gain related to the tLST suggests a strong selective pressure to maintain 13 core proteins which are present in all tLST variants and are necessary to protect multiple cellular components against multiple stressors. Resistance to heat and/or oxidising chemicals likely

facilitates dispersal of those *Enterobacteriaceae* that switch between animal and plant hosts but also may contribute to persistence of nosocomial pathogens in the hospital environment.

CHAPTER 6. Genetic Determinants of Stress Resistance in Desiccated *Salmonella enterica*

6.1 Introduction

Salmonella enterica causes disease in animals, including poultry, cattle, pigs, and rodents as well as humans (Kingsley and Bäumler, 2000). Some serovars, such as *S. enterica* serovar Typhimurium and *S.* Enteriditis, infect a wide spectrum of animals and humans but generally cause relatively mild symptoms, while other serovars, including *S.* Typhi, are host specific and cause more severe disease (Ellermeier and Slauch, 2007; Thomson et al., 2008; Tsolis et al., 1998). As pathogens, very few *Salmonella* form stable relationships with individual hosts. The transition from one host individual to another, or from one host species to another, exposes *Salmonella* to adverse environmental conditions, including low pH, osmotic stress, and desiccation or extreme temperatures (D'Aoust and Maurer, 2007; Spector and Kenyon, 2012). Desiccation tolerance enables survival and persistence of *Salmonella* on plant material, including food, and on inanimate surfaces (Billi and Potts, 2002). *Salmonella* are more capable of long-term survival in the dry state than related organisms, including *Escherichia coli*, *Enterobacter cloacae*, and many other *Enterobacteriaceae* (Barron and Forsythe, 2007).

The desiccation tolerance of *Salmonella* contributes to outbreaks of foodborne disease with dry or low water activity (a_W) foods ($a_W < 0.85$) that have consistently occurred over the past decades (Beuchat et al., 2011; Frelka and Harris, 2014; Gurtler et al., 2014; Laufer et al., 2015; Santillana Farakos and Frank, 2014). Dry foods contaminated with *Salmonella* include pet foods, nuts and nut products, spices, and infant formula (Behravesh et al., 2010; CDC, 2019; Jourdan et al., 2008). Desiccated *Salmonella* cells resist pathogen intervention treatments that are lethal to cells at high a_W. Interventions methods such as pasteurization, high pressure CO_2, or high hydrostatic pressure are effective decontamination treatments for high-a_W foods but are

insufficient to decontaminate dry foods (Chen et al., 2017; Molina-Höppner et al., 2004). *Salmonella* are inactivated within less than 1 to 10 min by treatment at 60 °C in high-a_W foods, however, decimal reduction times at 60 °C (D_{60} values) in low-a_W foods typically exceed 100 min (Finn et al., 2013). Treatments for inactivation of *Salmonella* in dry foods include treatment with propylene oxide, hot oil, or steam (Pan et al., 2012) or require temperatures exceeding 120 °C (Du et al., 2010; Podolak et al., 2010). These treatments also substantially impact food quality. Improving the safety of dry foods thus remains an unsolved problem for the food industry. The improvement of pathogen intervention technologies necessitates improved knowledge of the mechanisms of dry-heat resistance.

Survival of desiccated *Salmonella* is supported by the accumulation of compatible solutes, the expression of Fe-S cluster proteins, and the catabolism of fatty acids (Finn et al., 2013). Compatible solutes, including trehalose, glycine-betaine, and glutamate, prevent protein denaturation and maintain the membrane integrity in the dry state (Purvis et al., 2005). Iron-sulfur cluster proteins prevent oxidative damage after desiccation (Gruzdev et al., 2011); oxidative damage is a major contributor to the death of dry cell (Fang et al., 2020). Because unsaturated fatty acids are particularly prone to oxidation in the dry state, alterations of the composition of the membrane by increasing the proportion of saturated fatty acids and cyclopropane fatty acids also extends survival after desiccation (Finn et al., 2013). In addition to protein homeostasis, membrane composition, and transport of inorganic ions or compatible solutes, genes that were found to increase survival of desiccated *Salmonella* relate to energy production and conversion, regulation of biological processes, DNA metabolic process, and virulence factors (Jayeola et al., 2020; Jiang et al., 2004; Mandal and Kwon, 2017). Mechanisms that improve survival of enteric pathogens after desiccation, in particular the accumulation of compatible solutes, have been related to the

heat resistance of desiccated *Escherichia coli* (Li and Gänzle, 2016); however, mechanisms of dry-heat resistance of *Salmonella* remain largely unexplored.

Resistance of enteric pathogens to environmental stress is often strain-dependent (Liu et al., 2015; Tamber, 2018), indicating that many genetic determinants for stress resistance are encoded by the accessory rather than the core genome. The role of accessory genes encoded by mobile genetic elements in bacterial stress resistance was confirmed for wet heat and chlorine resistance of *E. coli* and *Klebsiella* (Kamal et al., 2021; Mercer et al., 2015) as well as the heat and pressure resistance of bacilli (Krawczyk et al., 2017; Li et al., 2019) Past studies identified wastewater isolates of *Salmonella* that exhibit exceptional tolerance to UV light (Prasad et al., 2021), heat (Gautam et al., 2020), and high-pressure CO_2 (Schultze et al., 2020) after desiccation. It remains unknown, however, whether the accessory genome of *Salmonella* contributes to resistance to desiccation or dry heat. This study aimed to investigate the genetic determinants for dry-heat resistance in *Salmonella* with a comparative genomics approach. The resistance of 108 strains of *Salmonella* to dry heat was determined, genes that were encoded in genomes of resistant strains but not in genomes of sensitive strains of *Salmonella* were identified, and the contribution of selected genes to the resistance to desiccation and dry heat was assessed in a functional genomics approach.

6.2. Materials and methods

6.2.1. Sample collection and dry-heat treatment

Wastewater isolates of *Salmonella* (50 strains) were isolated from a municipal wastewater treatment plant in Alberta. To achieve a wide range of different serotypes, an additional 58 *Salmonella* strains, from the SARB and SARC collections (Boyd et al., 1996, 1993), were obtained from the *Salmonella* Genetic Stock Centre, Calgary, AB, Canada (Table S6.1.). To determine the

dry-heat resistance, overnight cultures in tryptic soy broth (TSB) were washed by phosphate-buffered saline (PBS; Thermo Scientific, Wilmington, Delaware, USA), and 100 µL of culture from each strain was transferred in a 200-µL PCR tube. The tubes were placed in a vacuum desiccator (Thermo Scientific, Wilmington, Delaware, USA) with $CaSO_4$ as desiccant ($a_W < 0.1$) (Thermo Scientific, Wilmington, Delaware, USA) for 24 h. Dry cells were heated at 95 °C for 1 h, and cooled to 4 °C, and cell counts were determined by plating on trypticase soy agar (TSA; Difco, Becton Dickinson, Sparks MD) and incubation for 24 h at 37 °C.

6.2.2. Determination of heat resistance and high-pressure resistance

The heat resistance at different parameters of the 8 most dry-heat-resistant strains selected from 50 wastewater isolates and 58 SGSC strains was determined at different combinations of a_W and temperature to further confirm the resistance to dry heat. The following combinations of a_W and temperature were evaluated: a_W of 0.1 at 80°C for 1 h; a_W of 0.33 at 80°C for 30 min; and a_W of 0.75 at 80°C for 30 min. The 8 wastewater strains with highest resistance to dry-heat-resistant wastewater strains and the 8 most sensitive SGSC strains were additionally assessed with respect to resistance to treatment at 500 MPa for 1 min.

6.2.3. Genome sequencing and comparative genomics

The 8 most dry-heat-resistant wastewater isolates were selected for whole-genome sequencing as described (Mercer et al., 2015). In brief, genome sequencing was performed using an Illumina MiSeq system. Libraries were prepared with 1 ng of genomic DNA using the Nextera XT DNA Library preparation kit (Illumina Inc., SanDiego, CA) by following the manufacturer's instructions. Libraries were sequenced using the MiSeq Reagent Kit v3 (600-cycles) (Illumina Inc.) with the 2×300-bp pair-end chemistry. The adapter trimming in the Illumina FASTQ file generation pipeline was included to remove adapter sequences from the 3’ ends of the reads. Raw

reads were trimmed using Trimmomatic 0.36.4 by following the SLIDINGWINDOW operation with four bases to average across and 20 as the average quality. Trimmed reads were then *de novo* assembled with SPAdes 3.12.0, with k-mer sizes of 21, 33. Genome sequences of 58 SGSC strains were obtained from NCBI. Prokka was used to annotate the genomes of 8 water isolates and 58 SGSC strains (Seemann, 2014). Roary was used to assess the pangenome and generate the core genome alignment (Page et al., 2015), and a phylogenetic tree was constructed using FastTree2 (Price et al., 2010). Genes that were differentially distributed between heat resistant and heat sensitive cells were identified by Scoary (Brynildsrud et al., 2016). The SISTR web server was used to predict the serovar for 66 *Salmonella* strains.

6.2.4. Quantification of relative gene expression

Of the 8 dry-heat-resistant strains, *S. enterica* Muenchen FUA1903 was selected to quantify relative gene expression. The strain was grown in TSB or on a solid surface of agar plates aerobically. The cells were harvested from the two samples for RNA extraction and were desiccated for 24 h to an a_W of 0.10 and rehydrated in RNAprotect bacteria reagent (Qiagen, Hilden, Germany) for RNA extraction. The culture that was grown in broth without any further treatment served as control. RNA was isolated using the RNAeasy minikit (Qiagen) and reverse transcribed to cDNA by a QuantiTect reverse transcription kit (Qiagen) according to the manufacturer's protocols. The expression of 28 genes was quantified by using SYBR green reagent (Qiagen) and on a 7500 Fast PCR instrument (Applied Biosystems, Foster City, CA, USA). Negative controls included DNase-treated RNA and nontemplate controls. The gene coding for glyceraldehyde-3-phosphate dehydrogenase A (*gapA*) served as the reference gene. The gene expression ratio of 28 genes in cells grown on agar plates or desiccated cells relative to those cells grown in broth were calculated with the $\Delta\Delta C_T$ according to Pfaffl (Pfaffl, 2001).

6.2.5. Genetic complementation of putative functional genes

The 15 genes that were highly expressed after dry treatment were cloned into two dry-heat sensitive strains *S.* Arizona FUA10245 and *S.* Arizona FUA10246, which carry none of these genes. The genes were amplified using primers described in Table 6.1. The PCR products were cloned into pRK767 as HindIII/KpnI inserts and were transformed into *E. coli* DH5α. The pRK767 or pRK767-based recombinant strains were electroporated into *S.* Arizona FUA10245 and *S.* Arizona FUA10246. pRK767 was used as vector control. The plasmids used in this study were pRK767, pRK-*ahpD*, pRK-*cysJ*, pRK-*cysM*, pRK-*entD*, pRK-*fadK*, pRK-*fhuA*, pRK-*fixX*, pRK-*fliK*, pRK-*ndhI*, pRK-*pduF*, pRK-*phoC*, pRK-*pspE*, pRK-*sipA*, pRK-*sopD*, and pRK-*uspC*. Transfermants were cultivated in medium containing 15 mg/L tetracycline and were induced by 1 mM isopropyl-β-D-thiogalactopyranoside (IPTG).

6.2.6. Statistical analysis.

The gene expression of treated cells relative to the control was compared with 0 using one-sample t-test (P<0.05) in SPSS 21.0 software (SPSS Inc., Chicago, IL, USA). Data obtained from treatment lethality of transformants were analyzed with one-way analysis of variance (ANOVA). Tukey's test was used to test the difference among means using a P value of <0.05. Data are presented as means ± standard deviation (SD) from at least three biological replicates.

6.2.7. Data availability

The sequences of 8 dry-heat-resistant strains have been submitted to NCBI with accession numbers JAHWYY000000000, JAHWYZ000000000, JAHWZA000000000, JAHWZB000000000, JAHWZC000000000, JAHWZD000000000, JAHWZE000000000, and JAHWZF000000000.

6.3. Results

6.3.1. Variation of the dry-heat resistance of *Salmonella*

The screening for resistance to dry heat initially included stress-resistant wastewater isolated of *Salmonella*, which were complemented by strains form the Salmonella Genetic Stock Centre (SGSC) for a total of 108 strains representing 39 serotypes (Table S6.1.). The dry-heat resistance was determined at different combinations of temperature and a_W. All of the strains isolated from wastewater were extremely resistant to dry heat (Figure 6.1.). Of the wastewater isolates, 8 resistant strains were selected for genome sequencing and for genetic and physiological

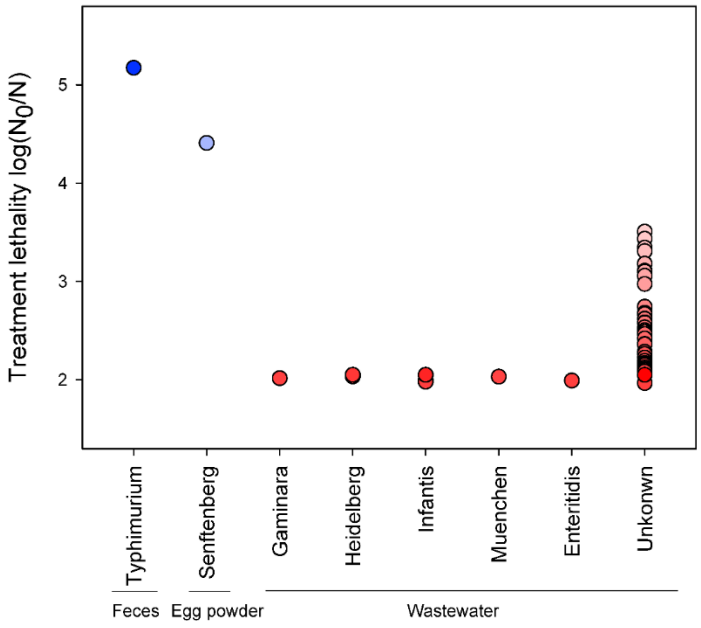

Figure 6.1. Treatment lethality of dry heat to *Salmonella* reference strains and 50 isolates of *Salmonella* from wastewater (Table S6.1.). The cells were desiccated for 24 h to a_W 0.10 and were heated at 80 °C for 1 h. Results are expressed as the log-transformed ratio of cell counts before treatment to the cell counts after treatment [$\log(N_0/N)$]. Data are shown as means for three independent experiments. The standard deviations were 0.60 log CFU/mL or less.

comparison to strains of *Salmonella* that were obtained from the SGSC. A core genome phylogenetic tree of the 8 wastewater isolates and 58 strains from the SGSC along with a heatmap

indicating resistance to 95 °C at an a_W of 0.1 for 1 h is shown in Figure 6.2. The cell counts after dry heating differed by about 5 log CFU/mL, indicating a substantial variation in the resistance of the strains.

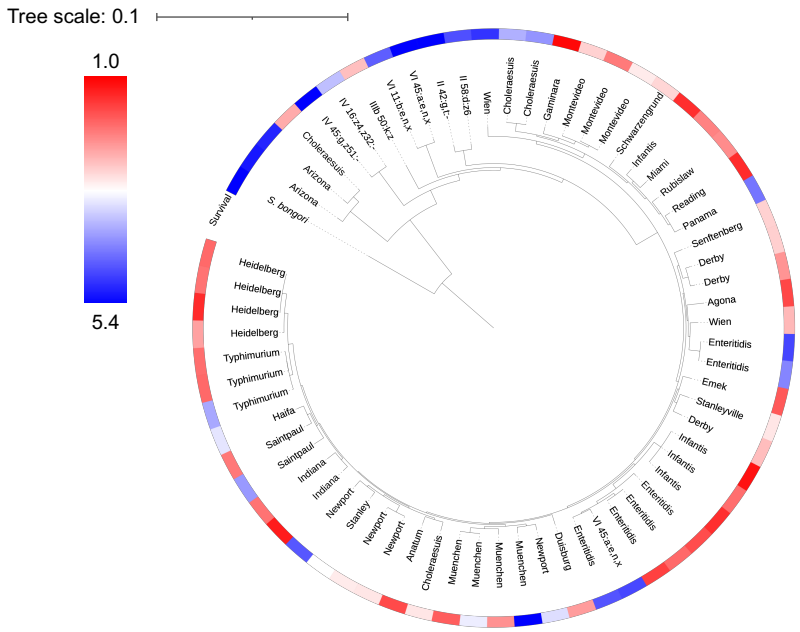

Figure 6.2. Core genome phylogenetic tree of *Salmonella enterica* using *Salmonella bongori* as outgroup. The core genome phylogenetic tree was constructed with the genome sequences of the 66 strains for which dry heat resistance was assessed (Tab. S1). Each leaf indicates the serotype of isolates. The heatmap indicates the survival of cells after dry-heat treatment (log CFU/mL). The overnight culture of each strain was dried in a vacuum desiccator for 24 h to reach a_W 0.10. The dry cells were heated at 95 °C for 1 h and then were cooled to 4 °C immediately. After the cells were rehydrated in PBS buffer back to original volume at room temperature for 10 min, cell counts were determined. Data are shown as means for three independent experiments. The standard deviations were 1.09 log CFU/mL or less.

To determine whether the dry-heat resistance of strains of *Salmonella* relates to the treatment conditions, the resistance of all 66 strains was assessed at 80 °C with an a_W of 0.1, 0.33 or 0.75. The treatment time was adjusted to obtain a reduction of cell counts ranging from > 1 to < 8 log CFU/mL. In *E.coli*, resistance to both desiccation and high pressure relates to oxidative stress; therefore, 16 strains were additionally evaluated with respect to their survival after

treatment with 500 MPa (Figure 6.3.). The treatment lethality of these 4 different treatments against strains of *Salmonella* (Figure 6.3.) was consistent with the resistance shown in Figure 6.2. Results also demonstrate a close relationship between the resistance to dry heat and the resistance to high pressure.

6.3.2. Phylogenetic distribution of resistant strains

The dry-heat resistance of strains was not related to their phylogenetic position (Figure 6.2.), indicating that the dry-heat resistance was mediated by genes of the accessory genome rather

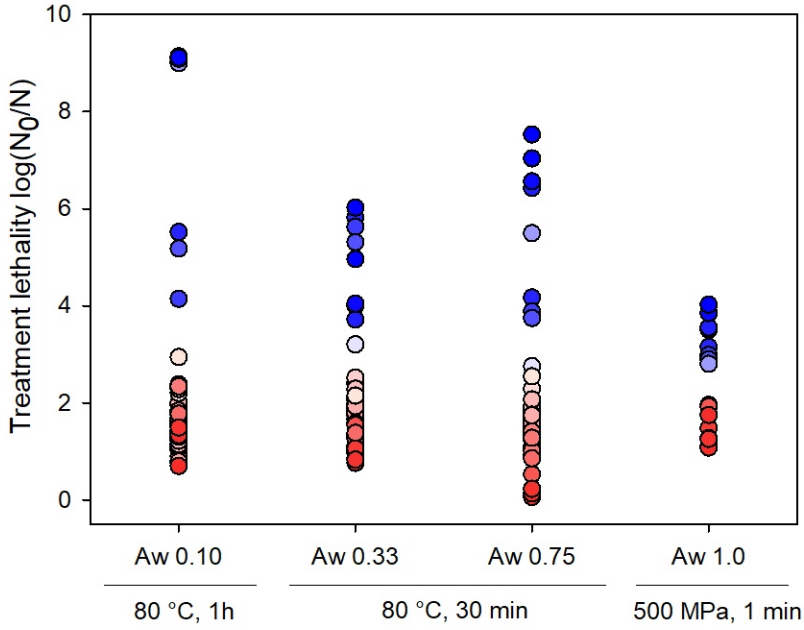

Figure 6.3. Treatment lethality of treatment with dry heat to 66 strains of *Salmonella*. The 66 strains used are the same as those shown in Figure 6.1. Dry-heat treatment was performed by equilibration of dry cells to an a_W of 0.10 and heating to 80 °C for 1 h. To determine the dry-heat resistance at different water activities, the cells were desiccated for 24 h at an a_W of 0.10, equilibrated to an a_W of 0.33 or an a_W of 0.75 for 24 h, and then heated at 80 °C for 30 min. The overnight culture of the 8 most resistant strains and 8 most sensitive strains were additionally treated at 500 MPa for 1 min. Results are expressed as the log-transformed ratio of cell counts before treatment to the cell counts after treatment [$\log(N_0/N)$]. Data are shown as means for three independent experiments. The standard deviations were 1.15 log CFU/mL or less.

than the core genome. To test the hypothesis that genes that are responsible for dry-heat resistance are part of the accessory genome, the 22 most resistant strains and the 8 most sensitive strains were selected for comparative genome analysis.

6.3.3. Identification of genes that potentially contribute to dry-heat resistance

To identify genes with a putative contribution to dry-heat resistance, genes that were differentially distributed among the 22 most resistant strains and the 8 most sensitive strains were identified with Scoary (Table S6.2.). Comparative genomic analysis identified 353 genes that were differentially distributed between the resistant and sensitive strains (Benjamini-Hochberg adjusted *P* value of < 0.03). Of these, 289 genes were present in all 22 dry-heat-resistant strains of *Salmonella* but absent in 4 or more of the 8 dry-heat-sensitive strains of *Salmonella*. To select candidate genes for subsequent confirmation, 22 proteins with a putative relationship to stress resistance were selected (Table 6.2.). The selected proteins are related with multiple stress responses, including oxidative stress, heat stress, acid stress, starvation stress, and virulence.

6.3.4. Quantification of gene expression

To further support a role of the 22 genes shown in Table 6.2., relative gene expression of these genes was assessed before and after desiccation. Three additional genes located on the same operon as one of the genes shown in Table 6.2. were additionally included (Figure 6.4.). After heating, the concentration of mRNA was too low to be detected (data not shown); therefore, gene expression was quantified after desiccation only. Since multiple genes identified in Table 6.2. relate to oxidative stress and starvation, the gene expression of cells grown as solid-state cultures on the surface of an agar plate were also compared to gene expression of planktonic cells growing in broth. The results indicated that 7 genes were overexpressed in both conditions; 2 genes were over-expressed ($P<0.05$) only by solid-state cultures on agar plates, and 6 genes were over-

expressed only after desiccation. In total, 15 genes were differentially expressed by solid-state cultures on agar plates or after desiccation. Genes that were overexpressed after desiccation relate to the osmotic (*ndhI* and *sopD*) or oxidative stress response (*ahpD*, *cysJ, cysM*, *entD, fhuA*, *fixX, pspE*, and *uspC*) but also to virulence of *Salmonella* (*pduF* and *sipA*) and other stress responses (*fadK*, *fliK*, and *phoC*).

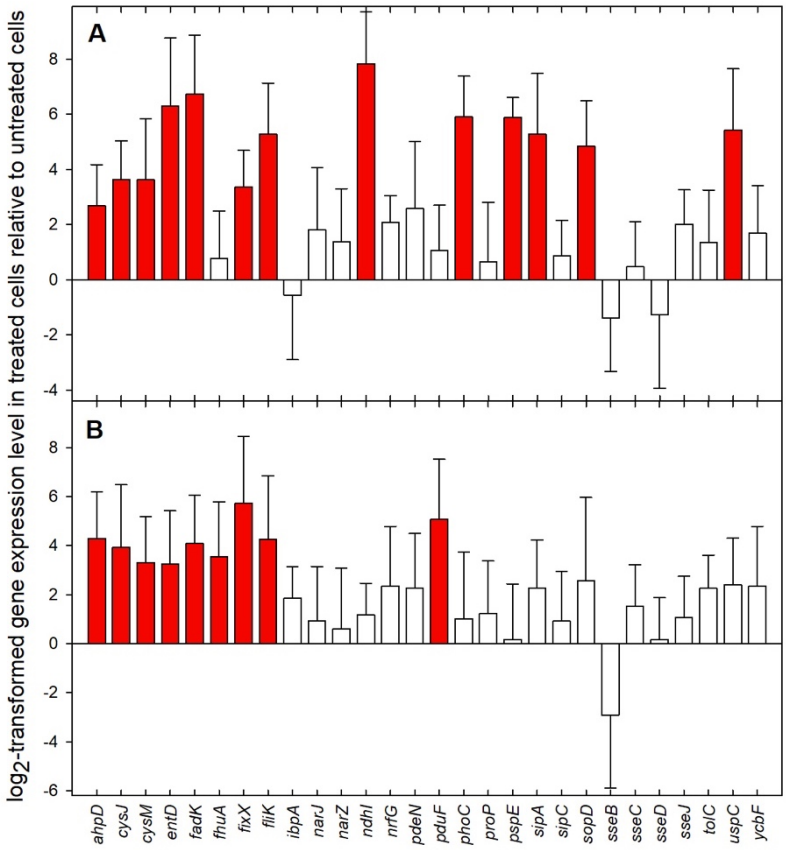

Figure 6.4. Relative expression of 28 genes in *S.* Muenchen FUA1903 after desiccation (Panel A) or solid-state incubation (Panel B). Relative gene expression was quantified by RT-qPCR with *gapA* as housekeeping gene and untreated cultures grown aerobically in broth were used as reference conditions. Desiccated cells were grown aerobically overnight and were desiccated for 24 h to a water activity 0.10. Bars are coloured if the expression was significantly (P<0.05) different from the reference conditions. Data are means ± standard error of five independent experiments.

6.3.5. Genes confer resistance to dry-heat or high pressure.

To verify the contribution of 15 genes in dry-heat or high-pressure resistance, these genes were introduced in two sensitive strains, *S.* Arizona FUA10245 and *S.* Arizona FUA10246, after cloning into the low-copy vector pRK767 under control of the inducible *lacZ* promotor. Cloning of the empty plasmid pRK767 served as control, and cultures were induced by IPTG prior to treatment. Cloning of *cysM*, *phoC*, *pspE*, *sopD*, and *uspC* increased the resistance to both dry heat

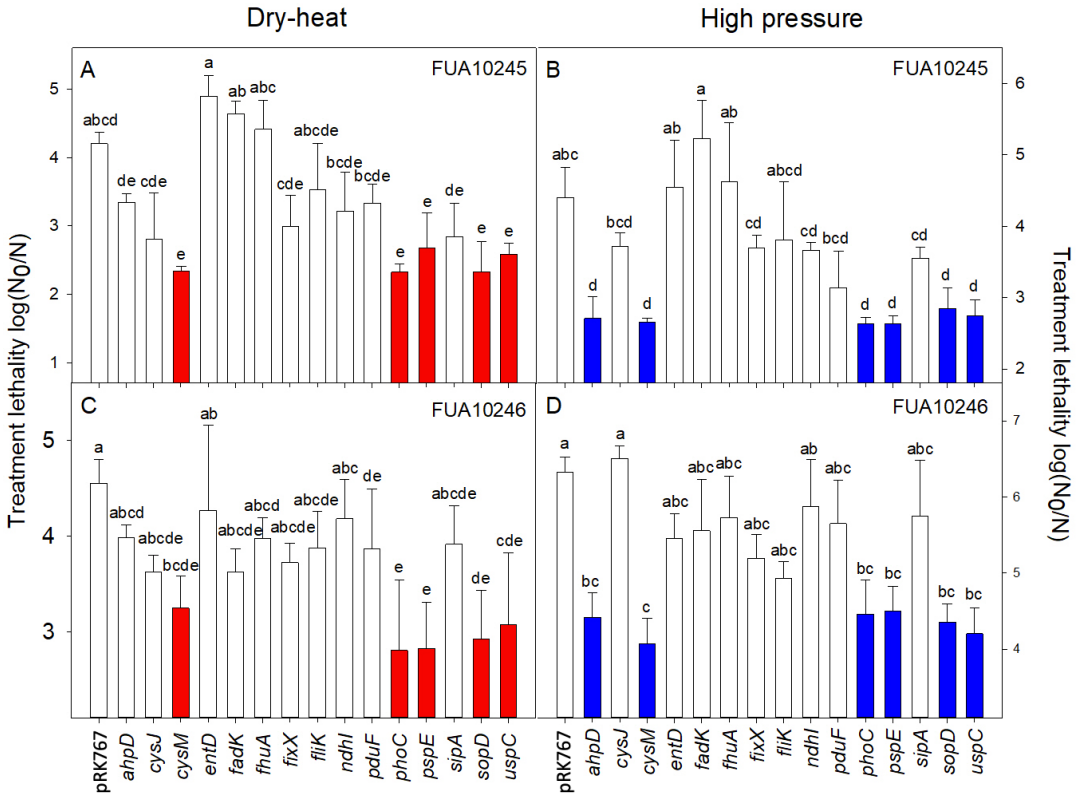

Figure 6.5. Lethality of treatments with dry-heat (Panel A and Panel C) or high pressure (Panel B and Panel D) towards *S.* Arizona FUA10245 (Panel A and Panel B) and *S.* Arizona FUA10246 (Panel C and Panel D). All strains harbored the plasmid pRK767 either as empty vector, or encoding the genes indicated on the x axis under control of the *lacZ* promotor. Treatment with dry heat was performed by desiccation and equilibration to an a_W of 0.10 and heating to 80 °C for 1 h. High-pressure treatment was performed by compression to 500 MPa for 1 min. Results are expressed as the log-transformed ratio of cell counts before treatment to the cell counts after treatment [$\log(N_0/N)$]. Values for different transformants that do not have a common superscript differ significantly ($P<0.05$). Bars are colored if the reduction of cell counts was significantly ($P<0.05$) different from the control strains transformed with empty pRK767. Data are means ± standard error for three independent experiments.

and high pressure (Figure 6.5.). The overexpression of *ahpD* only provided protection against high pressure (Figure 6.5.). The response of the two strains to overexpression was highly comparable (Figure 6.5.).

6.4. Discussion

This study extends prior knowledge by identification of genes of the accessory genome that contribute to dry-heat resistance of *Salmonella*. The identification of genes coding for resistance of *Salmonella* to dry heat or high hydrostatic pressure took advantage of the availability of several wastewater isolates of *S. enterica* that display an exceptional resistance to desiccation, dry heat, and oxidative stress (Du et al., 2020; Gautam et al., 2020; Schultze et al., 2020) and the availability of diverse strains of *S. enterica* from the SGSC. The strains of *S. enterica* differed substantially with respect to their dry-heat resistance, which matches prior observations for wet heat and pressure resistance of *Salmonella* as well as *E. coli* (Gill et al., 2019b; Liu et al., 2015; Mercer et al., 2015; Tamber, 2018). All of the wastewater isolates from a municipal wastewater treatment plant were resistant to dry heat. *E. coli* isolates from the same wastewater plant were previously demonstrated to resist chlorine treatment (Zhi et al., 2016). Because cell counts after treatments differed by more than 5 log CFU/mL, we considered comparative genomic analyses a feasible approach to identify those genes that contribute to the large difference in survival (Mercer et al., 2015).

Prior analyses identified genes with a putative or confirmed contribution to desiccation tolerance (Finn et al., 2013; Jayeola et al., 2020; Mandal and Kwon, 2017). Most of these genes, however, are part of the core genome of *Salmonella*, are also present in *E. colii*, and, thus, do not account for the large intraspecific or interspecies differences in resistance to desiccation and dry heat. Genetic determinants of pressure resistance in *Salmonella* (Tamber, 2018) have not been

elucidated, and genes that relate to pressure resistance in *E. coli* (Robey et al., 2001; Vanlint et al., 2013) are also part of the core genome. Comparative genomics identified 353 genes that were differentially distributed between resistant and sensitive strains; of these, 289 were present in all resistant strains of *Salmonella,* and 22 were annotated to have a relationship with stress resistance (Table 6.2. and Table S6.2). Of these 22 genes, 15 were overexpressed after desiccation or in solid-state culture on agar plates, and 6 genes were confirmed to contribute to dry-heat or high-pressure resistance by cloning and expression in sensitive cells. Our screen eliminated genes of the core genome, genes of unknown function, genes that contribute to stress resistance but are constitutively expressed, which is the case for, e.g., the transmissible locus of stress tolerance (tLST) in *E. coli* (Mercer et al., 2017a), as well as genes that act only in concert with other genes. Despite these limitations, the identification of 6 genes that contribute to resistance to multiple stressors substantially expands our knowledge of the tolerance of *Salmonella* to desiccation and intervention treatments after desiccation.

Genes that contributed to dry heat-resistance mapped to multiple pathways, including acid stress, osmotic stress, protein homeostasis, and oxidative stress, with the latter being the most prominent. Oxidative stress resistance is an important component of the desiccation tolerance of *Salmonella* (Finn et al., 2013). The cloning of *cysM* and *pspE* protected against oxidative stress (Nakatani et al., 2012; Wallrodt et al., 2013) and also increased the dry-heat resistance of sensitive *Salmonella* strains. The cysteine synthase B encoded by *cysM* synthesizes cysteine under anaerobic growth conditions (Filutowicz et al., 1982) and enables *Salmonella* to utilize thiosulfate ($S_2O_3^{2-}$) as a sulfur source (Nakamura et al., 1983) that reduces oxidative stress in the periplasm (Ohtsu et al., 2010). PspE is a periplasmic sulfurtransferase that may contribute to the cellular response to heat shock (Jovanovic et al., 2006). The acid phosphatase PhoC is involved in a high-affinity

phosphate uptake system that may contribute to the synthesis of membrane phospholipids after exposure to stress (Voegele et al., 1997). The secreted effector SopD plays a role in membrane fission during *Salmonella* invasion and was also shown to contribute to desiccation resistance (Maserati et al., 2017). The periplasmic proteins (CysM, PspE), membrane synthesis related proteins (PhoC, SopD), and general stress response protein (UspC) contributed the resistance to both dry heat and high pressure. Alkyl hydroperoxide reductase AhpD, a thioredoxin-like protein, provided oxidative defense under high-pressure stress rather than dry-heat shock (Bryk et al., 2002).

Our study expands current knowledge in two ways, first by analyzing the contribution of the multiple genes of the accessory genome of *Salmonella* to resistance to dry heat and high pressure, and, second, by demonstrating that these genes increase resistance to multiple stressors. Previous studies focused on individual stressors, including heat, oxidative stress, desiccation, and starvation (Hébrard et al., 2009; Jiang et al., 2004; McMeechan et al., 2007; Nguyen et al., 2017). Cytoplasmic and periplasmic oxidative stress and membrane integrity are key elements of the response of *E. coli* and *Salmonella* to desiccation as well as several intervention treatments after desiccation, e.g., dry heat, UV light, or high-pressure carbon dioxide (Chen and Gänzle, 2016; Fang et al., 2020; Finn et al., 2013; Malone et al., 2006). Our study further documents the contribution of membrane integrity and redox homeostasis to dry heat and high pressure; moreover, it is possible or even likely that the same genes also contribute to the resistance of the same strains to UV light after desiccation (Du et al., 2020) and to high-pressure CO_2 (Schultze et al., 2020). A genetic island termed the tLST, which is relatively frequently in *E. coli* and *Klebsiella* species, confers resistance to wet heat and oxidizing inorganic chemicals (Kamal et al., 2021). The virtual absence of the tLST in *Salmonella* (Kamal et al., 2021) and initial data on isogenic strains

of *S.* Typhimurium expressing the tLST1 or not (Seeras, 2017) suggest that the tLST decreases resistance to dry heat. Thus, mechanisms of dry-heat resistance differ from mechanisms of wet-heat resistance. Knowledge on convergent or divergent mechanisms for resistance to different decontamination methods will enable identification of intervention methods that target multiple pathogens of concern, e.g. *E. coli* and *Salmonella* in dry foods, as well as hurdle treatments with a complementary mode of action.

The evolution of *Salmonella* in vertebrates has resulted in thousands of serotypes that exhibit remarkable diversity in their host range and pathogenicity (den Bakker et al., 2011; Park and Andam, 2020). Serotypes of *Salmonella enterica* relate to phylogeny and host adaptation (Litrup et al., 2010); therefore, 39 serotypes were used in this study to investigate the relationship between dry-heat resistance and serotype or phylogeny. Horizontal gene transfer in the accessory genomes of *Enterobacteriaceae*, including pathogenic *E. coli* and *Salmonella*, are important for lifestyle adaptations (Pál et al., 2005). Horizontally acquired genes enhance virulence (Croxen et al., 2013; Tanner and Kingsley, 2018) or confer resistance to stress (Mercer et al., 2015; Nguyen et al., 2017). In contrast to *E. coli*, which includes free-living or plant-associated clades in addition to intestinal clades (Alm et al., 2011; Nguyen et al., 2017), *Salmonella* are obligate pathogens to humans and animals (Tanner and Kingsley, 2018).

Irrespective of the adaptation of specific clades or serotypes of *E. coli* and *Salmonella* to specific host species, neither organism forms stable relationships with host individuals (Tenaillon et al., 2010), and maintenance of the population requires horizontal transmission between individual hosts and survival in extraintestinal environments (Winfield and Groisman, 2003). Some virulence factors, like *pspE* and *sopD* in *Salmonella*, may be selected not only for host invasion but also for stress resistance in extraintestinal environments (Maserati et al., 2017).

Differences in the approach taken by *E. coli* and *Salmonella* to resist wet heat, desiccation, or dry heat were described above; these differences likely relate to the different approaches taken by *E. coli* and *Salmonella* to survival in extraintestinal habitats and host-to-host transmission. This implies that an improved understanding of the extraintestinal lifestyle of enteric pathogens (Winfield and Groisman, 2003) is important for their improved control in the food supply chain.

6.5. Conclusions

In conclusion, this study demonstrates that accessory genes coding for oxidative stress tolerance increase survival of *Salmonella* to dry heat and high pressure. Overexpression of these genes during growth on agar media and/or during desiccation increased dry-heat resistance. Resistance to oxidative stress and desiccation are critical to the long-term survival of *Salmonella* in extraintestinal environments. Genes related to virulence of *Salmonella* were also overexpressed after desiccation, which may contribute to the low infectious dose of *Salmonella* after ingestion of dry foods (Beuchat et al., 2013). Mechanisms of desiccation tolerance also enable *Salmonella* to overcome multiple stressors. *Salmonella* encounters multiple stresses throughout the food chain; therefore, mechanisms underlying dry-heat resistance and high-pressure resistance in a diversity of serotypes provide important clues for improved control of *Salmonella* in the food supply.

Table 6.1. Primers used in this study.

Experiment	Name	Sequence (5'→3')	Product size (bp)	Tm °
Gene expression	*ahpD*-qPCR-F	GTGCATTTTGCCTGGAGATG	234	60
	ahpD-qPCR-R	CGAAGGTCAGATCGCTGATT		
	cysJ-qPCR-F	AACTCAACCAGCTCCTTCAC	195	
	cysJ-qPCR-R	CAGCCCCTATACCAAAGACG		
	cysM-qCR-F	TACCAGCGAGGCGTTAAAAA	188	
	cysM-qPCR-R	GTCGCATCACCCATTTTGTC		
	entD-qCR-F	TATTGATAGCGATGAGCGCC	189	
	entD-qCR-R	GCTGGCAGCAGATATAACGA		
	fadK-qCR-F	AAATCGCCGTGGTCGATAAT	170	
	fadK-qCR-R	CAGGCAGGCCAGATAAATGA		
	fhuA-qCR-F	CAGGTGAACTGGTGGTCATT	209	
	fhuA-qCR-R	GAATACTTTGCTTTCGGCGG		
	fixX-qCR-F	CGTAGATGAAGGACACCCAC	180	
	fixX-qCR-R	AGAGTATTGCCGCAGAGAAC		
	fliK-qCR-F	CAGCATGATGAGAAAACGCC	250	
	fliK-qCR-R	GCTCGCTAAAAGAGAGCGTA		
	ibpA-qCR-F	TTCCCGTGTTTGCTGATTCT	195	
	ibpA-qCR-R	CGCCAACCGTTTCAATTTCA		
	narJ-qCR-F	TGATGGCACAGTATGAGCAG	228	
	narJ-qCR-R	CGATAACGGTATTCGCCAGT		
	ndhI-qCR-F	GGCAGGTCAGCATAGATACG	172	
	ndhI-qCR-R	TGCCAGAGAAGCAGTTCATC		
	nrfG-qCR-F	CCAGTCTGAACACTCCACTG	169	
	nrfG-qCR-R	CGTAAAGTCACGTAGCGGAT		
	pdeN-qCR-F	TGTGGATTCGCAGTATGTCC	250	
	pdeN-qCR-R	AAGACACAATGACAGCGGAA		
	pduF-qCR-F	TTTCACTGGCCGTTTACCTT	211	
	pduF-qCR-R	ACCATATGATGCGCAGTCTC		
	phoC-qCR-F	GGGCTATGCGATAAAGGGTT	174	
	phoC-qCR-R	TAGTAGCCGCCCATTTTCAG		
	proP-qCR-F	GGCGCCTTTGTTTTTGGTAA	174	
	proP-qCR-R	CAGCCCCTGTATAATTCGCA		
	pspE-qCR-F	TTCATAGCCATGCCGCTTTA	248	

	pspE-qCR-R	ATACCGCCCATATTCATCGC		
	sipA-qCR-F	GTGGATTCGACTACGCATCA	162	
	sipA-qCR-R	TTCTGACGTGACCACCTTTC		
	sipC-qCR-F	TAAAACGACAGCAAGCTCCA	169	
	sipC-qCR-R	TTTATCGATCTTCGCGGCAT		
	sopD-qCR-F	GGACGCTTCTCAGACACAAT	232	
	sopD-qCR-R	TGCATTTCCCGTCACTTCTT		
	sseB-qCR-F	CGTGAGCACGGTATTCTCAT	228	
	sseB-qCR-R	CCACTTACTGATAAGCCCCG		
	sseJ-qCR-F	ATCACATCCCAAGCCCAAAA	237	
	sseJ-qCR-R	GATGTACTTCCCCCTTCAGC		
	tolC-qCR-F	AACGGATTTTGGAGTGAGGG	243	
	tolC-qCR-R	CGCATATCAGATTGCATCGC		
	uspC-qCR-F	CTACTGGCTAAAGCGGTCTC	223	
	uspC-qCR-R	GCTGGCTTAACTCACCTGAT		
	ycbF-qCR-F	GCGCGATATATTGGTGCTTG	228	
	ycbF-qCR-R	TAAATAATGGCGGCGTGACT		
Plasmid construction	*ahpD*-HindIII	AAGCTTATGACAACGTTACGCCAACCCTATTATGA	442	60
	ahpD-KpnI	GGTACCTCACATTCGCATACCGATCGCCA		
	cysJ-HindIII	AAGCTTATGACGACACCGGCTCCACT	1810	
	cysJ-KpnI	GGTACCTTAGTAGACATCTCGCTGATAACGGCG		
	cysM-HindIII	AAGCTTGTGAATACATTAGAACAAACCATCGGCAATACG	962	
	cysM-KpnI	GGTACCTTAAATCCCTGCCCCCTGGCT		
	entD-HindIII	AAGCTTATGCTGACATCTCATTTTCCCCTTCCC	716	
	entD-KpnI	GGTACCTTTATCGGGGGATTGCGCTAAGTATAGAAGC		
	fadK-HindIII	AAGCTTATGAGTGTTACATTAACGTTTGACGCCG	1652	
	fadK-KpnI	GGTACCTTTATACCGCAGTGTGCTCCTGGC		
	fhuA-HindIII	AAGCTTATGGCGCGTCTTAAAACTGCTCA	2200	
	fhuA -KpnI	GGTACCTTAGAAACGGAAGGTTGCCGTTGC		
	fixX-HindIII	AAGCTTATGAGTTCGGACAATAAGGTGAATGTTGAC	304	
	fixX-KpnI	GGTACCTCAGCCGTAGCGAAACTCAACG		
	fliK-HindIII	AAGCTTATGATCACCCTGCCCCAACTGATC	1234	
	fliK-KpnI	GGTACCTTAGGCGAAGATATCCACTGCGCC		
	ndhI-HindIII	AAGCTTATGGTTAACCTGACGATCGATCCGG	874	
	ndhI-KpnI	GGTACCTTAAAGGCGCACAGCAAACTCAGG		
	pduF-HindIII	AAGCTTATGAATGATTCTCTAAAGGCGCAATGTGGT	805	

pduF-KpnI	GGTACCTTACAGTTCACAGCGGTTACAAGGTAAATTCT	
phoC-HindIII	AAGCTTATGAAAAGTCGTTATTTACTATTTTTTCTACCACTGATCG	763
phoC-KpnI	GGTACCTCAGTAATTAAGTTTGGGGTGATCTTCTTTACTCA	
pspE-HindIII	AAGCTTATGTTGAAAAAAGGAATATTTGCGTTAGCGTTATTCA	325
pspE-KpnI	GGTACCCTATTTTTTTACTTTAGGCATATCAAGACGACTGATACCG	
sipA-HindIII	AAGCTTATGGTTACAAGTGTAAGGACTCAGCCC	2068
sipA-KpnI	GGTACCTTAACGCTGCATGTGCAAGCCA	
sopD-HindIII	AAGCTTATGCCAGTCACTTTAAGCTTCGGTAATCA	964
sopD-KpnI	GGTACCTTATACCAGTAATATATTACGACTGCACCCATCTTTAC	
uspC-HindIII	AAGCTTATGAGCTACACCCATATTCTTGTCGCC	439
uspC-KpnI	GGTACCCTAGTCGCCCGCTAACGGTACC	

Table 6.2. List of genes that are present in all 22 heat resistant strains of *Salmonella* but absent in more than 4 of the 8 heat sensitive strains of *Salmonella*. Differentially distributed genes were identified in Scoary with a Benjamini-Hochberg adjusted *P*-value of less than 0.03. Of the 289 differentially distributed genes that were identified with these criteria (Table S6.2.) only those 25 with known function related to stress resistance or virulence are shown.

Gene	Annotation	Functions	References
fliK	Flagellar hook-length control protein	Acid stress	(Maurer et al., 2005)
ycbF	Putative fimbrial chaperone	Catabolic stress	(Hosoya et al., 2002)
uspC	Universal stress protein C	General stress response	(Heermann et al., 2009)
ndhI	NAD(P)H-quinone oxidoreductase subunit I	Osmotic stress	(Huihui et al., 2020)
proP	Proline/betaine transporter	Osmotic stress	(Racher et al., 1999)
sopD	Secreted effector protein	Osmotic stress	(Jiang et al., 2004)
cysJ	Sulfite reductase [NADPH] flavoprotein alpha-component	Oxidative stress	(Nakatani et al., 2012)
cysM	Cysteine synthase B	Oxidative stress	(Nakatani et al., 2012)
fixX	Ferredoxin-like protein	Oxidative stress	(Earl et al., 1987)
ahpD	Alkyl hydroperoxide reductase	Oxidative stress	(Hong et al., 2019)
entD	Enterobactin synthase component D	Oxidative stress	(Gehring et al., 1998)
fhuA	Ferrichrome outer membrane transporter/phage receptor	Oxidative stress	(Eisenhauer et al., 2005)
tolC	Outer membrane protein	Oxidative stress	(Lee et al., 2016)
nrfG	Formate-dependent nitrite reductase complex subunit	Oxidative stress (NO_2^-)	(Cole, 1996)
pspE	Thiosulfate sulfurtransferase	Oxidative stress (NO)	(Wallrodt et al., 2013)
narJ	Nitrate reductase molybdenum cofactor assembly chaperone	Protein homeostasis	(Blasco et al., 1998)
ibpA	Small heat shock protein	Protein homeostasis	(LeThanh et al., 2005)
fadK	Medium-chain fatty-acid--CoA ligase	Starvation stress	(Campbell et al., 2003)
pdeN	putative cyclic di-GMP phosphodiesterase	Starvation stress	(Herbst et al., 2018)
phoC	Acid phosphatase	Starvation stress	(Geiger et al., 1999)
pduF	Propanediol diffusion facilitator	Virulence	(Bobik et al., 1999)
sseB	Secreted effector protein	Virulence	(Freeman et al., 2002)
sseJ	Secreted effector protein	Virulence	(Ohlson et al., 2005)
sipA	Cell invasion protein	Virulence	(Bronstein et al., 2000)
sipC	Cell invasion protein	Virulence	(Hayward and Koronakis, 1999)

CHAPTER 7. General Discussion and Open Questions

The genomic information indicates adaptation of *Enterobacterales* to diverse habitats and lifestyles. The synthesis of phylogenomic, metabolic and functional data clearly provides clues on the evolution of lifestyles of *Enterobacterales* (Chapter 2). During this evolution, bacteria acquired resistance genes associated with specific host colonization to resist environmental stressors present in the given habitats. This Ph. D research explored the stress resistance mechanisms of *E. coli*, *Klebsiella* and *Salmonella* in non-host related environmental niches and ecological role of stress resistance in free-living lifestyle and symbiotic lifestyle.

7.1 Mechanisms of stress resistance in *Enterobacteriaceae*

The role of accessory genes encoded by mobile genetic elements in bacterial stress resistance was confirmed for the heat and pressure resistance of bacilli (Krawczyk et al., 2017; Chapter 3). The *spoVA*^{2mob} operon confers heat resistance on bacterial endospores and contributes to spore survival during baking (Berendsen et al., 2016a; Z. Li et al., 2020). This finding confirmed that accessory genes which mediate resistance are relevant for survival of spoilage bacteria or human pathogens during food processing. Therefore, this thesis investigated the mechanisms of wet heat and chlorine resistance of *E. coli* and *Klebsiella* (Chapter 4 and 5) and heat resistance of desiccated *Salmonella* (Chapter 6), which are conferred by accessory genes.

The tLST that occur in diverse *Enterobacteriaceae* confers resistance to heat, chlorine, and other oxidizing chemicals, which is consist of a protein homeostasis module, an envelope stress module, and an oxidative stress module (Mercer et al., 2017a). The protein homeostasis module encoding sHsp20, ClpK$_{GI}$, and sHsp$_{GI}$ is involved in protein folding and disaggregation in cytoplasm. Three periplasmic proteins encoded by the envelope stress module (*pscA*, *pscB* and *hdeD*$_{GI}$) contribute to both heat and chlorine resistance. KefB encoded by the oxidative stress

module is the only protein that specifically contributes to chlorine resistance by protecting membrane lipids. The maintenance of all core genes is necessary to give full protection to multiple cellular components against multiple stressors. The much lower frequency of the tLST in *Salmonella* relative to *E. coli* and *Klebsiella* indicate that *Salmonella* have different resistance mechanisms, thus the genetic determinants of dry-heat resistance and pressure resistance in *Salmonella* were identified in this study, including *cysM*, *pspE*, *phoC*, *sopD*, *uspC* and *ahpD*.

7.2 Ecological role of stress resistance in different lifestyles

Daqu fermentation selects for tLST-positive *Enterobacteriaceae* and *spoVA*^{2mob}-positive bacilli; Chlorination in wastewater treatment selects for tLST-positive strains of *E. coli*. A strong selective pressure like chlorination or thermization at 60 °C is required to maintain core proteins encoded by the tLST. In the absence of selective pressure, the tLST decreases the ecological fitness due to the high metabolic cost. Moreover, the selective pressure for the tLST is incompatible with the selective pressure for virulence factors in enteric pathogens. For example, the co-occurrence of the tLST and virulence factors of *Shigella*, STEC and UPEC has not been found by screening genomes. Strictly vertebrate-associated *Shigella* exclude the tLST but 2% of its parent species *E. coli* with blended lifestyles harboured this genetic island. High frequency of the tLST in those *Enterobacteriaceae* that have varied lifestyles of plant habitats and vertebrate intestines and absence of the tLST in unvaried-lifestyle species (Figure 7.1.) indicated the tLST may serve to overcome dispersal limitation by improving survival outside plant or vertebrate hosts during host transmission. Some species such as *E. coli* and *Klebsiella*, which are still in transition from plant-associated lifestyle to vertebrate-associated lifestyle, get benefits from the tLST for dispersal among environment and hosts, while this function is not necessary for *Salmonella* and some other obligate vertebrate-associated species.

Multiple stressors in wastewater treatment plants provide strong selective pressure for exceptional resistant strains of wide-spectrum species including *Enterobacterales* and *Pseudomonas*. Surprisingly, extremely resistant strains of tLST-positive *E. coli* and *Salmonella* have been isolated from the same source, wastewater, but they have distinct resistance mechanisms and lifestyles. The 6 genes identified in resistant strains of *Salmonella*, which confer dry-heat resistance or high pressure resistance, contributed to the long-term survival of *Salmonella* in non-host environments (Chapter 6). These findings support that the selective pressures in ecosystems maintain the genetic determinants against stressors and drive the evolution towards adaptation to specific hosts or niches.

7.3 Significant impact of the tLST on food safety and public health

Blended lifestyles facilitate gene acquisition related with stress resistance and provides selective pressure for antibiotic resistance independent of human activity (Chapter 2). Several nosocomial pathogens in *Enterobacteriaceae* frequently harbor the tLST, including *Enterobacter*, *Klebsiella*, and *Cronobacter*. These opportunistic human pathogens also acquire antimicrobial resistance genes, which leads to a concern of the spread of antibiotic resistance and urgent demand of new antibiotics. The tLST-mediated resistance to disinfection agents may facilitate bacterial persistence in hospitals and emergence of antibiotic resistant pathogens. The predicted function of several tLST-encoded proteins suggests a contribution to antibiotic resistance (Kamal et al., 2021). Genomic islands are mobile and transferable to pathogens by horizontal gene transfer. Some human-made environmental niches such as wastewater that may contaminate the food supply can enrich resistance genes and make it more likely to transfer among pathogens. Therefore, identification of genetic determinants that provide protection against multiple stressors in

Enterobacteriaceae and investigation of their ecological roles are important for controlling pathogenic *Enterobacterales*.

7.4 Open questions

This study proposed that tLST may facilitate the spread of antibiotic resistance, but the co-occurrence of the tLST and antibiotic resistance in *Enterobacteriaceae* has not been explored. Some human-made niches including chlorination and thermization treatments enriched the tLST, while whether some natural environments that harbor the tLST need further confirmation. For example, oxidative stress generated by the sunshine in water, oxidative stress in predatory protozoa, and heat stress from rotting plant may select for the tLST. The mutual exclusion between the tLST and virulence factors was discovered in this study but the reason is unclear. The presence of *orf1* in almost all tLST-positive *Enterobacterales* (Figure 7.1.) indicates its important role but the functions of *orf1* as well as other genes encoded by different variant of the tLST remain unknown. Besides heat and chlorine resistance, investigation of other potential functions of the tLST is necessary in the future. Last but not least, the ecological role of desiccation tolerance in *Salmonella* is unclear. The reason why *Salmonella* serovars are more desiccation resistant than other intestine-adapted *Enterobacteriaceae* (e.g. *Shigella*, STEC) remains unknown. The correlation between host adaptation and desiccation tolerance in *Salmonella* needs further investigation.

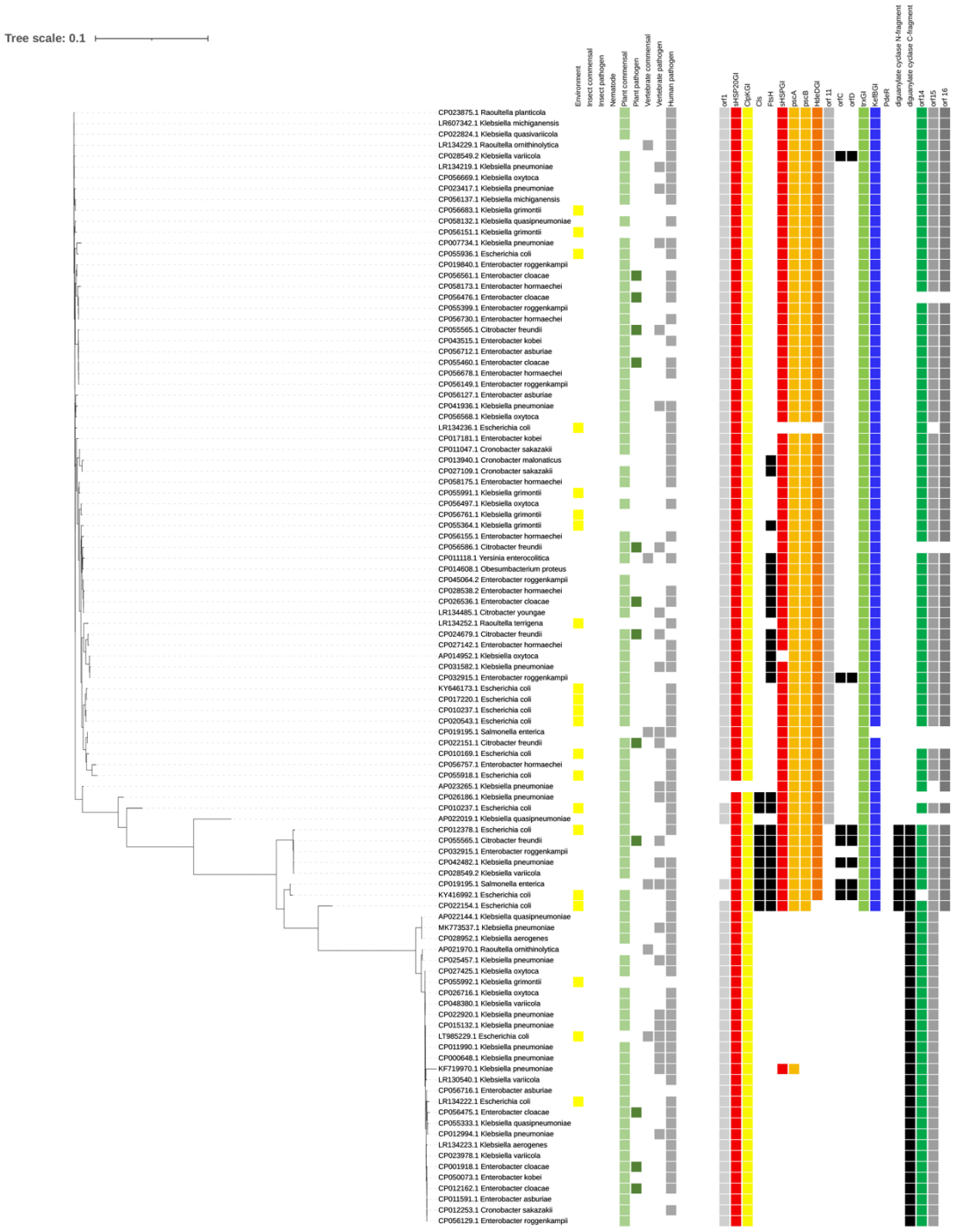

Figure 7.1. Presence of tLST-encoded genes in *Enterobacterales* genomes and their lifestyles. The assignment of species to lifestyle was based on different references (Table S2.4.), which included natural habitats of the species as environmental, insect commensal, insect pathogen, nematode, plant commensal, plant pathogen, vertebrate commensal, vertebrate pathogen, or human pathogen. Colored symbols indicate the presence or absence of each of the 20 genes encoded by the tLST2 of *S. enterica* serovar Senftenberg. The was modified from information provided by (Kamal et al., 2021).

BIBLIOGRAPHY

Achtman, M., Wain, J., Weill, F.-X., Nair, S., Zhou, Z., Sangal, V., Krauland, M.G., Hale, J.L., Harbottle, H., Uesbeck, A., 2012. Multilocus sequence typing as a replacement for serotyping in *Salmonella enterica*. PLoS Pathog 8, e1002776.

Adefisoye, M.A., Okoh, A.I., 2016. Identification and antimicrobial resistance prevalence of pathogenic *Escherichia coli* strains from treated wastewater effluents in Eastern Cape, South Africa. Microbiologyopen 5, 143–151.

Adegun, B.R., Oluduro, A.O., Aregbesola, O.A., 2019. Isolation and molecular characterization of *Citrobacter* species in fruits and vegetables sold for consumption in ILE-IFE, Nigeria. Sci. African 6, e00173.

Adeolu, M., Alnajar, S., Naushad, S., Gupta, R.S., 2016. Genome-based phylogeny and taxonomy of the *'Enterobacteriales'*: Proposal for *Enterobacterales* ord. nov. divided into the families *Enterobacteriaceae, Erwiniaceae* fam. nov., *Pectobacteriaceae* fam. nov., *Yersiniaceae* fam. nov., *Hafniaceae* fam. nov., *Morganellaceae* fam. nov., and *Budviciaceae* fam. nov. Int. J. Syst. Evol. Microbiol. 66, 5575–5599.

Alegbeleye, O.O., Singleton, I., Sant'Ana, A.S., 2018. Sources and contamination routes of microbial pathogens to fresh produce during field cultivation: a review. Food Microbiol. 73, 177–208.

Allahverdi, T., Rahimian, H., Ravanlou, A., 2016. First report of bacterial canker in mulberry caused by *Citrobacter freundii* in Iran. Plant Dis. 100, 1774.

Alm, E.W., Walk, S.T., Gordon, D.M., 2011. The niche of *Escherichia coli*. Popul. Genet. Bact. A Tribut. to Thomas S. Whittam. ASM Press. Washington, United States. 67–89.

Alnajar, S., Gupta, R.S., 2017. Phylogenomics and comparative genomic studies delineate six

main clades within the family *Enterobacteriaceae* and support the reclassification of several polyphyletic members of the family. Infect. Genet. Evol. 54, 108–127.

Anastasi, E.M., Matthews, B., Gundogdu, A., Vollmerhausen, T.L., Ramos, N.L., Stratton, H., Ahmed, W., Katouli, M., 2010. Prevalence and persistence of *Escherichia coli* strains with uropathogenic virulence characteristics in sewage treatment plants. Appl. Environ. 76, 5882–5886.

Anastasi, E.M., Wohlsen, T.D., Stratton, H.M., Katouli, M., 2013. Survival of *Escherichia coli* in two sewage treatment plants using UV irradiation and chlorination for disinfection. Water Res. 47, 6670–6679.

Baek, C., Shin, S.-K., Yi, H., 2019. *Limnobaculum parvum* gen. nov., sp. nov., isolated from a freshwater lake. Int. J. Syst. Evol. Microbiol. 69, 1826–1830.

Baquero, F., Tedim, A.-S.P., Coque, T.M., 2013. Antibiotic resistance shaping multi-level population biology of bacteria. Front. Microbiol. 4, 15.

Barret, M., Egan, F., Fargier, E., Morrissey, J.P., O'Gara, F., 2011. Genomic analysis of the type VI secretion systems in *Pseudomonas* spp.: novel clusters and putative effectors uncovered. Microbiology 157, 1726–1739.

Barron, J.C., Forsythe, S.J., 2007. Dry stress and survival time of *Enterobacter sakazakii* and other *Enterobacteriaceae* in dehydrated powdered infant formula. J. Food Prot. 70, 2111–2117.

Baylis, C., Uyttendaele, M., Joosten, H., Davies, A., 2011. The *Enterobacteriaceae* and their significance to the food industry. Enterobact. their significance to food Ind.

Beer, K.D., Gargano, J.W., Roberts, V.A., Hill, V.R., Garrison, L.E., Kutty, P.K., Hilborn, E.D., Wade, T.J., Fullerton, K.E., Yoder, J.S., 2015. Surveillance for waterborne disease outbreaks associated with drinking water—United States, 2011–2012. MMWR. Morb. Mortal. Wkly.

Rep. 64, 842.

Behravesh, C.B., Ferraro, A., Deasy, M., Dato, V., Moll, M., Sandt, C., Rea, N.K., Rickert, R., Marriott, C., Warren, K., 2010. Human *Salmonella* infections linked to contaminated dry dog and cat food, 2006–2008. Pediatrics 126, 477–483.

Berendsen, E.M., Boekhorst, J., Kuipers, O.P., Wells-Bennik, M.H.J., 2016a. A mobile genetic element profoundly increases heat resistance of bacterial spores. ISME J. 10, 2633–2642.

Berendsen, E.M., Koning, R.A.A., Boekhorst, J., de Jong, A., Kuipers, O.P.P., Wells-Bennik, M.H.J.H.J., 2016b. High-level heat resistance of spores of *Bacillus amyloliquefaciens* and *Bacillus licheniformis* results from the presence of a *spoVA* operon in a Tn1546 transposon. Front. Microbiol. 7, 1912.

Berendsen, E.M., Zwietering, M.H., Kuipers, O.P., Wells-Bennik, M.H.J., 2015. Two distinct groups within the *Bacillus subtilis* group display significantly different spore heat resistance properties. Food Microbiol. 45, 18–25.

Berg, G., Eberl, L., Hartmann, A., 2005. The rhizosphere as a reservoir for opportunistic human pathogenic bacteria. Environ. Microbiol. 7, 1673–1685.

Bernal, P., Llamas, M.A., Filloux, A., 2018. Type VI secretion systems in plant-associated bacteria. Environ. Microbiol. 20, 1–15.

Beuchat, L., Komitopoulou, E., Beckers, H., Betts, R., Bourdichon, F., Fanning, S., Joosten, H., Ter Kuile, B., 2013. Low–water activity foods: increased concern as vehicles of foodborne pathogens. J. Food Prot. 76, 150–172.

Beuchat, L., Komitopoulou, E., Betts, R., Beckers, H., Bourdichon, F., Joosten, H., Fanning, S., ter Kuile, B., 2011. Persistence and survival of pathogens in dry foods and dry food processing environments. ILSI Europe report series. 1–48.

Beuchat, L.R., 2002. Ecological factors influencing survival and growth of human pathogens on raw fruits and vegetables. Microbes Infect. 4, 413–423.

Billi, D., Potts, M., 2002. Life and death of dried prokaryotes. Res. Microbiol. 153, 7–12.

Blake, D.P., Hillman, K., Fenlon, D.R., Low, J.C., 2003. Transfer of antibiotic resistance between commensal and pathogenic members of the *Enterobacteriaceae* under ileal conditions. J. Appl. Microbiol. 95, 428–436.

Blasco, F., Dos Santos, J., Magalon, A., Frixon, C., Guigliarelli, B., Santini, C., Giordano, G., 1998. NarJ is a specific chaperone required for molybdenum cofactor assembly in nitrate reductase A of *Escherichia coli*. Mol. Microbiol. 28, 435–447.

Blekher, L., Siegman-Igra, Y., Schwartz, D., Berger, S.A., Carmeli, Y., 2000. Clinical significance and antibiotic resistance patterns of *Leminorella* spp., an emerging nosocomial pathogen. J. Clin. Microbiol. 38, 3036–3038.

Bobik, T.A., Havemann, G.D., Busch, R.J., Williams, D.S., Aldrich, H.C., 1999. The propanediol utilization (pdu) operon of *Salmonella enterica* serovar Typhimurium LT2 includes genes necessary for formation of polyhedral organelles involved in coenzyme B12-dependent 1, 2-propanediol degradation. J. Bacteriol. 181, 5967.

Boczek, L.A., Rice, E.W., Johnston, B., Johnson, J.R., 2007. Occurrence of antibiotic-resistant uropathogenic *Escherichia coli* clonal group A in wastewater effluents. Appl. Environ. Microbiol. 73, 4180–4.

Boll, E.J., Marti, R., Hasman, H., Overballe-Petersen, S., Stegger, M., Ng, K., Knøchel, S., Krogfelt, K.A., Hummerjohann, J., Struve, C., 2017. Turn up the heat - food and clinical *Escherichia coli* isolates feature two transferrable loci of heat resistance. Front. Microbiol. 8, 579.

Bommer, A., Böhler, O., Johannsen, E., Dobrindt, U., Kuczius, T., 2018. Effect of chlorine on cultivability of Shiga toxin producing *Escherichia coli* (STEC) and β-lactamase genes carrying *E. coli* and *Pseudomonas aeruginosa*. Int. J. Med. Microbiol. 308, 1105–1112.

Bond, W.W., Favero, M.S., 1977. *Bacillus xerothermodurans* sp. nov., a species forming endospores extremely resistant to dry heat. Int. J. Syst. Bacteriol. 27, 157–160.

Bortolaia, V., Kaas, R.S., Ruppe, E., Roberts, M.C., Schwarz, S., Cattoir, V., Philippon, A., Allesoe, R.L., Rebelo, A.R., Florensa, A.F., 2020. ResFinder 4.0 for predictions of phenotypes from genotypes. J. Antimicrob. Chemother. 75, 3491–3500.

Botzler, R.G., 1987. Isolation of *Yersinia enterocolitica* and *Y. frederiksenii* from forest soil, Federal Republic of Germany. J. Wildl. Dis. 23, 311–313.

Boyd, E.F., Wang, F.-S., Beltran, P., Plock, S.A., Nelson, K., Selander, R.K., 1993. *Salmonella* reference collection B (SARB): strains of 37 serovars of subspecies I. Microbiology 139, 1125–1132.

Boyd, E.F., Wang, F.S., Whittam, T.S., Selander, R.K., 1996. Molecular genetic relationships of the salmonellae. Appl. Environ. Microbiol. 62, 804–808.

Boyer, F., Fichant, G., Berthod, J., Vandenbrouck, Y., Attree, I., 2009. Dissecting the bacterial type VI secretion system by a genome wide in silico analysis: what can be learned from available microbial genomic resources? BMC Genomics 10, 1–14.

Breeuwer, P., 2014. Adaptation of Pathogenic Microorganisms to Dry Conditions. Microbiol. Saf. Low Water Act. Foods Spices. Springer, New York, NY, 37-48.

Brock, J.H., Williams, P.H., Liceaga, J., Wooldridge, K.G., 1991. Relative availability of transferrin-bound iron and cell-derived iron to aerobactin-producing and enterochelin-producing strains of *Escherichia coli* and to other microorganisms. Infect. Immun. 59, 3185–

3190.

Bronstein, P.A., Miao, E.A., Miller, S.I., 2000. InvB is a type III secretion chaperone specific for SspA. J. Bacteriol. 182, 6638.

Brown, E.W., Mammel, M.K., LeClerc, J.E., Cebula, T.A., 2003. Limited boundaries for extensive horizontal gene transfer among *Salmonella* pathogens. Proc. Natl. Acad. Sci. 100, 15676–15681.

Bryk, R., Lima, C.D., Erdjument-Bromage, H., Tempst, P., Nathan, C., 2002. Metabolic enzymes of mycobacteria linked to antioxidant defense by a thioredoxin-like protein. Science. 295, 1073–1077.

Brynildsrud, O., Bohlin, J., Scheffer, L., Eldholm, V., 2016. Rapid scoring of genes in microbial pan-genome-wide association studies with Scoary. Genome Biol. 17, 1–9.

Büttner, D., 2012. Protein export according to schedule: architecture, assembly, and regulation of type III secretion systems from plant-and animal-pathogenic bacteria. Microbiol. Mol. Biol. 76, 262-310.

Byappanahalli, M.N., Whitman, R.L., Shively, D.A., Sadowsky, M.J., Ishii, S., 2006. Population structure, persistence, and seasonality of autochthonous *Escherichia coli* in temperate, coastal forest soil from a Great Lakes watershed. Environ. Microbiol. 8, 504–513.

Cabiscol Català, E., Tamarit Sumalla, J., Ros Salvador, J., 2000. Oxidative stress in bacteria and protein damage by reactive oxygen species. Int. Microbiol. 3, 3-8.

Campbell, J.W., Morgan-Kiss, R.M., E. Cronan Jr, J., 2003. A new *Escherichia coli* metabolic competency: growth on fatty acids by a novel anaerobic β-oxidation pathway. Mol. Microbiol. 47, 793–805.

Campbell, M.A., Van Leuven, J.T., Meister, R.C., Carey, K.M., Simon, C., McCutcheon, J.P.,

2015. Genome expansion via lineage splitting and genome reduction in the cicada endosymbiont *Hodgkinia*. Proc. Natl. Acad. Sci. 112, 10192–10199.

Capella-Guti.rrez, S., Silla-Mart.nez, J.M., Gabald.n, T., 2009. trimAl: a tool for automated alignment trimming in large-scale phylogenetic analyses. Bioinformatics 25, 1972–1973.

CDC, 2019. Reports of selected *Salmonella* outbreak investigations. URL https://www.cdc.gov/salmonella/outbreaks.html (accessed 2.25.19).

Chen, Y.Y., Gänzle, M.G.M.G., 2016. Influence of cyclopropane fatty acids on heat, high pressure, acid and oxidative resistance in *Escherichia coli*. Int. J. Food Microbiol. 222, 16–22.

Chen, Y.Y., Temelli, F., Gänzle, M.G., 2017. Mechanisms of inactivation of dry *Escherichia coli* by high-pressure carbon dioxide. Appl. Environ. Microbiol. 83, e00062-17.

Cherepanov, P.P., Wackernagel, W., 1995. Gene disruption in *Escherichia coli*: TcR and KmR cassettes with the option of Flp-catalyzed excision of the antibiotic-resistance determinant. Gene. 158, 9–14.

Clemente, J.C., Pehrsson, E.C., Blaser, M.J., Sandhu, K., Gao, Z., Wang, B., Magris, M., Hidalgo, G., Contreras, M., Noya-Alarcón, Ó., Lander, O., McDonald, J., Cox, M., Walter, J., Oh, P.L., Ruiz, J.F., Rodriguez, S., Shen, N., Song, S.J., Metcalf, J., Knight, R., Dantas, G., Dominguez-Bello, M.G., 2015. The microbiome of uncontacted Amerindians. Sci. Adv. 1, e1500183.

Cole, J., 1996. Nitrate reduction to ammonia by enteric bacteria: redundancy, or a strategy for survival during oxygen starvation? FEMS Microbiol. Lett. 136, 1–11.

Cornelis, P., Wei, Q., Andrews, S.C., Vinckx, T., 2011. Iron homeostasis and management of oxidative stress response in bacteria. Metallomics 3, 540–549.

Cornforth, D.M., Foster, K.R., 2015. Antibiotics and the art of bacterial war. Proc. Natl. Acad. Sci.

U. S. A. 112, 10827–10828.

Croxen, M.A., Law, R.J., Scholz, R., Keeney, K.M., Wlodarska, M., Finlay, B.B., 2013. Recent advances in understanding enteric pathogenic *Escherichia coli*. Clin. Microbiol. Rev. 26, 822–880.

D'Aoust, J.-Y., Maurer, J., 2007. *Salmonella* species, in: Food Microbiology: Fundamentals and Frontiers, Third Edition. American Society of Microbiology, 187–236.

D'Costa, V.M., King, C.E., Kalan, L., Morar, M., Sung, W.W.L., Schwarz, C., Froese, D., Zazula, G., Calmels, F., Debruyne, R., Golding, G.B., Poinar, H.N., Wright, G.D., 2011. Antibiotic resistance is ancient. Nature. 477, 457–461.

Da Silva, R.M., Traebert, J., Galato, D., 2012. *Klebsiella pneumoniae* carbapenemase (KPC)-producing *Klebsiella pneumoniae*: A review of epidemiological and clinical aspects. Expert Opin. Biol. Ther. 12, 663–671.

Datsenko, K.A., Wanner, B.L., 2000. One-step inactivation of chromosomal genes in *Escherichia coli* K-12 using PCR products. Proc. Natl. Acad. Sci. U. S. A. 97, 6640–6645.

Davin-Regli, A., Lavigne, J.-P.P., Pagès, J.-M.M., 2019. Enterobacter spp.: Update on taxonomy, clinical aspects, and emerging antimicrobial resistance. Clin. Microbiol. Rev. 32, e00002-19.

De Maayer, P., Pillay, T., Coutinho, T.A., 2020. Flagella by numbers: comparative genomic analysis of the supernumerary flagellar systems among the *Enterobacterales*. BMC Genomics 21, 1–16.

Degrossoli, A., Müller, A., Xie, K., Schneider, J.F., Bader, V., Winklhofer, K.F., Meyer, A.J., Leichert, L.I., 2018. Neutrophil-generated HOCl leads to non-specific thiol oxidation in phagocytized bacteria. Elife 7, e32288.

den Bakker, H.C., Moreno Switt, A.I., Govoni, G., Cummings, C.A., Ranieri, M.L., Degoricija,

L., Hoelzer, K., Rodriguez-Rivera, L.D., Brown, S., Bolchacova, E., Furtado, M.R., Wiedmann, M., 2011. Genome sequencing reveals diversification of virulence factor content and possible host adaptation in distinct subpopulations of *Salmonella enterica*. BMC Genomics 12, 425.

den Besten, H.M.W., Berendsen, E.M., Wells-Bennik, M.H.J., Straatsma, H., Zwietering, M.H., 2017. Two complementary approaches to quantify variability in heat resistance of spores of *Bacillus subtilis*. Int. J. Food Microbiol. 253, 48–53.

Dibner, J.J., Richards, J.D., 2005. Antibiotic growth promoters in agriculture: history and mode of action. Poult. Sci. 84, 634–643.

Diepold, A., Armitage, J.P., 2015. Type III secretion systems: the bacterial flagellum and the injectisome. Philos. Trans. R. Soc. B Biol. Sci. 370, 20150020.

Dlusskaya, E.A., McMullen, L.M., Gänzle, M.G., 2011. Characterization of an extremely heat-resistant *Escherichia coli* obtained from a beef processing facility. J. Appl. Microbiol. 110, 840–849.

Dong, Y., Iniguez, A.L., Triplett, E.W., 2003. Quantitative assessments of the host range and strain specificity of endophytic colonization by *Klebsiella pneumoniae* 342, in: Plant and Soil. Springer, pp. 49–59.

Douglas, A.E., 1998. Nutritional interactions in insect-microbial symbioses: aphids and their symbiotic bacteria *Buchnera*. Annu. Rev. Entomol. 43, 17–37.

Doyle MP, B.R. (ed), 2012. Food microbiology: fundamentals and frontiers. ASM Press. Washington, United States.

Drazic, A., Tsoutsoulopoulos, A., Peschek, J., Gundlach, J., Krause, M., Bach, N.C., Gebendorfer, K.M., Winter, J., 2013. Role of cysteines in the stability and DNA-binding activity of the

hypochlorite-specific transcription factor HypT. PLoS One 8, e75683.

Du, L., Jaya Prasad, A., Gänzle, M., Roopesh, M.S., 2020. Inactivation of *Salmonella* spp. in wheat flour by 395 nm pulsed light emitting diode (LED) treatment and the related functional and structural changes of gluten. Food Res. Int. 127, 108716.

Du, W.X., Abd, S.J., McCarthy, K.L., Harris, L.J., 2010. Reduction of *Salmonella* on inoculated almonds exposed to hot oil. J. Food Prot. 73, 1238–1246.

Du, Z., Nandakumar, R., Nickerson, K.W., Li, X., 2015. Proteomic adaptations to starvation prepare *Escherichia coli* for disinfection tolerance. Water Res. 69, 110–119.

Earl, C.D., Ronson, C.W., Ausubel, F.M., 1987. Genetic and structural analysis of the *Rhizobium meliloti fixA*, *fixB*, *fixC*, and *fixX* genes. J. Bacteriol. 169, 1127.

Eden, P.A., Schmidt, T.M., Blakemore, R.P., Pace, N.R., 1991. Phylogenetic analysis of *Aquaspirillum magnetotacticum* using polymerase chain reaction-amplified 16S rRNA-specific DNA. Int. J. Syst. Bacteriol. 41, 324–325.

Edgar, R.C., 2004. MUSCLE: A multiple sequence alignment method with reduced time and space complexity. BMC Bioinformatics 5, 113.

Eisenhauer, H.A., Shames, S., Pawelek, P.D., Coulton, J.W., 2005. Siderophore transport through *Escherichia coli* outer membrane receptor FhuA with disulfide-tethered cork and barrel domains. J. Biol. Chem. 280, 30574–30580.

Ellermeier, J.R., Slauch, J.M., 2007. Adaptation to the host environment: regulation of the SPI1 type III secretion system in *Salmonella enterica* serovar Typhimurium. Curr. Opin. Microbiol. 10, 24–29.

Engels, C., Schwab, C., Zhang, J., Stevens, M.J.A., Bieri, C., Ebert, M.-O., McNeill, K., Sturla, S.J., Lacroix, C., 2016. Acrolein contributes strongly to antimicrobial and heterocyclic amine

transformation activities of reuterin. Sci. Rep. 6, 36246.

Ercumen, A., Pickering, A.J., Kwong, L.H., Arnold, B.F., Parvez, S.M., Alam, M., Sen, D., Islam, S., Kullmann, C., Chase, C., 2017. Animal feces contribute to domestic fecal contamination: evidence from *E. coli* measured in water, hands, food, flies, and soil in Bangladesh. Environ. Sci. Technol. 51, 8725–8734.

Esteban, M.-D., Conesa, R., Huertas, J.-P., Palop, A., 2015. Effect of thymol in heating and recovery media on the isothermal and non-isothermal heat resistance of Bacillus spores. Food Microbiol. 48, 35–40.

Esty, J.R., Meyer, K.F., 1922. The heat resistance of the spores of *B. botulinus* and allied anaerobes. XI. J. Infect. Dis. 31, 650–663.

Fang, Y., McMullen, L.M., Gänzle, M.G., 2020. Effect of drying on oxidation of membrane lipids and expression of genes encoded by the Shiga toxin prophage in *Escherichia coli*. Food Microbiol. 86, 103332.

Fang, Y., Mercer, R.G.R.G., McMullen, L.M., Gänzle, M.G., 2017. Induction of Shiga toxin encoding prophage by abiotic environmental stress in food. Appl. Environ. Microbiol. 83, e01378-17.

Fatica, M.K., Schneider, K.R., 2011. *Salmonella* and produce: survival in the plant environment and implications in food safety. Virulence. 2, 573–579.

Feeney, A., Johnston, C.D., Govender, R., O'Mahony, J., Coffey, A., Sleator, R.D., 2014. Analysis of the role of the *Cronobacter sakazakii* ProP homologues in osmotolerance. Gut Pathog. 6, 15.

Ferguson, G.P., Munro, A.W., Douglas, R.M., McLaggan, D., Booth, I.R., 1993a. Activation of potassium channels during metabolite detoxification in *Escherichia coli*. Mol. Microbiol. 9,

1297–1303.

Ferguson, G.P., Munro, A.W., Douglas, R.M., McLaggan, D., Booth, I.R., 1993b. Activation of potassium channels during metabolite detoxification in *Escherichia coli*. Mol. Microbiol. 9, 1297–1303.

Filloux, A., 2009. The type VI secretion system: a tubular story. EMBO J. 28, 309–310.

Filutowicz, M., Wiater, A., Hulanicka, D., 1982. Delayed inducibility of sulphite reductase in cysM mutants of *Salmonella* typhimurium under anaerobic conditions. Microbiology 128, 1791–1794.

Fink-Gremmels, J., van der Merwe, D., 2019. Mycotoxins in the food chain: contamination of foods of animal origin. Chem. hazards foods Anim. Orig. ECVPH Food Saf. Assur. Vet. Public Heal. 241–261.

Finn, S., Condell, O., McClure, P., Amézquita, A., Fanning, S., 2013. Mechanisms of survival, responses, and sources of *Salmonella* in low-moisture environments. Front. Microbiol. 4, 331.

Fisher, R.M., Henry, L.M., Cornwallis, C.K., Kiers, E.T., West, S.A., 2017. The evolution of host-symbiont dependence. Nat. Commun. 8, 1–8.

Forst, S., Dowds, B., Boemare, N., Stackebrandt, E., 1997. *Xenorhabdus* and *Photorhabdus* spp.: bugs that kill bugs. Annu. Rev. Microbiol. 51, 47–72.

Foxman, B., 2010. The epidemiology of urinary tract infection. Nat. Rev. Urol. 7, 653–660.

Freeman, J.A., Rappl, C., Kuhle, V., Hensel, M., Miller, S.I., 2002. SpiC is required for translocation of *Salmonella* pathogenicity island 2 effectors and secretion of translocon proteins SseB and SseC. J. Bacteriol. 184, 4971.

Frelka, J.C., Harris, L.J., 2014. Nuts and nut pastes, in: Gurtler, J., Doyle, M., Kornacki, J. (Eds.), The Microbiological Safety of Low Water Activity Foods and Spices. Springer, New York,

213–244.

Fu, S., Hiley, L., Octavia, S., Tanaka, M.M., Sintchenko, V., Lan, R., 2017. Comparative genomics of Australian and international isolates of *Salmonella* Typhimurium: correlation of core genome evolution with CRISPR and prophage profiles. Sci. Rep. 7, 1–12.

Fukatsu, T., Koga, R., Smith, W.A., Tanaka, K., Nikoh, N., Sasaki-Fukatsu, K., Yoshizawa, K., Dale, C., Clayton, D.H., 2007. Bacterial endosymbiont of the slender pigeon louse, *Columbicola columbae*, allied to endosymbionts of grain weevils and tsetse flies. Appl. Environ. Microbiol. 73, 6660–6668.

Gajdosova, J., Benedikovicova, K., Kamodyova, N., Tothova, L., Kaclikova, E., Stuchlik, S., Turna, J., Drahovska, H., 2011. Analysis of the DNA region mediating increased thermotolerance at 58 °C in *Cronobacter* sp. and other enterobacterial strains. Antonie Van Leeuwenhoek 100, 279–289.

Gänzle, M.G., 2015. Lactic metabolism revisited: Metabolism of lactic acid bacteria in food fermentations and food spoilage. Curr. Opin. Food Sci. 2, 106–117.

Gänzle, M.G., Hertel, C., Hammes, W.P., 1999. Resistance of *Escherichia coli* and *Salmonella* against nisin and curvacin A. Int. J. Food Microbiol. 48, 37–50.

Gautam, B., Govindan, B.N., Gänzle, M., Roopesh, M.S., 2020. Influence of water activity on the heat resistance of *Salmonella enterica* in selected low-moisture foods. Int. J. Food Microbiol. 334, 108813.

Ge, Y., Wang, B., Yang, J., Lai, X.-H., Zhang, G., Lu, S., Jin, D., Huang, Y., Cheng, Y., Zhang, X., 2021. *Jinshanibacter*, a new genus of *Budviciaceae*: identification of *Jinshanibacter zhutongyuii* sp. nov. and *Jinshanibacter xujianqingii* sp. nov. isolated from cloacal content of snow finch (*Montifringilla taczanowskii*). Int. J. Syst. Evol. Microbiol. 4653.

Gehring, A.M., Mori, I., Walsh, C.T., 1998. Reconstitution and characterization of the *Escherichia coli* enterobactin synthetase from EntB, EntE, and EntF. Biochemistry 37, 2648–2659.

Geiger, O., Röhrs, V., Weissenmayer, B., Finan, T.M., Thomas-Oates, J.E., 1999. The regulator gene phoB mediates phosphate stress-controlled synthesis of the membrane lipid diacylglyceryl-N, N, N-trimethylhomoserine in *Rhizobium* (*Sinorhizobium*) *meliloti*. Mol. Microbiol. 32, 63–73.

Gill, A., Tamber, S., Yang, X., 2019. Relative response of populations of *Escherichia coli* and *Salmonella enterica* to exposure to thermal, alkaline and acidic treatments. Int. J. Food Microbiol. 293, 94–101.

Goodrich-Blair, H., Clarke, D.J., Goodrich-Blair, H., Clarke, D.J., 2007. Mutualism and pathogenesis in *Xenorhabdus* and *Photorhabdus*: two roads to the same destination. Mol. Microbiol. 64, 260–268.

Gouliouris, T., Raven, K.E., Moradigaravand, D., Ludden, C., Coll, F., Blane, B., Naydenova, P., Horner, C., Brown, N.M., Corander, J., 2019. Detection of vancomycin-resistant *Enterococcus faecium* hospital-adapted lineages in municipal wastewater treatment plants indicates widespread distribution and release into the environment. Genome Res. 29, 626–634.

Gray, M.J., Jakob, U., 2015. Oxidative stress protection by polyphosphate—new roles for an old player. Curr. Opin. Microbiol. 24, 1–6.

Gray, M.J., Wholey, W.-Y., Parker, B.W., Kim, M., Jakob, U., 2013. NemR is a bleach-sensing transcription factor. J. Biol. Chem. 288, 13789–13798.

Groussin, M., Mazel, F., Alm, E.J., 2020. Co-evolution and co-speciation of host-gut Bacteria systems. Cell Host Microbe 28, 12–22.

Gruzdev, N., Pinto, R., Sela, S., 2011. Effect of desiccation on tolerance of *Salmonella enterica* to multiple stresses. Appl. Environ. Microbiol. 77, 1667–1673.

Gu, J., Neary, J.L., Sanchez, M., Yu, J., Lilburn, T.G., Wang, Y., 2007. Genome evolution and functional divergence in *Yersinia*. J. Exp. Zool. Part B Mol. Dev. Evol. 308, 37–49.

Guragain, M., Brichta-Harhay, D.M., Bono, J.L., Bosilevac, J.M., 2021. Locus of heat resistance (LHR) in meat-borne *Escherichia coli*: screening and genetic characterization. Appl. Environ. Microbiol. 87, e02343-20

Gurtler, J.B., Doyle, M.P., Kornacki, J.L., 2014. The microbiological safety of spices and low-water activity foods: correcting historic misassumptions, in: The Microbiological Safety of Low Water Activity Foods and Spices. Springer New York, New York, NY, 3–13.

Harrison, J.E., Schultz, J., 1976. Studies on the chlorinating activity of myeloperoxidase. J. Biol. Chem. 251, 1371–1374.

Harshey, R.M., 2003. Bacterial motility on a surface: many ways to a common goal. Annu. Rev. Microbiol. 57, 249–273.

Hayward, R.D., Koronakis, V., 1999. Direct nucleation and bundling of actin by the SipC protein of invasive *Salmonella*. EMBO J. 18, 4926–4934.

Healy, B., Cooney, S., O'Brien, S., Iversen, C., Whyte, P., Nally, J., Callanan, J.J., Fanning, S., 2010. *Cronobacter* (*Enterobacter sakazakii*): an opportunistic foodborne pathogen. Foodborne Pathog. Dis. 7, 339–350.

Hébrard, M., Viala, J.P.M., Méresse, S., Barras, F., Aussel, L., 2009. Redundant hydrogen peroxide scavengers contribute to *Salmonella* virulence and oxidative stress resistance. J. Bacteriol. 191, 4605–4614.

Heermann, R., Weber, A., Mayer, B., Ott, M., Hauser, E., Gabriel, G., Pirch, T., Jung, K., 2009.

The universal stress protein UspC scaffolds the KdpD/KdpE signaling cascade of *Escherichia coli* under salt stress. J. Mol. Biol. 386, 134–148.

Heiman, K.E., Mody, R.K., Johnson, S.D., Griffin, P.M., Gould, L.H., 2015. *Escherichia coli* O157 outbreaks in the United States, 2003–2012. Emerg. Infect. Dis. 21, 1293.

Herbst, S., Lorkowski, M., Sarenko, O., Nguyen, T.K.L., Jaenicke, T., Hengge, R., 2018. Transmembrane redox control and proteolysis of PdeC, a novel type of c-di-GMP phosphodiesterase. EMBO J. 37, e97825.

Herold, S., Karch, H., Schmidt, H., 2004. Shiga toxin-encoding bacteriophages – genomes in motion. Int. J. Med. Microbiol. 294, 115–121.

Hillion, M., Antelmann, H., 2015. Thiol-based redox switches in prokaryotes. Biol. Chem. 396, 415–444.

Hinnebusch, B.J., Erickson, D.L., 2008. *Yersinia pestis* biofilm in the flea vector and its role in the transmission of plague. Bact. biofilms 229–248.

Hinton, D.M., Bacon, C.W., 1995. *Enterobacter cloacae* is an endophytic symbiont of corn. Mycopathologia 129, 117–125.

Holmes, A., Pritchard, L., Hedley, P., Morris, J., McAteer, S.P., Gally, D.L., Holden, N.J., 2020. A high-throughput genomic screen identifies a role for the plasmid-borne type II secretion system of *Escherichia coli* O157: H7 (Sakai) in plant-microbe interactions. Genomics 112, 4242–4253.

Holmgren, A., 1979. Thioredoxin catalyzes the reduction of insulin disulfides by dithiothreitol and dihydrolipoamide. J. Biol. Chem. 254, 9627–9632.

Holt, K.E., Lassalle, F., Wyres, K.L., Wick, R., Mostowy, R.J., 2020. Diversity and evolution of surface polysaccharide synthesis loci in *Enterobacteriales*. ISME J. 14, 1713–1730.

Holt, K.E., Parkhill, J., Mazzoni, C.J., Roumagnac, P., Weill, F.-X., Goodhead, I., Rance, R., Baker, S., Maskell, D.J., Wain, J., 2008. High-throughput sequencing provides insights into genome variation and evolution in *Salmonella* Typhi. Nat. Genet. 40, 987.

Holý, O., Forsythe, S., 2014. *Cronobacter* spp. as emerging causes of healthcare-associated infection. J. Hosp. Infect. 86, 169–177.

Hommais, F., Krin, E., Coppee, J.-Y., Lacroix, C., Yeramian, E., Danchin, A., Bertin, P., 2004. GadE (YhiE): a novel activator involved in the response to acid environment in *Escherichia coli*. Microbiology 150, 61–72.

Hong, E.-J., Jeong, H., Lee, D.-S., Kim, Y., Lee, H.-S., 2019. The *ahpD* gene of *Corynebacterium glutamicum* plays an important role in hydrogen peroxide-induced oxidative stress response. J. Biochem. 165, 197–204.

Hosoya, S., Yamane, K., Takeuchi, M., Sato, T., 2002. Identification and characterization of the *Bacillus subtilis* D-glucarate/galactarate utilization operon *ycbCDEFGHJ*. FEMS Microbiol. Lett. 210, 193–199.

Hoy, M.A., 2019. Genetic systems, genome evolution, and genetic control of embryonic development in insects. Insect Mol. Genet. 103–175.

Hu, L., Peng, X., Chen, H., Yan, C., Liu, Y., Xu, Q., Fang, Z., Lin, Y., Xu, S., Feng, B., Li, J., Wu, D., Che, L., 2017. Effects of intrauterine growth retardation and *Bacillus subtilis* PB6 supplementation on growth performance, intestinal development and immune function of piglets during the suckling period. Eur. J. Nutr. 56, 1753–1765.

Hu, Y., Huang, H., Cheng, X., Shu, X., White, A.P., Stavrinides, J., K.ster, W., Zhu, G., Zhao, Z., Wang, Y., 2017. A global survey of bacterial type III secretion systems and their effectors. Environ. Microbiol. 19, 3879–3895.

Huihui, Z., Yue, W., Xin, L., Guoqiang, H., Yanhui, C., Zhiyuan, T., Jieyu, S., Nan, X., Guangyu, S., 2020. Chlorophyll synthesis and the photoprotective mechanism in leaves of mulberry (*Morus alba L.*) seedlings under NaCl and NaHCO3 stress revealed by TMT-based proteomics analyses. Ecotoxicol. Environ. Saf. 190, 110164.

Hyatt, D., Chen, G.-L., LoCascio, P.F., Land, M.L., Larimer, F.W., Hauser, L.J., 2010. Prodigal: prokaryotic gene recognition and translation initiation site identification. BMC Bioinformatics 11, 1–11.

Imamovic, L., Jofre, J., Schmidt, H., Serra-Moreno, R., Muniesa, M., 2009. Phage-mediated Shiga toxin 2 gene transfer in food and water. Appl. Environ. Microbiol. 75, 1764–1768.

Jang, J., Hur, H.G., Sadowsky, M.J., Byappanahalli, M.N., Yan, T., Ishii, S., 2017. Environmental *Escherichia coli*: ecology and public health implications—a review. J. Appl. Microbiol. 123, 570–581.

Jaradat, Z.W., Al Mousa, W., Elbetieha, A., Al Nabulsi, A., Tall, B.D., 2014. *Cronobacter* spp. – opportunistic food-borne pathogens. A review of their virulence and environmental-adaptive traits. J. Med. Microbiol. 63, 1023–1037.

Jayeola, V., McClelland, M., Porwollik, S., Chu, W., Farber, J., Kathariou, S., 2020. Identification of novel henes mediating survival of *Salmonella* on low-moisture foods via transposon sequencing analysis. Front. Microbiol. 11, 1–12.

Jeremić, S., Jakić-Dimić, D., Veljović, L.J., 2003. *Citrobacter freundii* as a cause of disease in fish. Acta Vet. Brno. 53, 399–410.

Jha, A.K., Bais, H.P., Vivanco, J.M., 2005. *Enterococcus faecalis* mammalian virulence-related factors exhibit potent pathogenicity in the Arabidopsis thaliana plant model. Infect. Immun. 73, 464–475.

Jiang, L., Wang, D., Lee, J.-S., Kim, D.-H., Jeong, J.C., Kim, C.Y., Kim, S.W., Lee, J., 2020. *Jejubacter calystegiae* gen. nov., sp. nov., moderately halophilic, a new member of the family *Enterobacteriaceae,* isolated from beach morning glory. J. Microbiol. 58, 357–366.

Jiang, X., Rossanese, O.W., Brown, N.F., Kujat-Choy, S., Galán, J.E., Finlay, B.B., Brumell, J.H., 2004. The related effector proteins SopD and SopD2 from *Salmonella enterica* serovar Typhimurium contribute to virulence during systemic infection of mice. Mol. Microbiol. 54, 1186–1198.

Johnston-Monje, D., Raizada, M.N., 2011. Conservation and diversity of seed associated endophytes in Zea across boundaries of evolution, ethnography and ecology. PLoS One 6, e20396.

Jourdan, N., Le Hello, S., Delmas, G., Clouzeau, J., Manteau, C., Désaubliaux, B., Chagnon, V., Thierry-Bled, F., Demare, N., Weill, F.X., 2008. Nationwide outbreak of *Salmonella enterica* serotype give infections in infants in France, linked to infant milk formula, September 2008. Eurosurveillance 13, 18994.

Jovanovic, G., Lloyd, L.J., Stumpf, M.P.H., Mayhew, A.J., Buck, M., 2006. Induction and function of the phage shock protein extracytoplasmic stress response in *Escherichia coli*. J. Biol. Chem. 281, 21147–21161.

Kakatkar, A.S., Gautam, R.K., Godambe, P.L., Shashidhar, R., 2017. Culture dependent and independent studies on emerging food-borne pathogens *Cronobacter sakazakii*, *Klebsiella pneumoniae* and *Enterococcus faecalis* in Indian food. Int. Food Res. J. 24, 2645–2651.

Kalyaanamoorthy, S., Minh, B.Q., Wong, T.K.F., von Haeseler, A., Jermiin, L.S., 2017. ModelFinder: Fast model selection for accurate phylogenetic estimates. Nat. Methods 14, 587–589.

Kamal, S.M., Rybtke, M.L., Nimtz, M., Sperlein, S., Giske, C., Trček, J., Deschamps, J., Briandet, R., Dini, L., Jänsch, L., Tolker-Nielsen, T., Lee, C., Römling, U., 2019. Two FtsH proteases contribute to fitness and adaptation of *Pseudomonas aeruginosa* Clone C strains. Front. Microbiol. 10, 1372.

Kamal, S.M., Simpson, D.J., Wang, Z., Gänzle, M., Römling, U., 2021. Horizontal transmission of stress resistance genes shape the ecology of beta- and gamma-Proteobacteria. Front. Microbiol. 12, 696522.

Kämpfer, P., Glaeser, S.P., Raza, M.W., Abbasi, S.A., Perry, J.D., 2014. *Pseudocitrobacter* gen. nov., a novel genus of the *Enterobacteriaceae* with two new species *Pseudocitrobacter faecalis* sp. nov., and *Pseudocitrobacter anthropi* sp. nov, isolated from fecal samples from hospitalized patients in Pa. Syst. Appl. Microbiol. 37, 17–22.

Kingsley, R.A., Bäumler, A.J., 2000. Host adaptation and the emergence of infectious disease: the *Salmonella* paradigm. Mol. Microbiol. 36, 1006–1014.

Kintz, E., Brainard, J., Hooper, L., Hunter, P., 2017. Transmission pathways for sporadic Shiga-toxin producing *E. coli* infections: A systematic review and meta-analysis. Int. J. Hyg. Environ. Health 220, 57–67.

Kojima, M., 1971. Studies on the effects of isothiocyanates and their analogues on microorganisms. I. Effect of isothiocyanates on the oxygen uptake of yeasts. J. Ferment. Technol. 49, 740–746.

Koleva, P.T., 2014. Non-digestible fibers and dietary interventions: alternative approaches for the treatment of inflammatory bowel disease. PhD thesis, Alberta of University.

Kort, R., O'Brien, A.C., Stokkum, I.H.M. van, Oomes, S.J.C.M.J.C.M., Crielaard, W., Hellingwerf, K.J.J., Brul, S., 0'Brien, A.C.C., Van Stokkum, I.H.M.H.M., Oomes, S.J.C.M.J.C.M., Crielaard, W., Hellingwerf, K.J.J., Brul, S., 2005. Assessment of heat

resistance of bacterial spores from food product isolates by fluorescence monitoring of dipicolinic acid release. Appl. Environ. Microbiol. 71, 3556–3564.

Koutsoumanis, K., Allende, A., Alvarez-Ordóñez, A., Bover-Cid, S., Chemaly, M., Davies, R., De Cesare, A., Herman, L., Hilbert, F., Lindqvist, R., Nauta, M., Peixe, L., Ru, G., Simmons, M., Skandamis, P., Suffredini, E., Jenkins, C., Monteiro Pires, S., Morabito, S., Niskanen, T., Scheutz, F., da Silva Felício, M.T., Messens, W., Bolton, D., Alvarez-Ordóñez, A., Bover-Cid, S., Chemaly, M., Davies, R., De Cesare, A., Herman, L., Hilbert, F., Lindqvist, R., Nauta, M., Peixe, L., Ru, G., Simmons, M., Skandamis, P., Suffredini, E., Jenkins, C., Monteiro Pires, S., Morabito, S., Niskanen, T., Scheutz, F., da Silva Felício, M.T., Messens, W., Bolton, D., 2020. Pathogenicity assessment of Shiga toxin-producing *Escherichia coli* (STEC) and the public health risk posed by contamination of food with STEC. EFSA J. 18, 5967.

Koutsoumanis, K., Allende, A., Álvarez-Ordóñez, A., Bolton, D., Bover-Cid, S., Chemaly, M., Davies, R., De Cesare, A., Herman, L., Hilbert, F., Lindqvist, R., Nauta, M., Ru, G., Simmons, M., Skandamis, P., Suffredini, E., Argüello, H., Berendonk, T., Cavaco, L.M., Gaze, W., Schmitt, H., Topp, E., Guerra, B., Liébana, E., Stella, P., Peixe, L., 2021. Role played by the environment in the emergence and spread of antimicrobial resistance (AMR) through the food chain. EFSA J. 19, 6651.

Kozlov, A.M., Darriba, D., Flouri, T., Morel, B., Stamatakis, A., 2019. RAxML-NG: a fast, scalable and user-friendly tool for maximum likelihood phylogenetic inference. Bioinformatics 35, 4453–4455.

Krawczyk, A.O., Berendsen, E.M., de Jong, A., Boekhorst, J., Wells-Bennik, M.H.J., Kuipers, O.P., Eijlander, R.T., 2016. A transposon present in specific strains of *Bacillus subtilis* negatively affects nutrient- and dodecylamine-induced spore germination. Environ.

Microbiol. 18, 4830–4846.

Krawczyk, A.O., de Jong, A., Omony, J., Holsappel, S., Wells-Bennik, M.H.J., Kuipers, O.P., Eijlander, R.T., 2017. Spore heat activation requirements and germination responses correlate with sequences of germinant receptors and with the presence of a specific *spoVA*^{2mob} operon in foodborne strains of *Bacillus subtilis*. Appl. Environ. Microbiol. 83, e03122-16.

Lasko, M.J., Nicolau, D.P., 2020. Carbapenem-resistant *Enterobacterales*: considerations for treatment in the era of new antimicrobials and evolving enzymology. Curr. Infect. Dis. Rep. 22, 1–12.

Lau, C.K.Y., Krewulak, K.D., Vogel, H.J., 2016. Bacterial ferrous iron transport: the Feo system. FEMS Microbiol. Rev. 40, 273–298.

Laufer, A.S., Grass, J., Holt, K., Whichard, J.M., Griffin, P.M., Gould, L.H., 2015. Outbreaks of *Salmonella* infections attributed to beef --United States, 1973-2011. Epidemiol. Infect. 143, 2003–2013.

Lawlor, K.M., Daskaleros, P.A., Robinson, R.E., Payne, S.M., 1987. Virulence of iron transport mutants of *Shigella flexneri* and utilization of host iron compounds. Infect. Immun. 55, 594–599.

Lawlor, M.S., O'connor, C., Miller, V.L., 2007. Yersiniabactin is a virulence factor for *Klebsiella pneumoniae* during pulmonary infection. Infect. Immun. 75, 1463–1472.

Lee, C., Franke, K.B., Kamal, S.M., Kim, H., Lünsdorf, H., Jäger, J., Nimtz, M., Trček, J., Jänsch, L., Bukau, B., Mogk, A., Römling, U., 2018. Stand-alone ClpG disaggregase confers superior heat tolerance to bacteria. Proc. Natl. Acad. Sci. 115, E273–E282.

Lee, C., Park, C., 2017. Bacterial responses to glyoxal and methylglyoxal: reactive electrophilic species. Int. J. Mol. Sci. 18, 169.

Lee, C., Wigren, E., Trček, J., Peters, V., Kim, J., Hasni, M.S., Nimtz, M., Lindqvist, Y., Park, C., Curth, U., 2015. A novel protein quality control mechanism contributes to heat shock resistance of worldwide-distributed *Pseudomonas aeruginosa* clone C strains. Environ. Microbiol. 17, 4511–4526.

Lee, H.-R.R.H.S., Lee, S., Kim, J.-S.S., Lee, H.-R.R.H.S., Shin, H.-C.C., Lee, M.-S.S., Jin, K.S., Kim, C.-H.H., Ku, B., Ryu, C.-M.M., Kim, S.J., 2019. Structural and physiological exploration of *Salmonella* Typhi YfdX uncovers its dual function in bacterial antibiotic stress and virulence. Front. Microbiol. 9, 3329.

Lee, J.-J., Wu, Y.-C., Kuo, C.-J., Hsuan, S.-L., Chen, T.-H., 2016. TolC is important for bacterial survival and oxidative stress response in *Salmonella enterica* serovar Choleraesuis in an acidic environment. Vet. Microbiol. 193, 42–48.

LeThanh, H., Neubauer, P., Hoffmann, F., 2005. The small heat-shock proteins IbpA and IbpB reduce the stress load of recombinant *Escherichia coli* and delay degradation of inclusion bodies. Microb. Cell Fact. 4, 1–12.

Letunic, I., Bork, P., 2019. Interactive Tree Of Life (iTOL) v4: recent updates and new developments. Nucleic Acids Res. 47, W256–W259.

Li, H., Gänzle, M., 2016. Some like it hot: Heat resistance of *Escherichia coli* in food. Front. Microbiol. 7, 01763.

Li, H., Mercer, R., Behr, J., Heinzlmeir, S., McMullen, L.M., Vogel, R.F., Gänzle, M.G., 2020. Heat and pressure resistance in *Escherichia coli* relates to protein folding and aggregation. Front. Microbiol. 11, 111.

Li, P., Aflakpui, F.W.K., Yu, H., Luo, L., Lin, W.-T., 2015a. Characterization of activity and microbial diversity of typical types of Daqu for traditional Chinese vinegar. Ann. Microbiol.

65, 2019–2027.

Li, P., Liang, H., Lin, W.-T., Feng, F., Luo, L., 2015b. Microbiota dynamics associated with environmental conditions and potential roles of cellulolytic communities in traditional Chinese cereal starter solid-state fermentation. Appl. Environ. Microbiol. 81, 5144–5156.

Li, P., Lin, W., Liu, X., Wang, X., Luo, L., 2016. Environmental factors affecting microbiota dynamics during traditional solid-state fermentation of Chinese Daqu starter. Front. Microbiol. 7, 1237.

Li, Z., Schottroff, F., Simpson, D.J., Gänzle, M.G., 2019. The copy number of the *spoVA*^{2mob} operon determines pressure resistance of *Bacillus* endospores. Appl. Environ. Microbiol. 85, e01596-19.

Li, Z., Siepmann, F.B., Rojas Tovar, L.E., Chen, X., Gänzle, M.G., 2020. Effect of copy number of the *spoVA*^{2mob} operon, sourdough and reutericyclin on ropy bread spoilage caused by *Bacillus* spp. Food Microbiol. 91, 103507.

Lin, X.B., Gänzle, M.G., 2014. Quantitative high-resolution melting PCR analysis for monitoring of fermentation microbiota in sourdough. Int. J. Food Microbiol. 186, 42–48.

Lin, X.B., Farhangfar, A., Valcheva, R., Sawyer, M.B., Dieleman, L., Schieber, A., Gänzle, M.G., Baracos, V., 2014. The role of intestinal microbiota in development of irinotecan toxicity and in toxicity reduction through dietary fibres in rats. PLoS One 9(1): e83644.

Litrup, E., Torpdahl, M., Malorny, B., Huehn, S., Christensen, H., Nielsen, E.M., 2010. Association between phylogeny, virulence potential and serovars of *Salmonella enterica*. Infect. Genet. Evol. 10, 1132–1139.

Liu, B., Zheng, D., Jin, Q., Chen, L., Yang, J., 2019. VFDB 2019: a comparative pathogenomic platform with an interactive web interface. Nucleic Acids Res. 47, D687–D692.

Liu, Y., Gill, A., Mcmullen, L., Gänzle, M., 2015. Variation in heat and pressure resistance of verotoxigenic and nontoxigenic *Escherichia coli*. J. Food Prot. 78, 111–120.

Loaces, I., Ferrando, L., Scavino, A.F., Fernández Scavino, A., 2011. Dynamics, diversity and function of endophytic siderophore-producing bacteria in rice. Microb. Ecol. 61, 606–618.

Łoś, J.M., Łoś, M., Węgrzyn, A., Węgrzyn, G., 2013. Altruism of Shiga toxin-producing *Escherichia coli*: recent hypothesis versus experimental results. Front. Cell. Infect. Microbiol. 2, 166.

Łoś, J.M., Łoś, M., Węgrzyn, G., Węgrzyn, A., 2009. Differential efficiency of induction of various lambdoid prophages responsible for production of Shiga toxins in response to different induction agents. Microb. Pathog. 47, 289–298.

Luo, C., Walk, S.T., Gordon, D.M., Feldgarden, M., Tiedje, J.M., Konstantinidis, K.T., 2011. Genome sequencing of environmental *Escherichia coli* expands understanding of the ecology and speciation of the model bacterial species. Proc. Natl. Acad. Sci. U. S. A. 108, 7200–7205.

Ma, A., Chui, L., 2017. Identification of heat resistant *Escherichia coli* by qPCR for the locus of heat resistance. J. Microbiol. Methods 133, 87–89.

Macauley, J.J., Qiang, Z., Adams, C.D., Surampalli, R., Mormile, M.R., 2006. Disinfection of swine wastewater using chlorine, ultraviolet light and ozone. Water Res. 40, 2017–2026.

Mafart, P., Couvert, O., Gaillard, S., Leguerinel, I., 2001. On calculating sterility in thermal preservation methods : Application of the Weibull frequency distribution model. Acta Hortic. 566, 107–114.

Malone, A.S., Chung, Y.K., Yousef, A.E., 2006. Genes of *Escherichia coli* O157:H7 that are involved in high-pressure resistance. Appl. Environ. Microbiol. 72, 2661–2671.

Mandal, R.K., Kwon, Y.M., 2017. Global screening of *Salmonella enterica* serovar Typhimurium

genes for desiccation survival. Front. Microbiol. 8, 1723.

Mardaneh, J., Soltan-Dallal, M.-M., 2014. Isolation and identification of *E. cowanii* from powdered infant formula in NICU and determination of antimicrobial susceptibility of isolates. Iran. J. Pediatr. 24, 261.

Margosch, D., Ehrmann, M.A., Buckow, R., Heinz, V., Vogel, R.F., Gänzle, M.G., 2006. High-pressure-mediated survival of *Clostridium botulinum* and *Bacillus amyloliquefaciens* endospores at high temperature. Appl. Environ. Microbiol. 72, 3476–3481.

Marti, R., Muniesa, M., Schmid, M., Ahrens, C.H., Naskova, J., Hummerjohann, J., 2016. Short communication: Heat-resistant *Escherichia coli* as potential persistent reservoir of extended-spectrum β-lactamases and Shiga toxin-encoding phages in dairy. J. Dairy Sci. 99, 8622–8632.

Maserati, A., Fink, R.C., Lourenco, A., Julius, M.L., Diez-Gonzalez, F., 2017. General response of *Salmonella enterica* serovar Typhimurium to desiccation: a new role for the virulence factors *sopD* and *sseD* in survival. PLoS One 12, e0187692.

Masuda, Y., Ozaki, M., Aoki, S., 1993. K+-driven sinusoidal efflux of glutathione disulfide under oxidative stress in the perfused rat liver. FEBS Lett. 334, 109–113.

Mates, A.K., Sayed, A.K., Foster, J.W., 2007. Products of the *Escherichia coli* acid fitness island attenuate metabolite stress at extremely low pH and mediate a cell density-dependent acid resistance. J. Bacteriol. 189, 2759–2768.

Mathys, A., Heinz, V., Schwartz, F.H., Knorr, D., 2007. Impact of agglomeration on the quantitative assessment of *Bacillus stearothermophilus* heat inactivation. J. Food Eng. 81, 380–387.

Maurer, L.M., Yohannes, E., Bondurant, S.S., Radmacher, M., Slonczewski, J.L., 2005. pH

regulates genes for flagellar motility, catabolism, and oxidative stress in *Escherichia coli* K-12. J. Bacteriol. 187, 304.

McCutcheon, J.P., 2010. The bacterial essence of tiny symbiont genomes. Curr. Opin. Microbiol. 13, 73–78.

McMeechan, A., Roberts, M., Cogan, T.A., Jørgensen, F., Stevenson, A., Lewis, C., Rowley, G., Humphrey, T.J., 2007. Role of the alternative sigma factors σ^E and σ^S in survival of *Salmonella enterica* serovar Typhimurium during starvation, refrigeration and osmotic shock. Microbiology 153, 263–269.

McQuiston, J.R., Herrera-Leon, S., Wertheim, B.C., Doyle, J., Fields, P.I., Tauxe, R. V, Logsdon, J.M., 2008. Molecular phylogeny of the salmonellae: relationships among *Salmonella* species and subspecies determined from four housekeeping genes and evidence of lateral gene transfer events. J. Bacteriol. 190, 7060–7067.

Mercer, R.G., Nguyen, O., Ou, Q., McMullen, L., Gänzle, M.G., 2017a. Functional analysis of genes encoded by the locus of heat resistance in *Escherichia coli*. Appl. Environ. Microbiol. 83, e1400-17.

Mercer, R.G., Walker, B.D., Yang, X., McMullen, L.M., Gänzle, M.G., 2017b. The locus of heat resistance (LHR) mediates heat resistance in *Salmonella enterica, Escherichia coli* and *Enterobacter cloacae*. Food Microbiol. 64, 96–103.

Mercer, R.G., Zheng, J., Garcia-Hernandez, R., Ruan, L., Gänzle, M.G., McMullen, L.M., 2015. Genetic determinants of heat resistance in *Escherichia coli*. Front. Microbiol. 6, 932.

Mezzatesta, M.L., Gona, F., Stefani, S., 2012. *Enterobacter cloacae* complex: clinical impact and emerging antibiotic resistance. Future Microbiol. 7, 887–902.

Minardi, D., d'Anzeo, G., Cantoro, D., Conti, A., Muzzonigro, G., 2011. Urinary tract infections

in women: etiology and treatment options. Int. J. Gen. Med. 4, 333.

Mlaga, K.D., Lotte, R., Montaudié, H., Rolain, J.-M., Ruimy, R., 2017. '*Nissabacter archeti*'gen. nov., sp. nov., a new member of *Enterobacteriaceae* family, isolated from human sample at Archet 2 Hospital, Nice, France. New microbes new Infect. 17, 81–83.

Mogk, A., Bukau, B., 2017. Role of *sHsps* in organizing cytosolic protein aggregation and disaggregation. Cell Stress Chaperones 22, 493–502.

Molina-Höppner, A., Doster, W., Vogel, R.F.R.F., Gänzle, M.G.M.G., 2004. Protective effect of sucrose and sodium chloride for *Lactococcus lactis* during sublethal and lethal high pressure treatments. Appl. Environ. Microbiol. 70, 2013–2020.

Moran, N.A., McCutcheon, J.P., Nakabachi, A., 2008. Genomics and evolution of heritable bacterial symbionts. Annu. Rev. Genet. 42, 165–190.

Moran, N.A., Mira, A., 2001. The process of genome shrinkage in the obligate symbiont *Buchnera aphidicola*. Genome Biol. 2, 1–12.

Moran, N.A., Russell, J.A., Koga, R., Fukatsu, T., 2005. Evolutionary relationships of three new species of *Enterobacteriaceae* living as symbionts of aphids and other insects. Appl. Environ. Microbiol. 71, 3302–3310.

Müller, A., Langklotz, S., Lupilova, N., Kuhlmann, K., Bandow, J.E., Leichert, L.I.O., 2014. Activation of RidA chaperone function by N-chlorination. Nat. Commun. 5, 5804.

Munson, M.A., Baumann, P., Kinsey, M.G., 1991. *Buchnera* gen. nov. and *Buchnera aphidicola* sp. nov., a taxon consisting of the mycetocyte-associated, primary endosymbionts of aphids. Int. J. Syst. Evol. Microbiol. 41, 566–568.

Nagano, T., Kiyohara, T., Suzuki, K., Tsubokura, M., Otsuki, K., 1997. Identification of pathogenic strains within serogroups of *Yersinia pseudotuberculosis* and the presence of non-

pathogenic strains isolated from animals and the environment. J. Vet. Med. Sci. 59, 153–158.

Naguib, Y.M.A., 1998. A fluorometric method for measurement of peroxyl radical scavenging activities of lipophilic antioxidants. Anal. Biochem. 265, 290–298.

Nakamura, T., Kon, Y., Iwahashi, H., Eguchi, Y., 1983. Evidence that thiosulfate assimilation by *Salmonella* typhimurium is catalyzed by cysteine synthase B. J. Bacteriol. 156, 656–662.

Nakatani, T., Ohtsu, I., Nonaka, G., Wiriyathanawudhiwong, N., Morigasaki, S., Takagi, H., 2012. Enhancement of thioredoxin/glutaredoxin-mediated L-cysteine synthesis from S-sulfocysteine increases L-cysteine production in *Escherichia coli*. Microb. Cell Fact. 11, 1–9.

Navarro-Garcia, F., Ruiz-Perez, F., Cataldi, Á., Larzábal, M., 2019. Type VI secretion system in pathogenic *Escherichia coli*: structure, role in virulence, and acquisition. Front. Microbiol. 10, 1965.

Nazarowec-White, M., Farber, J.M., 1997. Thermal resistance of *Enterobacter sakazakii* in reconstituted dried-infant formula. Lett. Appl. Microbiol. 24, 9–13.

Nguyen, S. V., Harhay, G.P., Bono, J.L., Smith, T.P.L., Harhay, D.M., 2017. Genome sequence of the thermotolerant foodborne pathogen *Salmonella enterica* serovar Senftenberg ATCC 43845 and phylogenetic analysis of loci encoding increased protein quality control mechanisms. mSystems 2, e00190-16.

Nováková, E., Hypša, V., 2007. A new *Sodalis* lineage from bloodsucking fly *Craterina melbae* (*Diptera*, *Hippoboscoidea*) originated independently of the tsetse flies symbiont *Sodalis glossinidius*. FEMS Microbiol. Lett. 269, 131–135.

Nykyri, J., Fang, X., Dorati, F., Bakr, R., Pasanen, M., Niemi, O., Palva, E.T., Jackson, R.W., Pirhonen, M., 2014. Evidence that nematodes may vector the soft rot-causing enterobacterial

phytopathogens. Plant Pathol. 63, 747–757.

Odonkor, S.T., Ampofo, J.K., 2013. *Escherichia coli* as an indicator of bacteriological quality of water: an overview. Microbiol. Res. 4, 2.

Ohlson, M.B., Fluhr, K., Birmingham, C.L., Brumell, J.H., Miller, S.I., 2005. SseJ deacylase activity by *Salmonella enterica* serovar Typhimurium promotes virulence in mice. Infect. Immun. 73, 6249.

Ohtsu, I., Wiriyathanawudhiwong, N., Morigasaki, S., Nakatani, T., Kadokura, H., Takagi, H., 2010. The L-cysteine/L-cystine shuttle system provides reducing equivalents to the periplasm in *Escherichia coli*. J. Biol. Chem. 285, 17479–17487.

Okochi, M., Yokokawa, H., Lim, T.-K., Taguchi, T., Takahashi, H., Yokouchi, H., Kaiho, T., Sakuma, A., Matsunaga, T., 2005. Disinfection of microorganisms by use of electrochemically regenerated periodate. Appl. Environ. Microbiol. 71, 6410–6413.

Page, A.J., Cummins, C.A., Hunt, M., Wong, V.K., Reuter, S., Holden, M.T.G., Fookes, M., Falush, D., Keane, J.A., Parkhill, J., 2015. Roary: rapid large-scale prokaryote pan genome analysis. Bioinformatics 31, 3691–3693.

Pál, C., Papp, B., Lercher, M.J., 2005. Adaptive evolution of bacterial metabolic networks by horizontal gene transfer. Nat. Genet. 37, 1372–1375.

Pan, Z., Bingol, G., Brandl, M.T., McHugh, T.H., 2012. Review of current technologies for reduction of *Salmonella* populations on almonds. Food Bioprocess Technol. 5, 2046–2057.

Park, C.J., Andam, C.P., 2020. Distinct but intertwined evolutionary histories of multiple *Salmonella enterica* subspecies. mSystems 5, e00515-19.

Parker, B.W., Schwessinger, E.A., Jakob, U., Gray, M.J., 2013. RclR is a reactive chlorine-specific transcription factor in *Escherichia coli*. J. Biol. Chem. 288, 32574–32584.

Parkhill, J., Wren, B.W., Thomson, N.R., Titball, R.W., Holden, M.T.G., Prentice, M.B., Sebaihia, M., James, K.D., Churcher, C., Mungall, K.L., 2001. Genome sequence of *Yersinia pestis*, the causative agent of plague. Nature 413, 523–527.

Parks, D.H., Imelfort, M., Skennerton, C.T., Hugenholtz, P., Tyson, G.W., 2015. CheckM: Assessing the quality of microbial genomes recovered from isolates, single cells, and metagenomes. Genome Res 25, 1043–1055.

Pavlova, A.S., Leontieva, M.R., Smirnova, T.A., Kolomeitseva, G.L., Netrusov, A.I., Tsavkelova, E.A., 2017. Colonization strategy of the endophytic plant growth-promoting strains of *Pseudomonas fluorescens* and *Klebsiella oxytoca* on the seeds, seedlings and roots of the epiphytic orchid, *Dendrobium* nobile Lindl. J. Appl. Microbiol. 123, 217–232.

Peleg, M., Cole, M.B., 2000. Estimating the survival of *Clostridium botulinum* spores during heat treatments. J. Food Prot. 63, 190–195.

Pendleton, J.N., Gorman, S.P., Gilmore, B.F., 2013. Clinical relevance of the ESKAPE pathogens. Expert Rev. Anti. Infect. Ther. 11, 297–308.

Perry, R.D., Balbo, P.B., Jones, H.A., Fetherston, J.D., DeMoll, E., 1999. Yersiniabactin from *Yersinia pestis*: biochemical characterization of the siderophore and its role in iron transport and regulation. Microbiology 145, 1181–1190.

Petersen, L.M., Tisa, L.S., 2013. Friend or foe? A review of the mechanisms that drive Serratia towards diverse lifestyles. Can. J. Microbiol. 59, 627–640.

Pfaffl, M.W., 2001. A new mathematical model for relative quantification in real-time RT-PCR. Nucleic Acids Res. 29.

Pilla, G., McVicker, G., Tang, C.M., 2017. Genetic plasticity of the *Shigella* virulence plasmid is mediated by intra-and inter-molecular events between insertion sequences. PLoS Genet. 13,

e1007014.

Pleitner, A., Zhai, Y., Winter, R., Ruan, L., McMullen, L.M., Gänzle, M.G., 2012. Compatible solutes contribute to heat resistance and ribosome stability in *Escherichia coli* AW1.7. Biochim. Biophys. Acta - Proteins Proteomics 1824, 1351–1357.

Podolak, R., Enache, E., Stone, W., Black, D.G., Elliott, P.H., 2010. Sources and risk factors for contamination, survival, persistence, and heat resistance of *Salmonella* in low-moisture foods. J. Food Prot. 73, 1919–1936.

Popa, L.I., Gheorghe, I., Barbu, I.C., Surleac, M., Paraschiv, S., Măruţescu, L., Popa, M., Pîrcălăbioru, G.G., Talapan, D., Niţă, M., 2020. Multidrug resistant *Klebsiella pneumoniae* ST101 clone survival chain from inpatients to hospital effluent after chlorine treatment. Front. Microbiol. 11, 3403.

Potter, R.F., D'Souza, A.W., Wallace, M.A., Shupe, A., Patel, S., Gul, D., Kwon, J.H., Beatty, W., Andleeb, S., Burnham, C.-A.D., 2018. *Superficieibacter electus* gen. nov., sp. nov., an extended-spectrum β-lactamase possessing member of the *enterobacteriaceae* family, isolated from intensive care unit surfaces. Front. Microbiol. 9, 1629.

Prasad, A., Gänzle, M., Roopesh, M.S., 2021. Antimicrobial activity and drying potential of high intensity blue light pulses (455 nm) emitted from LEDs. Food Res. Int. 110601.

Price, M.N., Dehal, P.S., Arkin, A.P., 2010. FastTree 2 – approximately maximum-likelihood trees for large alignments. PLoS One 5, e9490–e9490.

Pupo, G.M., Lan, R., Reeves, P.R., 2000. Multiple independent origins of *Shigella* clones of *Escherichia coli* and convergent evolution of many of their characteristics. Proc. Natl. Acad. Sci. 97, 10567–10572.

Purvis, J.E., Yomano, L.P., Ingram, L.O., 2005. Enhanced trehalose production improves growth

of *Escherichia coli* under osmotic stress. Appl. Environ. Microbiol. 71, 3761–3769.

Racher, K.I., Voegele, R.T., Marshall, E. V, Culham, D.E., Wood, J.M., Jung, H., Bacon, M., Cairns, M.T., Ferguson, S.M., Liang, W.-J., 1999. Purification and reconstitution of an osmosensor: transporter ProP of *Escherichia coli* senses and responds to osmotic shifts. Biochemistry 38, 1676–1684.

Rahoo, A.M., Mukhtar, T., Gowen, S.R., Pembroke, B., 2011. Virulence of entomopathogenic bacteria *Xenorhabdus bovienii* and *Photorhabdus luminescens* against *Galleria mellonella* larvae. Pak. J. Zool 43, 543–548.

Raymond, K.N., Dertz, E.A., Kim, S.S., 2003. Enterobactin: an archetype for microbial iron transport. Proc. Natl. Acad. Sci. 100, 3584–3588.

Reisch, C.R., Prather, K.L.J., 2015. The no-SCAR (Scarless Cas9 Assisted Recombineering) system for genome editing in *Escherichia coli*. Sci. Rep. 5, 15096.

Rekha, P.D., Hameed, A., Manzoor, M.A.P., Suryavanshi, M. V, Ghate, S.D., Arun, A.B., Rao, S.S., Bajire, S.K., Mujeeburahiman, M., Young, C.-C., 2020. First report of pathogenic bacterium *Kalamiella piersonii* isolated from urine of a kidney stone patient: draft genome and evidence for role in struvite crystallization. Pathogens 9, 711.

Ridgway, H.F., Olson, B.H., 1982. Chlorine resistance patterns of bacteria from two drinking water distribution systems. Appl. Environ. Microbiol. 44, 972–987.

Rijavec, M., Erjavec, M.S., Avguštin, J.A., Reissbrodt, R., Fruth, A., Križan-Hergouth, V., Žgur-Bertok, D., 2006. High prevalence of multidrug resistance and random distribution of mobile genetic elements among uropathogenic *Escherichia coli* (UPEC) of the four major phylogenetic groups. Curr. Microbiol. 53, 158–162.

Robey, M., Benito, A., Hutson, R.H., Pascual, C., Park, S.F., Mackey, B.M., 2001. Variation in

resistance to high hydrostatic pressure and *rpoS* heterogeneity in natural isolates of *Escherichia coli* O157:H7. Appl. Environ. Microbiol. 67, 4901–4907.

Rossmann, S., Dees, M.W., Perminow, J., Meadow, R., Brurberg, M.B., 2018. Soft rot Enterobacteriaceae are carried by a large range of insect species in potato fields. Appl. Environ. Microbiol. 84(12): e00281-18.

Sadiq, F.A., Li, Y., Liu, T., Flint, S., Zhang, G., Yuan, L., Pei, Z., He, G., 2016. The heat resistance and spoilage potential of aerobic mesophilic and thermophilic spore forming bacteria isolated from Chinese milk powders. Int. J. Food Microbiol. 238, 193–201.

Saha, P., Manna, C., Chakrabarti, J., Ghosh, M., 2016. Reversible thermal unfolding of a yfdX protein with chaperone-like activity. Sci. Rep. 6, 29541.

Sanders, W.E., Sanders, C.C., 1997. *Enterobacter* spp.: pathogens poised to flourish at the turn of the century. Clin. Microbiol. Rev. 10, 220–241.

Sandström, J.P., Russell, J.A., White, J.P., Moran, N.A., 2001. Independent origins and horizontal transfer of bacterial symbionts of aphids. Mol. Ecol. 10, 217–228.

Santillana Farakos, S.M., Frank, J.F., 2014. Challenges in the control of foodborne pathogens in low-water activity foods and spices, in: Gurtler, J., Doyle, M., Kornacki, J. (Eds.), The Microbiological Safety of Low Water Activity Foods and Spices. Springer , New York, pp. 15–34.

Sarowska, J., Futoma-Koloch, B., Jama-Kmiecik, A., Frej-Madrzak, M., Ksiazczyk, M., Bugla-Ploskonska, G., Choroszy-Krol, I., 2019. Virulence factors, prevalence and potential transmission of extraintestinal pathogenic *Escherichia coli* isolated from different sources: recent reports. Gut Pathog. 11, 10.

Schaible, U.E., Kaufmann, S.H.E., 2004. Iron and microbial infection. Nat. Rev. Microbiol. 2,

946–953.

Scheutz, F., Strockbine, N.A., 2005. Family I. *Enterobacteriaceae*, in: Garrity, G. (Ed.), Bergey's Manual of Systematic Bacteriology. Second Ed New York, USA: Springer. pp. 607–624.

Schmid, M., Iversen, C., Gontia, I., Stephan, R., Hofmann, A., Hartmann, A., Jha, B., Eberl, L., Riedel, K., Lehner, A., 2009. Evidence for a plant-associated natural habitat for *Cronobacter* spp. Res. Microbiol. 160, 608–614.

Schmidt, H., Hensel, M., 2004. Pathogenicity islands in bacterial pathogenesis. Clin. Microbiol. Rev. 17, 14–56.

Schultze, D.M., Couto, R., Temelli, F., McMullen, L.M., Gänzle, M., 2020. Lethality of high-pressure carbon dioxide on Shiga toxin-producing *Escherichia coli*, *Salmonella* and surrogate organisms on beef jerky. Int. J. Food Microbiol. 321, 108550.

Seemann, T., 2014. Prokka: rapid prokaryotic genome annotation. Bioinformatics 30, 2068–2069.

Seeras, A., 2017. Survival and persistence of dried *Salmonella enterica* in low water activity conditions. Thesis of master degree, University of Alberta.

Shanqimuge, Liang, H., Zhang, C., Shao, C., Peng, X., Liang, L., Su, J., Li, C., 2015. A DGGE marker-mediated fast monitoring of bacterial diversity and comprehensive identification of high-temperature Daqu starter. J. Food Sci. 80, M1519–M1525.

Shapiro, L.R., Seidl-Adams, I., De Moraes, C.M., Stephenson, A.G., Mescher, M.C., 2014. Dynamics of short-and long-term association between a bacterial plant pathogen and its arthropod vector. Sci. Rep. 4, 1–7.

Shigenobu, S., Watanabe, H., Hattori, M., Sakaki, Y., Ishikawa, H., 2000. Genome sequence of the endocellular bacterial symbiont of aphids *Buchnera* sp. APS. Nature 407, 81–86.

Siedler, S., Schendzielorz, G., Binder, S., Eggeling, L., Bringer, S., Bott, M., 2013. SoxR as a

single-cell biosensor for NADPH-consuming enzymes in *Escherichia coli*. ACS Synth. Biol. 3, 41–47.

Silva, H.S.A., Tozzi, J.P.L., Terrasan, C.R.F., Bettiol, W., 2012. Endophytic microorganisms from coffee tissues as plant growth promoters and biocontrol agents of coffee leaf rust. Biol. Control 63, 62–67.

Skórko-Glonek, J., Zurawa, D., Kuczwara, E., Wozniak, M., Wypych, Z., Lipinska, B., 1999. The *Escherichia coli* heat shock protease HtrA participates in defense against oxidative stress. Mol. Gen. Genet. MGG 262, 342–350.

Solomon, E.B., Yaron, S., Matthews, K.R., 2002. Transmission of *Escherichia coli* O157: H7 from contaminated manure and irrigation water to lettuce plant tissue and its subsequent internalization. Appl. Environ. Microbiol. 68, 397–400.

Soutar, C.D., Stavrinides, J., 2020. Phylogenetic analysis supporting the taxonomic revision of eight genera within the bacterial order Enterobacterales. Int. J. Syst. Evol. Microbiol. 70, 6524–6530.

Spector, M.P., Kenyon, W.J., 2012. Resistance and survival strategies of *Salmonella enterica* to environmental stresses. Food Res. Int. 45, 455–481.

Spurbeck, R.R., Dinh, P.C., Walk, S.T., Stapleton, A.E., Hooton, T.M., Nolan, L.K., Kim, K.S., Johnson, J.R., Mobley, H.L.T., Dinh Jr, P.C., Walk, S.T., Stapleton, A.E., Hooton, T.M., Nolan, L.K., Kim, K.S., Johnson, J.R., Mobley, H.L.T., 2012. *Escherichia coli* that carry *vat*, *fyuA*, *chuA*, and *yfcV* efficiently colonize the urinary tract. Infect. Immun. 80, IAI-00752.

Stevens, J.F., Maier, C.S., 2008. Acrolein: sources, metabolism, and biomolecular interactions relevant to human health and disease. Mol. Nutr. Food Res. 52, 7–25.

Streeter, K., Katouli, M., 2016. *Pseudomonas aeruginosa*: A review of their pathogenesis and

prevalence in clinical settings and the environment. Epidemiol. Infect. Microbiol. 2(1):25–32.

Tacconelli, E., Carrara, E., Savoldi, A., Harbarth, S., Mendelson, M., Monnet, D.L., Pulcini, C., Kahlmeter, G., Kluytmans, J., Carmeli, Y., 2018. Discovery, research, and development of new antibiotics: the WHO priority list of antibiotic-resistant bacteria and tuberculosis. Lancet Infect. Dis. 18, 318–327.

Tall, B.D., Gangiredla, J., Gopinath, G.R., Yan, Q., Chase, H.R., Lee, B., Hwang, S., Trach, L., Park, E., Yoo, Y., Chung, T., Jackson, S.A., Patel, I.R., Sathyamoorthy, V., Pava-Ripoll, M., Kotewicz, M.L., Carter, L., Iversen, C., Pagotto, F., Stephan, R., Lehner, A., Fanning, S., Grim, C.J., 2015. Development of a custom-designed, pan genomic DNA microarray to characterize strain-level diversity among *Cronobacter* spp. Front. Pediatr. 3, 36.

Tamber, S., 2018. Population-wide survey of *Salmonella enterica* response to high-pressure processing reveals a diversity of responses and tolerance mechanisms. Appl. Environ. Microbiol. 84, e01673-17.

Tanner, J.R., Kingsley, R.A., 2018. Evolution of *Salmonella* within hosts. Trends Microbiol. 26, 986–998.

Tenaillon, O., Skurnik, D., Picard, B., Denamur, E., 2010. The population genetics of commensal *Escherichia coli*. Nat. Rev. Microbiol. 8, 207–217.

Teng, T.Z.J., Junnarkar, S.P., Shelat, V.G., 2020. *Pluralibacter georgoviae* causing acute cholecystitis with perforation. Surg. Infect. 22(3): 353-353.

Teunis, P.F.M., Ogden, I.D., Strachan, N.J.C., 2008. Hierarchical dose response of *E. coli* O157:H7 from human outbreaks incorporating heterogeneity in exposure. Epidemiol. Infect. 136, 761–70.

Thomson, N.R., Clayton, D.J., Windhorst, D., Vernikos, G., Davidson, S., Churcher, C., Quail, M.A., Stevens, M., Jones, M.A., Watson, M., 2008. Comparative genome analysis of *Salmonella* Enteritidis PT4 and *Salmonella* Gallinarum 287/91 provides insights into evolutionary and host adaptation pathways. Genome Res. 18, 1624–1637.

Tovar-Rojo, F., Chander, M., Setlow, B., Setlow, P., 2002. The products of the *spoVA* operon are involved in dipicolinic acid uptake into developing spores of *Bacillus subtilis*. J. Bacteriol. 184, 584–587.

Troisfontaines, P., Cornelis, G.R., 2005. Type III secretion: more systems than you think. Physiology 20, 326–339.

Tsolis, E.M., Ficht, T.A., Ba, A.J., Adams, L.G., 1998. Evolution of host adaptation in *Salmonella enterica*. Infect. Immun. 66, 4579–4587.

Ueda, A., Saneoka, H., 2015. Characterization of the ability to form biofilms by plant-associated *Pseudomonas* species. Curr. Microbiol. 70, 506–513.

Valcheva, R., Koleva, P., Mart.nez, I., Walter, J., G.nzle, M.G., Dieleman, L.A., 2019. Inulin-type fructans improve active ulcerative colitis associated with microbiota changes and increased short-chain fatty acids levels. Gut Microbes 10, 334–357.

Valdebenito, M., Crumbliss, A.L., Winkelmann, G., Hantke, K., 2006. Environmental factors influence the production of enterobactin, salmochelin, aerobactin, and yersiniabactin in *Escherichia coli* strain Nissle 1917. Int. J. Med. Microbiol. 296, 513–520.

Vanlint, D., Rutten, N., Govers, S.K., Michiels, C.W., Aertsen, A., 2013. Exposure to high hydrostatic pressure rapidly selects for increased RpoS activity and general stress-resistance in *Escherichia coli* O157:H7. Int. J. Food Microbiol. 163, 28–33.

Voegele, R.T., Bardin, S., Finan, T.M., 1997. Characterization of the *Rhizobium* (*Sinorhizobium*)

meliloti high-and low-affinity phosphate uptake systems. J. Bacteriol. 179, 7226–7232.

Voor in ‘t holt, A.F., Mourik, K., Beishuizen, B., van der Schoor, A.S., Verbon, A., Vos, M.C., Severin, J.A., 2020. Acquisition of multidrug-resistant *Enterobacterales* during international travel: a systematic review of clinical and microbiological characteristics and meta-analyses of risk factors. Antimicrob. Resist. Infect. Control 9, 1–14.

Wallrodt, I., Jelsbak, L., Thorndahl, L., Thomsen, L.E., Lemire, S., Olsen, J.E., 2013. The putative thiosulfate sulfurtransferases PspE and GlpE contribute to virulence of *Salmonella* Typhimurium in the mouse model of systemic disease. PLoS One 8, e70829.

Walterson, A.M., Stavrinides, J., 2015. *Pantoea*: insights into a highly versatile and diverse genus within the *Enterobacteriaceae*. FEMS Microbiol. Rev. 39, 968–984.

Wang, H.-Y., Gao, Y.-B., Fan, Q.-W., Xu, Y., 2011. Characterization and comparison of microbial community of different typical Chinese liquor Daqus by PCR-DGGE. Lett. Appl. Microbiol. 53, 134–140.

Wang, Z., Fang, Y., Zhi, S., Simpson, D.J., Gill, A., McMullen, L.M., Neumann, N.F., Gänzle, M.G., 2020. The locus of heat resistance confers resistance to chlorine and other oxidizing chemicals in *Escherichia coli*. Appl. Environ. Microbiol. 86, e02123-19.

Wang, Z., Li, P., Luo, L., Simpson, D.J., Gänzle, M.G., 2018. *Daqu* fermentation selects for heat-resistant *Enterobacteriaceae* and bacilli. Appl. Environ. Microbiol. 84, e01483-18.

Weibull, W., 1951. A Statistical Distribution Function of Wide Applicability. J. Appl. Mech. 18, 293–297.

White, A.P., Sibley, K.A., Sibley, C.D., Wasmuth, J.D., Schaefer, R., Surette, M.G., Edge, T.A., Neumann, N.F., 2011. Intergenic sequence comparison of *Escherichia coli* isolates reveals lifestyle adaptations but not host specificity. Appl. Environ. Microbiol. 77, 7620-7632.

WHO, 2015. WHO Global action plan on antimicrobial resistance. WHO. URL http://www.who.int/antimicrobial-resistance/publications/global-action-plan/en/ (accessed 4.9.21).

Winfield, M.D., Groisman, E.A., 2003. Role of nonhost environments in the lifestyles of *Salmonella* and *Escherichia coli*. Appl. Environ. Microbiol. 69, 3687–3694.

Winter, J., Linke, K., Jatzek, A., Jakob, U., 2005. Severe oxidative stress causes inactivation of DnaK and activation of the redox-regulated chaperone Hsp33. Mol. Cell 17, 381–392.

Wyckoff, E.E., Boulette, M.L., Payne, S.M., 2009. Genetics and environmental regulation of *Shigella* iron transport systems. Biometals 22, 43–51.

Xi, C., Zhang, Y., Marrs, C.F., Ye, W., Simon, C., Foxman, B., Nriagu, J., 2009. Prevalence of antibiotic resistance in drinking water treatment and distribution systems. Appl. Environ. Microbiol. 75, 5714–5718.

Xiao, C., Lu, Z.-M., Zhang, X.-J., Wang, S.-T., Ao, L., Shen, C.-H., Shi, J.-S., Xu, Z.-H., 2017. Bio-heat is a key environmental driver shaping microbial community of medium-temperature Daqu. Appl. Environ. Microbiol. 83(23): e01550-17.

Xiu, L., Kunliang, G., Hongxun, Z., 2012. Determination of microbial diversity in Daqu, a fermentation starter culture of Maotai liquor, using nested PCR-denaturing gradient gel electrophoresis. World J. Microbiol. Biotechnol. 28, 2375–2381.

Xu, Z., Xia, M., Huo, Y.-X., Yang, Y., 2020. *Intestinirhabdus alba* gen. nov., sp. nov., a novel genus of the family *Enterobacteriaceae*, isolated from the gut of plastic-eating larvae of the *Coleoptera* insect *Zophobas atratus*. Int. J. Syst. Evol. Microbiol. 70, 4951–4959.

Yahia, H. Ben, Chairat, S., Gharsa, H., Alonso, C.A., Sallem, R. Ben, Porres-Osante, N., Hamdi, N., Torres, C., Slama, K. Ben, 2020. First report of KPC-2 and KPC-3-producing

Enterobacteriaceae in wild birds in Africa. Microb. Ecol. 79, 30–37.

Yan, Q., Fanning, S., 2015. Strategies for the identification and tracking of *Cronobacter* species: an opportunistic pathogen of concern to neonatal health. Front. Pediatr. 3, 38.

Zhang, L., Simpson, D., McMullen, L., Gänzle, M., 2018. Comparative genomics and characterization of the late promoter *p*R' from Shiga toxin prophages in *Escherichia coli*. Viruses 10, 595.

Zheng, J., Wittouck, S., Salvetti, E., Franz, C.M.A.P., Harris, H.M.B., Mattarelli, P., O'Toole, P.W., Pot, B., Vandamme, P., Walter, J., Watanabe, K., Wuyts, S., Felis, G.E., Gänzle, M.G., Lebeer, S., 2020. A taxonomic note on the genus *Lactobacillus*: Description of 23 novel genera, emended description of the genus *Lactobacillus beijerinck* 1901, and union of *Lactobacillaceae* and *Leuconostocaceae* . Int. J. Syst. Evol. Microbiol. 70, 2782–2858.

Zhi, S., Banting, G., Li, Q., Edge, T.A., Topp, E., Sokurenko, M., Scott, C., Braithwaite, S., Ruecker, N.J., Yasui, Y., McAllister, T., Chui, L., Neumann, N.F., 2016. Evidence of naturalized stress-tolerant strains of *Escherichia coli* in municipal wastewater treatment plants. Appl. Environ. Microbiol. 82, 5505–5518.

Zhi, S., Banting, G., Stothard, P., Ashbolt, N.J., Checkley, S., Meyer, K., Otto, S., Neumann, N.F., 2019. Evidence for the evolution, clonal expansion and global dissemination of water treatment-resistant naturalized strains of *Escherichia coli* in wastewater. Water Res. 156, 208–222.

Zou, Q.H., Li, R.Q., Liu, G.R., Liu, S.L., 2016. Genotyping of *Salmonella* with lineage-specific genes: correlation with serotyping. Int. J. Infect. Dis. 49, 134–140.

APPENDIX

Supplemental Table S2.1. Information of 364 types strains of *Enterobacterales* in this study (provided as Excel file). https://doi.org/10.7939/r3-7tgc-qd31

Supplemental Table S2.2. Pairwise cAAI values (provided as Excel file). https://doi.org/10.7939/r3-xd7f-zw67

Supplemental Table S2.3. Lifestyles of type strains in the *Enterobacterales* with references (provided as Excel file). https://doi.org/10.7939/r3-kkr6-q023

Supplemental Table S2.4. Location of *Enterobacterales* in phyllosphere, rhizosphere or endophytes (provided as Excel file). https://doi.org/10.7939/r3-cth7-1v85

Supplemental Table S2.5. List of type strains that were isolated before 1943 (provided as Excel file). https://doi.org/10.7939/r3-0n2v-0g62

Supplemental Method 2.1. Pan genome analysis and species phylogeny inference

Genome sequences of the 310 type strain belonging to the 310 species or subspecies in the order Enterobacterales, and 28 genomes from the family Pasteurellales were obtained from Genbank at June 10, 2021. The quality of these genomes were assessed by CheckM (Parks et al., 2015). All the genomes were re-annotated through Prokka (Seemann, 2014), which implements Prodigal for gene prediction(Hyatt et al.,2010). All the protein sequences from all the used genomes were combined and an all-against-all blastP were performed on this protein dataset, with the *E*-value threshold of 10^{-5}. Then the protein sequences clustering were conducted by FastOrtho (https://github.com/olsonanl/FastOrtho). The pan and core gene of these genomes were calculated through local Perl scripts.

For each of the 1306 core gene family shared by at least 90% of the 338 genomes, protein sequences were extracted from all the used genomes, and aligned by MUSLCE (Edgar, 2004). TrimAl ws used to remove spurious sequences or poorly aligned regions in all 1306 alignments (Capella-Gutiérrez et al., 2009). Then the cleaned alignments were concatenated to form a new alignment (Kalyaanamoorthy et al., 2017). ModelFinder was used to evaluate the best fitting evolutionary model for this alignment. Maximum likelihood (ML) based phylogenetic analysis was performed by RAxML-NG with the best model (LG+I+G), with 500 bootstrap replicates (Kozlov et al., 2019). The tree was visualized through ITOL (https://itol.embl.de) (Letunic and Bork, 2021).

The genome size and GC content were computed by the assembly-stats tool (https://github.com/sanger-pathogens/assembly-stats) and local Perl script. Core genome average amino acid identity (cAAI) was computed based on the 1306 core gene families. AAI and cAAI

were analyzed through compareM (https://github.com/dparks1134/CompareM) and plotted using R.

Supplemental Method 2.2. Gene content analysis

Microbial genome-wide association studies (mGWAS) analysis on the pan gene clusters established above using Scoary was performed to predict the family-specific genes (Brynildsrud et al., 2016). It used the gene presence and absence pattern file and a trait file. Traits were defined as a strain belonging to a certain family ("1") or not ("0"). Scoary was run with 1,000 permutation replicates, gene families were reported as specific if all the three types of *P*-values (naive, Benjamini-Hochberg-corrected, empirical) are less than 0.05, and both specificity and sensitivity are above 70%. The overall distribution of all the family specific genes among all the studied genomes were plotted as a heatmap through the package pheatmap of R (Fig. 2.6). The distribution of a few family specific genes with interesting metabolic functions among all the genomes analyzed were visualized by ITOL.

For different subtypes of type III secretion system (T3SS) and type VI secretion system (T6SS), the database sequences were collected from Genbank according to the associated papers. For virulence factor gene analysis, the database dataset was downloaded from the VFDB website (Liu et al., 2019). The protein sequences of all the used genomes were used as query to Blast against the database, with the E-value threshold of 10^{-10}. The candidate sequences were extracted when the coverage is above 60% and the identity is above 50%. Each candidate was checked by conserved domain scanning. The subtypes of T3SS and T6SS were determined according the descriptions of Hu *et al* (2017) and Bernal *et al* (2018), respectively. ABRicate (https://github.com/tseemann/abricate) was used identify antibiotics resistance genes (ARGs) from each of the used genomes using ResFinder 4.0 as database (Bortolaia et al., 2020). The gene

presence and absence profiles and the total numbers for each genome were summarized by local script and were visualized through ITOL (Letunic and Bork, 2021).

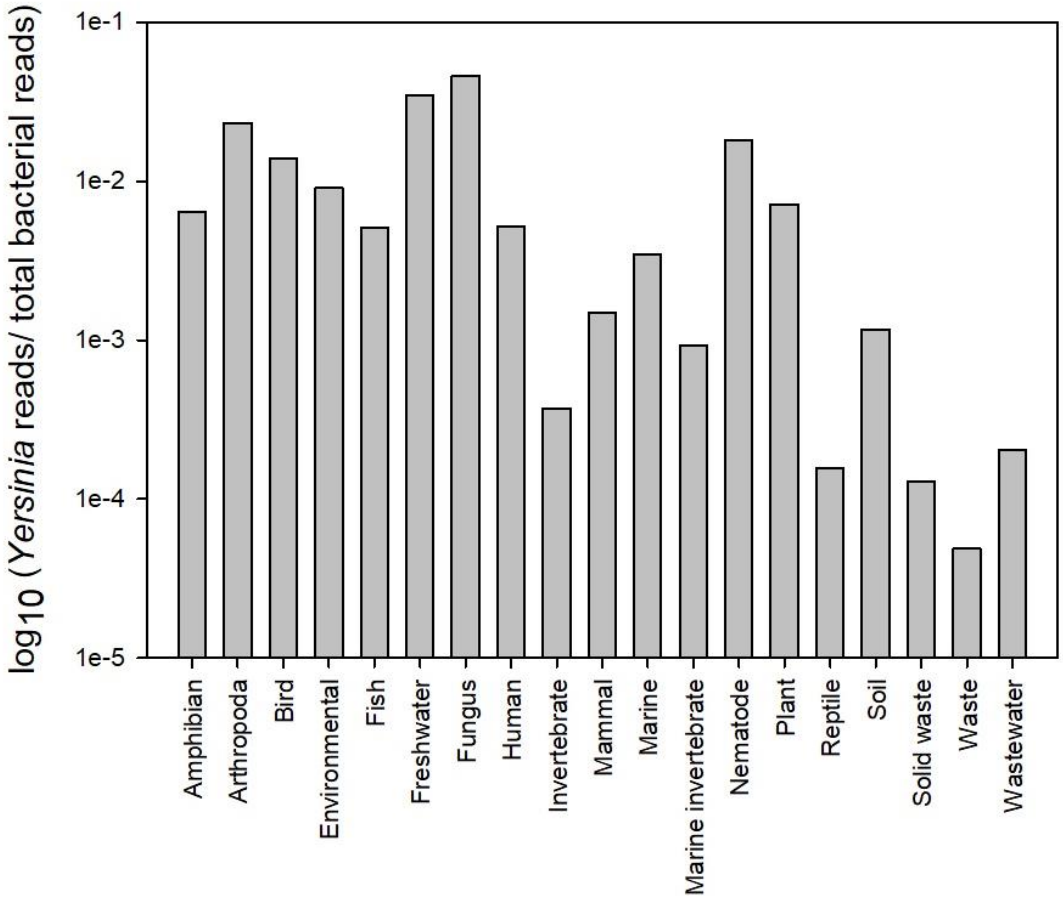

Supplemental Figure S2.1. Origin of 16S rRNA gene sequences corresponding to *Yersinia* species in the metagenome datasets available on the integrated microbial NGS platform (IMNS, https://www.imngs.org/).

Supplemental Table S4.1. Screening of the transmissible locus of stress tolerance (tLST), IS30 and virulence genes in 70 wastewater *E. coli* strains (+: positive and -: negative)

	Targets						
	tLST	IS30	*papC*	*saf/foc*	*ibeA*	*fuyA*	*iroN*
BB04US10-31	-	-	-	-	-	-	-
BB05DS10-34	-	-	-	-	-	-	-
BB05SLO10-25	-	-	-	-	-	-	-
BB06DS10-31	-	-	-	-	-	-	-
BB06SLO10-33	-	-	-	-	-	-	-
BB07DS110-3	-	-	-	-	-	-	-
BB07SLO210-3	-	-	-	-	-	-	-
BB08DS110-3	-	-	-	-	-	-	-
BB08DS210-3	-	-	-	-	-	-	-
BB08DS310-3	-	-	-	-	-	-	-
BB08US510-6	-	-	-	-	-	-	-
BB09DS110-3	-	-	-	-	-	-	-
BB09DS210-3	-	-	-	-	-	-	-
BB09DS410-3	-	-	-	-	-	-	-
BB09US410-5	-	-	-	-	-	-	-
BB09US510-5	-	-	-	-	-	-	-
BB09SLO310-1	-	-	-	-	-	-	-
BB10US210-6	-	-	-	-	-	-	-
BB10SLO310-2	-	-	-	-	-	-	-
BB10SLO510-2	-	-	-	-	-	-	-
BB11US110-6	-	-	-	-	-	-	-
PC02DS410-4	-	-	-	-	-	-	-
PC02DS510-4	-	-	-	-	-	-	-
BB04US10-33	-	-	-	-	-	-	-
BB04US10-34	-	-	-	-	-	-	-
BB05SLO10-22	-	-	-	-	-	-	-
BB05SLO10-23	-	-	-	-	-	-	-
BB08SLO410-2	-	-	-	-	-	-	-
BB12DS510-3	-	-	-	-	+	-	-
BB02DS210-4	-	-	-	-	+	-	-
BB09SLO110-1	-	-	-	-	-	-	+
BB04DS10-32	-	-	+	-	-	+	-
BB04US10-73	-	-	+	-	-	+	-
BB06DS10-34	-	-	-	-	-	+	-
BB06SLO10-32	-	-	-	-	-	+	-
BB08SLO510-4	-	-	-	-	-	+	-
BB09DS510-3	-	-	-	-	-	+	-
BB12US410-7	-	-	+	-	-	+	-
BB12DS410-3	-	-	-	-	-	+	-
PC02DS110-4	-	-	-	+	-	+	-
BB04US10-32	-	-	-	-	-	+	-
BB05US10-53	-	-	-	-	-	+	-
BB09US110-5	-	-	-	-	+	+	-
BB04DS10-31	-	-	-	-	-	+	+
BB01DS110-3	-	-	+	+	-	+	+

BB04DS10-33	-	-	+	+	+	+	+
BB05US10-51	-	-	-	-	+	+	+
BB09SLO210-1	-	-	+	+	+	+	+
BB09SLO410-1	-	-	-	-	+	+	+
BB10DS310-4	-	-	-	-	+	+	+
BB10US310-6	-	-	-	-	+	+	+
BB12DS210-3	-	-	+	+	+	+	+
BB01DS410-3	-	-	+	+	+	+	+
PC01DS310-4	-	-	-	+	+	+	+
BB06US10-63	+	-	-	-	-	-	-
BB06SLO10-34	+	-	-	-	-	-	-
BB07US210-6	+	-	-	-	-	-	-
BB08DS410-3	+	-	-	-	-	-	-
BB08US110-6	+	-	-	-	-	-	-
BB08US410-6	+	-	-	-	-	-	-
BB09DS310-3	+	-	-	-	-	-	-
BB11DS310-3	+	-	-	-	-	-	-
BB11DS510-3	+	-	-	-	-	-	-
BB05US10-55	+	-	-	-	-	-	-
BB05SLO10-21	+	-	-	-	-	-	-
BB06DS10-32	+	-	-	-	-	-	-
BB05DS10-35	+	+	-	-	-	-	-
BB06DS10-33	+	+	-	-	-	-	-
BB07US110-6	+	-	-	-	-	+	-
BB10UD410-6	+	-	-	-	-	+	-

Supplemental Table S4.2. Flow cytometric quantification of the oxidation of membrane lipids in *E. coli* AW1.7, *E. coli* AW1.7 ΔpRK1 using C11-BODIPY$^{581/591}$ after H_2O_2 treatment (n=8).

Proportion in population	*E. coli* AW1.7	*E. coli* AW1.7ΔpRK1
Unoxidized cells	39.6 ± 6.3	29.1 ± 6.6*
Oxidized cells	28.0 ± 5.8	44.3 ± 4.1*
Non-stained cells	32.3 ± 5.1	26.6 ± 6.1

Values for different strains within a row that are marked with an asterisk are significantly different (P<0.05).

Supplemental Table S4.3. Heat resistance and presence of the tLST of Shiga-toxin producing *Escherichia coli*. Data for heat resistance are from Gill et al., 2019; PCR conditions for screening of the three fragments of the LHR are described in the Chapter 4.2. (+: positive and -: negative)

Reduction of cell counts (log cfu/mL) after heating for 2 min at 60°C							
ID	**Serotype**	**Isolation**	**Mean**	**SD**	**Fragment 1**	**Fragment 2**	**Fragment 3**
1934	O157:H7	Beef	3.55	0.36	-	-	-
1931	O157:H7	Beef	3.59	0.39	-	-	-
LCDC 7282	O157:H7	Beef	3.48	0.36	-	-	-
LCDC 7283	O157:H7	Beef	3.83	0.08	-	-	-
06-0434	O103:H2	Human	3.76	0.61	-	-	-
05-4161	O111:NM	Human	3.92	0.43	-	-	-
04-7099	O145:NM	Human	2.91	0.11	-	-	-
161-84	O157:H7	Human	3.75	0.29	-	-	-
1011-84	O157:H7	Human	4.32	0.35	-	-	-
HCO 62	O157:H7	Human	3.49	0.49	-	-	-
HCO 59	O157:H7	Human	4.06	0.18	-	-	-
A9619.C2	O145:H2	Human	2.83	0.42	-	-	-
75-83	O145:H2	Human	3.84	0.72	-	-	-
05-6545	O45:H2	Human	2.29	0.26	-	-	-
04-2446	O103:H2	Human	3.26	0.13	-	-	-
99-2076	O103:H2	Human	3.60	0.76	-	-	-
98-8338	O111:NM	Human	4.03	0.31	-	-	-
00-4748	O111:NM	Human	3.56	0.33	-	-	-
03-2832	O121:H19	Human	3.37	0.37	-	-	-
87-1215	O157:H7	Human	3.25	0.23	-	-	-
05-6544	O26:H11	Human	2.80	0.42	-	-	-
03-4064	O121:NM	Human	3.08	0.09	-	-	-
03-4699	O145:NM	Human	1.69	0.32	-	-	-
85-0489	O91:H21	Human	3.53	0.29	-	-	-
C0283	O157:H7	Cattle	2.46	0.01	-	-	-
E0122	O157:H7	Cattle	2.62	0.01	-	-	-
CFS2	O26:H11	Cattle	4.03	0.50	-	-	-
99-4610	O26:H11	Human	3.71	0.14	-	-	-
03-2816	O26:H11	Human	2.59	0.03	-	-	-
01-5870	O26:H11	Human	2.98	0.52	-	-	-
04-2445	O45:H2	Human	3.51	0.43	-	-	-
01-6102	O103:H2	Human	2.93	0.33	-	-	-
00-4440	O26:H11	Human	3.85	0.25	-	-	-
03-3991	O26:H11	Human	3.35	0.52	-	-	-
04-1449	O145:NM	Human	2.36	0.03	-	-	-
11-3088	O104:H4	Human	2.86	0.30	-	-	-
03-6430	O145:NM	Human	2.39	0.42	-	-	-

11-3581	O26:H11	Human	2.54	0.23	-	-	-
11-4969	O26:H11	Human	3.27	0.55	-	-	-
11-4211	O103:H21	Human	3.33	0.10	-	-	-
11-5595	O103:H21	Human	2.49	0.35	-	-	-
11-3925	O121:H19	Human	2.53	0.06	-	-	-
11-3926	O121:H19	Human	3.41	0.37	-	-	-
11-5594	O121:H1	Human	2.63	0.10	-	-	-
11-5597	O121:H1	Human	2.97	0.08	-	-	-
11-2925	O121:H19	Human	2.88	0.42	-	-	-
F5-28-2	O26:H11	Cattle	2.54	0.28	-	-	-
85-X-40c R3	O26:H11	Cattle	2.85	0.27	-	-	-
3267-95	O26:H11	Human	5.00	0.00	-	-	-
3285-96	O26:H11	Human	3.83	0.40	-	-	-
89-39	O26:H11	Human	2.86	0.30	-	-	-
SET2M6P2	O103:H2	Cattle	4.77	0.19	-	-	-
112.1	O103:H2	Cattle	3.55	0.06	-	-	-
79-C-43hiiR3	O111:H8	Cattle	2.94	0.17	-	-	-
8448-100.8	O111:H8	Cattle	3.47	0.09	-	-	-
LC#*2*	O111:NM	Cattle	3.76	0.69	-	-	-
O157-3	O121:H19	Cattle	3.47	0.21	-	-	-
2454-01	O145:NM	Human	2.40	0.40	-	-	-
VT113-5	O145:NM	Human	3.54	0.09	-	-	-
ECI-1285	O91:H21	Bovine	ND	ND	-	-	-
F17-A BEADS	O113:H4	Cattle	3.20	0.04	-	-	-
FM4-5-B	O113:H4	Cattle	3.30	0.17	-	-	-
LAAFC O157-1	O157	Cattle	4.72	0.40	-	-	-
LAAFC O157-2	O157	Cattle	2.70	0.25	-	-	-
LAAFC O157-3	O157	Cattle	4.02	0.36	-	-	-
LAAFC O157-4	O157	Cattle	3.18	0.25	-	-	-
LAAFC O157-5	O157	Cattle	4.49	0.03	-	-	-
LAAFC O157-6	O157	Cattle	3.89	0.25	-	-	-
LAAFC O157-7	O157	Cattle	3.18	0.22	-	-	-
LAAFC O157-8	O157	Cattle	3.76	0.06	-	-	-

LAAFC O157-9	O157	Cattle	3.23	0.93	-	-	-
LAAFC O157-10	O157	Cattle	2.72	0.28	-	-	-
LAAFC O157-11	O157	Cattle	3.08	0.21	-	-	-
LAAFC O157-12	O157	Cattle	3.20	0.01	-	-	-
LAAFC O157-13	O157	Cattle	3.41	0.09	-	-	-
LAAFC O157-14	O157	Cattle	3.48	0.40	-	-	-
LAAFC O157-15	O157	Cattle	3.65	0.64	-	-	-
LAAFC O157-16	O157	Cattle	3.60	0.54	-	-	-
LAAFC O157-17	O157	Cattle	4.04	0.43	-	-	-
LAAFC O157-18	O157	Cattle	3.16	0.16	-	-	-
LAAFC O157-19	O157	Cattle	2.89	0.26	-	-	-
LAAFC O157-20	O157	Cattle	4.02	0.06	-	-	-
LAAFC O157-21	O157	Cattle	3.80	0.10	-	-	-
LAAFC O157-22	O157	Cattle	ND	ND	-	-	-
LAAFC O157-23	O157	Cattle	3.13	0.20	-	-	-
LAAFC O157-24	O157	Cattle	3.48	0.64	-	-	-
LAAFC O157-25	O157	Cattle	3.72	0.33	-	-	-
LAAFC O157-26	O157	Cattle	3.81	0.54	-	-	-
LAAFC O157-27	O157	Cattle	3.34	0.09	-	-	-
LAAFC O157-28	O157	Cattle	3.03	0.85	-	-	-
LAAFC O157-29	O157	Cattle	2.90	0.23	-	-	-
LAAFC O157-30	O157	Cattle	3.42	0.30	-	-	-
LAAFC O157-31	O157	Cattle	3.22	0.09	-	-	-
LAAFC O157-32	O157	Cattle	2.78	0.06	-	-	-
LAAFC O157-33	O157	Cattle	3.10	0.22	-	-	-

LAAFC O157-34	O157	Cattle	2.89	0.06	-	-	-
LAAFC O157-35	O157	Cattle	4.33	0.38	-	-	-
LAAFC O157-36	O157	Cattle	4.08	0.16	-	-	-
LAAFC O157-37	O157	Cattle	3.97	0.56	-	-	-
LAAFC O157-38	O157	Cattle	2.87	0.37	-	-	-
LAAFC O157-39	O157	Cattle	3.81	0.01	-	-	-
LAAFC O157-40	O157	Cattle	3.61	0.22	-	-	-

Supplemental Table S5.1. Occurrence and prevalence of the tLST in strains of *Klebsiella pneumononiae* and *Cronobacter sakazakii* of different origin.

Species	# of genomes	% tLST positive genomes
Cronobacter sakazakii	355	15
Clinical isolates	101	8
Environmental isolates	81	8
Klebsiella pneumoniae	4162	7
Clinical isolates	250	4
Environmental isolates	360	2

Supplemental Table S5.2. List of genomes that were analyzed for presence or absence of the tLST (provided as Excel file). https://doi.org/10.7939/r3-8ta6-jq68

Supplemental Table S5.3. Strains used in Figure 3.3. and their origin or source of isolation.

Strains	tLST variant	Source	Latitude	Longitude	Reference
E.coli FUA10289	tLST1	North Saskatchewan River	53.5317	-113.5119	This study
E.coli FUA10290	-[a)]	North Saskatchewan River	53.5317	-113.5119	This study
E.coli FUA10291	tLST1	Hawrelak Park	53.5272	-113.5490	This study
E.coli FUA10292	tLST1	Unknown Lake	52.1542	-117.0097	This study
E.coli FUA10293	-	Unknown Lake	52.1542	-117.0097	This study
E.coli FUA10296	tLST1	Chain Lakes	50.2030	-114.1926	This study
E. coli FUA10297	tLST1, tLSTa	Pond beside highway	50.3426	-113.7657	This study
K. pneumoniae FUA10298	tLSTa	Sheep river	50.7129	-113.8813	This study
K. pneumoniae FUA10329	-	Clinical isolate[b)]			
K. pneumoniae FUA10330	-	Clinical isolate[b)]			
K. pneumoniae FUA1427	tLST1	Human intestine			Koleva, 2014; Valcheva et al., 2019
K. oxytoca FUA10326	-	Clinical isolate[b)]			
K. oxytoca FUA10327	-	Clinical isolate[b)]			
K. oxytoca FUA10328	-	Clinical isolate[b)]			
K. oxytoca FUA1261	-	Rat mesenteric lymph nodes			Lin et al., 2014
K. oxytoca FUA1266	-	Rat mesenteric lymph nodes			Lin et al., 2014
K. oxytoca FUA1271	-	Rat mesenteric lymph nodes			Lin et al., 2014

[a)] "-"indicates tLST-negative; [b)] The clinical isolates were obtained by Michael E. Stiles prior to 1985 and the exact source of isolation is unknown.

Supplemental Table S5.4. Primers and probes used in Chapter 5.

Assay	Primer/probe name	Primer/probe sequence (5'-3')	Tm (°C)
tLST versions	tLST1-F1-F	GTCGTCTACAAGCGTGATCC	60
	tLST1-F1-R	CAGAGGATCAGGTGAACAGAC	
	tLST1-F2-F	CGATATTTTCGCTGGCAGTCAG	
	tLST1-F2-R	CCTTCAGCAGGTCAAATGGAAA	
	tLST1-F3-F	AGCTCATCTCCATCGTCTTCAC	
	tLST1-F3-R	TCTTGACCTGGATGATGCTGTC	
	tLST2-F1-F	CGTTCAACCCGACATTGATTCC	
	tLST2-F1-R	ACGAAAGTGCAAATCGTGACAG	
	tLST2-F2-F	GTGCAGCTGCCACTATCTATCT	
	tLST2-F2-R	CGATGACGCGCATATATGTGTC	
	tLST2-F3-F	TCAATGATACCTATGGGCACGG	
	tLST2-F3-R	TTCCAACAACACAGCGAATTCC	
MG1655 *lacZ::*LHR construction	sgRNA-lacZ-F	GGCCAGTGAATCCGTAATCAGTTTTAGAGCTAGAAATAGCAAG	62
	sgRNA-lacZ-R	TGATTACGGATTCACTGGCCGTGCTCAGTATCTCTATCACTGA	
	Targeting sequence	GGCCAGTGAATCCGTAATCA	
	tLST-16-F	CGGTATCGCCGTCGACGACG	
	lacZ-upstream	GCTGTTGCCCGTCTCACTGG	
	tLST-2-R	GCCGGAATTTCCCCGTGTGC	
	lacZ-downstream	GGACGACGACAGTATCGGCC	
Cm^R cassette	*orf1*-P2	TTGGCCGGAACCGCAAAGCGACGCGATTGGAGAGGGTGAGATGGGAATTAGCCATGGTCC	65
	orf1-P1	GTCCATGTCATACCTCCAGAAAAATTGGAAAACGAGTTACGTGTAGGCTGGAGCTGCTTC	
	sHsp20-P2	GCTTGAGTAACTCGTTTTCCAATTTTTCTGGAGGTATGACATGGGAATTAGCCATGGTCC	
	sHsp20-P1	CTCGGGACGGGTTTTTCTTGTGACGAACGAGCCGGCGACGGTGTAGGCTGGAGCTGCTTC	
	$clpK_{GI}$-P2	GAGGTGCTGGCCCGGCGCAAGAAGAACAACCCGGTGCTGAATGGGAATTAGCCATGGTCC	
	$clpK_{GI}$-P1	GCCAGGCCCTTGGGGTCGGACACGGCAGCCTCGCCCGCCAGTGTAGGCTGGAGCTGCTTC	
	$sHsp_{GI}$-P2	GCGTCATCCAATTCGTCGGCATTGTTCAAGGAGAACCGATATGGGAATTAGCCATGGTCC	
	$sHsp_{GI}$-P1	TGGCTGTTTGATATTCATGATCTTGGGCTCCTGATTGAAGGTGTAGGCTGGAGCTGCTTC	
	pscA-P2	GAAATCTCAGTCAACTAACTTCAATCAGGAGCCCAAGATCATGGGAATTAGCCATGGTCC	
	pscA-P1	CGCGAGACTGACCGACAGAGCAGTCAGCCCCTTCATCACCGTGTAGGCTGGAGCTGCTTC	
	pscB-P2	GATTCGCCTATTTTCACTATCTCATACGAGGCATATCACCATGGGAATTAGCCATGGTCC	
	pscB-P1	AGGGGCGAGACGCGCCCCTCTTACGCCCTATCCAGCGGTTGTGTAGGCTGGAGCTGCTTC	
	$hdeD_{GI}$-P2	GTTTGCTTTTTCACCCCATTAGATCTTTAGGAGATATAGCATGGGAATTAGCCATGGTCC	
	$hdeD_{GI}$-P1	CGAGGATGCTCATATCCATAGATTTTGGTTTGGCACGCTCGTGTAGGCTGGAGCTGCTTC	

	orf11-P2	GATTCATGCCTCCATAGAAATGACATCGAAGGAGTCATACATGGGAATTAGCCATGGTCC	
	orf11-P1	GCGGTTGATGGACTGGCAGTGCGGGCAGACGAGGTGAAGAGTGTAGGCTGGAGCTGCTTC	
	trx_{GI}-P2	CGAAGCGAGGCAGCCTCACTGTGGTCCAAGGAGGCGAACCATGGGAATTAGCCATGGTCC	
	trx_{GI}-P1	CCAGCAGGATTAGTGTAGTGCCGAGCAAGCCCTGCATCGGGTGTAGGCTGGAGCTGCTTC	
	kefB-P2	CATCGTGCGCTGGACGTCGACGCAAGTGGGACGCTGACCGATGGGAATTAGCCATGGTCC	
	kefB-P1	TGGTCACGTAAGACCTGAAATGGGTTAAGGCGTGTTGATTGTGTAGGCTGGAGCTGCTTC	
	orf14-P2	GCCGTCTCGACAGCAGCCGTTTACCAGGGAGTTCATCGTCATGGGAATTAGCCATGGTCC	
	orf14-P1	GCGGTTGAGCCAGCGGTGTTGCAAGAGCGCCGTGCGCGGAGTGTAGGCTGGAGCTGCTTC	
	orf15-P2	CTGCGCAAGCGCGGCGACCGCGCCGCCGAGACCTCTGAGCATGGGAATTAGCCATGGTCC	
	orf15-P1	GGTCGAGATAGGCCATGAGACGTCTCCTGTTGATGGGCAAGTGTAGGCTGGAGCTGCTTC	
	$degP_{GI}$-P2	CGGGCTGTGGCGCTGATTGCCCATCAACAGGAGACGTCTCATGGGAATTAGCCATGGTCC	
	$degP_{GI}$-P1	CTTGGCTGCTTCGCTGTGCAGATCCATGACCCACTTTCCAGTGTAGGCTGGAGCTGCTTC	
Mutants check (Up/Down)	*orf1*-Up-F	TGCAAGGATTTCCTTGGCCG	58
	orf1-Down-R	CCTTAGAAGGTTGAAAAGGTTGAGG	
	sHsp20-Up-F	AATTTTTCTGGAGGTATGAC	
	sHsp20-Down-R	TGAGATTGGCTTCCACCC	
	$clpK_{GI}$-Up-F	AAAACCCGTCCCGAGACG	
	$clpK_{GI}$-Down-R	CCTTGGCCTCATCCCCCCCC	
	$sHsp_{GI}$-Up-F	CGGCTCTGTTCAGTGCG	
	$sHsp_{GI}$-Down-R	CAGAGGGTGCTGCAGCA	
	pscA-Up-F	CAACTAACTTCAATCAGGAGCCC	
	pscA-Down-R	GCTGCTTACCGCGGC	
	pscB-Up-F	TCGCATTCAGCCCCAATAGA	
	pscB-Down-R	TGGTGGGGTCATCCGC	
	$hdeD_{GI}$-Up-F	CTCTCTTGGCTCAGGAGTGTT	
	$hdeD_{GI}$-Down-R	AGCTCTCTGCCAAGGTTCAT	
	orf11-Up-F	CTTCGCAAAACGCGCCT	
	orf11-Down-R	CAAGGGCTGCTGGCAGC	
	trx_{GI}-Up-F	AGGCGTTGATTGGTTGGC	
	trx_{GI}-Down-R	GGGGCCCAGTACAACGC	
	kefB-Up-F	TCGTGCGCTGGACGT	
	kefB-Down-R	GCAGCGTGAAGACGATGG	
	orf14-Up-F	GACACATCAGCGCAATGCG	
	orf14- Down-R	GGCAAACAGCGCGAGC	
	orf15-Up-F	TACTGGCTGCTGCGCA	
	orf15-Down-R	ACCATGCCTCGATGGCG	

	degP$_{GI}$-Up-F	TCCGGCAACGCAAGAGC	
	degP$_{GI}$-Down-R	GCTGTGCAGATCCATGACC	
Mutants check (absence)	*orf1*-check-F	GGTGATTTTCACGCTCGATG	60
	orf1-check-R	TCGGATGACTTCTGCTGTTC	
	sHsp20-check-F	TACAAGATTGCCCTGGAAGT	
	sHsp20-check-R	CTTGATCGAATCCTGGTTGG	
	clpK$_{GI}$-check-F	CCATTCTTATGTCGGTCCAGAG	
	clpK$_{GI}$-check-R	CCACCTTGCTGACCTGTT	
	sHsp$_{GI}$-check-F	TCCGGGAACTGGATGAATTG	
	sHsp$_{GI}$-check-R	AGATCCAGCTTGAGGAGGAA	
	pscA-check-F	TCGGTAAAGAAAGCGGTCAAG	
	pscA-check-R	CATCGGAAGGTTGTCGGTTT	
	pscB-check-F	CAAACACCGAATCCCAATGC	
	pscB-check-R	GCCTCATCGAGGACTTGTTT	
	hdeD$_{GI}$-check-F	ATTGTCGGCATACTTACGGG	
	hdeD$_{GI}$-check-R	ACAAGACGATAGCACCAAGG	
	orf11-check-F	GAAGCGATTGTCCGAGCTAAG	
	orf11-check-R	TGCTTGCCACTTCGTTATCC	
	trx$_{GI}$-check-F	ATCGGAACATCCCAACTGTG	
	trx$_{GI}$-check-R	CAGCCTCGGTATTCACCTTC	
	kefB-check-F	TTGCTGGGGTATCTCTCTGT	
	kefB-check-R	CAGCCACATCAATAGCAGGA	
	orf14-check-F	GTTTTTACGAGCGCTTCGAG	
	orf14-check-R	GAATGCTTGAACTCCATCGC	
	orf15-check-F	GCTAATGAGGATCTGCGTGT	
	orf15-check-R	GGCGATACGGCCAATAACAA	
	degP$_{GI}$-check-F	CGGAATCAATACCGCCATCT	
	degP$_{GI}$-check-R	GTCACGCGCAATACGAATAC	
Cm^R position	Cm-Insert	ATCCCTGGGTGAGTTTCACCAG	58
Complementation	*sHsp20*-NotI	GCGGCCGCAGTAAATGGACATCGATTTCAAGAA	60
	sHsp20-HindIII	AAGCTT TCAGCCGTTGATCGGGATCG	
	clpK$_{GI}$-NotI	GCGGCCGCAGTAAATGGCCAGAAAACAATGCCA	
	clpK$_{GI}$-HindIII	AAGCTTTCAAGATGCGTCGCTCGCCG	
	sHsp$_{GI}$-NotI	GCGGCCGCAGTAAATGTCTGCATTGACTCCGTG	
	sHsp$_{GI}$-HindIII	AAGCTTTTAGTTGACTGAGATTTCAA	
	pscA-NotI	GCGGCCGCAGTAAATGAATATCAAACAGCCAC	

	pscA-HindIII	AAGCTTTCAAAACAGCTTTTGGATGC	
	pscB-NotI	GCGGCCGCAGTAAATGAATGAGCAAACACCGAA	
	pscB -HindIII	AAGCTTTCAGAACAACCTGGACAGCT	
	$hdeD_{GI}$-NotI	GCGGCCGCAGTAAATGAATACAGACACCATCAC	
	$hdeD_{GI}$-HindIII	AAGCTTTTACCCCAGGCGCGTTTTGC	
	kefB-NotI	GCGGCCGCAGTAAATGCAGGGCTTGCTCGGCAC	
	kefB-HindIII	AAGCTTTCATGACGATGAACTCCCTG	
ddPCR	tLST-F	AGGTCTATTGGCCTGGTCTA	60
	tLST-R	AGCGGATTCCGGCAAAAA	60
	tLST-probe	/56-FAM/TGGCGTCCG/ZEN/TGCTGGCAAAA/3IABkFQ/	63
	WT-F	CCAGGCAAAGCGCCATTC	60
	WT-R	CTTTATGCTTCCGGCTCGTA	60
	WT-probe	/5HEX/GGCCTCTTC/ZEN/GCTATTACGCC /3IABkFQ/	63

Supplemental Table S5.5. *E. coli* mutants used in Chapter 5.

Strain	Plasmids used in this strain	
	Complementation plasmid Chloramphenicol (34 mg/L)	Probe plasmid Ampicillin (100 mg/L)
E. coli MG1655		pCC_roGFP2_Orp1
E. coli MG1655 lacZ::LHR	pCA24N	pCC_roGFP2_Orp1
E. coli MG1655 lacZ::LHR Δ*orf1*		pCC_roGFP2_Orp1
E. coli MG1655 lacZ::LHR Δ*sHsp20*	pCA-*sHsp20*	pCC_roGFP2_Orp1
E. coli MG1655 lacZ::LHR Δ$clpK_{GI}$	pCA-$clpK_{GI}$	pCC_roGFP2_Orp1
E. coli MG1655 lacZ::LHR Δ$sHsp_{GI}$	pCA-$sHsp_{GI}$	pCC_roGFP2_Orp1
E. coli MG1655 lacZ::LHR Δ*pscA*	pCA-*pscA*	pCC_roGFP2_Orp1
E. coli MG1655 lacZ::LHR Δ*pscB*	pCA-*pscB*	pCC_roGFP2_Orp1
E. coli MG1655 lacZ::LHR Δ$hdeD_{GI}$	pCA-$hdeD_{GI}$	pCC_roGFP2_Orp1
E. coli MG1655 lacZ::LHR Δ*orf11*		pCC_roGFP2_Orp1
E. coli MG1655 lacZ::LHR Δtrx_{GI}		pCC_roGFP2_Orp1
E. coli MG1655 lacZ::LHR Δ*kefB*	pCA-*kefB*	pCC_roGFP2_Orp1
E. coli MG1655 lacZ::LHR Δ*orf14*		pCC_roGFP2_Orp1
E. coli MG1655 lacZ::LHR Δ*orf15*		pCC_roGFP2_Orp1
E. coli MG1655 lacZ::LHR Δ$degP_{GI}$		pCC_roGFP2_Orp1

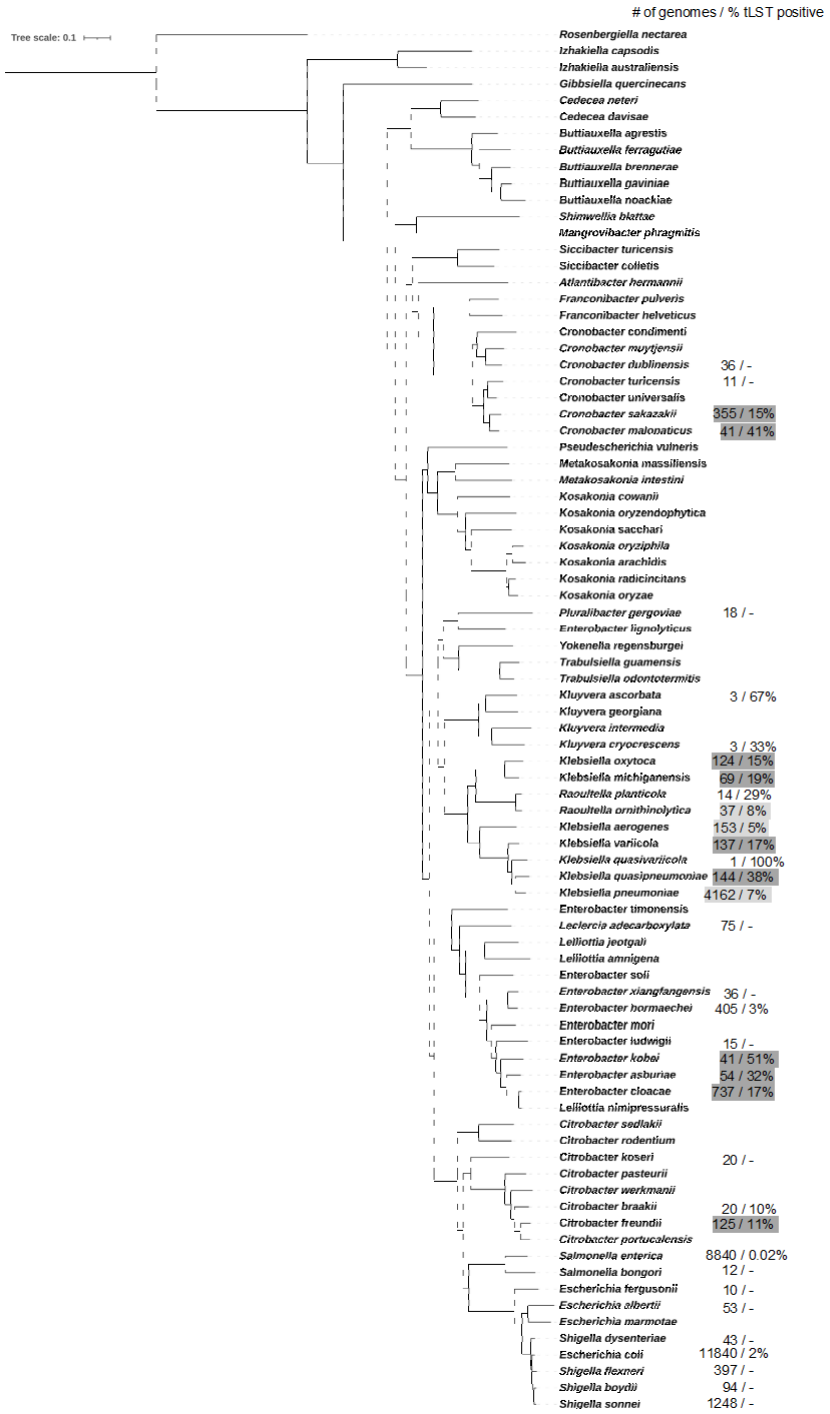

Supplemental Figure S5.1. Phylogenetic tree of representative genomes of type strains of the *Enterobacteriaceae* (left) with indication of the number of genomes and the percent of genomes that are positive for one of the two tLST variants. The number of genomes is indicated only for those species that were represented by 10 or more genomes in the genome database (Table S5.2.);

Supplemental Figure S5.1. legend (con't)

gray shading identifies those species that are represented by more than 30 genomes and include more than 5% tLST positive genomes; dark gray shading identifies those species that are represented by more than 30 genomes and include more than 15% tLST positive genomes. The core genome phylogenetic tree was constructed as described (Zheng et al., 2020). In brief, genomes are labelled as "ncbi_type_material" in the family *Enterobacteriaceae* were retrieved in June 2021. Core genes were identified with Roary (Page et al., 2015) with 80% identity. Core genes (289) were used to construct maximum likelihood (ML) phylogenetic tree (Price et al., 2010).

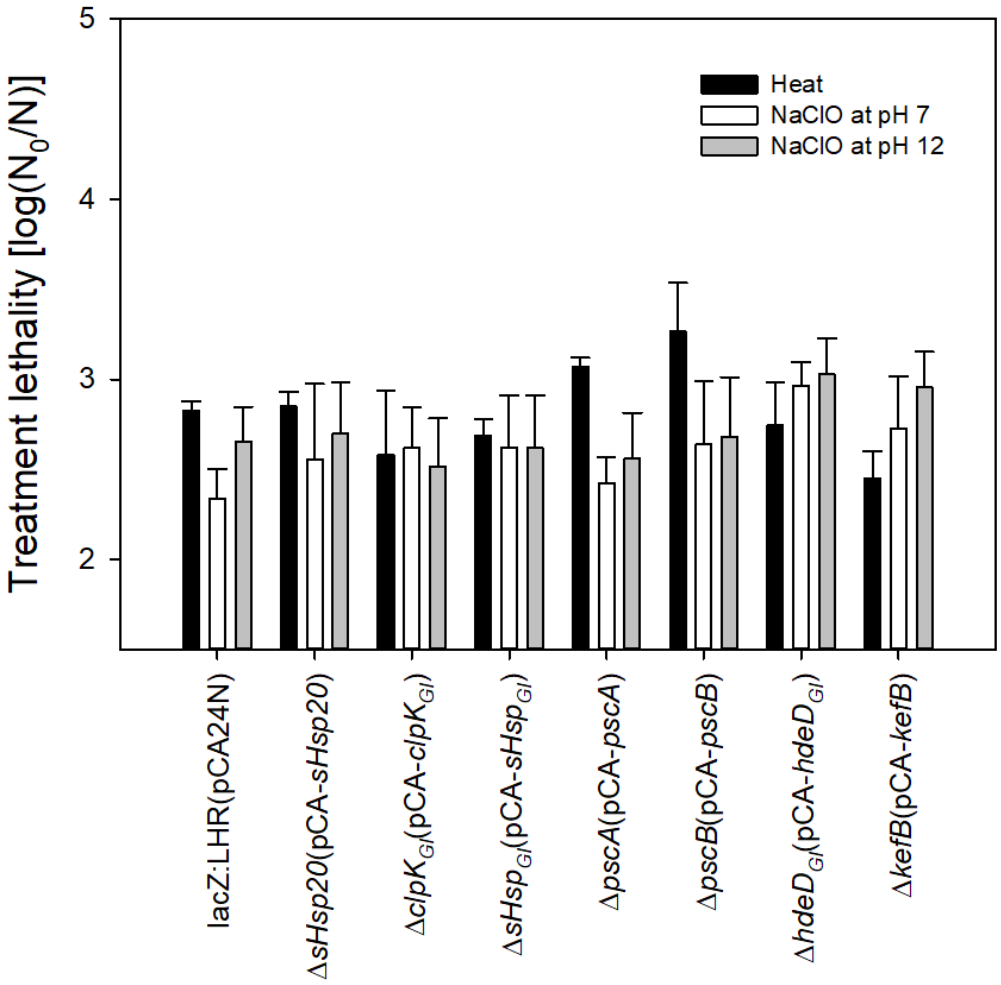

Supplemental Figure S5.2. Lethality of heat and chlorine treatments to cultures of complemented *E. coli* MG1655 *lacZ::*LHR with single deletion. The empty vector pCA24N was transformed to *E. coli* MG1655 *lacZ::*LHR as negative control. The treatment lethality was expressed as the log-transformed ratio of cell counts before treatment (N_0) over the cell counts after treatment (N). Black bars represent cells treated after 63 °C for 5 min; white bars represent cells treated with 50 mM NaClO for 5 min at pH 7; grey bars represent cells treated with 8 mM NaClO for 5 min at pH 12. Values for different strains within a treatment are not significantly different (P>0.05). Data are shown as means ± standard deviation of three independent experiments.

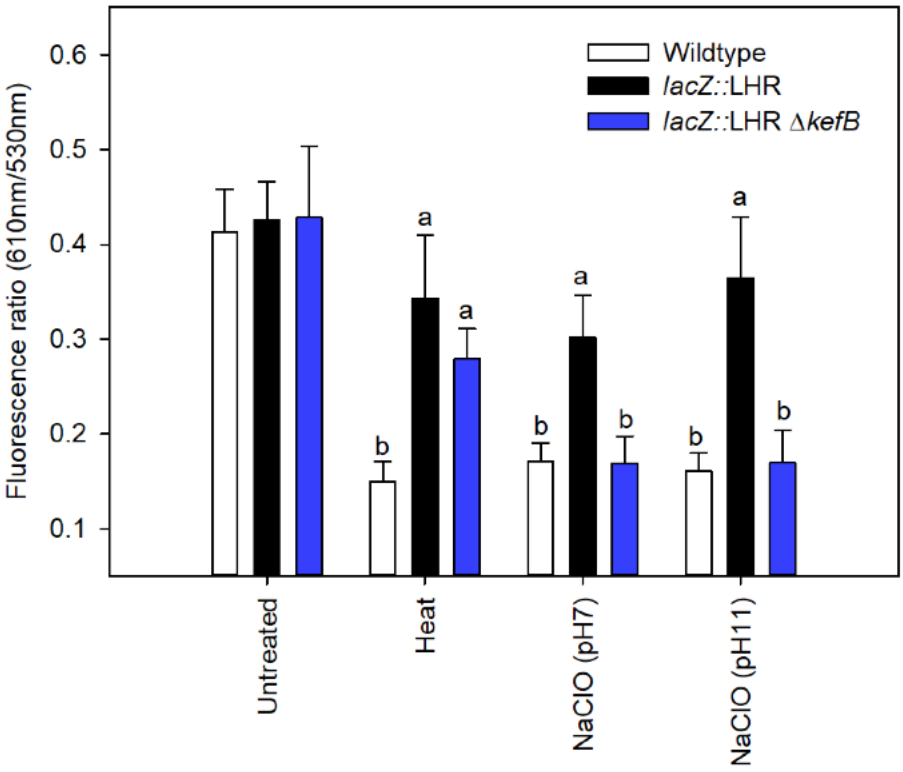

Supplemental Figure S5.3. Quantification of the membrane potential in *E. coli* MG1655, *E. coli* MG1655 *lacZ::*LHR and *E. coli* MG1655 *lacZ::*LHR Δ*kefB*. The ratio of the fluorescence intensity at emission wavelengths of 610 and 530 nm was calculated to indicate the membrane potential. Cells were stained with 30 µM DiOC2(3) and then were treated with 60 °C, 25 mM NaClO at pH 7 or 4 mM NaClO at pH 11 for 5 min to cause reduction of cell counts from 0.5 to 5 logCFU/mL. Values for different strains that do not have a common superscript are significantly different (P<0.05). Data are shown as means ± standard deviation of at least three independent experiments.

Supplemental Figure S6.1. Information of 110 strains of *Salmonella* (provided as Excel file). https://doi.org/10.7939/r3-zprf-he87

Supplemental Figure S6.2. List of genes that were differentially distributed among the 22 most resistant strains and the 8 most sensitive strains (provided as Excel file). https://doi.org/10.7939/r3-skag-pv26

References

Bernal, P., Llamas, M.A., Filloux, A., 2018. Type VI secretion systems in plant-associated bacteria. Environ. Microbiol. 20, 1–15.

Bortolaia, V., Kaas, R.S., Ruppe, E., Roberts, M.C., Schwarz, S., Cattoir, V., Philippon, A., Allesoe, R.L., Rebelo, A.R., Florensa, A.F., 2020. ResFinder 4.0 for predictions of phenotypes from genotypes. J. Antimicrob. Chemother. 75, 3491–3500.

Brynildsrud, O., Bohlin, J., Scheffer, L., Eldholm, V., 2016. Rapid scoring of genes in microbial pan-genome-wide association studies with Scoary. Genome Biol. 17, 1–9.

Capella-Guti.rrez, S., Silla-Mart.nez, J.M., Gabald.n, T., 2009. trimAl: a tool for automated alignment trimming in large-scale phylogenetic analyses. Bioinformatics 25, 1972–1973.

Edgar, R.C., 2004. MUSCLE: A multiple sequence alignment method with reduced time and space complexity. BMC Bioinformatics 5, 113.

Gill, A., Tamber, S., Yang, X., 2019. Relative response of populations of *Escherichia coli* and *Salmonella enterica* to exposure to thermal, alkaline and acidic treatments. Int. J. Food Microbiol. 293, 94–101.

Hu, Y., Huang, H., Cheng, X., Shu, X., White, A.P., Stavrinides, J., K.ster, W., Zhu, G., Zhao, Z., Wang, Y., 2017. A global survey of bacterial type III secretion systems and their effectors. Environ. Microbiol. 19, 3879–3895.

Hyatt, D., Chen, G.-L., LoCascio, P.F., Land, M.L., Larimer, F.W., Hauser, L.J., 2010. Prodigal: prokaryotic gene recognition and translation initiation site identification. BMC Bioinformatics 11, 1–11.

Kalyaanamoorthy, S., Minh, B.Q., Wong, T.K.F., von Haeseler, A., Jermiin, L.S., 2017. ModelFinder: Fast model selection for accurate phylogenetic estimates. Nat. Methods 14, 587–589.

Koleva, P.T., 2014. Non-digestible fibers and dietary interventions: alternative approaches for the treatment of inflammatory bowel disease. PhD thesis, Alberta of University.

Kozlov, A.M., Darriba, D., Flouri, T., Morel, B., Stamatakis, A., 2019. RAxML-NG: a fast, scalable and user-friendly tool for maximum likelihood phylogenetic inference. Bioinformatics 35, 4453–4455.

Letunic, I., Bork, P., 2021. Interactive Tree Of Life (iTOL) v5: an online tool for phylogenetic tree display and annotation. Nucleic Acids Res. 49, W293–W296.

Lin, X.B., Farhangfar, A., Valcheva, R., Sawyer, M.B., Dieleman, L., Schieber, A., Gänzle, M.G., Baracos, V., 2014. The role of intestinal microbiota in development of irinotecan toxicity and in toxicity reduction through dietary fibres in rats. PLoS One 9(1): e83644.

Liu, B., Zheng, D., Jin, Q., Chen, L., Yang, J., 2019. VFDB 2019: a comparative pathogenomic platform with an interactive web interface. Nucleic Acids Res. 47, D687–D692.

Page, A.J., Cummins, C.A., Hunt, M., Wong, V.K., Reuter, S., Holden, M.T.G., Fookes, M., Falush, D., Keane, J.A., Parkhill, J., 2015. Roary: rapid large-scale prokaryote pan genome analysis. Bioinformatics 31, 3691–3693.

Parks, D.H., Imelfort, M., Skennerton, C.T., Hugenholtz, P., Tyson, G.W., 2015. CheckM: Assessing the quality of microbial genomes recovered from isolates, single cells, and metagenomes. Genome Res 25, 1043–1055.

Price, M.N., Dehal, P.S., Arkin, A.P., 2010. FastTree 2 – approximately maximum-likelihood trees for large alignments. PLoS One 5, e9490–e9490.

Seemann, T., 2014. Prokka: rapid prokaryotic genome annotation. Bioinformatics 30, 2068–2069.

Valcheva, R., Koleva, P., Mart.nez, I., Walter, J., G.nzle, M.G., Dieleman, L.A., 2019. Inulin-type fructans improve active ulcerative colitis associated with microbiota changes and increased short-chain fatty acids levels. Gut Microbes 10, 334–357.

Zheng, J., Wittouck, S., Salvetti, E., Franz, C.M.A.P., Harris, H.M.B., Mattarelli, P., O'Toole, P.W., Pot, B., Vandamme, P., Walter, J., Watanabe, K., Wuyts, S., Felis, G.E., G.nzle, M.G., Lebeer, S., 2020. A taxonomic note on the genus *Lactobacillus*: Description of 23 novel genera, emended description of the genus *Lactobacillus beijerinck* 1901, and union of *Lactobacillaceae* and *Leuconostocaceae*. Int. J. Syst. Evol. Microbiol. 70, 2782–2858.